EXPRESSION STUDIES OF THE ACC OXIDASE GENE FAMILY OF WHITE CLOVER

(*Trifolium repens* L.)

A thesis presented in partial fulfillment of the
requirements for the degree of

Doctor of Philosophy

in

Molecular Plant Biotechnology

at Massey University, Palmerston North,
New Zealand

Chih-Ming (Balance) Chen

2005

Abstract

Four ACO promoters and four ACO genomic sequences have been isolated and cloned from *Trifolium repens* L. The promoter sequences were cloned using Gene Walker™ technology, and are defined as the 5′ flanking sequences upstream of the ATG translation start codon, and designated p*TR-ACO1* (1006 bp), p*TR-ACO2* (1510 bp), p*TR-ACO3* (1350 bp), and p*TR-ACO4* (1250 bp). To confirm that each 5′ flanking sequences represents distinct genes, Southern analysis was undertaken with each of the 5′ flanking sequences used as probes. For *TR-ACO1* and *TR-ACO2,* Southern analysis indicated that the genome of white clover contains two copies of each gene, while single copies of *TR-ACO3* and *TR-ACO4* are evident. However, the pattern of recognition of p*TR-ACO3* differs from p*TR-ACO4* confirming *TR-ACO4* as a newly identified member of the ACO gene family of white clover. The four genomic sequences isolated cover sequences downstream of the ATG codon to the stop codon, and each comprises 4 exons interspersed by 3 introns. In terms of sequence identity, for exon 1, identities over the four genes ranges from 69% to 94%, with 94% identity between exon 1 of *TR-ACO3* and *TR-ACO4,* while for exon 2, identities range from 60% to 99%, with 99% identity between *TR-ACO3* and *TR-ACO4.* For exon 3, sequence identities ranged from 71% to 89%, with 89% identity between *TR-ACO3* and *TR-ACO4,* while for exon 4, identities range from 62% to 100%, with 100% sequence identity between *TR-ACO3* and *TR-ACO4.* For the intron sequences, significantly lower identities are observed, with again, highest identities were observed for *TR-ACO3* and *TR-ACO4.* For intron 1, identities ranged from 40% to 81% with the highest identity of 81% observed between *TR-ACO3* and *TR-ACO4.* For intron 2, an identity range of 32% to 72% was observed with 72% identity between *TR-ACO3* and *TR-ACO4,* while identity values of 13% to 79%, with 79% between *TR-ACO3* and *TR-ACO4.* Analysis, *in silico,* of the 5′ flanking sequences was undertaken to identify putative transcriptional binding domains using the PLACE and Mat-Inspector programmes. The

TR-ACO1 5′ flanking sequence contains a higher proportion of domains that are associated with young developing tissues, while the *TR-ACO2* 5′ flanking sequence contains domains that are associated with environmental/hormonal cues. In contrast, the *TR-AC*O3 and *TR-ACO4* 5′ flanking sequences contain a higher proportion of ethylene-response and wound associated domains. The expression pattern, *in vivo,* directed by all four 5′ flanking sequences during leaf development has been examined using GUS fusions and transformation into both tobacco and white clover. In tobacco, the p*TR-ACO1* directed expression in the terminal bud and in axillary buds of younger leaves, with expression declining in the older tissues. The p*TR-ACO2* directed expression in the petioles and mature-green and senescent leaves, while the *TR-ACO3* and *TR-ACO4* promoters directed expression in the axillary buds, petioles and leaves of mature-green tissues and those in the early stages of senescence. In white clover, the *TR-ACO1* 5′ flanking sequence directed highest expression in the apical tissues, axillary buds, and leaf petiolules in younger tissues and then declines in the ageing tissues, while the p*TR-ACO2* directed expression in the axillary buds and leaf petiolules in mature-green tissues. The *TR-ACO3* and *TR-ACO4* 5′ flanking sequences direct more expression in the ontological older tissues, including the axillary buds and leaf petiolules. However, in association with this ontological pattern, all of the 5′ flanking sequences directed expression in most cell types examined during leaf ontogeny. In younger tissues, the *TR-ACO1* 5′ flanking sequence directed expression in the ground meristem and newly emerged leaf tissue at the apical bud of the stolon, the ground meristem tissue of axillary buds, vascular tissue, pith and cortex of the internode and node, and the cortex and vascular tissue of the leaf petiolule. In ontological older tissue, the *TR-ACO3* and *TR-ACO4* 5′ flanking sequences directed expression in the ground meristem of the axillary buds, the vascular tissue of the stolon and petiolule. However, staining could be observed in the pith and cortex of the stolon, and the cortex of the leaf petiolule, but at a reduced intensity. These expression studies suggest that in leaf development of white clover, the primary cues for the transcriptional regulation of the ACO gene family are

ontological in nature.

Acknowledgements

I would really like to offer a very large thank you to my supervisor, Associate Professor Michael T. McManus, Institute of Molecular Biosciences, Massey University, for his excellent guidance, understanding, patience, and encouragement throughout the course of Ph.D. project. I am especially grateful for the time he has been spent towards the end of my writing, editing my Asia's style English, and offering a valuable perspective on this thesis. I feel I cannot say enough, thank you again Michael.

I thank to Dr. Richard Scott, his enthusiastic helping me in many aspects. Especially, I thank you for your valuable discussion when I encountered problems, although I still own you some chocolate fishes. I also thank to Ms. Anya Lambert and Miss Susanna Leung for their chemical ordering help always in a fast mode and with patient to listen my requests.

I thank to Ms. Trish McLenachan and Dr. Rissa Ota. Their warmly smiling to listen my stories and enthusiastically encouragement that helps me to accelerate lab works. Greg Clack, an interest lab mate, thank you companied me for rest of lab time. From you, I recognized the delicious flavor of milkshake. I also appreciate rest crew of MTM lab, Dr. Simon, Dr. Trish, Dr. Ning, Cait, Mathew, Fiona, Rachael, Ludervin, and Marrisa who have created a real-world-like place to work.

To the many staffs and students of the Institute Molecular BioScience who I have for reason or another asked for assistance, thank you.

My appreciation also goes out to the staffs of Plant Molecular Genetics Lab at AgResearch, Gresslands. All of whom have been kindly and friendly helped me during Ph.D. period, especially thank to Dr. Derek White and Roy Meeking their patient to teach me the white clover plant transgenic techniques and Dr. Nena Alvarez and Dr. Alicia Scott their consultation in GUS activity and *in-situ* hybridization assays.

I also thank to Dr. David Lewis and Mr. Ian King from Crop and Food Research, their kindly provided the GMO glasshouse for rescuing my transgenic plants when the period of GMO glasshouse of Massey University was re-constructed.

I would like to thank to my co-supervisor Dr. Mike Hay and AgResearch, Grasslands, for lab research funding support, also thank to Bright Future Scholarship providing financial assistance throughout my Ph.D. research period.

My final and very special thank to my all family members. I cannot thank them enough for all the support and encouragement they have given to me.

Table of Contents

List of Figures

List of Tables

List of Abbreviations

$A_{280\ nm}$	Absorbance at 280 nm
ABA	Abscisic acid
ACC	1-aminocyclopropane-1-carboxylic acid
ACO	ACC oxidase
ACS	ACC synthase
AdoMet	S-adenosyl-$_L$-methionine
AEC	1-amino-2-ethyl-cyclopropane-1-carboxylate
AM	Apical meristem
Amp^{100}	Ampicillin (100 mg/ml)
APS	Ammonium persulfate
ATP	Adenosine-5′-triphosphate
AVG	Aminoethoxyvinylglycine
BCIP	5-bromo-4-chloro-3-indoyl phosphate
bp	Base pair
BSA	Bovine serum albumin
°C	Degrees celsius
ca	Approximately
CaMV	Cauliflower mosaic virus
Cef^{100}	Cefotaxime (100 mg/ml)
CTR	Constitutive triple response
CNBr	Cyanogen bromide
DEA	Diethanolamide
DEAE	Diethylaminoethyl
DEPC	Diethyl pyrocarbonate
DMF	Dimethylformamide
DMSO	Dimethyl sulphoxide
DNA	Deoxyribonucleic acid
DPX	Dibutyl phthalate xylene
DTT	Dithiothreitol

E.coli	*Escherichia coli*
EDTA	Ethylenediaminetetraacetic acid
EFE	Ethylene forming enzyme
EIN	Ethylene insensitive
ELISA	Enzyme-linked immunosorbent assay
EMS	Ethylmethane sulfonate
ETR	Ethylene triple response
FPLC	Fast protein liquid chromatography
EtBr	Ethidium bromide
FW	Fresh weight
g	Gram
g	Acceleration due to gravity (9.8 m/s^2)
GACC	1-(gamma-L-glutamylamino) cyclopropane-1-caboxylate
GC	Gas chromatography
GUS	*E.coli* β-glucuronidase
h	Hour
HCL	Hydrochloric acid
HIC	Hydrophobic interaction chromatography
IAA	Indole-3-acetic acid
IPTG	Isopropyl-β-$_D$-thiogalactopyranoside
Kan^{100}	Kanamycin (100 mg/ml)
Kb	Kilo basepair
kDa	Kilo daltons
K_M	Substrate concentration at half maximum reaction rate
L	Litre
Log	Logarithm
LB	Luria-Bertani (media or broth)
M	Molar, moles per litre
MACC	1-(malonylamino) cyclopropane-1-carboxylate
MADS	The conserved domain of MCM1, AGAMOUS, DEFICIENS and SRF
1-MCP	1-methylcyclopropene

mg	Milligram
Milli-Q water	Water purified by a Milli-purification system
min	Minute
ml	Millilitre
Mr	Relative molecular mass (g/mol)
MS	Murashige and Skoog base media
n	Number of replicates
NAA	1-naphthaleneacetic acid
NaOAc	Sodium acetate
NBT	Nitrotetrazolium blue chloride
NCBI	National center for biotechnology information
nl	Nanolitre
nmol	Nanomole
NPT II	Neomycin phosphotransferase II
PAGE	Polyacrylamide gel electrophoresis
PBSalt	Phosphate buffered saline
PCR	Polymerase chain reaction
Pers.comm.	Personal communication
pH	-Log [H^+]
pI	Isoelectric point
ppm	Parts per million
PVDF	Polyvinylidine difluoride
RO	Reverse osmosis
RT-PCR	Reverse transcriptase-dependent PCR
SAG	Senescence associated gene
SAM	S-adenosyl-$_L$-methionine
SAM	Shoot apical meristem
SDS	Sodium dodecyl sulphate
S.E.	Standard error of the mean
TBA	Tertiary butyl alcohol
TCA	Trichloroacetic acid

TEMED	N, N, N', N'-tetramethylethylenediamine
TFBD	Transcription factors binding domain
T_m	PCR anneal temperature
TR-ACO	*Trifolium repens*-ACC oxidase
Tris	Tris(hydroxymethyl)aminomethylycine
µg	Microgram
µl	Microlitre
µM	Micromolar
µm	Micrometer
UTR	Untranslated region
UV	Ultra violet light
V	Volts
V/V	Volume per volume
WT	Wild type
W/V	Weight per volume
W/W	Weight per weight
X-Gal	5-Bromo-4-chloro-3-indolyl β-$_D$-galactopyranoside
X-Gluc	5-Bromo-4-chloro-3-indolyl β-$_D$-glucuronide cyclohexylamine salt

Chapter 1 Introduction

1.1 Ethylene in plant development

It has long been known that ethylene is the causal agent of plant defoliation. In the 19th century, city streets were lit with gas lamps, and the leaked gas was found to cause defoliation of shade trees along the streets. At the start of the 20th century, D. Neljubov was the first person to demonstrate that ethylene was the active component of the illuminating gas (Neljubov, 1901; cited in (Abeles et al., 1992)). He exposed pea seedlings to the gas and found that it caused the stem to grow in a horizontal direction. He also reported the ethylene can cause the etiolation of pea seedlings with a thickening of the stem, inhibition of root and hypocotyl elongation, and a more pronounced curvature of the apical hook: the triple response phenotype to ethylene.

After this important finding, ethylene, as the first phytohormone, has been studied for more than 100 years, and the following lists some of the more important roles of ethylene in plant growth and development :

Seed germination: Ethylene is proposed to break seed dormancy in different species, including cocklebur seeds (Yoshiyama et al., 1996), lettuce seeds (Kepczynski and Kepczynska, 1997), and seeds of *Amaranthus* (Kepczynski and Kepczynska, 1997).

Emergence of seedlings from the soil: Ethylene can promote the newly germinated seedlings to emerge through soil. For example, when the *etr-1* mutation of *Arabidopsis thaliana,* with an absence of the triple response phenotype, is treated with 10 μL/L ethylene, these plants were less able to emerge through soil when compared with the same treatment of wild-type seedlings (Harpham et al., 1991).

Root formation: Evidence for a role in the promotion of root formation includes the observation that the numbers of root primordia at the cutting site of sunflower hypocotyls

were higher than when the equivalent tissues were treated with the ethylene biosynthesis inhibitor aminoethyoxyvinyl glycine (AVG) prior to cutting (Liu et al., 1990).

Root elongation: Observations that suggest a role for ethylene in the inhibition of root growth include one in which the root elongation rate of sunflower seedlings treated for 12 h, with 10 μM 1-aminocyclopropane-1-carboxylic acid (ACC; the precursor to ethylene) was 40 % less than un-treated seedlings. This inhibition of elongation can be reversed by the addition of silver thiosulphate (STS), an inhibitor of ethylene action (Finlayson et al., 1996).

Shoot elongation: In young tissue, ethylene can limit shoot elongation. For example, applied ethylene can promote the triple response in etiolated pea seedlings with thickening of the stem and inhibition of hypocotyl elongation (Petruzzelli et al., 1994).

Leaf senescence: Ethylene can promote the rate of leaf senescence. For example, ethylene has been shown to induce the expression of a series of cDNAs termed senescence associated genes (SAGs) from treated leaves of *Arabidopsis* (Gepstein et al., 2003). As well, ethylene evolution has been shown to increase during leaf senescence (Hunter et al., 1999; Miller et al., 1999), and the expression of genes coding for the ethylene forming enzymes, ACC synthase and ACC oxidase expression has also been shown to increase.

Floral tissues senescence: Ethylene production is induced, and has been shown to promote senescence of floral plant parts. Ethylene evolution has been shown to increase in senescent floral tissues of carnation or rose (Sisler et al., 1996). These phenomena can be inhibited and retarded by pre-treating these tissues with 1-methylcyclopropene (1-MCP; an inhibitor of ethylene action) (Sisler and Serek, 1997).

Sexual determination: Treatment with ethylene can induce the formation of female flowers in cucumber (Reid, 1995). The gynoecious cucumber plants (female flowers) have an additional copy of a gene (*CS-ACS1*) that encodes the ethylene biosynthesis enzyme, ACC synthase. The allele for this gene has been shown to be closely linked to the locus F which determines the expression of female floral tissues (Trebitsh et al., 1997).

Fruit ripening: Ethylene can control the biosynthesis of fruit pigments and other biochemical and physiological changes that give rise to aromas, textures and flavours in climacteric fruits (Lelievre et al., 1997). For example, after harvest kiwifruit become soft and this is accompanied by a two-fold increases in ethylene production, and a two-fold increase in the content of soluble solids (Sfakiotakis et al., 1997). In another example, in early experiments with transgenic tomato fruit with an ACC synthase gene in the anti-sense orientation, the ripening time of the fruit was postponed (Oeller et al., 1991).

Nodule formation: Ethylene may prevent infection of legume roots by *Rhizobium* species. For example, the ethylene insensitive mutant (*sickle)* of *Medicago trunculata* was found to exhibit an increase in the number of *Rhizobium* infections and nodule formation when compared with wild type plants (Penmetsa and Cook, 1997).

Wound response: Ethylene maybe involved in tissue recovery after wounding. For example, in spear tissues of asparagus, the level of ethylene evolution increased 2-6 fold after wounding when compared with un-wounded tissue (Bhowmik and Matsui, 2004).

Pathogen response: Ethylene has been shown to be associated with pathogen defense mechanisms in plants. For example, in leaves of tobacco, the expression of ACC oxidase (the ethylene forming enzyme) was shown to increase in response to infection with the tobacco mosaic virus (Kim et al., 1998).

Abscission: Ethylene has been shown to promote the rate of abscission of leaves and fruits. For example, in the abscission zone of *Lupinus angustifolius*, the rate of ethylene evolution was higher than in the non-abscission tissues, and the pI-9.5 cellulase gene, which is involved in xyloglucan hydrolysis, is induced by ethylene treatment (Henderson et al., 2001).

Together, all these roles for ethylene during plant growth and development underline the complexity of ethylene biosynthesis, perception and signal transduction. To dissect these phenomena, it is necessary to first look at the regulation of ethylene biosynthesis, before examining ethylene perception and signal transduction.

1.2 Ethylene biosynthesis pathway

Typically, in higher plants which include the cycads, gymnosperms, and angiosperms, ethylene production is regulated by both developmental and external cues, including biotic and abiotic factors (Osborne et al., 1996). During plant development, higher rates of ethylene evolution occur from young tissues (fruit, vegetative and floral tissues) that display a high rate of cell division. During the ensuing cell expansion and elongation stages, ethylene production then declines in these tissues. Finally, ethylene production increases again during fruit ripening and leaf and floral senescence (Abeles et al., 1992). External biotic stresses in plants are caused by tissue invasion by pathogens, including viruses, bacteria, fungi or insects, and external abiotic stresses are due to the wounding, bending, tissue abrasion, radiation, high temperature, chilling, dehydration, flooding, and varied chemical stimuli. Most of these external stress factors can induce ethylene evolution from affected tissues usually as a sharp burst. This phenomenon is termed stress ethylene (Abeles et al., 1992).

The study of ethylene biosynthesis in plants is mainly through the elucidation of the ACC-mediated pathway (Figure 1.1) that begins with *S*-adenosyl-$_L$-methionine (AdoMet or SAM), which is derived from the amino acid methionine by the action of SAM synthetase [E.C. 2.5.1.6]. The SAM is then converted to methylthio-adenosine (MTA) and ACC by ACC synthase (ACS) [E.C. 4.4.1.14] followed by oxidation of ACC to CO_2, HCN and ethylene by ACC oxidase (ACO) reviewed in [E.C.1.4.3] (Yang and Hoffman, 1984; Imaseki, 1991; Kende, 1993; Zarembinski and Theologis, 1994; Fluhr and Mattoo, 1996).

To support high rates of ethylene production without depleting the levels of methionine in cells, the MTA is then converted, through the Yang cycle (methionine cycle), back to methionine (Baur and Yang, 1972).

In addition to the conversion into ethylene, ACC can either be conjugated into 1-(malonylamino) cyclopropane-1-carboxylic acid (MACC) by MACC transferase which is

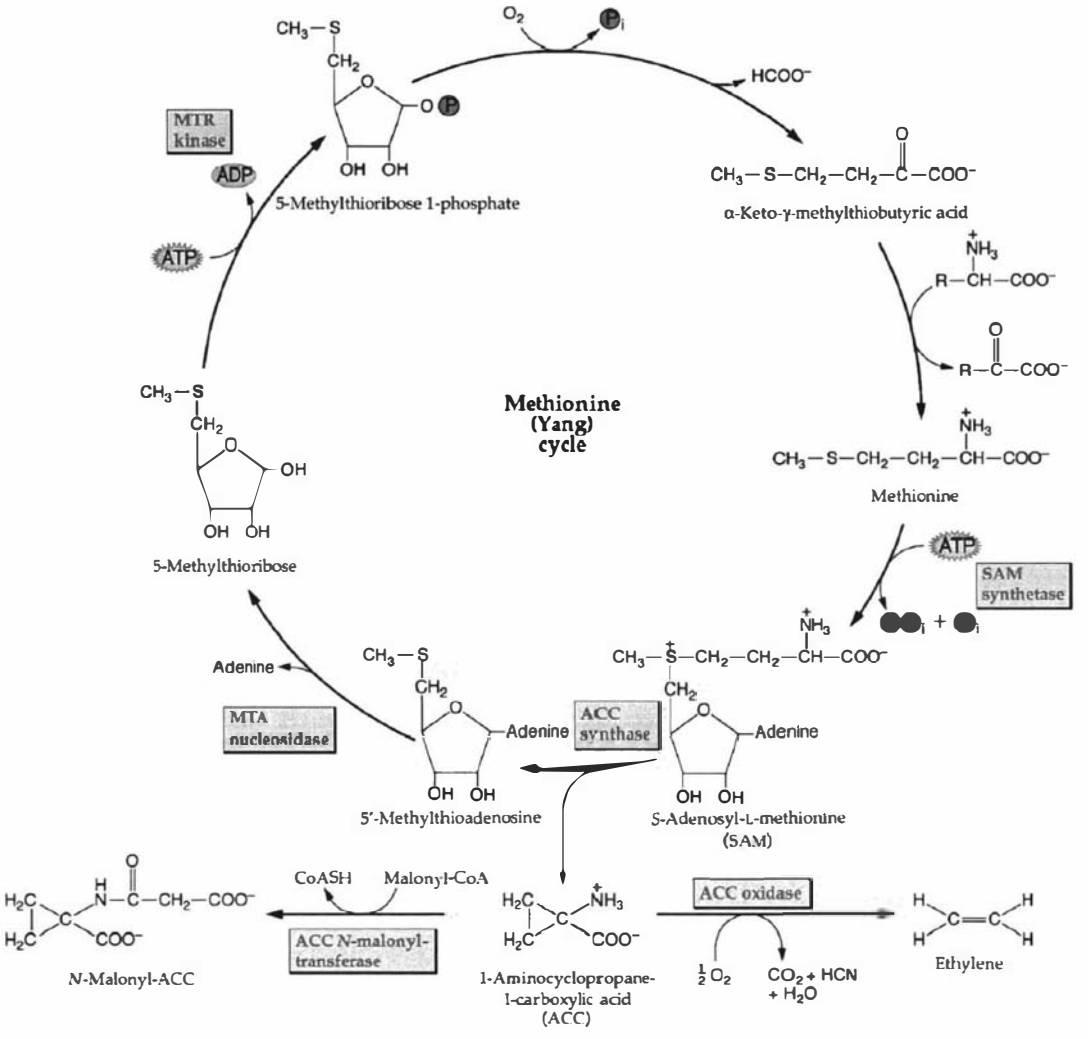

Figure 1.1 The ethylene biosynthetic pathway (edited from Bleecker et al., 2000)

the major ACC-conjugate in plants (Amrhein et al., 1981). Alternatively, ACC can be conjugated, in tomato fruit, into 1-(gamma-$_L$-glutamylamino) cyclopropane-1-carboxylase acid (GACC) by GACC transferase (Martin and Saftner, 1995).

The cyanide product (HCN) is degraded to β-cyanoalanine and asparagine by β-cyanoalanine synthase (Yip et al., 1991). The accumulation of high levels of asparagine indicates a high correlation between activation of ACO and β-cyanoalanine synthase and supports the proposed detoxification mechanism of the cyanide product (Manning, 1988).

1.2.1. SAM synthetase

The ethylene biosynthesis pathway begins conventionally with the conversion of *L*-methionine to *S*-adenosyl-$_L$-methionine (SAM). This step is catalysed by SAM synthetase, which uses ATP as a substrate for this reaction (Yang and Hoffman, 1984). SAM synthetase is an ubiquitous enzyme found in both prokaryote and eukaryote (Tabor and Tabor, 1984). It is classified as a house-keeping enzyme, because it has an important role in cellular biochemistry (Fluhr and Mattoo, 1996). In plants, SAM is not only a precursor for ethylene biosynthesis, but is also a precursor for polyamine biosynthesis (Peleman et al., 1989) and in the transmethylation of proteins, nucleic acids, lipids and carbohydrates. The link between polyamine production and ethylene biosynthesis is of particular interest as application of polyamines has been shown to inhibit ethylene production in some plants. For example, the application of spermine to cut carnation flowers delayed flower senescence, and reduced ethylene or ACC production. Spermine can also reduce the transcription rate of ACC synthase and ACC oxidase genes (Lee et al., 1997).

Since SAM is a universal methylating agent in plants, the enzyme-catalysed conversion of SAM to ACC is regarded generally as the committed step in the ethylene biosynthetic pathway (Yang and Hoffman, 1984; Imaseki, 1991). It has been suggested originally that SAM synthetase is not an important regulatory enzyme in the ethylene biosynthetic pathway

(Peleman et al., 1989). However, more recently SAM synthetase has been shown to occur as multiple isoforms, and there is evidence that expression of the multigene family is under development and environmental control (Schroder et al., 1997). For example, the gene family members have been shown to be expressed differentially during senescence in carnation flowers (Woodson et al., 1992), and in response to treatment of pea ovaries with auxin (Gomez-Gomez and Carrasco, 1998). The existence of multiple controls on SAM synthetase suggests that during optimal plant growth the level of SAM produced by the constitutive enzyme is sufficient, but may not be under stress conditions. In this regard, expression of SAM synthetase genes is increased by a variety of environmental factors including drought stress (Mayne et al., 1996), salt stress (Espartero et al., 1994), fungal and bacterial elictors (Kawalleck et al., 1992; Arimura et al., 2002), mechanical stimuli (Kim et al., 1994), and ozone exposure (Tuomainen et al., 1997). Differential regulation of the SAM synthetase gene family has also been observed during fruit ripening. In fruit of *Actinidia chinensis*, SAM synthetase transcripts were shown to be induced by exposure to exogenous ethylene (Whittaker et al., 1997). This is an important result, as it shows that ethylene can alter SAM synthetase transcription in a feedback regulatory manner. Further, the enzyme has been suggested to play an important role in replenishing the level of SAM, particularly during periods of high ethylene production (Whittaker et al., 1997). Taken together, these observations suggest that an important role of ethylene is to replenish SAM during periods of enhanced ethylene synthesis (Boerjan et al., 1994). With further biochemical and molecular characterization, it may be, therefore, that this enzyme-catalysed step can be included as a committed step in the ethylene biosynthesis pathway.

1.2.2. ACC synthase (ACS)

The second step of the ethylene biosynthetic pathway is the conversion of SAM into ACC (Yang and Hoffmen, 1984), a conversion catalysed by ACC synthase. ACC synthase also

produces 5′-methythioadenosine (MA) which is recycled as part of the Yang cycle to regenerate methionine (Yang and Hoffman, 1984). ACC synthase was first purified from ripened tomato pericarp after a wounding pretreatment (Bleecker et al., 1986), and was subsequently purified from mung bean hypocotyls (Tsai et al., 1988), and from mesocarp tissue of *Cucurbita maxima* after treatment with lithium ions (Nakajima et al., 1990), and apple fruit (Yip et al., 1991).

The enzyme is localised in the cytosolic fraction of plant cells and requires pyridoxal-5′-phosphate as a cofactor. This cofactor requirement has been characterized, as well as the determination that the activity of the enzyme can be inhibited by AVG and aminooxyacetic acid (AOA) (Imaseki, 1991). It also has been shown that the enzyme occurs in low abundance and is very labile (Bleecker et al., 1986), because the level of ACC synthase protein measured in ripened tomato pericarp is only *ca.* 0.0001 % of total protein. However, once treated with a wounding stimuli, the protein concentration may rise 100-fold (Bleecker et al., 1986). In mung bean hypocotyls, the half life of ACC synthase after extraction was reduced from 23.5 min to 12.0 min, whereas the concentration of SAM increased from 40 to 150 μM (Satoh and Esashi, 1986). The lability of this enzyme is due to a catalytic-based inactivation where a covalent linkage is formed at the active site between ACC synthase and its substrate, SAM (Casas et al., 1993).

ACC synthase is coded for by a multi-gene family that has been isolated from many different plant species. In tomato, ten gene members have been isolated (Alexander and Grierson, 2002), in mung bean seven gene family members have been isolated (Song et al., 2003), and at least 12 gene family members have been sequenced in *Arabidopsis* (Yamagami et al., 2003). In addition, three have been isolated from potato (Destefanobeltran et al., 1995), and five in white lupin (*Lupinus albus* L) (Bekman et al., 2000). Although these genes belong to ACC synthase, their amino acid sequences vary in identity from 48 % to 97 %. This suggests that gene regulation and function may also vary (Woltering and Devrije, 1995).

ACC synthase is considered to catalyze the rate-determining step in the ethylene biosynthetic pathway, because of its very low abundance in cells, and it is the first committed step of the pathway (Yang and Hoffman, 1984; Yang and Dong, 1993). Very early studies showed that ethylene production increased in plant organs after application of ACC (Hoffman and Yang, 1980), and that the levels of endogenous ACC were higher in tissue that also produced higher amount of ethylene. For example, at certain stages of development (eg. fruit ripening, flower senescence), and in response to stimulation by physiological factors (eg. wounding, chilling, pathogen attack, or auxin application), ACC levels and ethylene concentration are also induced (Yang and Hoffman, 1984). However, pre-treatment of tissues with AVG can prevent accumulation of both ACC and ethylene (Yang and Hoffman, 1984). The measurement of ACC synthase activity *in vitro* has confirmed that enzyme activity is higher in tissues that have elevated levels of endogenous ACC and ethylene. This has been shown in ripening tomato fruits (Boller et al., 1979), in auxin-pre-treated mung bean hypocotyls (Yu et al., 1979), in senescing carnation petals (Park et al., 1992), and in wounding potato tubers (Burns and Evensen, 1986). Taken together, these studies suggest that ACC levels and ethylene production are highly dependent upon the activity of ACC synthase; observations that are considered to support the hypothesis that ACC synthase is a rate-determining enzyme.

Most physiological factors which have been shown to induce ethylene production in plants have been also shown to either increase ACC synthase activity or induce gene expression (Bleecker et al., 1988). It is now apparent that the ability of different stimuli to influence the activity of ACC synthase is not through multiple regulations of the same gene; instead, it is through regulation of distinct genes which do or do not contain specific regulatory elements. For example, different ACC synthase genes cloned from the same species can have distinct expression patterns. These can be tissue-specific (eg. in fruit or root), or expressed at a specific developmental stage (eg. during ripening or senescence), or in response to specific stress factors (eg. wounding or chilling). In seedlings of *Arabidopsis*, it was shown very early

that each ACS family gene has a specific response to wounding, anaerobiosis, and treatment with lithium chloride and auxin (Liang et al., 1992). Further, in leaf development of *Arabidopsis*, *AT-ACS1* expression is highest at leaf emergence and decreases sharply in rapidly expanding leaves (Smalle et al., 1999), while *AT-ACS6* expression is induced in senescent leaves during ozone exposure (Miller et al., 1999). In tomato suspension cells, only a subset of genes are induced in response to yeast elicitors (Oetiker et al., 1997), and in tomato fruit in response to wounding (Lincoln et al., 1993). In carnation floral tissue, different tissues express specific genes (TenHave and Woltering, 1997), and in mung bean hypocotyls, a specific ACS gene is induced by auxin treatment (Yu et al., 1998). In *Stellaria longipes,* specific ACS genes respond to photoperiod and temperature (Kathiresan et al., 1998), and in the wounded tissues of *C. maxima*, specific ACS genes are induced in response to ethylene treatment (Nakajima et al., 1990). These studies support the notion that different members of the ACS gene family have specific regulatory functions.

In most cases, ethylene production rates are positively correlated with increasing transcriptional rates of ACC synthase genes. Some examples include: in zucchini fruit (*Cucurbita pepo*) (Sato and Theologis, 1989) and etiolated hypocotyls tissues (Huang et al., 1991). Positive correlations are also observed in wounded fruit of tomato (Olson et al., 1991), the senescence stages of tomato floral tissue (Rottmann et al., 1991) and in fruit (pericarp) tissue of pepper (*Capsicum annuum*) (Harpster et al., 1996). These studies support the idea that stimuli, or specific developmental stages promote ACC synthase transcription, and the ethylene produced is thus controlled at this gene transcription level. But not every stress-induced, tissue-specific or developmental cue correlates with the rate of ACC synthase transcription. For example, in the styles of cut carnation flowers (TenHave and Woltering, 1997), the elicitor-induced ethylene production in tomato suspension cultures (Oetiker et al., 1997), wounded floral tissues of carnation (Park et al., 1992), and the light-induced rhythm of ethylene production in *S. longipes* (Kathiresan et al., 1998). In these cases, transcription of

ACS genes did not show any correlation with ethylene production. This maybe due to the fact that other (as yet un-discovered) ACS gene family members are induced, or the mRNA undergoes post-transcriptional processing and the protein post-translational modification. This also implies that ethylene biosynthesis is not only controlled at the level of ACC synthase, but can be regulated at other levels, including ACC conjugation and the regulation of ACC oxidase. These mechanisms have been studied and will be discussed later.

In some cases, ACC synthase genes may be modified during transcription. In one example, an auxin-inducible ACC synthase cDNA from pea (*PS-ACS1*) was found to be recognized two RNA transcripts of *ca.* 1.6 kb and 1.9 kb on northern blots. The large transcript was not considered to be a product of incomplete processing of introns, but instead the transcript may arise due to the presence of an alternative promoter within the sequence of the large transcript (Peck and Kende, 1998).

In another example of post-transcriptional processing, the *LE-ACS3* gene of tomato showed multiple RNA sizes using northern blot analysis. Using specific probes, three different size of *LE-ACS3* were identified that all contained the same coding sequence but two of them contained extra intron sequences. This reflects a different splicing mechanism that may also control ACC synthase expression at the post-transcriptional level (Olson et al., 1995).

In addition to regulation at the transcription and the post-transcriptional level, ACC synthase can be regulated at the post-translational level. For example, the COOH-terminal end of most ACC synthase proteins display differences in residue number and sequence identity despite a high degree of similarity in the rest of the protein (Theologis et al., 1992). However, when 46 to 52 amino acid residues of the tomato ACS1 protein were deleted from the COOH-terminal, the truncated protein had 9-times higher affinity for SAM, when compared with the wild-type, when expressed in *E.coli* (Li and Mattoo, 1994). In *Arabidopsis*, the *ACS5* gene specifically responds to cytokinin treatment. However, the phenotype of the *acs5* mutation, with a single base pair insertion 35 bp upstream of stop codon (which caused a frame-shift mutation change

to the 12 terminal amino acids of ACS5 from RVSYTDRVPDER to PGFMDRSCT), showed a 20-fold over-production of ethylene under cytokinin application, whereas the wild type only had less than two-fold increase in ethylene production in response to the same treatment (Vogel et al., 1998). It was proposed that cytokinin action may interfere with some negative regulators in the C-terminal region of the ACS5 protein. In tomato, a 50 kDa molecular weight monomer form was purified (Van Der Straeten et al., 1989), but when this gene was expressed in *E.coli*, a 55 kDa protein product was purified, suggesting that some post-translational modification occurs in tomato that does not occur in the *E. coli* background (Van Der Straeten et al., 1990).

A key element in the post-translational modification of ACS enzyme activity is the regulation of the stability of the protein. More recently, a stress-specific response mitogen activated protein kinase (MAPK) has been isolated and characterized from tobacco (Liu and Zhang, 2004). This kinase (SIPK) is able to phosphorylate the ACS-2 and ACS-6 proteins from *Arabidopsis*, and elevates the levels of cellular ACS accumulation and ethylene production. They also used a gain-of-function mutant (ACS-6^{DDD}) phenotype to confirm that the phosphorylation site is in the C-terminal of ACS-6 protein (Liu and Zhang, 2004). The significance of phosphorylation of the C-terminal has been highlight more recently with the characterization of the function of the ETO-1 protein of *Arabidopsis*. The *eto* mutants of *Arabidopsis* were those that displayed the triple response without ethylene added, and subsequent experiments showed that these mutants over-produced ethylene (Wang et al., 2004). Wang et al. (2004) have shown that ETO-1 binds to the truncated isoforms (ACS-5). Further, over expression of ETO-1 inhibits the induction of ethylene production by the plant growth regulator cytokinin (Vogel et al., 1998), and promotes ACS-5 protein degradation (Chae et al., 2003; Wang et al., 2004). These studies also show that at least two signaling pathways through post-translational mechanisms regulate the ACS proteins. One is from exogenous stimuli (eg. biotic or abiotic stress) through the MAPKs phosphorylation/

de-phosphorylation mechanisms, while the second is from endogenous cues (eg. cytokinin) through kinases or inhibitor proteins (eg. ETO-1) that regulate ACS protein activation (Ecker, 2004).

1.2.3. Conjugation of ACC

The product of the ACC-synthase-catalysed reaction, ACC, has two fates. ACC oxidase can convert ACC into ethylene, or ACC can be conjugated with malonyl CoA to form malonyl-ACC (MACC) (Yang and Hoffman, 1984), a reaction catalysed by MACC transferase. In some plant species (eg. tomato), ACC can be conjugated with glutathione to form glutamyl-ACC (GACC), a reaction catalysed GACC transferase (Peiser and Yang, 1998).

MACC is found throughout the plant, including vegetative tissue, seeds and in ripening fruit (Amrhein et al., 1981; Satoh and Esashi, 1984; Yang and Dong, 1993). It is proposed to be synthesized in the cytosol and stored in the vacuole (Bouzayen et al., 1989). MACC transferase has been isolated from the hypocotyls of mung bean (Benichou et al., 1995) and tomato fruit (Martin et al., 1995). In mung bean, two iso-forms of MACC transferase with different molecular masses and kinetic parameters have been characterized. A 36 kDa isoenzyme exhibits a lower temperature optimum (40°C), and a seven-fold lower apparent Km for ACC when compared with the 55 kDa isoenzyme (Benichou et al., 1995). In tomato, the MACC transferase activity was found to be enhanced by ethylene in treated immature green fruit, but not in ripening fruit (Martin et al., 1995).

In some plant tissues, MACC is considered to be an inactive form of ACC, and cannot be hydrolysed to release free ACC (Hoffman et al., 1983). There is some evidence that this enzyme might act as a negative regulatory component in the ethylene biosynthesis pathway, and its function is to control the rate of ethylene production, by depleting cellular pools of ACC. For example, in tomato fruits, the activity of MACC transferase increases just after a

period of high ethylene production (Yang and Hoffman, 1984; Martin and Saftner, 1995). During ripening of bananas, the peel produces up to 80-fold less ethylene than the pulp even though it has seven-fold more ACC oxidase activity. This reduction in ethylene production maybe due to the higher level of ACC conjugation observed in the peel as compared with the pulp (Dominguez and Vendrell, 1993).

In contrast, GACC appears only when sufficient glycine, serine, histidine tripeptide is available. GACC transferase activity has been measured in ripening tomato fruit, but not in any other plant organs, even when these are producing high levels of ethylene. This implies that GACC is not a universal conjugation form, but might act as a tissue-specific regulatory component (Peiser and Yang, 1998).

1.2.4. ACC oxidase (ACO)

In contrast to ACC synthase, ACC oxidase was thought originally to be expressed in a constitutive manner in many plant tissues, since the ACC is readily converted to ethylene when added to growth medium or plant tissues (Yang and Hoffman, 1984). But recent studies at the molecular level reveal that the ACO expression rate is correlated to the ethylene production rate. Thus regulation of ACO activity may act as an extra tier for controlling ethylene biosynthesis in higher plants.

1.2.4.1 Identification of EFE as ACC oxidase

Due to early difficulties in measuring ACC oxidase enzyme activity in a cell-free system, the identification of this enzyme was first achieved at the cDNA level. In 1985, Slater et al. published the screening of a cDNA library made from ripe tomato fruit to isolate cDNAs that were differentially expressed in mature and ripe fruits. Nineteen non-homologous groups of ripening related clones were identified (Slater et al., 1985). One clone, designated pTOM13, was shown to be homologous to a mRNA that accumulated after mechanical wounding of un-ripe tomato pericarp and leaf tissue, and prior to the wounding-induced peak of ethylene

production (Smith et al., 1986). It was suggested, therefore that the pTOM13 transcript was either involved in ethylene production or was induced by ethylene, since it was also shown that it can be induced by treatment of mature green tomato fruit with ethylene (Maunders et al., 1987). In later experiments, the pTOM13 cDNA was transformed into tomato plants in the anti-sense orientation, and the transformants showed decreased ethylene synthesis in both wounded leaf tissue and ripening fruit in a gene dose-dependent manner. This indicated that this sequence was involved in ethylene production, perception or metabolism (Hamilton et al., 1990).

The confirmation that the pTOM13 cDNA as an EFE sequence was obtained through heterologous expression in yeast of a full-length identical clone of pTOM13 designated as pRC13. When exogenous ACC was applied to the yeast cells transformed with pRC13, the cells converted ACC to ethylene, whereas un-transformed cells did not have this ability (Hamilton et al., 1991). This gene product in yeast also displayed similar characteristics to ethylene-forming activity found in plant tissue, including strong inhibition by cobalt ions (Co^{2+}) and 1,10-phenanthroline (PA; a metal chelator). Therefore, from these experiences, the pTOM13/pRC13 sequence was proposed to code for the ethylene forming ethylene.

The deduced amino acid from the cDNA sequence of pTOM13 has highly identical to flavanone 3-hydroxylase cDNA of *Antirrhinum majus* (Hamilton et al., 1990) and their amino acid sequence shared 33 % identity and 58 % similarity. The flavonone 3-hydroxylase enzyme required ascorbate and iron (Fe^{2+}) as co-substrates/co-factors for activity and also needed anoxic conditions during extraction (Britsch and Grisebach, 1986). Therefore, when using these same extraction and assay conditions, active ACC oxidase was successfully recovered from the soluble fraction of melon fruit (Ververidis and John, 1991). With this observation, it was possible to explain subsequently that previous assays from tissue homogenates that lacked ACC oxidase was due to the loss of iron and ascorbate during extraction. The previously observed relative higher enzyme activity rates from extracts of intact protoplasts

and vacuoles was due to the fact that the integral membrane structure kept the enzyme cofactors in the extract (Fernandez Maculet and Yang, 1992). Subsequently, CO_2 has also been reported to increase the activity of apple ACO (Fernandez Maculet and Yang, 1992).

1.2.4.2 Biochemical characterization of ACC oxidase

After pTOM13 protein was identified as the ACC oxidase enzyme and the biochemical cofactors identified, numerous ACC oxidase enzyme activities were demonstrated in many plant species, such as apple (Dong et al., 1992; Pirrung et al., 1995); avocado (McGarvey and Christoffersen, 1992); pear (Vioque and Castellano, 1994); banana (Moya-Leon and John, 1995); citrus (Dupille and Zacarias, 1996).

The common co-substrate/co-factors for ACO activity identified for pTOM13 (ascorbate and Fe^{2+}) were similar in both dicot (eg. tomato) and monocot (eg. banana) plant species (John, 1997). When 2-oxoglutarate replaced ascorbate in the assay mixture extracted from pear fruit, enzyme activity was lost. This suggested the ascorbate can not be replaced by any other 2-oxoacids (Vioque and Castellano, 1994). When an ion chelator (EDTA or PA) was added to a citrus extract, ACO activity was lost. If other divalent metal ions (eg. Zn^{2+}, Mg^{2+}, Mn^{2+}, and Cu^{2+}) replaced Fe^{2+} in the assays, ACO activity was again lost confirming that Fe^{2+} serves as important cofactor for the ACO enzyme (Dupille and Zacarias, 1996). Examination of the ACO protein sequence of apple reveals that this ACO protein structure did not contain the prosthetic-heme group for Fe^{2+} binding (Dupille et al., 1993), but through subsequent recombinant ACO proteins studies it was determined that His_{177}, Asp_{179}, His_{211}, and His_{234} may form the $Fe2^{+}$ binding site (Tayeh et al., 1999). The CO_2 requirement for ACO activity has been studied from many plant species. For example, the activity in pear fruit extracts increased 14 % with applied CO_2 (Vioque and Castellano, 1994), and in melon fruit, a similar stimulation was observed (Smith and John, 1993). Therefore, CO_2 acts as a co-factor and as a product.

The inhibitors of the ACO activity have been well characterized in both *in vivo* and *in vitro* assays. Aminoisobutyric acid (AIB) and Co^{2-} both can inhibit ACO enzyme activity when added in the extract (Vioque and Castellano, 1994) and they were often used to confirm the ACO-mediated ethylene biosynthesis pathway.

Using SDS-PAGE, a molecular mass of 35 kDa was determined for an ACO from apple fruit, and by using gel filtration for an ACO protein from the same source, a mass of 39 kDa was calculated (Dong et al., 1992). Also, electrospray-mass spectroscopy determined a mass of 35.3318 kDa for an ACO purified from apple fruit (Pirrung et al., 1993). A central conclusion from these determinations is that ACO in apple fruit exists as a monoer.

Through cell fractionation techniques and immunoblot analysis, the cellular location of the ACO protein has been determined in tomato suspension cultured cells. In these studies, ACO protein was found in the cytoplasm of cells and was not found in the vacuole and the cell membrane (Reinhardt et al., 1994). Although most studies and sequence analysis reveals that the ACO protein is located in the cytoplasm, it is also possible that it may also occur in the extracellular space of plant cells. Using the electron microscope and immunogold-labeled antibodies, the ACO protein was located in the apoplasm of breaker tomato fruit. Using immuno-localisation studies, the antibody stained the cell walls of apple fruit and breaker tomato fruit (Rombaldi et al., 1994). In addition, in proteinase K-treated protoplasts from cultured apple cells, much less detection of ACO protein by Western blot analysis was observed, supporting the view that the enzyme may also occur in the extracellular space in tomato and apple fruits (Ramassamy et al., 1998).

ACO enzyme activity has also been shown to alter in different developmental stages and in response to different physiological stimuli. In climacteric fruit, ACC oxidase activity is normally lower in the early unripe green fruit stage, and then rises rapidly as fruits start to ripen, after which activity declines again in the over-ripe stage (Moya-Leon and John, 1995). For example, activity in banana fruit has been reported to increase from 2 to 35 $nLFWg^{-1}h^{-1}$

(pulp), and in the peel, activity increased from 35 to 130 nLFWg^{-1} h^{-1} (Moya-Leon and John, 1995). In melon fruit, activity was increased from 5 to 260 nLFWg^{-1} h^{-1} (Ververidis and John, 1991), and in ripe tomato fruit activity increased from 10 to 196 protein $mg^{-1}h^{-1}$ (Barry et al., 1996). Although each plant species displayed a different degree of activity increase, these examples confirm that ACO activity responds to developmentally-specific cues. In terms of physiological stimuli, wounding can normally induce ACO activity in some plant tissues. For example, in wounded mesocarp tissue of *C. maxima,* ACO activity increased four-fold when compared with un-wounded tissues after a period of 40 h incubation (Hyodo et al., 1993). Similarly, in wounded flavedo discs of mandarin fruit, ACO activity increased four-fold after 24 h (Dupille and Zacarias, 1996).

In early studies, ACO in different tissues were shown to have different affinities for CO_2 and ascorbate, and this implied the existence of ACO isoforms and that these function in a tissue-specific manner. For example, the leaves of sunflower or corn plants contain low CO_2 and high ascorbate concentrations when compared with root tissues, but the ACO enzymes showed a higher affinity (low K_m) to CO_2 and lower affinity to ascorbate in the leaf tissues, whereas the root, ACO just showed a higher affinity (low K_m) to ascorbate and a lower affinity to CO_2. This result implies that there are ACC oxidase isoforms that exist in different plant tissues, and these respond differentially to environmentally- and developmentally-specific cues. Thus to define these multiple family members, molecular analysis is necessary.

1.2.4.3 Molecular characterization of ACC oxidase

Following identification of the first ACC oxidase cDNA in tomato (designated as pTOM13) (Slater et al., 1985), numerous ACC oxidase genes have now been isolated from a diversity of plants species. Through screening genomic libraries, multiple members of ACC oxidase gene families have been identified, including four members in *Petunia hybrida* (Tang et al., 1993),

four members in tomato (Barry et al., 1996; Nakatsuka et al., 1998), three members in cantaloupe melon (Lasserre et al., 1996), and three members in tobacco (Kim et al., 1998). By screening cDNA libraries, two members have been identified in mung bean (Kim and Yang, 1994), two members in banana fruit (Huang et al., 1997), three members in sunflower seedlings (Liu et al., 1997), one in apricot fruit (Mbeguie-A-Mbeguie et al., 1999), and three members in broccoli floral tissue (Pogson et al., 1995; Yang et al., 2003).

In general, most ACC oxidase gene sequences share high identity from species to species. By comparing more than 30 ACC oxidase gene sequences, a high nucleotide sequence identity (70-95%) was observed both within the same family and between families from different plant species (Lasserre et al., 1996). The gene families of tomato and *Petunia* are highly similar with 88-94% identity over three genes of tomato, compared with 88-95% identity over three genes of *Petunia* in terms of their amino acid sequences (Lasserre et al., 1996). In contrast, the 5′-untranslated regions (UTRs) of the four gene members of *Petunia* display only 42-43% identity, and their 3′-UTRs display 50-57% identity (Tang et al., 1994). For the three tomato ACO gene family members, the 5′-UTR sequences show 58 to 60 % identity and the 3′-UTR regions have 44 to 52 % identity (Barry et al., 1996). This suggests that both the 5′- and 3′- untranslated regions of ACO genes have significant sequence diversity.

Originally, the expression of ACC oxidase activity was thought to be constitutive in plant tissues (Yang and Hoffman, 1984), but it is clear now that this constitutive expression in plants is not due to a single ACC oxidase gene. Multigene families from many species have now been studied in terms of their expression patterns. The results show that these genes display differential temporal and spatial patterns of expression. For example, in mung bean hypocotyls, *VR-ACO1* is highly expressed in most seedling tissues, but the *VR-ACO2* gene only has a basal level expression during seedling development (Kim and Yang, 1994). In broccoli, the *ACC-Ox1* gene was detectable in senescent tissue and reproductive tissues, but *ACC-Ox2* is expressed only in reproductive tissues (Pogson et al., 1995). Expression of the

tomato gene family has been examined during flower development. The first gene, *LE-ACO1,* is dominant in petals, stigma and style, *LE-ACO2* can be detected in the anther cone only, and the *LE-ACO3* transcripts were shown to accumulate in all the floral organs, except the sepals (Barry et al., 1996). A fourth gene, *LE-ACO4* with low sequence identity to the other genes, has been shown to be expressed at the initiation of fruit ripening (Nakatsuka et al., 1998). In melon tissues, all three ACO genes are highly expressed in hypocotyl tissue during seedling growth. After this stage, *CM-ACO1* is expressed in senescent leaves and fruits, *CM-ACO2* is expressed mainly in mature green leaves and floral tissues (Lasserre et al., 1997). In the tobacco species *Nicotiana glutinosa*, *NG-ACO1* and *NG-ACO3* are both expressed highly in root and senescent leaves, but *NG-ACO2* was shown only to be expressed constitutively in leaves and stems (Kim et al., 1998). In sunflower, *ACCO1* is highly expressed in apical buds and root tips, *ACCO2* is detected predominantly in roots and aerial part of plants, and *ACCO3* is expression constitutively in all plant parts (Liu et al., 1997).

ACC oxidase genes do not only display a tissue-specific expression pattern, but also show specific responses to environmental and physiological stimuli. For example, the expression of *VR-ACO1* from mung bean is induced by wounding, but expression decreased following application with 5 μM methyl-jasmonate (Kim and Yang, 1994). In *Arabidopsis, AT-ACO1* expression can be induced by wounding, and treatment with ACC (10 mM), iron (0.2 mM) and ethylene (1 mM) (Gomez Lim et al., 1993). Expression of *ACC-Ox1* from broccoli can not be induced by ABA or ethylene treatment, whereas, expression of *ACC-Ox2* can be induced by these treatments (Pogson et al., 1995). In tobacco, the expression of both *NG-ACO1* and *NG-ACO3* can be induced by various stress factors (TMV infection, wounding, salicylic acid, Cu_2SO_4, ethylene and methyl-jasmonate), but these treatments did not alter the expression of *NG-ACO2* (Kim et al., 1998).

ACO gene expression is not only regulated at the transcriptional level, but also post-transcriptional mechanisms are involved. For example, in sunflower, expression of the

ACCO1 gene can be induced by wounding and treatment with silver ions, but accumulation of the ACO protein did not correlate with this increased of *ACCO1* RNA accumulation (Liu et al., 1997). A similar trend has been observed in mung bean. The *VR-ACO1* gene, which can be induced by ethylene treatment, has a higher transcription rate when compared with the protein accumulation rate (Jin et al., 1999).

1.3 Ethylene signal transduction pathway

Ethylene biosynthesis comprises the conversion of SAM through several steps to become the gaseous hormone. Once synthesized, the action of the hormone is *via* perception and the down-stream signal transduction pathways (Figure 1.2).

1.3.1. Ethylene perception

Through screening mutants of *Arabidopsis* with an altered triple response, the ethylene triple response (*etr*) and ethylene insensitive (*ein*) mutants were isolated (Bleecker et al., 1988; Guzman and Ecker, 1990). The phenotype of this mutant family showed a reduced or no response to exogenous ethylene and abnormal growth and development. For example, in the *etr1* line, plants treated with ethylene displayed elongated hypocotyls (similar to the wild-type grown in dark without ethylene treatment), and the rate of seed germination was slower than the wild-type (Bleecker et al., 1988).

A comparison of the sequence of *ETR1* with other prokaryote and eukaryote signalling proteins, revealed that this protein may code for a two-component signal transducer (Chang et al., 1993). When the ETR1 protein was over-expressed in yeast, and the cells treated with [C^{14}]-ethylene, evidence was gathered that the transformants could bind ethylene (Schaller and Bleecker, 1995). This binding activity has been reported to require copper (Cu I) to act as a transition metal, and the metal ion binding site was shown to be located in the second hydrophobic motif at the N-terminal end of the ETR1 protein (Rodriguez et al., 1999). Evidence for the metal ion requirement comes from the ethylene inhibitor (trans-cyclooctene)

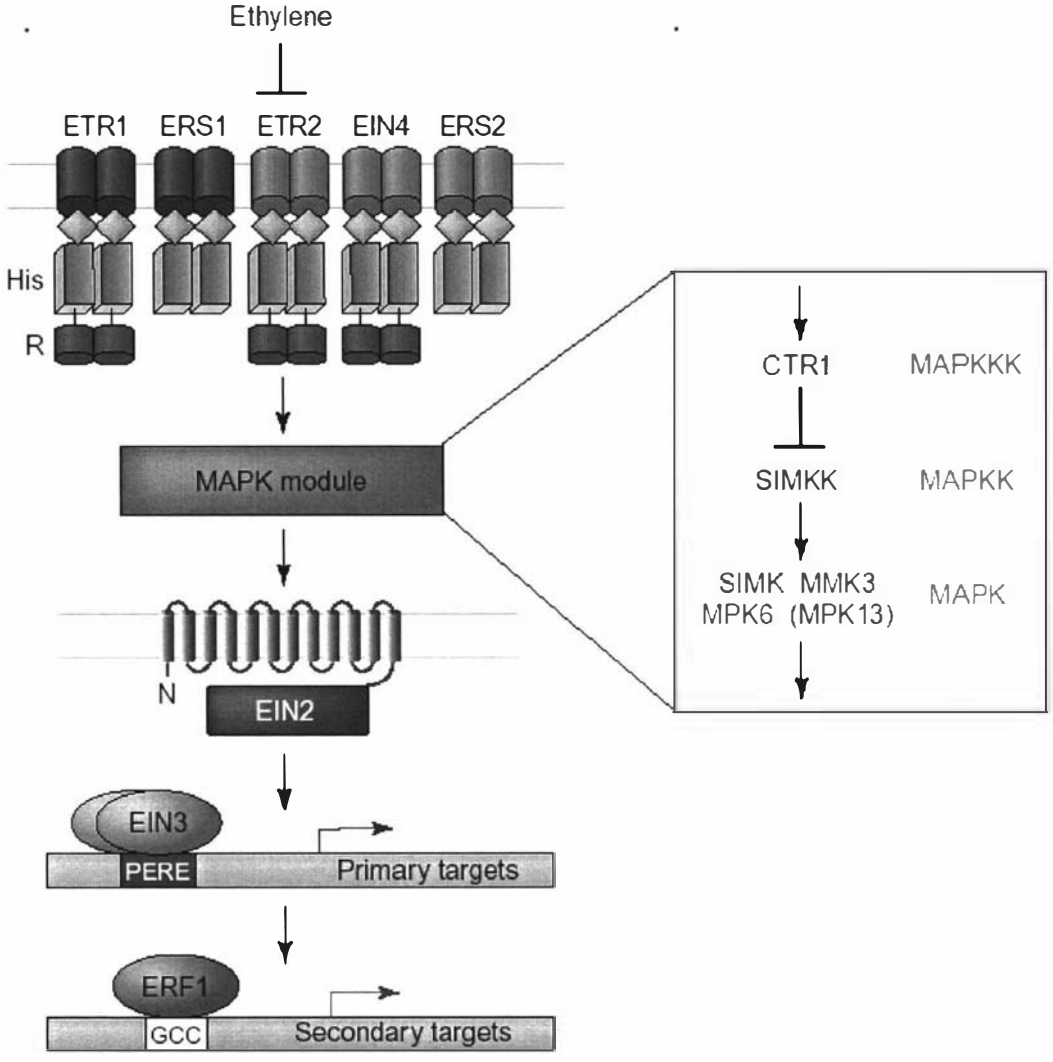

Figure 1.2 Model of the ethylene signalling pathway in *Arabidopsis*

ETR1, ERS1, ETR2, EIN4, ERS2 = five members of ethylene receptor protein family

His = histidine kinase domain, R = receiver domain

CTR1 = constitutive triple response 1, a Raf-like kinase; a member of the MAPKKK family

SIMKK = a MAPKK family member, isolated from *Medicago*

SIMK, MMK = a MAPK family member, isolated from *Medicago*

MPK6, MPK13 = a MAPK family member, isolated from *Arabidopsis*

EIN2 = ethylene in-sensitive 2; presume presumed to be a nuclear membrane spanning kinase

PERE = primary ethylene response element

ERF1 = ethylene-response factor 1

sensitive mutant, *ran 1*, which has been characterized as a copper-transporting P-type ATPase. The observation that ETR1 is a trans-membrane protein, forms homodimers (Schaller et al., 1995) and has histidine-kinase activity (Gamble et al., 1998) supported the proposal that ETR1 is a ethylene receptor protein (Chang, 1996; Bleecker, 1999).

Additional *ETR1* family members were then identified through cDNA screening from *Arabidopsis* genome (Figure 1.2), and these designated as *ETR2, ERS1, ERS2,* and *EIN4* (Hua et al., 1995; Hua et al., 1998; Sakai et al., 1998). The structure of these proteins is highly conserved at the N-terminus domain, which is the site of the membrane-spanning regions and for extra-cellular ethylene binding, and in the C-terminal region (excluding *ERS1* and *ERS2*) which have identity with bacteria histidine protein kinase (HPK) receptors. These proteins were proposed to initiate signal transduction through His autophosphorylation on the His kinase domain followed by transfer of the phosphate to a conserved aspartate residue in the cognate receiver domain (C-terminal domain) (Chang and Bleecker, 2004). In *Arabidopsis*, these receptors have been grouped into two subfamilies. Sub-family-1 comprises *ETR1* and *ERS1*, contain all the defined His kinase sequence motifs, whereas subfamily-2 (*ETR2, EIN4* and *ERS2*) are substantially divergent in terms of the content of these domains (Chang and Stadler, 2001). In tomato, six *ETR* like genes have been isolated and designated as *LeETR1*, *LeETR2* and *LeETR3* (also known as *NR*), *LeETR4*, *LeETR5* and *LeETR6* (Lashbrook et al., 1998; Tieman et al., 2000; Moussatche and Klee, 2004). The *LeETR1* and *LeETR2* genes were cloned from a root cDNA library, and their structure has been shown to be similar to the *ETR1* gene, and so contain all the major structures of the two-component regulator domains (Lashbrook et al., 1998). In contrast, the LeETR3 protein differs from the other two family members, as it does not have the HPK domain in its structure, and so is similar to the ERS1 and ERS2 proteins of *Arabidopsis* (Lashbrook et al., 1998). Although these HPK domain are conversed in many of ethylene receptors, other serine domains also play an important role in the ethylene receptor families. For example, autophosphorylation of NTHK-1, a tobacco

subfamily-2 ethylene receptor, has been demonstrated on serine and threonines *in vitro* (Zhang et al., 2004), and all five receptor proteins from *Arabidopsis* have been shown to display autophosphorylation *in vitro*. Moussatche and Klee, (2004) have found that autophosphorylation is predominantly on serine residues, and that mutation of the histidine residues conserved in two-component systems does not abolish this serine autophosphorylation function (Moussatche and Klee, 2004).

The occurrence of multiple ethylene receptors might imply that they are involved in different functions in plant development. The *LeETR1* gene is expressed constitutively throughout plant tissues, whereas *LeETR2* also shows low expression through the plant, but is induced during seed germination, and then down-regulated during etiolated seedling elongation and during leaf senescence (Lashbrook et al., 1998). *LeETR3* displays a high level of tissue-specific expression since it can be detected only in the ovary and at the onset of ripening fruit tissues (Lashbrook et al., 1998). Although the expression of all *LeETR* genes overlaps throughout plant tissues, at certain developmental stages, only specific receptors are expressed to give these spatial and temporal patterns (Lashbrook et al., 1998). This suggests that each individual ethylene receptor maintains a distinct functional identity *via* the capacity to respond differentially to developmental and environmental cues.

With the discovery of the putative ethylene receptor, investigation then turned to the down-stream signaling components. However, as these studies were being done, critical experiments by Hua and Meyerowitz (1998) changed the concept as to how the ETR protein interacts with its downstream component. In these, the generation of double (*ers1* and *etr1*), triple (*etr2*, *ein4* and *ers2*) and quadruple (*etr1, etr2, ein4* and *ers2*) lost-of-function mutants of *Arabidopsis* did not show an (expected) decrease in ethylene sensitivity but a constitutive ethylene response instead (Hua and Meyerowitz, 1998; Zhao et al., 2002; Hall and Bleecker, 2003). This genetic evidence supported the proposal that the wild-type active ethylene receptors or their complexes appear to repress ethylene signaling in air. This suggests that

when ethylene is bound to the receptors, the receptor switches to an inactive state and ceases to repress the down-stream signal kinases (Hua and Meyerowitz, 1998).

1.3.2. Ethylene signal transduction

Through screening T-DNA insertion lines of *Arabidopsis*, one phenotype was identified that displayed the triple response without ethylene treatment, and therefore the "constitutive triple response" (*ctr1*) mutant was identified (Kieber, 1993). The *CTR1* gene was sequenced and shown to have high identity to the Raf-like kinase family of eukaryotes which contains a conserved motif for an intrinsic Ser/Thr kinase at the C-terminal end of the protein. The CTR protein family has been characterized as MAPKKK proteins (Mitogen Activate Protein Kinase Kinase Kinases) which act in phosphorylation-based cascade-signalling (Ouaked et al., 2003). By using a yeast two hybridization system and *in vitro* affinity assays, CTR1 has been demonstrated to interact physically with the ETR1 and ERS1 proteins (Clark, 1998). Therefore, an epistatic relationship has been determined in which CTR1 acts downstream of the ethylene receptor and may be controlled by the phosphorylation status of the ETR protein. Since CTR1 acts as a negative regulator of the ethylene response, this suggests that without ethylene, the receptor complex (eg. ETR1) may associate with CTR1 to mediate downstream kinase-based phosphorylation signaling to repress the ethylene response. In the presence of ethylene, the ETR1 dimer might become dephosphorylated, and CTR1 then ceases its downstream phosphorylation function (Bleecker, 1999). The association of ETR with CTR has been supported by the localisation of these proteins in cells. Using immunoelectron microscopy, the ETR1 receptor has been localized in endoplasmic reticulum (ER) (Chen et al., 2002), and furthermore, the CTR1 protein, but not the mutant protein, has also been detected to be associated with the ER membrane through immunoblot assays (Gao et al., 2003).

Through in-gel kinase assays, the downstream MAPK module members have been isolated and characterized. Two proteins from *Medicago truncatula* have been isolated and designated

as SIMK and MMK3, and one protein isolated from *Arabidopsis* is designated as MPK6. All of these proteins are activated immediately by treatment with ACC, and are inactive by treatment with ethylene biosynthesis inhibitors. Therefore, they have been confirmed as downstream MAPK module members (Ouaked et al., 2003). After that, by using hemagglutinin epitope (HA)-tagged versions of SIMK, one MAPKK protein was isolated, and designated as SIMKK. This kinase can be rapidly activated by ACC treatment, which can also activate SIMK and MMK3 (Ouaked et al., 2003). That suggests that ethylene is a positive regulator of the SIMKK and SIMK or MMK3 proteins.

Over-expression of SIMKK in *Arabidopsis* resulted in an ethylene constitutive response phenotype. Since this is the same as the *ctr1* phenotype, it suggests that the SIMKK protein has an opposite function to the CTR1 protein which is upstream of the MAPK module component. Through the gain-of-function assays in the *etr1* mutant of *Arabidopsis*, MPK6 activity is lost, even when treated with ethylene, which suggests that signalling downstream of the MAPK module kinase activity is dependent on the ethylene receptors (Ouaked et al., 2003).

Taken together, ethylene signal transduction in the cytoplasm is through the MAPK cascade module mechanism (Figure 1.2), but within this module family, the upstream (CTR1) and the downstream components (SIMKK, and SIMK) have opposite functions in mediating ethylene response. Also the multiple numbers of this module component (eg. SIMK and MMK3) may have other regulatory mechanisms for controlling this signal transduction pathway.

1.3.3. Ethylene responses in the nucleus

Using similar approaches as that used to isolate the *etr1* mutants (EMS mutagenesis), two ethylene insensitive phenotypes mutants were isolated and designed as *EIN2* and *EIN3*. By using double mutant gain-of -function assays, both loci were found to be epistatic to the *ctr1* allele, and functionally *CTR1* can repress the *EIN2* and *EIN3* phenotype (Roman et al., 1995).

This suggests that both EIN2 and EIN3 act as ethylene activators in the signal transduction pathway. Examination of the protein sequence and structure of EIN2 reveals that it contains a membrane spanning region in the N-terminal region, and also a coiled-coil structure in the COOH-terminal region which has a role in protein-protein interactions. The EIN2 protein has been proposed to be located at the nuclear membrane for ethylene signal transduction into the nucleus (Chang and Shockey, 1999), although its final localization is yet to be determined.

Plants of *Arabidopsis*, in which *EIN3* is over-expressed, display the ethylene constitutive response phenotype (Bleecker and Kende, 2000), and the *ein3* mutant did not or only partially alter *EIN2* function in the gain-of-function assay, suggesting that the EIN3 protein may act downstream of *EIN2* (Bleecker and Kende, 2000). Examination of the EIN3 protein sequence and structure, suggests that it is a nuclear-localised protein (Guo and Ecker, 2004), and the protein has been found to be bound to the promoter sequences of the glutathione synthesis transferase (GST-1) gene (ltzhaki et al., 1994), the *E4* gene (Montgomery et al., 1993), the *LE-ACO1* gene (Blume and Grierson, 1997), and the ethylene response factor (ERF1) (Solano et al., 1998). These observations suggest that *EIN3* acts as a transcription activator (Chang and Shockey, 1999). Another three *EIN3*-like genes have been isolated, and their functions and sequences are highly similar to the *EIN3* gene (Roman et al., 1995), implying that the ethylene response in the nucleus can be controlled by multiple factors for different responses.

An interesting finding is *ERF1*, the transcription of which is regulated by the EIN3 protein. The ERF1 protein is also a transcription factor, and has been found to bind to the specific ethylene response domain, the GCC-box, which occurs in the promoter regions of many ethylene-related genes, including β-chitinase (Shinshi et al., 1995), *PDF 1.2* (Penninckx et al., 1996), *Hookless 1* (Lehman et al., 1996). Therefore, the ethylene signal response in the nucleus may occur through a transcription cascade that can induce the transcription of a wide array of genes.

1.4 Regulation of ACC oxidase gene expression in higher plants

Families of multiple ACC oxidase genes have been isolated and differentially expressed in tissues of many plant species, and these have been shown to respond to different stimuli. Thus, ACO genes appear to be involved in regulating functions in a tissue-specific manner (Barry et al., 1996).

1.4.1. Tissue specific patterns of expression

Through the use of specific probes for each ACO isoform, many members of ACO gene families display tissue-specific expression patterns. For example, in the tomato ACO family, both *LE-ACO1* and *LE-ACO3* expression is dominant in senescent leaves, fruit, and flower tissues (Barry et al., 1996), whereas *LE-ACO1* and *LE-ACO4* are expressed in preclimacteric fruit, and then expression increases greatly when ripening commences (Nakatsuka et al., 1998). Most *LE-ACO* genes are spatially regulated throughout flower development with *LE-ACO1* expressed predominately in petals, the stigma, and the style, *LE-ACO2* expression is limited to the anther cone, whereas *LE-ACO3* transcripts accumulate in all of the floral organs excluding the sepals (Barry et al., 1996). In common with expression during development in tomato, the expressions of four members of the ACO gene family of *Petunia* are also regulated in floral tissue. The mRNA for *PH-ACO1* is detected in sepals, the corolla, anthers, and pistils, while expression of *PH-ACO3* and *PH-ACO4* is restricted to the pistils (stigma, style, and ovary) of the flowers (Fernandez Maculet and Yang, 1992). Moreover, expression of these genes in the pistil depends upon the developmental stage of the flower. In the stigma and style, these three genes are expressed in a co-ordinated fashion, but the transcript in the ovary is primarily *PH-ACO1* (Fernandez Maculet and Yang, 1992). From these studies with tomato and *Petunia*, the expression patterns of the ACO gene families reveal that at least in flower tissues, these genes have a tissue-specific expression pattern, and

this may relate to their developmental functions. In broccoli, expression of *ACC-Ox1* has been detected in senescent tissue and reproductive tissues, but ACC-Ox2 is only expressed in reproductive tissues (Pogson et al., 1995). Three members of ACO gene family in melon also show a tissue-specific expression pattern. Expression of *CM-ACO1* is induced in ripe fruit, while *CM-ACO2* is expressed at a low level in etiolated hypocotyls, while expression of *CM-ACO3* is predominantly in flower tissues (Lasserre et al., 1996). There are two distinct ACO genes reported in peach, with expression of *PP-ACO1* detectable in flowers, fruitlet abscission zones, the fruit mesocarp and young fully expanded leaves (Ruperti et al., 2001). The accumulation of this transcript strongly increases during fruitlet abscission, mesocarp ripening, and leaf senescence. In contrast, the expression of *PP-ACO2* can only be detected during early development of fruit tissue. During seedling growth, both genes can be detected in the epicotyl and root with *PP-ACO2* more highly expressed when compared with *PP-ACO1* (Ruperti et al., 2001). In mung bean hypocotyls, only two ACO genes have been isolated. The expression of *VR-ACO1* is high in all tissues of seedlings, while only low levels of expression of the second gene, *VR-ACO2*, can be detected in the hypocotyls (Kim and Yang, 1994). These studies reveal that regulation of ACO gene expression is not only limited to certain developing stages of specific tissues (eg. reproductive tissues) but are expressed in a range of tissues throughout the life cycle of the plant from seed germination to fruit ripening and leaf senescence. As well, the expression of gene members can overlap in some specific stages of development, but usually the expression of one is higher than the others in family. (Kim and Yang, 1994; Ruperti et al., 2001).

In vegetative tissues of sunflower, expression of the *ACCO1* gene is high in root tissues, while the expression of the *ACCO2* is mainly confirmed to leaf and hypocotyl tissues. The remaining member of the gene family, *ACCO3,* can be detected in leaves, hypocotyls, and roots during seedling growth, but at a lower, constitutive level (Liu et al., 1997). In potato, expression of both *ST-ACO1* and *ST-ACO2* is high in leaf tissues, but is lower in the root and

tuber tissues. In leaves, the expression of *ST-ACO1* is predominantly in the senescent leaves, whereas *ST-ACO2* is expressed in young and green leaves only (Nie et al., 2002). In tobacco, the expression of *NG-ACO1* and *NG-ACO3* is high in senescent leaves, while *NG-ACO2* is constitutively expressed during all stages of leaf development. In root tissues, both *NG-ACO1* and *NG-ACO3* are highly expressed, whereas *NG-ACO2* is expressed predominantly in stem tissue (Kim et al., 1998). In tomato leaf tissues, *LE-ACO1* is barely detectable in green leaves, but at the onset of senescence, gene expression increases 27-fold, and continues to rise through to the mid-senescence stage and then declines slightly at the late senescence stage. The *LE-ACO2* and *LE-ACO4* transcripts were not detectable in leaves either at the young developing or senescent developmental stages. The expression of *LE-ACO3* can only be detected in senescent leaves, but its level of expression is only half that of *LE-ACO1* (Barry et al., 1996). These observations suggest that in vegetative tissues, members of the ACO gene families may have distinct expression patterns as well as overlapping regulation patterns in some developing tissues, such as is observed during seed germination or senescence of leaves.

1.4.2. Patterns of ACO expression induced by external cues

Since most ACC oxidase genes display a tissue-specific pattern of expression at different plant developmental stages, it follows that developmental and/or environmental cues may also regulate expression of different members of ACO gene families. In tomato, when leaf tissues are wounded, an increase in expression of *LE-ACO1* only can be detected (up to 11-fold) (Barry et al., 1996). This gene not only responds to wounding, but also can be quickly induced in leaves by exposure to ozone (Moeder et al., 2002), ethylene or by pathogen attack (Blume and Grierson, 1997). Thus in tomato, it appears that only one of the ACO genes is responsive to stress signals. This type of regulation can also be found in other plant species. For example, in melon the expression of *CM-ACO1* is increased sharply after wounding and/or ethylene treatment, whereas *CM-ACO3* did not show any change in expression under

the same treatment (Lasserre et al., 1997). The response to wounding and ethylene is proposed by the authors to involve distinct mechanisms. As evidence of this, if tissues were pre-treated with 1-MCP (an inhibitor for ethylene action), the ethylene-induced *CM-ACO1* transcripts was inhibited, but the wounding-induced increase of *CM-ACO1* expression was not (Bouquin et al., 1997). In the peach ACO family, both ethylene and wounding induces the expression of *PP-ACO1* in senescent leaves and in ripe fruits, but not *PP-ACO2* (Ruperti et al., 2001). In apple, the *AP4* ACC oxidase gene (ACO1), which is specifically expressed in ripening fruit, can also be induced by ethylene and wounding in fruit tissue. Interestingly, the time of induction in response to ethylene (3-5 days) differs from the timing of the response to wounding (24 h) (Dong et al., 1992; Ross et al., 1992). A similar response can also be detected in papaya, in which *CP-ACO2* is induced by ethylene in ripening fruit and senescent leaves, but not the other ACO family member, *CP-ACO1* (Chen et al., 2003). In potato, *ST-ACO1* is highly expressed in wounded leaves, but *ST-ACO2* expression is not affected (Nie et al., 2002). In mung bean, only *VR-ACO1* expression is induced by wounding and ethylene treatment, although in this tissue the wound response appears to be induced by ethylene. As evidence, the addition of AOA (aminooxyacetic acid) and NBD (2,5-norbornadiene; inhibitor of ethylene action) can block the wound induction, but exogenous ethylene can restore the effect (even in the presence of the inhibitor). This suggests that in this tissue, the induction of *VR-ACO1* by wounding is mediated by ethylene (Kim and Yang, 1994), and also implies that both the ethylene and wounding responses can either be mediated *via* individual pathways or can be co-ordinated.

In addition to the wounding and ethylene stimuli, ACO gene expression can also be induced by the other hormones. During seed germination of chick-pea, ACO expression declined during the post-germinative period, but the application of IAA ceased the decline in expression and induced more ACO transcripts. In contrast, ABA treatment inhibited the induction of ACO gene expression (Gomez-Jimenez et al., 2001). In rice, expression of the

OS-ACO2 was markedly increased by IAA treatment of etiolated seedlings, but the expression of *OS-ACO3* was greatly increased by ethylene treatment. Interestingly, the auxin-induced increase in *OS-ACO2* expression was partially inhibited by ethylene, whereas the ethylene-induced expression of *OS-ACO3* was completely blocked by auxin treatment (Chae et al., 2000). This observation suggests that hormone cross-talk can be mediated through the biosynthetic pathway at a transcription level. In most orchid flower tissues, ACO gene expression can be induced by both IAA and ethylene and responses to both stimuli show similar patterns in most flower parts (Zhang et al., 1999). Another interesting example is in mung bean, in which expression of the *VR-ACO1* gene is induced by ethylene treatment (Kim and Yang, 1994), but this induction can be suppressed by IAA and N_6-benzyladenine (BA) treatment. In mung bean hypocotyls tissue, addition IAA or BA did not change the basal expression of ACO, but when combined with ethylene, specific transcripts of *VR-ACO1* were induced. This suggests that *VR-ACO1* expression may have a positive feedback control, but this feedback regulation can be suppressed by added IAA or cytokinin (Kim et al., 2001). In epicotyls of azuki bean, *AB-ACO1* expression can be repressed by GA_3 treatment after 10 h of incubation, whereas applied IAA did not alter the level of *AB-ACO1* transcripts. Interestingly, GA_3 treatment also stimulated ethylene production (Kaneta et al., 1997) implying that GA may have different regulatory effects on the multi-ACO gene family of azuki bean. In cucumber fruit, the expression of *CS-ACO1* can be induced either by wounding or IAA treatment, but the expression of *CS-ACO2* is not affected by either stimulus (Shiomi et al., 1998).

Through screening of ABA-treated lines of sunflower for drought-tolerance, five clones were isolated, and one of these had increased expression of *HA-ACO* (Ouvrard et al., 1996). This implies that ACO expression can be induced by ABA treatment under drought stress. In mung bean, ABA treatment of hypocotyls reduced the ethylene-induced accumulation of *VR-ACO1* (Kim et al., 1997). That suggests the ethylene can interact with ABA to regulate the response

to different environmental cues. Taken together, these observations support the view that most of the main plant hormones can control ACO expression in a tissue/function-specific manner and so regulate ethylene biosynthesis. This also confirms that in common with most plant physiological and developmental responses, hormones to act synergistically with each other.

ACO expression is not only regulated by wounding or other hormonal cues, but is also regulated by environmental signals. For example, in sorghum, a mutant deficient in functional phytochrome B exhibits reduced photoperiodic sensitivity (Finlayson et al., 1999). Further, its ethylene production is increased 10-fold, but this synthesis is only commensurate with the abundance of *SB-ACO2* expression in the mutant when compared with the wild-type. When both mutants and wild-type plants were treated with shading, increased expression of *SB-ACO2* can be detected in both cultivars. This suggests that *SB-ACO2* gene regulation is coupled to a diurnal rhythm mechanism, and that light can also control ACO gene expression (Finlayson et al., 1999). The other case of light regulation in ACO expression is observed in *Chenopodium rubrum* seedlings in which ACO enzyme activity increased when plants were transferred from light to dark and decreased when plants where placed back in the light (Machackova et al., 1997). ACO activity did not change in continuous light, whereas if plants were incubated in constant dark, high activity was only observed at an initial time and then expression decreased (Machackova et al., 1997). This implies that at least two separate mechanisms maybe involved in generating the ethylene production rhythm; one in response to the loss of phytochrome B function and another is response to shading (Finlayson et al., 1999).

There are many studies that report that stress factors can induce ethylene production, which implies that ACO gene expression is also regulated by stress factors. In potato, heat (40°C), cold (0°C) and/or soil-flooding treatments to the shoots or tuber tissues, results in the induction of *ST-ACO1*, whereas expression of *ST-ACO2* is only induced by the cold stress (Nie et al., 2002). In addition, inoculation of leaf, stem and tuber tissues of potato with the

potato virus A (PVA) only induces the expression of *ST-ACO1*. Together, these data suggest that most stress factors that induce ACO expression do so in a gene-specific manner (Nie et al., 2002). Exposure of plant tissues to ozone can also induce ACO gene expression. In tomato, an increase in expression of *LE-ACO1* coincided with the rate of ethylene production of leaves increasing when exposed to ozone, but the transcription of the wound-inducible proteinase inhibitor II gene was undetectable in same ozone treated leaves. This suggests that the response to ozone stress may differ from the wounding stress pathway in terms of regulating *LE-ACO1* expression (Nakajima et al., 2001). Exposure to plant pathogens also regulates ACO gene transcript level in tobacco. In response to TMV infection, the expression of both *NG-ACO1* and *NG-ACO3* were significantly induced, but in a mock treatment which caused mild wounding, only *NG-ACO3* increased in expression. In addition, treatment of tobacco leaf tissues with salicylic acid, methyl jasmonate and $CuSO_4$ resulted in differential expression, with both *NG-ACO1* and *NG-ACO3* induced. In contrast, *NG-ACO2* expression did not change in response to any stress stimulus treatment. This reflects that stress and wounding regulatory mechanisms are different in the *NG-ACO* gene family, and confirms that the stress response also can occur in a gene-specific manner (Kim et al., 1998).

Mechanisms of phosphorylation and de-phosphorylation are also involved in controlling many biological processes, including metabolism, catabolism, signal transduction or even the circadian rhythm. This post-translational mechanism has also been reported to be involved in regulating ACO gene expression. For example, in rice, *OS-ACO2* expression is induced by auxin, but suppressed by ethylene treatment. This cross-talk between the hormonal networks can also be regulated by applying okadaic acid (an inhibitor of protein phosphatases). For example, the auxin induction of *OS-ACO2* can be suppressed by okadaic acid treatment suggesting that protein dephosphorylation plays a role in controlling IAA signals that regulate ACO gene expression (Chae et al., 2000). In mung bean, the expression of *VR-ACO1* can be stimulated by ethylene treatment, but if staurosporine (an inhibitor of protein kinase) is added,

this ethylene-induced effect is repressed. When okadaic acid is applied to mung bean alone, no changes in *VR-ACO1* expression are observed but when ethylene is added, the increase in *VR-ACO1* expression is not as marked. This suggests that the ethylene signal transduction may be tightly coupled to protein phosphorylation/ de-phosphorylation and that this affects the feedback regulation by ethylene on its own biosynthesis pathway (Kim et al., 1997).

1.4.3. Analysis of the ACO gene promoter

To obtain further information on the regulation of ACO gene expression *in vivo,* there have been studies in which ACO promoter sequences have been analysed. In general, these have involved the use of promoter: reporter gene fusions and the use of plant transgenic backgrounds. In tomato, *LE-ACO1* is the major gene expressed during ripening, leaf senescence, and in response to wounding (Barry et al., 1996). Using deletion assays from the 5'end, these authors determined that a short sequence (124 bp) of the *LE-ACO1* promoter can direct a basal level of tissue-specific expression (eg. fruit-ripening-specific), but responses to the other stimuli are lost. In contrast, two other promoter constructs (396 bp, designated as p396 and 1825 bp, designated as p1825) did direct more intense expression in tissues and did respond to different stimuli. Both of the two longer promoter constructs (p396 and p1825) also displayed different expression patterns in response to stimuli. For example, when treated with ethylene, the p396 construct directed twice the expression when compared with the p1825 construct in mature green fruit, but in leaf tissues, the expression patterns directed from both promoters is similar. In response to methyl jasmonate treatment, the p396 construct directed significantly higher expression when compared with the p1825 construct, but in response to powdery mildew infection, the differences in the level of expression was reversed. Further, the p396 construct directed two-fold more expression when compared with the p1825 construct in senescent leaves and in the petiole abscission zone (Blume and Grierson, 1997). These results demonstrate that ACC oxidase is regulated at the transcriptional level, and that

different regions of the promoter provide domains for different stimuli to regulate ACO gene expression. Further individual domains can interact with other domains to form complex regulatory mechanisms (Blume and Grierson, 1997).

The apple *AP4-ACO* gene promoter has also been studied through a series of 5′ deletions fused to the GUS reporter gene, followed by transformation into tomato. The results from this heterologous expression system reveals that the shorter promoter construct (450 bp) directs a basal fruit tissue-specific pattern, but without the ripening developmental pattern. However, two longer promoter constructs (1159 bp and 1966 bp) did both direct tissue- and ripening-specific expression. Of interest is that the shorter promoter sequence (1159 bp) contains an *agamous* (AG) binding site which is involved in floral tissue developmental identity. The 1996 bp sequence contains two potential ethylene response elements (EREs) which are found in many ethylene response gene promoters. Therefore, the *AP4* promoter has at least 3 major regions: one related to tissue-specific regulation, one related to ripening-specific expression, and the third related to ethylene responses (Atkinson et al., 1998). This implies that regulation of the ripening process, tissue-specificity, and the ethylene response are all directed by different binding factors. In other studies on ACO gene promoters using transgenic approaches, the promoters from two ACO genes of melon, *CM-ACO1* and *CM-ACO3*, were each fused with the GUS reporter gene and transformed into tobacco. The results showed that p*CM-ACO1* driven GUS activity increased sharply with the onset of leaf chlorophyll breakdown, but did not drive expression in floral tissues, whereas GUS driven from the p*CM-ACO3* was highly expressed in mature green leaves and declined at the onset of senescence. Further, dense GUS staining was apparent in most floral tissues. This expression pattern is consistent with the expression patterns of the gene family established using northern analysis. When the transgenics were treated with other factors, the results showed that GUS expression driven from the *CM-ACO1* promoter can be induced by ethylene, wounding, and heavy metal ($CuSO_4$) treatment. In each of these, expression was 2 to 3-fold high than

expression directed from the *CM-ACO3* promoter. For auxin treatment, both promoter constructs did not show any response, but when infected with pathogens, the *CM-ACO1* promoter was activated rapidly, whereas the *CM-ACO3* promoter did not show any response in terms of directing GUS expression. Therefore, the senescence-tissue associated *CM-ACO1* promoter can be activated by a range of stress factors including pathogen infection, whereas the green-tissue-associated *CM-ACO3* promoter only has a basal response to stress and can not be activated by pathogen infection. The reason for these patterns of activation maybe due to the promoter sequence structure. In the *CM-ACO1* promoter, two EREs, seven wounding-response-element (WUNs), two drought response elements (DREs) and three elictor response elements (designated PI, ELI and BRE) can be identified. In contrast, the *CM-ACO3* promoter sequence contains seven stigma/style specific elements (SLG13 boxes), two flower-specific Myb binding elements (H-boxes), three drought response elements (DREs) and two heavy metal response element (MTREs) (Lasserre et al., 1997). These observations imply that the tissue-specific and response-specific regulation patterns may depend on the transcription factor domains within each promoter sequence.

Similar experiments have also been applied to the peach ACO family. In these, the *PP-ACO1* and *PP-ACO2* promoters have been isolated, fused to the GUS gene and both constructs transformed into a heterologous host, tomato. The results showed that the GUS expression driven from the *PP-ACO1* promoter was observed throughout most developmental stages of the leaf, whereas GUS expression driven by the *PP-ACO2* promoter was only observed in senescent leaf tissue, and at a lower level when compared with *PP-ACO1* at the same developmental stage. The *PP-ACO1* promoter can also drive expression in mature green fruit tissues, and increased GUS activity is observed during the initial ripening stage, while the *PP-ACO2* promoter directed only very low expression in fruit tissues. When transgenic plants were wounded or treated with ethylene, the *PP-ACO1* promoter was activated in senescent leaf tissues and in fruit at the immature stage, whereas the *PP-ACO2* promoter did not drive

any increase in expression in leaves and fruits: in fact a slight decrease in GUS activity was observed. Of interest are observations in the abscission zones of fruits and leaves. In these tissues, both promoters can drive equal levels of expression, but neither respond to an ethylene stimulus (Rasori et al., 2003). Variable lengths of promoter also showed GUS expression difference among tissues. In a 403 bp *PP-ACO1* promoter::GUS construct, GUS expression was detected in tomato fruit, but not in other tissues. If a 901 bp region was used, more GUS staining was observed in the fruit, and a 2141 bp construct can drive GUS expression in fruit from the green stage to the mature stage (Moon and Callahan, 2004).

In a more detailed analysis of each promoter, the *PP-ACO1* promoter sequence has been examined for possible transcription factor binding domains and one primary ethylene response element (PERE), a secondary ethylene response element (SERE), one putative repressor region (N-), an enhancer element (CATT-box) and two auxin response elements (AUX-re) have been identified. Further, these authors also undertook 5′ deletion assays in combination with transient expression assays in peach fruit tissue. The results revealed that in ethylene-treated fruit tissues, GUS activity can be induced from the full length promoter sequence, but once the AUX-re and CATT-boxes are deleted, activity was reduced significantly to only 33 % of the full-length sequence. In contrast, if the SERE and N- elements are deleted, GUS activity was slightly increased constitutively, but there was no increase in response to ethylene treatment (Rasori et al., 2003). This suggests that *PP-ACO1* gene expression is tightly linked to the ethylene response factors, and other transcription factors which are derived from different signals.

Together, these promoter analyses with expression *in vivo* using transgenic plants reveals that the expression of ACO multi-gene families in plants is controlled mainly at the transcriptional level. The function and the nature of transcription factor binding domains necessary for tissue-specific expression is still not clear, but for those stress factors (eg. pathogen infection , wounding) and the other hormones response factors (eg. IAA, ethylene), the identification of

their binding elements is becoming more reliable.

1.5 ACC oxidase gene studies in white clover

In pastures, white clover (*Trifolium repens* L.) is one of the most economically important agronomic species among the 200 to 300 species that comprise the genus *Trifolium*, and is considered the most important pasture legume in many temperate climates throughout the world (Baker and Williams, 1987). In New Zealand, it is grown in mixed swards with rye grass (*Lolium perenne*) and as the clover provides fixed nitrogen to the pasture ecosystem, the mixed sward is considered to provide a high quality feed for livestock (Brougham et al., 1978).

White clover has a stoloniferous growth habit, with the basic structure of the stolon comprising of a series of internodes separating the nodes which form as a result of growth at the apical bud. Each node contains a long petiole which supports the trifoliate leaf, two root primordia, and an axillary bud as the basic structure. The uppermost root primordium is normally dormant when compared with the lower one, whereas the lower primordium can give rise to a fibrous root in moist conditions. The axillary bud from each node is also normally in the dormant state, but during development and in response to some environmental cues, the bud can differentiate into an inflorescence structure or produce another lateral stolon. The trifoliate leaf is comprised of three leaf blades, each supported by a small petiolule, that acts as a pulvinus, and connects the leaf blade to the petiole. These trifoliate leaf blades have nastic movements that follow a diurnal cycle to fold and un-fold the leaves (Baker and Williams, 1987). The growth of the stolon is indeterminate, but normally during spring time, many stolons senesce and fragment to produce a higher proportion of plants with first order branching (Hay et al., 1989). In summer, plants often possess up to six orders of branching from the initial main stolon (Brock et al., 1988).

Carbohydrate is the major storage form of carbon, which is stored in the stolon. The

carbohydrate is produced primarily in the leaves, but is also reallocated from older stolon fragments to the apical tissues and younger stolon tissues (Chapman and Robson, 1992). During senescence of old tissues, the stolon tissues and the older leaves change from being a reservoir of carbohydrate to exporters of carbon. This reallocation process can be initiated by a variety of environmental cues, including shading, drought, pathogen infection or nutrient deficiency (Thomas and Stoddart, 1980). During normal development, and without other stimuli, leaf senescence is regulated in an age-dependent manner (Lohman et al., 1994). Therefore, leaf senescence is a highly regulated developmental phase where degraded macromolecules are mobilized to young, developing or storage tissues (Buchanan Wollaston, 1997). This developmental change also may be important in preventing the maintenance of a leaf past its useful role of supplying carbohydrate to the distant apical tissues (Bleecker and Patterson, 1997). This also implies that senescence of leaves and stolons is a key factor in the persistence of white clover in pastures.

The white clover stoloniferous growth pattern, therefore, provides a good model system for studying leaf ontogeny in which leaves at different developmental stages from initiation at the apex, to mature-green to senescence and then necrosis can be excised from the same stolon. The use of this system is also useful in providing genetically identical tissues through the vegetative propagation of stolon material in the glasshouse.

Several studies have used this sequential nature of white clover stolon growth to analyse ethylene biosynthesis and physiology in relation to leaf ontogeny. Firstly, the ethylene produced from white clover has been characterized during leaf ontogeny (Butcher et al., 1996). High ethylene production is observed at the apex which then declines as the chlorophyll concentration starts to increase. In node numbers 3 to 9, the leaves are expanding and the chlorophyll content increases but ethylene production is at a consistently low level. After the leaf is fully expanded and the onset of senescence is observed, the chlorophyll content starts to decline, but the ethylene evolution increases (Butcher et al., 1996; Hunter,

1998). This increase in ethylene evolution maybe due to the increased activity of the ACC-mediated biosynthetic pathway (Butcher et al., 1996). After this physiological characterization, three ACC oxidase cDNAs have been isolated and cloned from white clover leaf tissues, and designated as *TR-ACO1*, *TR-ACO2*, and *TR-ACO3* (Hunter, 1998; Yoo, 1999) The expression of *TR-ACO1* is predominantly in the apical tissues, *TR-ACO2* expression is mainly in the green leaf tissues, with highest expression in newly initiated leaf tissues, and *TR-ACO3* expression is initiated in newly senescent leaf tissues and increases with leaf yellowing and then declines at leaf necrosis (Hunter et al., 1999). Southern blot analysis, using the *TR-ACO3* coding sequence as a probe detected two copies of the gene, but when using 3′ UTR sequences as a probe only a subset of fragments were recognized, suggesting that a fourth ACO gene may exist that has identity to the reading frame of *TR-ACO3*, but a distinct 3′-UTR region. In further experiments, it has been shown that *TR-ACO2* expression is induced by ethylene, and is negatively regulated by ageing, In contrast, *TR-ACO3* expression can be induced by wounding and ageing but expression of the gene is not induced by ethylene (Hunter, 1998; Yoo, 1999).

1.6 Research aims

In this study, the focus was mainly on the extension of studies that examined the three ACO genes of white clover. The aim was to initiate the understanding of factors that regulate the developmental-stage-specific expression of this gene family during leaf ontogeny. Therefore, the specific objectives of this thesis were:

I. To isolate the promoter sequences corresponding to *TR-ACO1*, *TR-ACO2* and *TR-ACO3*.

II. To analyze each promoter sequence using bioinformatic approaches to identify any candidate transcription factor binding domains.

III. To construct p*TR-ACO::GUS* reporter gene fusions and express these in a heterologous

host, tobacco, and in white clover to determine the tissue-specific nature of promoter-directed GUS expression.

Chapter 2 Materials and Methods

2.1 Plant material

White clover (*Trifolium repens* L.) genotype 10F of cultivar Grasslands Challenge (AgResearch Grasslands, Palmerston North, NZ) was used for most wild-type experimental analysis in this study (Figure 2.1). The plants were propagated in horticultural grade bark/peat/ pumice (50:30:20) (Dalton Nursery Mix, Tauranga, NZ) with potting mix nutrients [dolomite (3 g/L), agricultural lime (3 g/L), iron sulphate (0.5 g/L), osmocote (5 g/L)] added, and the plants grown in temperature-controlled greenhouses (Plant Growth Unit, Massey University, Palmerston North, NZ). The temperature was set at a minimum of 12°C during the night, 20°C during the day, and with venting when the temperature reached 25°C. Plants were watered at 10 am and 5 pm for 5 min each using a time-controlled dropped watering system (Automation Services Ltd., Auckland, NZ). Aphids and whitefly were controlled by spraying with the insecticide Attack® (Crop Care Holdings Ltd., Richmond, Nelson, NZ).

2.2 Chlorophyll quantification

Leaf tissue was excised free from the leaf midrib, ground in liquid nitrogen and 50 to 200 mg aliquots mixed with 1 mL of dimethylformamide (DMF). The mixture was then incubated at 4°C for 48 h in the dark, the sample was mixed vigorously by vortexing and the cellular debris pelleted by centrifugation at 20 800 x g for 5 min. An aliquot (100μL) of supernatant was then mixed with 900 μL of DMF in a fresh tube, the diluted solution then placed into a 1 mL glass cuvette and the absorbance at 647 nm and 665 nm determined using a spectrophotometer (LKB Novaspec®II, Pharmacia, Biochrom Ltd. Cambridge, UK). The chlorophyll concentration was calculated using the following formula:

Chlorophyll a = $12.7\ A_{665} - 2.79\ A_{647}$ (mg/mL)

Chlorophyll b = $20.7\ A_{647} - 4.62\ A_{665}$ (mg/mL)

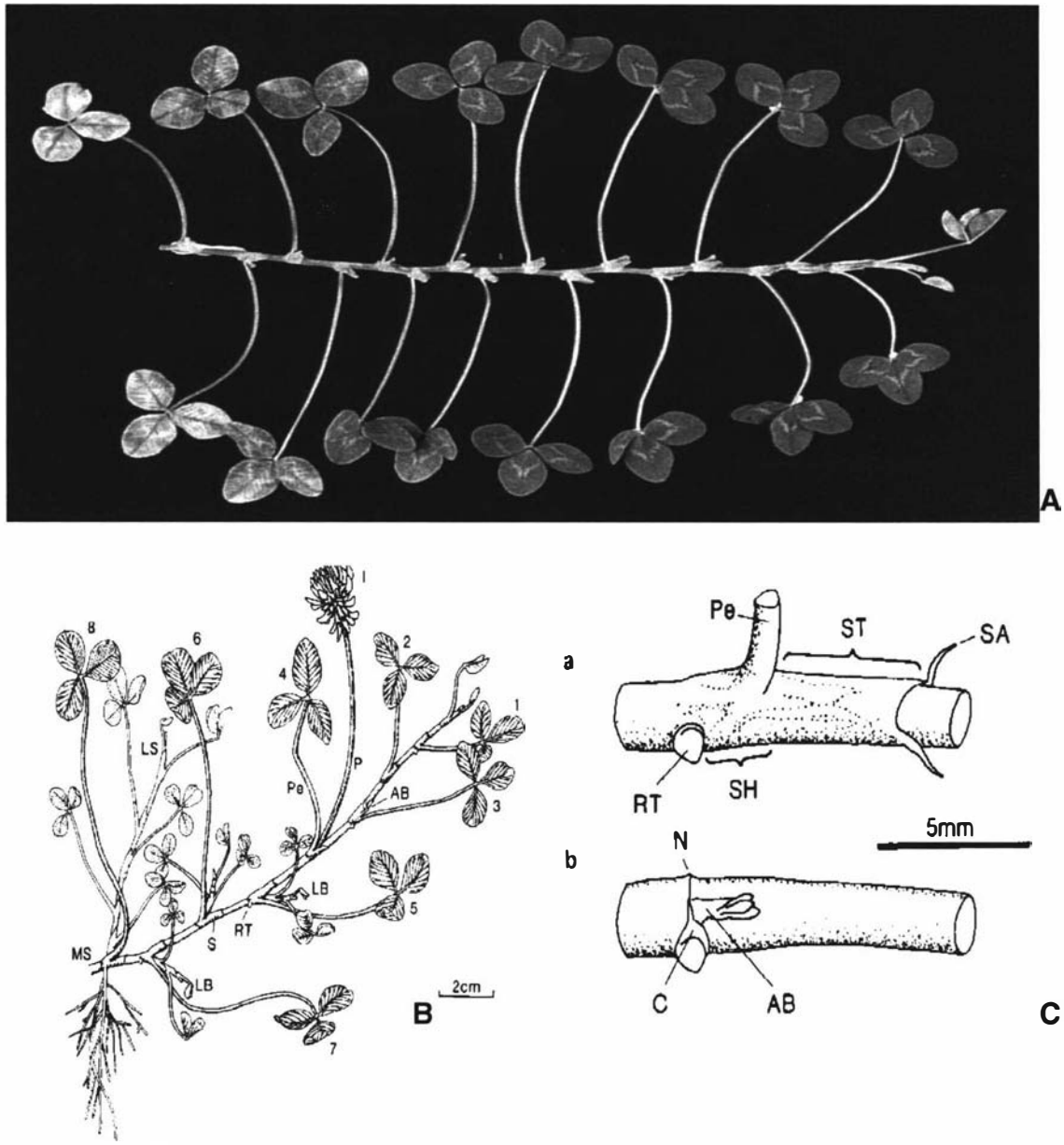

Figure 2.1 White clover plant material and tissue structures

A An individual stolon comprising leaf tissue at different developmental stages

B Diagrammatic representation of the structure of a stolon of white clover (from Baker et al., 1987)

C Diagrammatic representation of the structure of a node (from Baker et al., 1987)

MS= main stolon, AB= axillary bud, LB= lateral branches, LS= lateral stolons, S= stipule, Pe, petiole, RT, nodal root primordium, I= inflorescence, P= peduncle, ST= stipular tube, N= node, SA= stipule apex, SH= leaf sheath. The numbers represent the node number.

Total Chlorophyll = $17.9\,A_{647} - 8.08\,A_{665}$ (mg/mL)

2.3 Chemicals

Unless otherwise stated, the chemical regents used were analytical grade, obtained from either BDH Laboratory Supplies (Pool, Dorset, England), or Sigma-Aldrich Chemical Company (St. Louis, Mo., USA). The laboratory supply of purified water used for making solutions was itself produced by reverse-osmosis (RO), followed by microfitration (Milli-Q, Millipore Crop., Bedford, MA, USA).

2.4 Isolation of genomic DNA

Genomic DNA was isolated either using the Nucleon PhytoPure™ kit (Amersham Pharmacia Biotech, Piscataway, NJ, USA), or by a modified method of Junghans and Metzlaff, (1990). For the kit method, approximately 0.1 g of fresh or frozen young leaf tissue was ground to a powder in a pre-chilled mortar containing liquid nitrogen. The powder was transferred into a 2-mL capacity centrifuge tube, and was mixed thoroughly in 600 μL of Reagent-1 (Nucleon PhytoPure™). Following the addition of 200 μL of Reagent-2 (Nucleon PhytoPure™), the mixture was inverted several times until a homogeneous suspension was obtained. The mixture was then incubated at 65°C for 10 min, with gentle agitation, and then on ice for 20 min, after which a 500 μL aliquot of pre-chilled (-20°C) chloroform and 100 μL of DNA extraction resin suspension (Nucleon PhytoPure™) were added to the mixture. After shaking end-over-end for 10 min, the mixture was centrifuged at 1300 x g for 10 min at 4°C, and the upper (DNA-containing) phase transferred to a fresh centrifuge tube. The nucleic acid was precipitated by the addition of an equal volume of ice-cold isopropanol, and then collected by centrifugation at 20 800 x g for 5 min. The pellet was washed with 1 ml of ice cold 70 % (v/v) ethanol and again centrifuged at 20 800 x g for 5 min to pellet the DNA. Finally, the pellet was air dried for 10 min, and resuspended in 100 μL of sterile water.

For the modified Junghans and Metzlaff (1990) method, approximately 1.5 g of fresh or frozen leaf tissue was ground to a powder in a pre-cooled mortar containing liquid nitrogen. The powder was thawed in 10 mL of lysis buffer (50 mM Tris-HCl, pH 7.6, 100 mM NaCl, 50 mM EDTA, 0.5 % (w/v) SDS) and 10 mL of Tris-buffer phenol (6 mL of 1 M Tris-HCl (pH 8.0), 130 mL H_2O, 500 g commercial phenol crystals, adjust to pH 7.5 by using 2M NaOH) and the mixture shaken vigorously for 3 min. Five mL of chloroform : isoamyl alcohol (24 : 1) was added and after shaking for another 3 min, the cellular debris was pelleted by centrifugation at 26 000 x g for 10 min at 4°C, The aqueous phase was transferred to a new centrifuge tube containing 5 mL of Tris-buffered phenol and shaken for 3 min. A further 5 mL of chloroform : isoamyl alcohol (24 : 1) was added and the mixture shaken again for 3 min, the aqueous and organic phases separated by centrifugation (26 000 x g for 10 min, 4°C), and the aqueous phase was then transferred to 10 mL of chloroform : isoamyl alcohol (24 : 1) and shaken for a further 3 min. The aqueous phase was again separated by centrifugation, transferred to a new tube and cold isopropanol (0.67 volumes) added and the mixture gently inverted to precipitate the nucleic acid, which was then pelleted by centrifugation at 26 000 x g for 10 min. The pellet was then rinsed with 80 % (v/v) ethanol, air-dried, re-suspended in 4 mL TES/RNase solution (10 mM Tris-HCl, pH 8.0, 100 mM NaCl, 1 mM EDTA, 5 μL RNase A (10 mg/ml)) and was incubated at 37°C for 20 min. After the addition of 2 mL of Tris-buffered phenol, the mixture was shaken for 3 min, two mL of chloroform : isoamyl alcohol (24:1) added and the solution shaken for further 3 min. The aqueous phase was separated by centrifugation, transferred to 4 mL of chloroform : isoamyl alcohol (24: 1), shaken for 3 min, the centrifugation repeated and the aqueous phase transferred to a new tube and the nucleic acid precipitated with ethanol (section 2.10.3). The pellet was re-suspended in 500 μL of 0.25 M NaCl and 0.35 volumes of 100 % (v/v) ice-cold ethanol was slowly added to the tube. The precipitate was incubated on ice for 15 min, centrifuged (20 800 x g for 5 min at 4°C) and the supernatant transferred to new tube, ethanol

precipitated, and the DNA resuspended in sterile water.

2.5 Digestion of genomic DNA

Digestion of genomic DNA was undertaken using one of two methods, depending on the application. For digestion to make the GenomeWalk™ libraries, an aliquot (2.5 μg/μL) of genomic DNA was mixed with 8 μL of blunt end restriction enzyme [*Dra* I (10 unit/μL), *Eco* RV (10 unit/μL), *Pvu* II (10 unit/μL), *Stu* I (10 unit/μL), *Sma* I (10 unit/μL) or *Nae* I (10 unit/μL) (Roche Diagnostics, IN, USA)], 10 μL of 10 X restriction enzyme buffer (Roche, Mannheim, Germany) and then made up to 100 μL with Milli-Q water. The mixture was gently inverted several times and incubated for 2 h at 37°C. The reaction was then gently vortexed and incubated at 37°C for 16-18 h.

For Southern analysis, genomic DNA was digested with three restriction endonuclease enzymes (*Eco* RI, *Xba* I, and *Bam* HI for wild type plants, and *Eco* RI, *Bam* HI, and *Hin*d III were used for transgenic plants). Each digest mixture consisted of 30 μg of DNA, 80 U of restriction enzyme, 20 μL of 10 X restriction buffer and sterile water added to 200 μL. After mixing, the digested reactions were incubated at 37°C overnight, after which, another 30 μL of restrction enzymes with 10 μL of 10 X restriction buffer and 60 μL of sterile water was added. The reaction mixtures were incubated for a further 3 h at 37°C, the DNA precipitated with either ethanol or isopropanol (section 2.10.3), re-suspended in 20 μL of sterile water, and mixed with 1/10 volume of 10 X SUDE (0.1 M EDTA, pH 8.0, 50 % (v/v) glycerol, 1 % (w/v) SDS, 0.025 % (w/v) bromophenol blue) resolution by agarose gel electrophoresis (section 2.10.1).

2.6 Purification of digested genomic DNA

After restriction enzyme incubation, an equal volume of Tris-buffered phenol was added to the DNA and the mixture vortexed gently. After centrifugation at 20 800 x g for 5 min to separate the aqueous and organic phases, the upper (DNA-containing) phase was then

transferred to a fresh tube, and an equal volume of chloroform added. After vortexing and centrifugation (5 min, 20 800 x g), the upper (DNA-containing) phase was transferred to fresh tube, and two volumes of ice-cold 95 % (v/v) ethanol, 1/10 volume of NaOAc (3 M, pH 4.5) and 20 μg of glycogen were added. Following vortexing and centrifugation for 10 min at 20,800 x g, the supernatant was decanted and the pellet was washed in 100 μL of ice-cold 80% (v/v) ethanol. The pellet was centrifuged for a further 5 min at 20 800 x g, the resultant supernatant decanted, and the pellet air dried for 30 min. The purified genomic DNA was then resuspended in 20 μL of TE buffer (10 mM Tris, 0.1 mM EDTA, pH 7.5).

2.7 Ligation of genomic DNA with adaptors

Four μL of digested genomic DNA (0.1μg/μL; section 2.6), 1.9 μL of GenomeWalker™ adaptor (25 μM, Clontech, Palo Alto, CA, USA) (Figure 2.2), and 1.6 μL of 10 X ligation buffer (Clonetech) were placed in a 0.2 mL tube. The reaction was mixed by gently vortexing for 10 sec, 0.5 μL of T4 DNA ligase (6 U/μL, Clonetech) was added and mixed and the mixture incubated at 16°C, overnight. The reaction was then stopped by incubation at 70°C for 5 min, and the mixture diluted to 80 μL with TE buffer.

2.8 PCR methods

2.8.1. Primary PCR

The sequences of each gene-specific primer and the adaptor primer for primary PCR for promoter isolation using the Genome Walker™ method are shown as Figure 2.2. The gene-specific primers (Sigma) were dissolved in sterile water to give a final concentration of 1 mM and stored at -20°C. For working stocks, the concentration of the primer was adjusted to 10 μM. Each PCR reaction contained 37.8 μL of Milli-Q water, 5 μL of 10 X *Tth* PCR Reaction buffer (Clontech), 1 μL of dNTP (10 mM each of dATP; dTTP; dGTP; dCTP, (Roche)), 2.2 μL of $Mg(OAc)_2$ (25 mM), 1μL of adaptor primer-1 (10 μM, Clontech), 1 μL of

Adaptor Sequence

5'-GTAATACGACTCACTATAGGGCACGCGTGGTCGACGGCCCGGGCTGGT-3'

3'--**H_2N**– CCCGACCA-PO_4-5'

Adaptor Primers

AP1 = 5'—GTAATACGACTCACTATAGGGC—3'
(first round adaptor primer 1)

AP2 = 5'—ACTATAGGGCACGCGTGGT—3'
(second round nested adaptor primer 2)

First round gene specific primers

GW-TR1- R1 = 5'—GGAAGATGGCGCAAAAAGAAAGTGCTTTCC—3'
(specific sequence in *TR-ACO1*)

GW-TR-2+3-CON-R1 = 5'--TCC CAR TCC ATR TCT TTG ACC TCA GTT TG—3'
(specific conserving sequence in *TR-ACO2* and *TR-ACO3*)

Second round gene specific primers

GW-TR1-R2 = 5'— ACTGAACACACTCCAAACCTTTGCTTGAAACC—3'
(specific sequence in *TR-ACO1*)

GW-TR-2–R2 = 5'-- GTTGGCCACCAAATCCTTGAATCTTTGTTC—3'
(specific sequence in *TR-ACO2*)

GW-TR-3–R2 = 5'-- GACCTAGAATATGAATGTGGAACC—3'
(specific sequence in *TR-ACO3*)

Figure 2.2 Sequence of the adaptor and the primers for promoter isolation using the Genome Walker™ method

gene specific primer-1 (10 μM) and 1 μL of *Tth* DNA polymerase (5 unit/μL, Promega, Madison, WI, USA). The reaction was mixed well, 1 μL of genomic library DNA with adaptor, (section 2.7) was then added, the mixture briefly centrifuged for 5 sec.

The tubes were placed in the Peltier Thermal Cycler (PTC-200; MJ Research Inc., Watertown, MA, USA), and two-step cycle parameters were programmed for: 7 cycles of 94°C for 25 sec; 72°C for 3 min; 32 cycles of 94°C for 25 sec; 67°C for 3 min, and 7 min at 67°C.

2.8.2. Secondary PCR

The sequences of each gene-specific primer and the adaptor primer for secondary PCR are shown as Figure 2.2. Each PCR reaction contained 37.8 μL of Milli-Q water, 5 μL of 10 X *Tth* PCR Reaction buffer (Clontech), 1 μL of dNTP (10 mM each of dATP; dTTP; dGTP; dCTP, Roche), 2.2 μL of $Mg(OAc)_2$ (25 mM), 1μL of adaptor primer-2 (10 μM, Clontech), 1 μL of gene specific primer-2 (10 μM) and 1 μL of *Tth* DNA polymerase (5 unit/μL, Promega). After mixing, 1.0 μL of 50-fold diluted primary PCR product (section 2.8.1) was added, the mixture briefly spun for 5 sec, and then each tube was placed in a PTC-200 (Peltier Thermal Cycler) and the PCR reaction carried out using the following two-step cycle parameter: 5 cycles of 94°C for 25 sec; 72°C for 3 min; 20 cycles of 94°C for 25 sec; 67°C for 3 min, and 7 min at 67°C.

2.9 RT-PCR assay

2.9.1. RNA isolation

Fresh leaves were harvested and powdered with liquid N_2 in a pre-baked mortar (180°C, 6 h). One mL of TRI-REAGENT® (Cincinnati, OH, USA) was mixed with every 0.1 g of leaf tissue powder and the mixture vortexed vigorously for 1 min until it became homogenised. The sample was then incubated at room temperature for 5 min, after which 0.2 mL chloroform was added, the mixture shaken vigorously for 15 sec, and then incubated for a

further 15 min at room temperature. After centrifugation at 12 000 x g for 15 min at 4°C, the upper aqueous phase was transferred to a fresh tube and mixed with 0.8 volumes (v/v) of isopropanol. After incubating the mixture at room temperature for 10 min, the RNA was pelleted by centrifugation at 12 000 x g at 4°C for 8 min, the supernatant removed and the pellet washed twice with 1 mL of 75 % (v/v) ethanol. After removing the trace ethanol and air drying the pellet, the RNA was dissolved in 50 µL of diethyl pyrocarbonate (DEPC) (Sigma) treated water at 55°C for 15 min, and stored at -20°C until required.

2.9.2. Reverse transcriptase synthesis of cDNA

The extracted RNA (1 µg) was mixed with 2 µL of the appropriate primers at a concentration of 10 mM, and the volume then made to 10 µL with DEPC treated water. The mixture was then incubated at 70°C for 10 min, subsequently placed on ice for 5 min, and then the following components added: 4 µL of 5 X expand reverse transcriptase buffer (Roche), 2 µL of 100 mM DTT, 2 µL of 10 mM dNTP mixture (Roche), and 0.5 µL of RNase inhibitor (40 U/µL, Roche). After mixing well and incubating at 42°C for 2 min, 1 µL of expand reverse transcriptase (50 U/µL, Roche) was added and the mixture was incubated for a further 1 h at 42°C. The cDNA was placed on ice to stop the reaction, and was then used immediately for PCR (section 2.9.3) or stored at -20°C.

2.9.3. PCR amplification of cDNA

The first round of PCR used 5 µL of the cDNA (synthesized as described in section 2.9.2) mixed with 25 µL of PCR master mixture (Promega), 2 µL each of 10 mM primers and then water added to make a final volume of 50 µL. The reaction was set to the following parameters: one cycle at 94°C for 2 min; 35 cycles at 94°C for 45 sec; 45°C for 1 min, 72°C for 30 sec; and 72°C for 3 min and stop reaction at 4°C. The second round PCR reaction used 2 µL of the first round PCR products as template with the other reactants and PCR programme the same as used for the first round.

2.10 DNA cloning procedures

2.10.1. Electrophoresis of DNA

Agarose gels (0.7 % to 1.2 % (w/v)) were prepared by dissolving agarose (UltraPure™ agarose, GIBCO BRL, Grand Island, NY, USA) in 1 X TAE buffer (20 X TAE: 0.8 M Tris, 0.4 M glacial acetic acid, 20 mM EDTA, pH 8.0), and pouring the molten agarose solution into either a horizontal DNA Mini Sub Cell™ (70 cm^2 gel bed, Bio-Rad Laboratory, Hercules, CA, USA) for general applications or a horizontal DNA Sub Cell™ (225 cm^2 gel bed, Bio-Rad) for Southern blot analysis. The DNA samples, including molecular size markers (1 Kb Plus DNA ladder, Invitrogen, Carlsbad, CA, USA), were mixed with a 0.1 volume of 10 X SUDS and loaded into the pre-formed wells. The samples were separated by electrophoresis in 1 x TAE, at 100 volts for 1 to 3 hr. For general applications, gels were stained with 0.1 μg mL^{-1} of ethidium bromide for 10 min before being visualized on a short wavelength (340 nm) UV transilluminator (UVP inc., San Gabriel, CA, USA), and digitally photographed with the Alpha imager™ 2000 Documentation and Analysis System (Alpha Innotech Corporation, San Leandro, CA, USA). After electrophoresis of DNA fragments for Southern analysis, the gel was processed further (section 2.12.1).

2.10.2. DNA recovery from agarose gels

After agarose electrophoresis, DNA fragments of interest were excised under long-wave UV light using a sterile scalpel blade. The excised gel piece was then placed in a 1.5 mL tube, weighed and thirty μL of gel solubilization buffer (CONCERT™ Gel Extraction Systems; GIBCO BRL) added. The mixture was then incubated at 50°C for 15 min, with shaking every 3 min for 5 sec, and once the gel had dissolved, the sample was incubated for a further 5 min. The mixture was transferred to a cartridge (CONCERT™) contained in a 2 mL capacity tube, centrifuged at 12 000 x g for 1 min, the flow-through solution was discarded and another 500 μL of gel solubilization buffer (CONCERT™) added. After centrifugation at 12 000 x g for 1

min, the flow-through was again discarded, 700 µL of wash buffer (CONCERT^{TM}) was then added and the cartridge incubated at room temperature for 5 min. The tube was then centrifuged at 12 000 x g for 1 min, after which the flow-through was discarded, and then centrifuged again for another 1 min to remove residual wash buffer. The cartridge was transferred into a fresh 1.5 mL tube, 50 µL of pre-warm (50°C) TE buffer was then applied directly to the centre of the cartridge, the tube incubated for 1 min, and then centrifuged at 12 000 x g for 2 min.

2.10.3. Precipitation of DNA

Precipitation of nucleic acids was carried out with either ethanol or isopropanol. For ethanol precipitation, 0.1 volumes of 3 M NaOAc and 2.5 volumes of ice-cold 100 % ethanol was added to the DNA solution, the mixture incubated at -20°C for 30 min or 4°C over night, and then centrifuged at 20 800 x g for 20 min at 4°C. The supernatant was discarded and the pellet twice rinsed with 80 % (v/v) ethanol. The residual ethanol was removed with a pipette following collection by a pulse-centrifugation. The pellet was air dried or dried in a heating block at 40°C for 3 min and resuspended in sterile water.

For isopropanol precipitation, 0.6 to 1.0 volumes of ice-cold isopropanol was added to the DNA solution, the mixture gently inverted several times then centrifuged at 20 8000 x g for 5 min. The following wash steps were identical to those described for ethanol precipitation.

2.10.4. DNA quantification

DNA solutions were diluted 50- and 100- fold with water to a total volume of 100 µL. The diluted samples were loaded into a quartz cuvette, and the absorbance measured against a water blank at 260 nm with a 1 cm light path. The absorbances at 260 nm and 280 nm were used to calculate DNA concentration and purity. An absorbance of 1.0 corresponds to approximately 50 µg/ mL of double strand DNA, and the relative purity of nucleotide solution can be gauged by examining the ratio of 260 nm/280 nm. The pure DNA is equal to 1.8

(Sambrook et al., 1989). The formula used for calculating DNA concentration of the sample is as follows:

A_{260} nm x dilute factor x 50 = DNA conc. in μg/ mL

2.10.5. DNA ligation with the T-vector system

The DNA fragments produced by PCR contain a single deoxyadenosine to the 3′ end of the duplex molecule. Therefore, following the recovery of the PCR product from the agarose gel (section 2.10.2), the DNA fragments were ligated into the pGEM®-T Easy™ vector system (Promega)(Figure.2.3). For each ligation reaction, the amount of DNA was in a 3:1 (insert : vector) ratio and the following formula was used:

X ng (DNA) = 3 x (size of insert (kb)) x (50 ng of pGEM vector) / 3.0 kb (vector size)

The insert DNA was added, as calculated, to 5 μL of 2 X T4 DNA ligase buffer (Promega) and pGEM®-T Easy vector (50 ng/μL). One μL of T4 DNA ligase (3 Weiss units/μL)(Promega) was then added and the reaction made up to a final volume of 10 μL with Milli-Q water. The reaction was mixed by pipetting and incubated at 4°C for overnight.

2.10.6. Transformation of *E.coli* competent cells

2.10.6.1 Preparation of competent cells

Cells of the *E.coli* strain DH-5α (GIBCO BRL) were inoculated from glycerol stocks into 10 mL of LB (Luria-Bertani) broth (1 % (w/v) tryptone, 0.5 % (w/v) yeast extract, 1 % (w/v) NaCl, pH 7.5) and incubated overnight at 37°C with shaking at 180 rpm. Four hundred μL of the broth was then transferred to a fresh 40 mL of LB broth and incubated at 37°C, with shaking at 180 rpm, for 2 to 2.5 hr or until the OD_{600} reached 0.4. The cell culture was then transferred to a pre-cooled (4°C) centrifuge tube, centrifuged at 4000 x g for 5 min, the supernatant discarded and 10 ml of ice-cold $CaCl_2$ (60 mM) added to resuspend the pellet through gently vortexing. The mixture was kept on ice for 30 min, centrifuged at 4000 x g for 3 min at 4°C, the supernatant discarded and the pellet was resuspended gently in 4 mL of

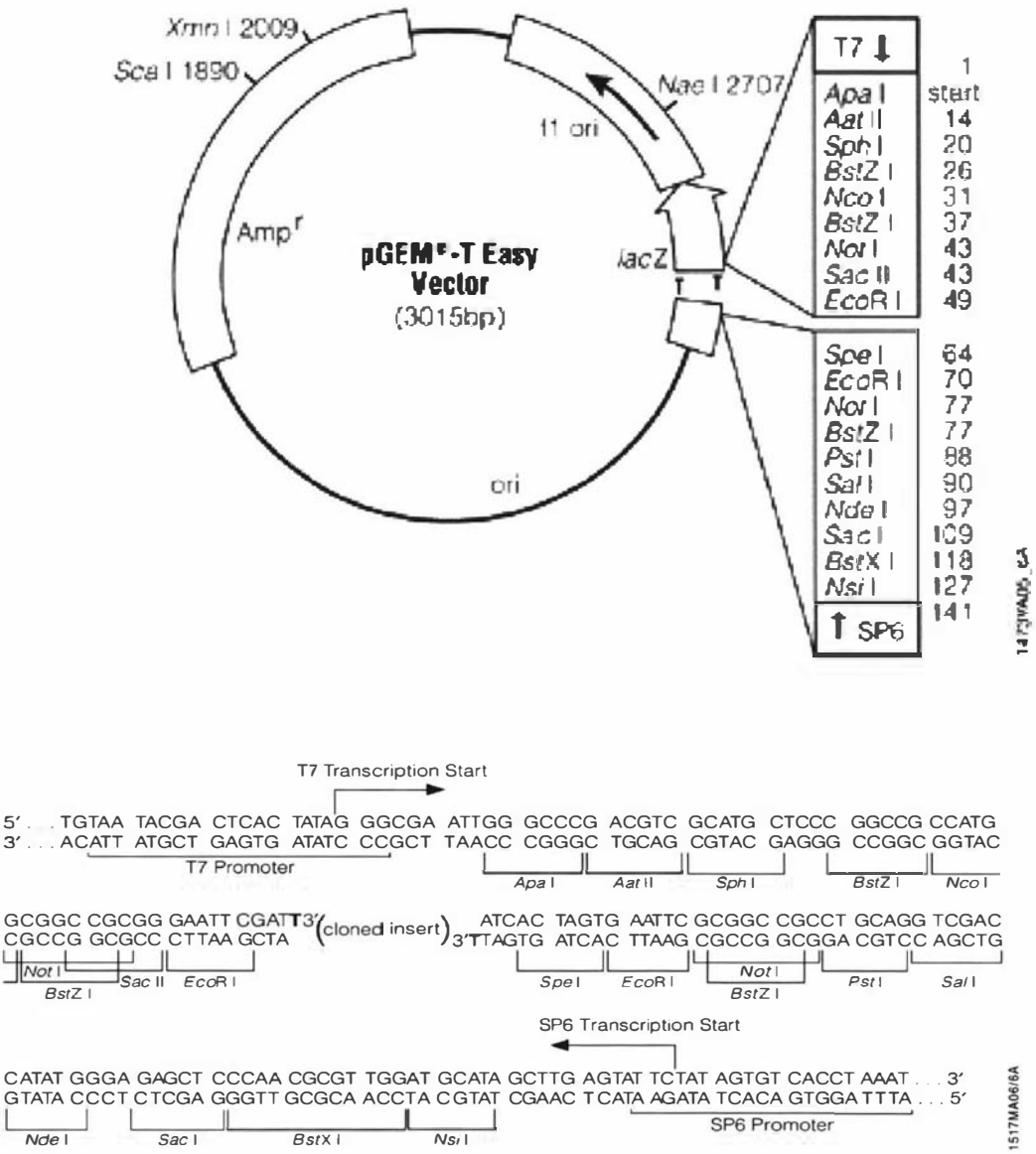

Figure 2.3 Diagram of the pGEM-T-Easy vector used for T-A-cloning of PCR generated sequences

The sequence of the multiple cloning site is shown. The SP6 promoter and T7 promoter sequences used in *in-situ* hybridization assays are also indicated. This figure is reproduced from the pGEM®-T-Easy instruction manual.

$CaCl_2$ (60 mM) containing 15 % (v/v) glycerol. The competent cells were then stored as 300 µL aliquots at -80°C.

2.10.6.2 Transformation using the heat shock method

Aliquots of competent cells were thawed on ice for 5 min, then 50 to 150 µL added to the ligation reaction (section 2.10.5), the suspension gently mixed and then incubated on ice for 20 min. The mixture was then incubated at 42°C for 45-50 sec, immediately placed on ice for 2 min, 950 µL of LB broth added and the cells incubated at 37°C for 2 h with shaking at 180 rpm. Putative transformed cells were then spread onto LB plates (LB broth with 1.5 % (w/v) bacto-agarose) using the appropriate selection (section 2.10.7) and incubated overnight at 37°C.

2.10.7. Selection of transformants

After transformation (section 2.10.6.2), 200 µL of the transformation mixture was transferred to a fresh tube. The remaining broth was spun at 6 500 x g for 1 min and the supernatant discarded. The cell pellets was resuspended with fresh LB broth, and both concentrated and un-diluted cell cultures were spread onto either LB^{AMP100} plates (LB plates with 100 mg L^{-1} ampicillin) for general selection or spread onto $LB^{AMP100/IPTG/X\text{-}Gal}$ plates [LB^{AMP100} plate pre-spread with 100 µL of IPTG (100 mM) and 20 µL of X-Gal (50 mg/mL)] for blue-white selection. The plates were incubated overnight at 37°C, and white colonies were selected and inoculated in 10 mL of LB^{AMP100} broth. The tubes were incubated overnight at 37°C with shaking (180 rpm).

2.10.8. Isolation of plasmids

2.10.8.1 Alkaline lysis miniprep method

After overnight incubation, cell cultures of *E. coli* (section 2.10.7) were pelleted by centrifugation at 3 000 x g for 5 min at room temperature, and the supernatant discarded. The

pellet was resuspended completely in 200 µL of freshly prepared alkaline lysis solution-A (25 mM Tris-HCl, pH 8.0, 50 mM glucose, 10 mM EDTA), and after transferring the resuspended pellet to a fresh 1.5 mL centrifugation tube, the cells were lysed with the addition of 400 µL of freshly prepared alkaline lysis solution-B (0.2 M NaOH, 1 % (w/w) SDS). The contents were mixed by gentle inversion, incubated on ice for 10 min and the contaminating chromosomal DNA and protein was then precipitated by the addition of 300 µL of alkaline lysis solution-C (3 M KOAc, 2 M glacial acetic acid). After the solution was shaken vigorously and incubated on ice for 15 min, the mixture was centrifuged at 20 800 x g for 5 min and 700 µL of supernatant was transferred to a fresh 1.5 mL centrifugation tube. Ice-cold isopropanol (800 µL) was then added to the supernatant, the contents inverted several times, and the precipitated plasmid DNA collected by centrifugation at 20 800 x g for 5 min. The pellet was washed twice with 80 % (v/v) of ethanol, air-dried and then dissolved in 50 µL of sterile water.

2.10.8.2 Column miniprep method

For DNA sequencing purposes, plasmids were isolated using the QIAprep® Miniprep kit (QIAGEN, Valencia, CA, USA). The *E. coli* cell culture (section 2.10.7) was pelleted by centrifugation at 3 000 x g for 5 min, the supernatant discarded and the pellet resuspended in 250 µL of buffer P1 containing RNaseA (QIAGEN), before transfer to 250 µL of buffer P2 (QIAGEN). The suspension was gently inverted 4-6 times in order to lyse the cells, buffer N3 (350 µL) (QIAGEN) was then added to the mixture which was immediately but gently inverted (4-6 times) until the solution became cloudy. After centrifugation at 20 800 x g for 10 min, the supernatant was transferred to a QIAprep column (QIAGEN) contained in a 2-mL capacity collection tube, the assembly centrifuged at 20 800 x g for 1 min and the flow through discarded. The column was then washed with 0.75 mL of buffer PE (QIAGEN) and centrifuged at 20 800 x g for 1 min. After discarding the flow through, the column was

centrifuged for an additional 1 min to remove any residual wash buffer. The cartridge was then placed in a fresh 1.5 mL tube and 50 μL of buffer EB (QIAGEN) was pipetted to the centre. After 1 min incubation at room temperature, the plasmid DNA was collected by centrifugation at 20 800 x g for 1 min.

2.10.9. Restriction digestion of plasmid DNA

Plasmid DNA (0.5 μg) was mixed with 5 units of restriction enzyme (Roche), 0.1 volumes of 10 x restriction buffer (Roche), 10 μg RNaseA (Sigma) and then sterile water added to a total volume of 15 μL. After mixing, the reaction was incubated at 37°C for 2 h, 0.1 volumes of 10 X SUDS loading dye was added and the digested DNA was resolved by electrophoresis (section 2.10.1).

2.10.10. DNA sequencing procedures

2.10.10.1 PCR of terminator dye reaction

The templates for sequencing reactions included plasmid DNA (section 2.10.8), linear DNA recovered from agarose gel (section 2.10.2) or PCR products (section 2.8.2). The requirement of the template from the PCR product was that only one band was produced in the PCR reaction and before sequencing, the products were cleaned up in order to remove RNA and primers. The cleanup reaction consisted of 2μL of SAP (shrimp alkaline phosphatase) (1U/ μL, USB Corp., OH, USA), 1μL of Exo I (exonuclease I)(10U/ μL, USB) and a half-volume (25 μL) of the PCR products. This mixture was incubated at 37°C for 30 min, and the reaction terminated by incubation at 80°C for 15 min. The different types of template also used different amounts of DNA for the terminator dye reaction. For plasmid DNA, the reaction required 0.5~1.0 μg of DNA, but for the gel-excised linear DNA or PCR products, usually 50~100 ng was required for the reaction.

The terminator reaction contained 2 μL of BigDyeTM Terminator (Version 3.1, Applied Biosystems, Foster city, CA, USA), 3 μL of sequencing buffer (Applied Biosystems), 3.2

pmol of the appropriate primer, and the appropriate amount of DNA template, with sterile water added to a total volume of 20 µL. The mixture tube was placed in a Peltier Thermal Cycler (MJ Research Inc.) and a one step reaction programme used as follows: 25 cycles set at 96°C for 10 sec, then rapid thermal ramp (1°C/ sec) to 50°C; 50°C for 5 sec, then rapid thermal ramp (1°C/ sec) to 60°C; 60°C for 4 min. After 25 cycles, the reaction was ended, and held at 4°C until the sequence products were purified further.

2.10.10.2 Precipitation of terminator DNA and automated DNA sequencing

The sequenced DNA after the terminator reaction required precipitation and purification before automated sequencing could be performed. The product of terminator dye reaction (section 2.10.10.1) was precipitated with the addition of 2 µL of EDTA (125 mM), 2 µL of NaOAc (3 M), and 50 µL of 100 % (v/v) ethanol. The mixture was inverted 5 times, incubated at room temperature for 15 min, and then centrifuged (20 800 x g) at 4°C for 25 min. The supernatant was removed immediately and the pellet was washed twice with 70 µL of 70 % (v/v) ethanol and then collected by centrifugation at 4°C at 20 800 x g for 5 min. After the supernatant was removed, pellet was air dried and the sample submitted to the Allan Wilson Centre, Institute of Molecular BioSciences, Massey University, Palmerston North, NZ for automated sequencing using ABI PRISM® BigDye™ Terminator Cycle Sequencing (Applied Biosystems).

2.11 Plant transformation and growth

2.11.1. Construction of binary transformation vectors

2.11.1.1 Modification of binary vector system

The binary plant transformation vector used for this study was pRD-410 (Datla et al., 1992) (Figure. 2.4) which was provided by Dr. Derek White, AgResearch, Palmerston North, NZ.

The features of pRD-410 are that it contains a wild type *NPT* II sequence and a cauliflower mosaic virus 35S (CaMV 35S) promoter fused with the *E.coli* β-glucuronidase (GUS) reporter gene. Therefore, the first manipulation was to excise the CaMV 35S sequence, and to replace this promoter with the *TR-ACO* promoters.

The pRD-410 vectors were transformed into *E.coli* competent cells (DH-5α strain) (section 2.10.6), and then the positively selected (section 2.10.7) cells were inoculated into LB^{AMP100} broth and incubated at 37°C for 24 h. Plasmid DNA was isolated using the alkaline lysis miniprep method (section 2.10.8.1), and after DNA quantification, 30 μg of plasmid DNA was mixed with 20 units of *Bam* HI and *Hind* III (Roche), 0.1 volumes of 10 x restriction buffer B (Roche), 30 μg RNaseA (Sigma) and sterile water added to make a total volume of 100 μL. The reaction was incubated at 37°C for 5 h, 0.1 volumes of 10 X SUDS loading dye was then added and the digested plasmid was resolved by electrophoresis (section 2.10.1). Bands of interest in the agarose gel were excised, and the DNA fragments were recovered through column method (section 2.10.2).

2.11.1.2 Modification of promoter sequences by the PCR method

To insert sequences of interest into the linear and modified pRD-410 vector that contains sticky compatible for both *Bam* HI and *Hin*d III (section 2.11.1.1), promoter sequences were re-amplified by PCR. The *Hin*d III sequence and six bp of non-sense nucleotides were added to the 5′ end of the reverse primers, while the *Bam* HI sequence and another six bp of non-sense nucleotides were added before the 5′ end of forward primer sequence (Figure 2.5). One μL (50 ng/μL) of each promoter sequence in the $pGEM\text{-}T^{\text{-EASY}}$ vectors (section 2.10.5) was used as a template. The final reaction contained the template, 25 μl of PCR master mixture solution (Promega), 22 μL of Milli-Q water and 1μL each of the forward and reverse primers (10 μM) (Figure 2.5). The PCR reaction programme was set for one cycle of

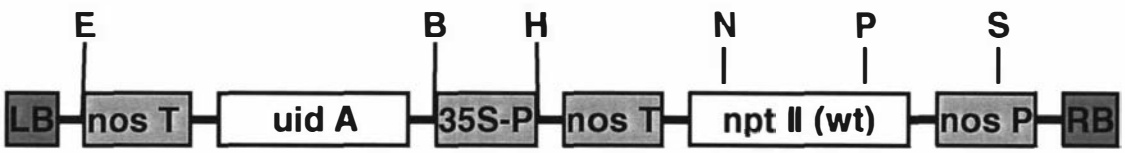

pRD- 410

Figure 2.4 Diagrammatic representation of the pRD-410 vector used for *Agrobacterium* transformation

LB = left border of T-DNA sequence
nos T = nopaline synthase terminator sequence
uid A = GUS coding sequence
35S-P = cauliflower mosaic virus 35S promoter sequence
npt II (wt) = wild type neomycin phosphotransferase II sequence
nos P = nopaline synthase promoter sequence
RB = right border of T-DNA sequence

E = *Eco* RI, **B** = *Bam* HI, **H** = *Hind* III, **N** = *Nco* I, **P** = *Pst* I, **S** = *Sst* II

TR1-Clone-F =5'—*GACGAC***AAGCTT**AAATATTATTCTTACTGCTTATTTTTTTC—3'

TR1-Clone-R = 5'--*GACGAC***GGATCC**TTTGCTTCTTTCAATTTTCT—3'

TR2-Clone-F =5'—*GACGAC***CAGCTG**ACCAGCATCTACCAAAAGTG—3'

TR2-Clone-R = 5'--*GACGAC***GGATCC**ATCTCTCAAACAAACTCTTAAC—3'

TR3-Clone-F =5'—*GACGAC***AAGCTT**AAACTGATCCCACTAACCCAC—3'

TR3-Clone-R = 5'--*GACGAC***GGATCC**AACTTAAACTCAAAGTAACTCTC—3'

TR4-Clone-F =5'—*GACGAC***AAGCTT**CCTACATGTCTTAAACCTACTGTATC—3'

TR4-Clone-R = 5'--*GACGAC***GGATCC**TTCTTAAACTCAAGGTAACTCCC—3'

Figure 2.5 Sequence of the primers used in cloning the *TR-ACO* promoter sequences, as indicated, into the pRD-410 vector

GACGAC = non-sense nucleotide

AAGCTT = *Hin*d III enzyme cutting sequence

GGATCC = *Bam* HI enzyme cutting sequence

CAGCTG = *Pvu* II enzyme cutting sequence

incubation at 94°C for 2 min; denaturing was set at 30 cycles of 94°C for 30 sec; annealing was set at 5°C below the melting temperature (T_m) of the promoter sequence for 30 sec; extension was set at 72°C for 45 sec/kb of the amplified size; one cycle was set at 72°C for 5 min followed by holding at 4°C. Recovery of the PCR products was achieved through ethanol precipitation (section 2.10.3). To provide *Bam* HI and *Hin*d III sites, twenty-five units of each enzyme was mixed with 5 μg of purified PCR-generated DNA, 0.1 volumes of restriction buffer was added and the reaction made up to a total volume of 70 μL with sterile water. After 5 h of incubation at 37°C, the digested DNA was resolved by agarose gel electrophoresis (section 2.10.1), and the DNA fragment of interest was excised and recovered by the column method (section 2.10.2).

2.11.2. Ligation of promoters and binary vectors

The ligation ratio for vector: insert fragments was set at 3 : 2. The size of the modified vectors (section 2.11.1.1) was approximately 12 kb, and 200 ng of DNA was used for each reaction. The size of inserted DNA (section 2.11.1.2) ranged from 1.0 kb to 1.5 kb. Therefore, the amount of DNA for insertion was calculated using the following formula:

insert DNA (ng) = (200 ng vector) x (insert DNA size, 1~1.5 kb) x 1.5 / (vector size,12 kb)

The mixture of DNA fragments (calculated from the formula above) were added to a 0.1 volume of 10 x ligation buffer (Roche), 1.5 μL of T4 DNA ligase (10 Weiss unit/ μL) (Roche), and the reaction made to 10 μL with sterile water. The reaction was incubated at 4°C overnight, and then transformed into *E.coli* competent cells (section 2.10.6). Cells containing plasmids with putative inserts were selected from LB $^{Amp100, Kan50}$ plates, inoculated into LB^{Kan50} broth for growth overnight, and the plasmid DNA isolated using the alkaline lysis miniprep method (section 2.10.8.1). To confirm inserts of the correct size, the restriction enzymes *Bam* HI and *Hind* III were used to excise the inserted fragments (section 2.11.2) and

these were resolved by gel electrophoresis (section 2.10.2). Further confirmation was performed through PCR, with the same primers used to amplify each promoter sequence (section 2.11.1.2) and then sizing the products by gel electrophoresis (section 2.10.1). The positive plasmids selected by these confirmation methods were isolated by the column miniprep method (section 2.10.8.2) and stored at -20°C until required (section 2.11.3).

2.11.3. Transformation of competent cells of *Agrobacterium tumefaciens*

To transform competent cells of *Agrobacterium tumefaciens* (LBA 4404, LifeTechnologies™, Invitrogen) with the modified binary vectors (pRD 410) containing an insert promoter fused with the GUS reporter gene, electroporation was used. To do this, a 1μL volume of the modified binary vector pRD410 (50 ng/ μL) (section 2.11.2) was mixed with 20 μL of the LBA 4404 cells. The mixture was transferred into the gap of an electroporation metal cuvette (Bio-Rad) and the cuvette placed into the electric shock cassette (Bio-Rad). An electric current of 400 V and 15 amp was used to pulse shock the mixture, and following the shock treatment, the mixture was transferred to 1 mL of LB broth and incubated at 28°C with agitation at 180 rpm for 3 h. After centrifugation at 6 500 x g for 1 min to collect the pellet, the cells were spread onto a $LB^{Kan\ 50}$ agarose plate and incubated at 28°C for 3 days.

2.11.4. Confirmation of the binary vector transformation

The colonies selected from the $LB^{Kan\ 50}$ plates (section 2.11.3) were re-inoculated into 10 mL of $LB^{Kan\ 100}$ broth and incubated at 28°C with agitation (180 rpm) for 2 days. The cells were then collected by centrifugation at 6 500 x g for 1 min, and the binary plasmids were isolated by the column miniprep method (section 2.10.8.2). In order to confirm that the binary vectors had been correctly transformed into the *Agrobacterium tumefaciens* cells, the isolated plasmids were digested with restriction enzymes (*Bam* HI and *Hin*d III) to excise the inserted fragments (section 2.11.1.2) and the products resolved by gel electrophoresis (section 2.10.2).

Further confirmation was carried at using PCR. The same primers used for the modification of promoter sequences (section 2.11.1.2) were used to re-amplify the insert fragments. The size of the PCR product was verified by gel electrophoresis (section 2.10.2). Colonies that contained plasmids with the correct size inserts, after these two selection procedures, were then sequenced. The primers used for sequencing were the reverse primer that was complementary to a region of the GUS coding sequence, and the forward primer that was complementary to a region in the *Npt* II sequence (Figure 2.6). The terminator dye reaction and sequencing procedures were as outlined in (section 2.10.10). Once the binary vector was confirmed by DNA sequencing, pellets from fresh broths were resuspended with 700 µL of LB broth and 300 µL of 50% (v/v) glycerol. The mixture was snapped frozen in liquid nitrogen, and stored at -80°C until required for plant transformation (section 2.11.5; 2.11.6).

2.11.5. Transformation of tobacco procedures

2.11.5.1 Tobacco plant material

The tobacco cultivar Wisconsin-38 (W-38) was used for transformation. About 50 mg of seeds were sterilized in 25 mL of 6 % (v/v) H_2O_2 solution for 3 min with gentle agitation. The H_2O_2 was then decanted and the seeds washed four times with sterile water before sowing in sterile water agar (0.8 % (w/v) PhytoAgar™, GIBCO BRL). The seeds were kept in the dark at 4°C for 3 days, before transfer to a plant growth cabinet (SANYO, Japan), where they were incubated at 25°C in a constant light (1500 lux). The germinated seedlings were incubated for one month, after which they were transferred to a tissue culture pot (Bio-Lab) containing fresh water agar (four plantlets per pot). The plants were grown in the same conditions until required for transformation (section 2.11.5).

2.11.5.2 Tobacco transformation methods

The *Agrobacterium tumefaciens* cells containing the binary vectors (section 2.11.3) were inoculated into 10 mL of $TY^{Kan\ 100}$ broth [0.5 % (w/v) tryptone, 0.3 % (w/v) yeast extract, 1.3

TR1-GUS-F =5'—**AAGCTT**AAATATTATTCTTACTGCTTA—3'

TR2-GUS-F =5'—**CAGCTG**ACCAGCATCTACCAAAAGTG—3'

TR3-GUS-F =5'—**AAGCTT**AAACTGATCCCACTAACCCAC—3'

TR4-GUS-F =5'—**AAGCTT**CCTACATGTCTTAAACCTAC—3'

GUS-R = 5'-- CCAACGCTGATCAATTCCACAGT—3'

NPT II-F = 5'-- CGCCTTCTATCGCCTTCTTGACG—3'

Figure 2.6 Sequence of the primers used in confirming the *TR-ACO* promoter sequences, as indicated, cloned into the pRD-410 vector

AAGCTT = *Hin*d III enzyme cutting sequence

GGATCC = *Bam* HI enzyme cutting sequence

CAGCTG = *Pvu* II enzyme cutting sequence

μg/mL $CaCl_2$, 100 μg/mL of kanamycin sulphate (Sigma)] and grown at 25°C with shaking (180 rpm) for 2 days. After incubation, the broth was centrifuged at 6 500 x g for 5 min, the supernatant discarded, and the cells resuspended in 10 mL of sterile 10 mM $MgSO_4$. Young tobacco leaves were excised and cut into 1 cm^2 leaf discs, dipped into the cells/ $MgSO_4$ mixture for 5 min and then blotted on sterile blot paper (3mm Chr, Whatman International Ltd, Maidstone, England) to remove excess solution. Fifteen pieces of the blot-dried leaf discs were placed onto Nic I media [MS media (Table 2.1), 30 % (w/v) sucrose, 1 mg/L 6-benzyl aminopurine (BAP), 0.1 mg/L 1-naphthaleneacetic acid (NAA), 0.8 % (w/v) agar, pH 5.7], and incubated at 25°C with light (1500 lux) until the regeneration steps (section 2.11.5.3).

2.11.5.3 Regeneration and growth of transgenic tobacco plants

After co-cultivation of the leaf discs with the *A. tumefaciens* solution for three days (section 2.11.5.2), the leaf discs were transferred to Nic $I^{Kan\ 100;\ Cef\ 100}$ media (Nic I media, 100μg/mL kanamycin, 100 μg/mL cefotaxime (ATF Pharmaceuticals, Auckland, NZ)), and incubated at 25°C under light until callus formation had occurred. The calluses were transferred onto fresh Nic II $^{Kan\ 100;\ Cef\ 100}$ media (MS media (Table 2.1), 30 % (w/v) sucrose, 1.0 mg/L BAP, 0.2 mg/L NAA, 0.8 % (w/v) agar, pH 5.7, 100μg/mL kanamycin, and 100 μg/mL cefotaxime) to generate shoots, and the tissues incubated at 25°C in continuous light and the plant tissue transferred to fresh media every 7 days. Once shoots had reached the 3 to 4 leaf stage, the plants were transferred to fresh Nic III $^{Kan\ 100}$ media (MS media (Table 2.1), 30 % (w/v) sucrose, 0.8 % (w/v) agar, pH 5.7, 100μg/mL kanamycin) in order to generate roots and develop further shoots. To do this, plant tissues were incubated at 25°C in continuous light, with tissues transferred to fresh pots every 10 days until the shoots and roots were well developed. When the shoot height had reached approximately 4 to 5 cm, selected plants were transferred to pots containing soil (Seed Raise™, ORDERINGS, Palmerston North, NZ), and then the plants were transferred to a containment PC2 glasshouse where they were grown in

Macro Stock	**per litre:**
NH_4NO_3	16.5 g
KNO_3	19.0 g
$MgSO_4 . 7H_2O$	3.70 g
$CaCl_2 . 2H_2O$	4.40 g
KH_2PO_4	1.70 g

Micro Stock	**per litre:**
$MnSO_4 . H_2O$	17.0 g
$ZnSO_4 . 7H_2O$	8.60 g
H_3BO_3	6.20 g
KI	830 mg
$NaMoO_4 . 2H_2O$	182.5 mg
$CuSO_4 . 5H_2O$	25 mg
$CoCl_2 . 6H_2O$	26 mg

Vitamins	**per litre:**
aneurine . HCl	10 mg
pyridoxine . HCl	50 mg
nicotine acid	20 mg
glycine	200 mg

FeNaEDTA	**per litre:**
$NaEDTA . 2H_2O$	3.73 g
$FeSO_4 . 7H_2O$	2.78 g

MS media composition (pH 5.8)	**per litre:**
Macro stock	100 mL
Micro stock	1 mL
Vitamins	10 mL
FeNaEDTA	10 mL
Myo-Inositol	100 mg
Sucrose	20 g

Table 2.1 Murashige and Skoog (MS) basal salt mixture

75 % humidity at 23°C, with watering once per day.

2.11.6. Transformation of white clover

2.11.6.1 White clover plant material

White clover cultivar Huia (AgResearch Grassland, Palmerston North, NZ) was used for transformation. Approximately 150 mg of seeds were sterilized with 15 mL of 70 % (v/v) ethanol for 1 min in a 15 mL tube, and after decanting the ethanol, 15 mL of mercuric chloride solution (0.2 % (v/v) $HgCl_2$, 0.5 % (v/v) HCl) was added, and the seeds mixed on a circular mixer for 8 min. The mercuric chloride solution was then discarded, the seeds rinsed four times with sterile water, and then transferred to a Petri dish and covered with sterile water. The seeds were then incubated at 15°C in the dark for 17 h.

2.11.6.2 White clover transformation procedures

After overnight incubation, the majority of seeds had started to germinate and the incubation water in the Petri dish was discarded and 6 % (v/v) H_2O_2 solution was added for 3 min with occasional stirring for the final sterilization. The seeds were rinsed five times with sterile water and finally covered with sterile water. Removal of the seed coat and endosperm from the seed was performed using fine forceps and a scalpel under a dissecting microscope. The cotyledons were cut and separated into two. Each cotyledon was placed onto the CR7 media (MS media (Table 2.1),1 mg/L BAP, 50 µg/L NAA, pH 5.7, 0.8 % (w/v) phytoagar) with a layer of filter paper (3mm Chr, Whatman). The *A. tumefaciens* cells that contained the appropriate binary vectors (section 2.11.4) were inoculated into 10 mL of $TY^{Kan\ 100}$ broth and incubated at 25°C with shaking (180 rpm) for 2 days. After incubation, the broth was centrifuged at 6 500 x g for 5 min and the supernatant discarded. The resulting pellet was resuspended in 10 mL of sterile 10 mM $MgSO_4$, and 3 µL of the solution was applied to each cotyledon, and the tissue incubated in CR7 media at 28°C under continuous light.

After 4 days co-cultivation with the *A. tumefaciens* solution, the cotyledons were transferred

to fresh $CR7^{Kan200;\ Cef300}$ media (CR7 media, plus 200µg/mL kanamycin, 300 µg/mL cefotaxime, 0.8 % phytoagar) and incubated at 28°C for 10 days continuous light. After 10 days, the cotyledons were transferred to a fresh $CR7^{Kan200;\ Cef300}$ media plate, and the dead cotyledons removed from the selection. After a period of 20 days, all live cotyledons were switched onto $CR5^{Kan200;\ Cef300}$ media (MS media (Table-2.1), 30 % (w/v) sucrose, 0.1 mg/L BAP, 0.05 mg/L NAA, 0.8 % (w/v) phytoagar, pH 5.7, 200µg/mL kanamycin, 300 µg/mL cefotaxime) and incubated at 28°C in continuous light until shoots had generated. Sets of live cotyledons were switched to fresh $CR5^{Kan200;\ Cef300}$ media every 21 days. Over this period of regeneration, the cotyledons were checked regularly for contamination and when necessary, shifted onto fresh media. After approximately two months, the plantlets that had started rooting were transferred to $CR0^{Kan200}$ media (MS media (Table 2.1), 30 % (w/v) sucrose, 0.8 % (w/v) Phytoagar, pH 5.7, 200µg/mL kanamycin) to continue generating plants. Once selected plant shoots were approximately 3 to 5 cm high, these were transferred into pots containing soil (SeedRaise™, ORDERINGS), sealed in a plastic bag and contained in a tray with water. Water was also sprayed into the plastic bag to create a humid environment. The plants were incubated at 25°C in a long-daylight environment (15 h) for 15 days, and after that, plants were transferred to the containment glasshouse and grown at 23°C in 75 % humidity, with watering once per day.

2.12 Southern analysis

2.12.1. Transfer of genomic DNA

After digested genomic DNA (section 2.5) was separated by electrophoresis (section 2.10.1), the DNA was transferred to a nylon membrane by the capillary transfer method (Chomczynski, 1992). The gel (section 2.10.1) was first immersed in depurination solution (0.25 M HCl) for 5 min with gentle agitation, rinsed twice with RO water and then immersed in neutralisation solution (1.5 M NaCl, 0.4 M NaOH) for 1 h with gentle agitation. After

rinsing twice with RO water, the gel was immersed in transfer solution (3 M NaCl, 8 mM NaOH, pH 11.4) for 15 min with gentle agitation.

To transfer the DNA, four pieces of dry blotting paper (3mm Chr, Whatman) were first lined up on a 5 cm high stack of paper towels, and then a gel-sized piece of blotting paper, pre-wetted with transfer solution, was placed onto the top of the dry blotting paper. A gel-sized piece of Hybond^{TM} –N+ nylon membrane (Amersham), pre-soaked in transfer solution for 5 min, was placed on top of the wet blotting paper, and then the gel was placed face-up on top of the nylon membrane and smoothed to remove any air bubbles. Three pieces of blotting paper, pre-wetted with transfer buffer, were placed onto the gel. Four pieces of longer and pre-wetted blotting paper were then used as a capillary wick with one end covering the top of the blotting assembly and the other end dipped into the transfer solution. After 16 h of blotting, the membrane was post-fixed by UV-crosslinking (UV Stratalinker®2400; STRATAGENE, La Jolla, CA, USA) for 2 min, neutralized in neutralization solution (0.1 M $Na_2PO_4.2H_2O$, pH 7.2) for 10 min, and then sealed in a plastic bag and stored at 4°C until required.

2.12.2. Labeling DNA for Southern analysis with [α-^{32}P]-dCTP

DNA probes (Figure 2.7; 2.9) were labeled with [α-^{32}P]-dCTP (3 000 Bq/mmol; Amersham) using the Ready-To-Go ^{TM} DNA labeling kit (Amersham). To do this, an aliquot of DNA was diluted to 25 ng with sterile water, denatured in a boiling water bath for 2 min and then immediately chilled on ice for 2 min. The denatured DNA was collected at the bottom of the tube by pulse centrifugation and added to the Ready-To-Go reagent beads. After gentle mixing the beads with the DNA solution, an aliquot (5 μL) of the [α-^{32}P]-dCTP was added to the mixture, and the reaction incubated for 15 min at 37°C. The labeled DNA was then separated from unincorporated nucleotides by chromatography through a Sephadex G-50

***TRACO1*-southern promoter probe**

5'—CTTTGCCAATTCTTCTATGTACCAAAAAAAAAGTACAGTATGATTTTTGTTCCAATTTAAGTGGATTGATTTTTTACATTT
GAATTTAATCCACATAAAATCTCATTATAAATTGATACATTAGATTTTTTTTTCTTTCACTACCAGTTTAATCTGGTTCGGTGGTCAG
TTCTGACATCAAGTGATTCTAATCTCCTTCTGATCGCAGCTGCGGAAGTATCAAACTGTGATCCTCTCTACCAAACACCAATCAT
CACTTAACCCACTAACGATTTCTTGACACATCAAAATTCTATGCCAAGAGACTTTGGAACAAAATTTCTTATATACTACTTTCTTAA
TTAGTTTTAATTAATAATAGATTTTATTCTAAGATTCACTGAGAGCCTTGG—3'

***TRACO2*-southern promoter probe**

5'—GACCACACCAATTCGAGTTCGGTGGTTTATACTATGTTAGAATGTGCGTCCAAAAAACATTTTCGTTTGGGAAATGCG
AGTTCGAGGCTCCTTCTTAAACATCATTTTCAAATGCATTTAAAAAATGTNAAATAAAATAGAGAACAAATAGAGGTTGCGGCAG
CCTTAGANGTTGAATTTGGTCAAATGTTCAAGAGGAAAAACCAGCCATCAAGTAGGNCCAACCNTATGCCCAGTGTTTTTGACA
AATCAACCAAAAGAACCCAAAATAAACACAAGCTTCTGATTAGAACTATTAATAATAAACAAAGAAAATTAAGCTGAACAAATCAT
ACTATTAAAATATAAAATATATTCAATTAGATTTAAAATAATAATAAGTTGTCTATTTGGTCTTGTGATGTAAAGGTC—3'

***TRACO3*-southern promoter probe**

5'—CTCTCAAAGCGTTAACCATGTCTGGTATGCCTTTTTCTGTTGTTTTTTTATTTTTACCAGCCCTACGACTCACTATAGGG
CACGCGTGGTCGACGGCCCGGGCTGGTAAACATAAACGAATTGATTAAACAGAAATTGTTTTCAATCTGTTTAAACGACTCACT
ATAGGGCACGCGTGGTCGACGGCCCGGGCTGGTAAACATAAACGAATTGATTAAACAGAAATTGTTTTCAATCTGTTTAAACGA
CTCACTATANGGCACGCGTGGTCGACNGCCCGGGCTGGTCCTGCGTGTCTAAAAGC—3'

***TRACO4*-southern promoter probe**

5'—CCTACATGTCTTAAACCTACTGTATCTTAAAATCTAAAAAGTCAATTTTTTTAGGATAAGTAGGCTTATACCCCCCTGTAA
TGTAGGCAAGTTTTGTTTTCCCCCTGTAATTTTTTTTTTTGTGACTCGCCCTTTGCAATGTTGAATATTTTTTTTCCCAGTTCATTTT
ACCCCATGTAATGTTGGCCTTTACTCCCCTGCAAGGGGTAAAAATGAACTAAAAGAGAAAAAAATCAACATTGCAAGGGGCAA
GTCAGACAAAAAAAAATTATAGGGGGAAAACCAAAACTCGCCCATATTAAGGGGATATTAACCTATTTACC—3'

Figure 2.7 Sequences, as indicated, of the probes used in Southern blot analysis

The boxed regions represent the primer sequences for the forward (clear background) and reverse (shaded background) primers used to amplify each probe.

***TR-ACO3*-3'UTR-southern probe**

5'—**CAAGCTAAGGAACCAAGAT**TTGAAGCACTGAAAGCATGAAATGTGAATTTGGGTTCAA
TTGCAATTGTTTTGAATTTAAACAAGTAACATAAAATAGGCAAAGATGCATGTGCTCCTCAA
ATGAAAATAATAAAAAATAGATTTAAATATGATGCGAGTCATGCAAATATATTATGTGTTAGTTT
TTGTAAGTTTATTTTTAATAGATAAACGAAATGTGTGTTAATACAAATTCACACAGTAAATTGA
AGGGATTAGAGTTCGAACATCGG**TTATGGTGTCAGACTCATTTTGG**—3'

Figure 2.8 Sequence of the probe used in Southern blot analysis for distinguishing between *TR-ACO3* and *TR-ACO4* genes

The boxed regions represent the primer sequences for the forward (clear background) and reverse (shaded background) primers used to amplify each probe.

GUS-southern probe

5'—**CGATGCGGTCACTCATTACGGC**AAAGTGTGGGTCAATAATCAGGAAGTGATGGAGCAT
CAGGGCGGCTATACGCCATTTGAAGCCGATGTCACGCCGTATGTTATTGCCGGGAAAAGT
GTACGTATCACCGTTTGTGTGAACAACGAACTGAACTGGCAGACTATCCCGCCGGGAATG
GTGATTACCGACGAAAACGGCAAGAAAAAGCAGTCTTACTTCCATGATTTCTTTAACTATG
CCGGAATCCATCGCAGCGTAAT**GCTCTACACCACGCCGAACACCTG**—3'

Figure 2.9 Sequences of the probe used in Southern blot analysis for genome copy number confirmation in transgenic plants

The boxed regions represent the primer sequences for the forward (clear background) and reverse (shaded background) primers used to amplify each probe.

Micro column (Amersham) by centrifugation at 735 x g for 2 min. The collected DNA was then denatured in a boiling water bath for 2 min, immediately cooled on ice for 2 min and then added to a hybridization solution (pre-equilibrated at 65°C) containing with the blotted membrane (section 2.12.4.).

2.12.3. Labeling DNA for Southern analysis with [α-^{32}P]-dATP

DNA probes (Figure 2.8) were labeled with [α-^{32}P]-dATP (3 000 Bq/mmol; Amersham) using the Megaprime ™ DNA labeling kit (Amersham). The probe DNA was diluted to 5 ng/μL with Milli-Q water, denatured in a boiling water bath for 2 min and immediately chilled on ice for 2 min. The denatured DNA was collected at the bottom of the tube by pulse centrifugation and mixed with 4 μL each of un-labeled nucleotides (dGTP, dCTP and dTTP), 5 μL of reaction buffer, 17 μL of sterile water, and 2 μL of enzyme (1 unit/μL DNA polymerase I Klenow fragment). Finally, 5 μL of [α-^{32}P]-dATP was added, the mixture incubated for 15 min at 37°C, and 5μL of 0.2 M EDTA was then added to stop the reaction. This mixture was then transferred to a Sephadex G-50 Micro column (Amersham) and the labeled DNA separated from unincorporated nucleotides by centrifugation at 735 x g for 2 min. The collected DNA was then denatured in a boiling water bath for 2 min, immediately cooled on ice for 2 min, and then placed on a blotting membrane soaked in hybridization solution (pre-equilibrated at 65°C).

2.12.4. Hybridization, washing and development of DNA blots

The blotted membrane (section 2.12.1) was rolled (nucleic acid facing inwards) and placed into a Hybaid™ glass tube (Amersham) containing 25 mL of Church hybridization solution (0.25 M $Na_2PO_4.2H_2O$, pH 7.2, 7 % (w/v) SDS, 1 % (w/v) BSA fraction V, 1 mM EDTA, pH 8.0) and the membrane pre-incubated in a rotary oven at 65°C. After 3 h, the labeled probe (section 2.12.2 or 2.12.3) was added to the hybridization solution and the membrane was incubated for 16 h at 65°C. A series of washes were then processed undertaken at 65°C. At the

conclusion of hybridization, the membrane was washed with the hybridization wash solution (20 mM $Na_2PO_4.2H_2O$, pH 7.2, 5 % (w/v) SDS, 0.5 % (w/v) BSA fraction V, 1 mM EDTA, pH 8.0) for 20 min and then with dilutions of a 20 X SSPE solution (0.2M Na_2HPO_4, pH 6.5, 3.6 M NaCl, 20 mM EDTA). The first of these was in 2 X SSPE (2X SSPE, pH 6.5, 0.1 % (w/v) SDS) for 20 min, 1 X SSPE (1X SSPE, pH 6.5, 0.1 % (w/v) SDS) for 20 min, and then 0.2 X SSPE (0.2X SSPE, pH 6.5, 0.1 % (w/v) SDS). The membrane was finally washed in 0.1 X SSPE (0.1X SSPE, pH 6.5, 0.1 % (w/v) SDS) for 40 min, wrapped in cling film, and either placed onto a Phosphor-Image cassette (FujiFilm, Tokyo, Japan) for 5 hr and the image was developed in a Phosphor-Image (FLA-5000; FujiFilm) or placed with an X-OMATIC intensifying screen and an XAR-5 X-ray film (Kodak) at -80°C for 2 weeks. After this time, the film was developed in an automatic X-ray film processor (100Plus™, All-Pro Image, Hickville, NY, USA).

2.13 GUS staining histochemical assays

2.13.1. Staining procedures

Tissues which were required for analysis were excised fresh, or kept at 4°C until dipped in 90 % (v/v) of ice-cold acetone and incubated on ice for 15 min. The fixed tissues were then rinsed with 50 mM of Na_2HPO_4 (pH 7.2), immersed into X-gluc staining solution (2 mM 5-bromo-4-chloro-3-indolyl β-$_D$-glucuronide cyclohexylamine salt (Sigma), 50 mM Na_2HPO_4, pH 7.2) and placed under vacuum at 50 kPa for two periods of 15 min. The entire solution and tissues were then wrapped in tin foil and incubated at 37°C overnight.

2.13.2. Tissue fixation and embedding

The stained tissues normally display a blue colour, and for shoot tissue this is seen against a green chlorophyll background. To remove chlorophyll and for tissue fixation purposes, tissues were initially destained in 15 % to 30 % (v/v) ethanol for 30 min each, and then transferred to

the FAA fixative solution (50 % (v/v) ethanol, 5 % (v/v) acetic acid, 3.7 % (v/v) formaldehyde) with vacuum filtration at 50 kPa for 15 min. After incubation for 4 h to overnight, the tissues were immersed in 70 %, 85 %, 95 % (v/v) ethanol solutions for 30 min at each step, and then immersed twice in 100 % ethanol for 2 h. The de-stained tissues can be kept in 100 % ethanol at 4°C for several months. To obtain tissue sections, the fixed tissues required the following clean-up and embedding steps. The de-stained tissues were incubated in 25 % (v/v) xylene and 75 % (v/v) ethanol for 1 h, then immersed in 50 % : 50 % and then 75 % : 25 % (v/v) of xylene : ethanol for 1 h in each solution. After a final incubation in 100 % xylene for 1h, paraplast chips (TYCO healthcare, Mansfield, MA., USA) were gradually added to the xylene solution at 42°C with gentle agitation. The chips were continually added until the wax volume was equal to the xylene volume, and the mixture then incubated for 2h. After that, the tissues were switched to fresh wax and incubated at 60°C overnight, after which the wax was changed twice per day for three days. A histochemical embedder (BioLab) was used to prepare wax blocks. The tissue was placed in a pre-warmed embedding boat, filled with molten wax, covered with an embedding cassette (BioLab) and finally switched to a cold plate to solidify the wax.

2.13.3. Sectioning and mounting

The wax block was trimmed of un-wanted wax and pre-cooled on ice until sectioning. The embedding cassette was placed on the microtome (Leica, Bensheim, Germany) and the tissue sectioned from 8 μm to 35 μm using disposable blades. The wax sections were floated in water pre-heated to 42°C, captured onto polysine microscope slides (BDH) and placed on the top of the slide backer (Agar Scientific, UK) at 42°C overnight. To de-wax, the slides were dipped twice into 100 % xylene for 10 min, before mounting with dibutyl phthalate xylene (DPX) solution (Sigma).

2.14 *In Situ* hybridization

2.14.1. Sub-cloning of probes

The sequences of the 3'-UTR regions of *TR-ACO1* and *TR-ACO3* were used as probes for *in-situ* hybridization (Figure 2.10). Since these 3'-UTR sequences were cloned originally (Hunter et al., 1999) into the pCR2.1® vector (Invitrogen), which does not contain the SP6 promoter sequence, these sequences were first sub-cloned into the pGEM™-T-Easy vector that contains both T7 and SP6 promoters. To do this, cells from a glycerol stock were inoculated into 5 mL of LB^{AMP100} broth and the cells incubated at 37°C for overnight with shaking (180 rpm). The broth was then centrifuged at 6 500 x g for 5 min to collect the pellet, and the alkaline lysis miniprep method (section 2.10.8.1) used to obtain plasmid DNA. The DNA insert of interest was identified by restriction digestion (section 2.10.9), the digested DNA resolved by gel electrophoresis (section 2.10.1) and the band of the expected size excised and recovered using the column method (section 2.10.8.2). After confirmation by DNA sequencing (section 2.10.10), the nucleic acid fragments were ligated into pGEM™-T-Easy (section 2.10.5) (Figure 2.3), transformed into *E. coli* (DH-5α strain) competent cells with ampicillin selection (section 2.10.7) and plasmids with the correct inserts were identified by restriction digestion of plasmid DNA (section 2.10.9).

2.14.2. RNA probe synthesis

The sub-cloned plasmid DNA (section 2.14.1) was used as template for PCR using the forward and reverse M13 primers and the amplification products treated with 2 μL of SAP (1 U/ μL, Invitrogen) and 1μL of Exo I (10 U/ μL, Invitrogen). Since the sense probe will be used as negative control, both RNA probes (sense and antisense) were synthesised using T7 and SP6 RNA polymerases. The reaction mixture used comprised 1 μL of DNA template (400 ng/μL) mixed with 2 μL of 10 x transcription buffer (Roche), 1 μL of RNase inhibitor (20U/μL, Roche), 2 μL of NTP labeling mixture (100 μM ATP, 100 μM CTP, 100 μM GTP, 65

TR-ACO1-3'UTR-*in-situ* probe

5'—**CAAGCTAAGGAACCAAGAT**TTGAAGCACTGAAAGCATGAAATGTGAATTTGGG
TTCAATTGCAATTGTTTTGAATTTAAACAAGTAACATAAAATAGGCAAAGATGCATGT
GCTCCTCAAATGAAAATAATAAAAAATAGATTTAAATATGATGCGAGTCATGCAAATAT
ATTATGTGTTAGTTTTTGTAAGTTTATTTTTAATAGATAAACGAAATGTGTGTTAATAC
AAATTCACACAGTAAATTGAAGGGATTAGAGTTCGAACATCGG**TTATGGTGTCAGA**
CTCATTTTGG—3'

TR-ACO3-3'UTR-*in-situ* probe

5'—**CAAGCTAAGGAACCAAGAT**TTGAAGCACTGAAAGCATGAAATGTGAATTTGGG
TTCAATTGCAATTGTTTTGAATTTAAACAAGTAACATAAAATAGGCAAAGATGCATGT
GCTCCTCAAATGAAAATAATAAAAAATAGATTTAAATATGATGCGAGTCATGCAAATAT
ATTATGTGTTAGTTTTTGTAAGTTTATTTTTAATAGATAAACGAAATGTGTGTTAATAC
AAATTCACACAGTAAATTGAAGGGATTAGAGTTCGAACATCGG**TTATGGTGTCAGA**
CTCATTTTGG—3'

Figure 2.10 Sequences, as indicated, of the probes used in *in-situ* hybridization analysis for *TR-ACO1* and *TR-ACO3*

The boxed regions represent the primer sequences for the forward (clear background) and reverse (shaded background) primers used to amplify each probe.

μM UTP, and 35 μM DIG-UTP, (Roche)), 12 μL of diethyl pyrocarbonate (DEPC)-treated water (Sigma) and 2 μL of T7 or SP6 RNA polymerase (20 U/μL, Roche). After incubation at 37°C for 3 h, 2 μL of DNase I (10 U/μL, Roche) was added, and the mixture incubated at 37°C for 30 min. Finally, the reaction was terminated by the addition of 2 μL of 200 mM EDTA (pH 8).

The labeled probes were precipitated by adding 2.5 μL of 4 M LiCl and 75 μL of 100 % (v/v) ethanol to the mixture. After an overnight incubation at -20°C, the precipitate was collected by centrifugation at 20 800 x g for 15 min, the supernatant removed, and the pellet washed with 150 μL of 70 % (v/v) ethanol. The pellet was recovered by centrifugation at 20 800 x g for 5 min, washed twice more with 70 % (v/v) ethanol, once with 100 % (v/v) ethanol, air-dried and resuspended in 100 μL of DEPC-treated water.

2.14.3. Hydrolysation and precipitation of probes

The labeled probes required hydrolysation to reduce the probe size and achieve efficient penetration into the tissue. To do this, the reaction mix contained half of the probe solution (50 μL) (section 2.14.2) mixed with 20 μL of 200 mM $NaHCO_3$ (pH 10.2), and 30 μL of 200 mM Na_2CO_3 (pH 10.2). The mixture was incubated at 60°C for a time calculated using the formula:

Incubation time $T = (L0-Lf) / [(K) * (L0) * (Lf)]$

Where T = hydrolysis time (min)

L0 = starting length (kb)

Lf = final length (kb) (= 0.1 kb)

K = rate of constant for hydrolysis (= 0.11 $kb^{-1}min^{-1}$)

After incubation, 10 μL of 1 M NaOAc, (pH 4.7), was added to stop the reaction, the hydrolysed probes precipitated by the addition of 1 μL of glycogen (20 mg/mL, Sigma), 10

μL of 4 M LiCl and 300 μL of ice-cold 100 % (v/v) ethanol. The mixture was incubated at -20°C for overnight, the probes collected by centrifugation at 20 800 x g for 15 min, washed twice with 70 % (v/v) ethanol, air dried and resuspended in 500 μL of 50 % (v/v) formamide.

2.14.4. Quantification of probes

The labeled probes and the control labeled RNA (supplied by Roche) were serially diluted into different ratios ranging from 1:10 to 1:1000, with 1 μL of each dilution spotted onto Hybond™ –N+ nylon membrane. After post-fixing by UV-crosslinking (UV Stratalinker®2400; STRATAGENE) for 2 min, the membrane was placed in wash buffer (100 mM maleic acid (pH 7.5), 0.15 mM NaCl, 0.3 % (v/v) Tween 20) for 5 min with gentle agitation and then covered with blocking buffer (1 % (w/v) blocking reagent (Roche), 100 mM maleic acid (pH 7.5), 0.15 mM NaCl) for 30 min with gentle agitation. The membrane was then incubated in a 1:5000 dilution of anti-DIG-alkaline phosphatase (Roche) for 30 min at room temperature, rinsed twice with wash buffer and then placed into detection buffer (100 mM Tris-HCl, pH 9.5, 100 mM NaCl, 50 mM $MgCl_2$) for 5 min. Finally, the membrane was incubated overnight in 10 mL of detection solution (3.37 μg of Nitroteazolium blue chloride (NTB), 1.75 μg of 5-Bromo- 4-chloro-3-indolyl phosphate (BCIP) in 10 mL of detection buffer) in the dark at room temperature, after which the probe was compared with the density of staining of the control RNA and the probe concentration calculated.

The concentration was also quantified using the NanoDrop® method. The labeled probes were diluted with 50 % (v/v) formamide to give 1: 5 and 1:10 fold dilutions, and 2μL of each dilution was then loaded on the pedestal of the NanoDrop® (ND-1000, NanoDrop Technologies, Montchanin, DE, USA) and the probe concentration was calculated.

2.14.5. Fixation and dehydration of plant tissue materials

The paraformaldehyde fixation method was mainly used for *in-situ* hybridazation in this study. Fresh plant tissues were excised and immediately placed into an ice-cold fixation solution (4

% (w/v) paraformadehyde, 130 mM NaCl, 7 mM Na_2HPO_4, 3 mM NaH_2PO_4, pH 7.0) and tissue placed under vacuum (-35 kPa) for 10 min until all tissue descended to the bottom of the vessel containing the fixative. After the pressure was released, fixation was continued at 4°C for 12 h.

Subsequent to fixation, the plant tissues were placed into 0.85 % (w/v) NaCl at 4°C for 30 min with gentle agitation, after which the tissue was placed in 15 % (v/v) ethanol containing 0.85 % NaCl (w/v) for 1 h, then transferred to 30 % (v/v) and 50 % ethanol each containing 0.85 % NaCl (w/v) for 1 h each. The 50 % (v/v) ethanol was then replaced by 50 % (v/v) TBA (tertiary butyl alcohol) for a 1 h incubation, followed by incubation in 70% (v/v) TBA overnight at 4°C. After the overnight incubation, the tissues were transferred and incubated, at 37°C, for 1 h each in a series of TBA solutions as follows 70 % (v/v), 85 % (v/v), 90 % (v/v) before incubation in 100 % pure TBA twice for 2 h each, and then incubation overnight in fresh 100 % TBA solution at 37°C.

2.14.6. Wax infiltration

After incubation in TBA, tissues were transferred to a solution of 50 % (v/v) paraffin oil and 50 % (v/v) TBA at 37°C for 30 min, before placing the fixed tissues onto the top of semi-solid wax and incubating at 60°C for 3 h. After that, the tissues were placed into fresh wax and incubated overnight at 60°C. The wax was changed twice per day for a further three days, after which a histochemical embedder was used to prepare wax blocks which were stored in 4°C until required for sectioning (section 2.14.7).

2.14.7. Tissue sectioning

After removal of unwanted wax, the tissue sample was sectioned from 8 μm to 20 μm using disposable blades in a microtome (Leica), the wax sections floated onto DEPC-treated water at 42°C, and then captured onto polysine microscope slides (BDH). The microscope slides were placed overnight onto a slide incubator at 42°C.

2.14.8. Pretreatments of samples

The baked microscope slides were placed into a de-waxing solution (Histoclear®, National Diagnostics, Atlanta, GA, USA) for 10 min, with this procedure being performed twice in order to effectively remove wax from the sectioned samples. The sections were then rehydrated through an ethanol series from 100 % (v/v) ethanol for two rinses of 30 sec, and then the sections transferred sequentially for two rinses of 30 sec in 95 % (v/v), 85 % (v/v), 70 % (v/v), 50 % (v/v), 30 % (v/v) and 15 % (v/v) ethanol, each with 0.85 % (w/v) of NaCl, until a final wash with 0.85 % NaCl for 30 sec. After this, the slides were incubated in pronase solution (0.125 mg/ml pronase, (Sigma); 50 mM Tris-HCl, pH 7.5; 5 mM EDTA, pH 8.0) at 37°C for 35 min, the reaction stopped by transferring the slides to glycine solution (0.2 % (w/v) glycine, 130 mM NaCl, 7 mM Na_2HPO_4, 3 mM NaH_2PO_4, pH 7.0) for 2 min, then each slide was rinsed twice in 1 x PBS buffer (130 mM NaCl, 7 mM Na_2HPO_4, 3 mM NaH_2PO_4, pH 7.0) for 2 min each and then in 0.85 % (w/v) NaCl solution for 2 min.

2.14.9. RNA hybridization and washing

RNA probes (section 2.14.3) were diluted to the required concentration with hybridization buffer (50 % (v/v) formamide, 300 mM NaCl, 10 mM Tris, pH 7.5, 1 mM EDTA, pH 8.0, 5 % (w/v) dextran sufate, 1 % (w/v) blocking reagent (Roche), 150 μg/mL tRNA (Roche)), with the required concentration calculated from the following formula:

$$\text{Probe conc.} = 200 \text{ ng} / (S) / (P)$$

Where (S) = the volume (mL) of hybridization solution applied to each slide

(P) = the probe size (kb)

Approximately 100 μL of diluted hybridization solution was applied to each of the pre-treated slides (section 2.14.8), these were covered with a cover slip and the slides laid on an elevated level in a container lined with blotting paper (3mm Chr, Whatman) pre-wet with 2 x SSC

(0.03 M sodium citrate, pH 7.0, 0.3 M NaCl) in 50 % (v/v) formamide. The slides were then incubated overnight at 55°C, and following probe hybridization, low and high stringency washes were applied to the slides. The slides were washed twice in low stringency saline solution (2 x SSPE) at room temperature for 10 min, and then with the high stringency wash (0.2 X SSPE solution) at 55°C for 1h with gentle agitation. RNase treatment was completed by immersing the slides twice in RNase buffer (10 mM Tris-HCl, pH 7.5, 1 mm EDTA, 500 mM NaCl) at 37°C for 5 min, then transferring to a RNase A solution (5 μg/mL RNase A (Sigma) in RNase buffer) at 37°C for 30 min. The slides were subsequently washed twice in fresh RNase buffer at 37°C for 5 min each, then transferred to fresh 0.2 x SSPE buffer and a high stringency wash was repeated at 55°C for 1 h. The slides were then rinsed twice with fresh 0.2 x SSPE at 37°C for 5min.

2.14.10. Immunological detection

The washed slides (section 2.14.9) were transferred into 1 X blocking solution (1 % (w/v) blocking reagent (Roche), 100 mM maleic acid (pH 7.5), 150 mM NaCl) for 45 min and then into BSA wash solution (1 % (w/v) BSA fraction V (Invitrogen), 0.3 % (v/v) Triton-X 100, 100 mM Tris-HCl, pH 7.5, 150 mM NaCl) with gentle agitation for 45 min. Before applying antibody to the slides, the anti-DIG-AP fragments (Roche) were diluted 1:1000 with the BSA wash solution, and then 100 μL applied to a slide and a cover slip placed on top. After incubating at room temperature for 2 h, the slides were washed three times with BSA wash buffer for 45 min each, then dipped twice in detection buffer (100 mM Tris-HCl, pH 9.5, 100 mM NaCl, 50 mM $MgCl_2$) for 5 min. One hundred μL of detection solution (NTB (3.375mg/mL), BCIP (1.75 mg/mL) in detection buffer) was then applied to each slide, the slides incubated in the dark and in a humid environment at room temperature for 36 h. The reaction was stopped by washing three times with TE buffer (for 5 min, before being processed in a series of dehydration steps sequentially from 70 % (v/v), 85 % (v/v), 95 % (v/v)

ethanol, and then twice in 100 % ethanol for 1 min for each step. The final step was to soak the slides in a de-waxing solution (Histoclear®) for 1 min, and after drying in the fume hood, the slides were mounted with DPX (Sigma) before analysis.

2.15 General microscopy methods

To capture GUS stained and those generated by *in-situ* hybridization images, the slides were examined using a compound light microscope (Olympus-BX51, Olympus Ltd. Japan), and the images captured using an Optronics U-TV0.5XC camera (Olympus Ltd.).

Chapter 3 Results

3.1 Isolation of *TR-ACO* promoter sequences

3.1.1. *TR-ACO1* promoter isolation

3.1.1.1 Amplification of the *TR-ACO1* promoter using Genome Walker™ PCR

Five libraries were amplified using the Genome Walker™ method with nested PCR primers. The primers used were nested forward primers based on the commercially-available 5′ adaptor sequence, (AP-F1; AP-F2) and reverse primers based on the known 3´ sequence of the *TR-ACO1* cDNA (designated GW-ACO1-R1; GW-ACO1-R2, Section 2.8) (Figure 2.2). Prior to PCR amplification, DNA was digested with different restriction enzymes, an adaptor sequence for the AP-F1 primer was then annealed to the 5´ ends of the fragments and then these used as templates for PCR. After two rounds of PCR, amplified products were present in three libraries (L). A 1500 bp product was amplified from L1 (*Dra* I digested), 800 bp and 1600 bp products from L2 (*Eco* RV digested), and 1200 bp and 700 bp products from L4 (*Stu* I digested) (Figure 3.1.1). Only low molecular weight amplification products were obtained from genomic templates generated using *Pvu* II (L3) and *Sma* I (L5).

3.1.1.2 Screening of putative *TR-ACO1* promoter inserts in p-GEM vector

The three amplified products from the L1 and L2 libraries were purified, ligated into the p-GEM vector and transformed into *E.coli* strain DH-5α. After plating onto selection media, colonies were selected, the plasmid DNA isolated and then digested. Preliminary screening (Figure 3.1.2 A) showed that five colonies contained putative inserts from the original 1500

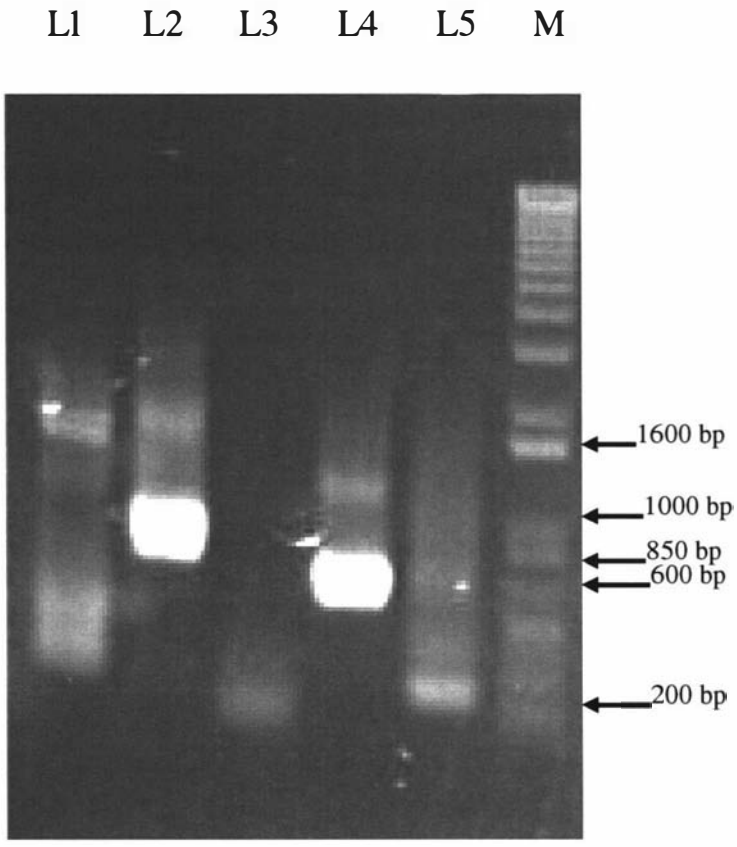

Figure 3.1.1 *TR-ACO1* promoter isolation using PCR

PCR-generated DNA fragments, using the GW-ACO1-R1 and AP-F1 primers for round one, and the GW-ACO1-R2 and AP-F2 primers for round two. PCR products were separated by electrophoresis on a 0.75 % (w/v) agarose gel and visualized with ethidium bromide. The relative sizes of the DNA ladder are indicated on the right.

L1: Two rounds of PCR amplification from a *Dra* I digested library
L2: Two rounds of PCR amplification from a *Eco* RV digested library
L3: Two rounds of PCR amplification from a *Pvu* II digested library
L4: Two rounds of PCR amplification from a *Stu* I digested library
L5: Two rounds of PCR amplification from a *Sma* I digested library

bp purified PCR product from the L1 library and colony # 2 was chosen for further DNA sequencing. Two colonies with *ca.* 800 bp inserts from the original 1600 bp purified product from the L2 library were obtained, and colony # 2 was chosen for DNA sequencing (Figure 3.1.2 B). Three colonies from the original 800 bp purified PCR product from the L2 library were obtained, and colony # 4 was chosen for DNA sequencing (Figure 3.1.2 C).

3.1.1.3 Sequencing of the putative *TR-ACO1* promoter

The results of DNA sequencing showed that a 1440 bp insert was obtained from colony # 2 of the L1 (1500 bp) library (colony # 2, Figure 3.1.2 A). The sequenced colony from the L2 (1600 bp) library (Figure 3.1.2 B) had a 730 bp insert, and the L2 (800 bp) library product transformation had a 600 bp insert (colony #4, Figure 3.1.2 C). Both of these two sequences (from the L2 library) are contained within the L1 sequence. So, the 1440 bp sequence from the L1 library was used for further analysis (Figure 3.1.3).

3.1.1.4 Confirmation of putative *TR-ACO1* promoter sequence

3.1.1.4.1. TR-ACO1 promoter sequence analysis using BLAST-n

The alignment results from the NCBI BLAST-n database indicated that a 387 bp primary sequence was most closely related to the *TR-ACO1* gene isolated from white clover with 99 % identity (Hunter et al., 1999). At least 90 different ACC oxidase genes were aligned, and highly conserved first intron and 5′ and 3′ splice sites can also be detected in the *TR-ACO1* sequence (data not shown). Excluding the white clover *TR-ACO1* sequence, the second most identical sequence is an ACC oxidase cDNA from pea (*Pisum sativum*), *PE8*, and then an ACC oxidase cDNA sequence from mung bean (*Vigna radiata*) *VR-ACO1* (Figure 3.1.4). A 131 bp sequence from *TR-ACO1* isolated in this thesis is aligned with *TR-ACO1* (GI 4704655) and the *PE8* sequence (GI 169040) and shown to have 95 % identity (Figure 3.1.4). In contrast with the reading frame, the upstream sequence from the putative ATG does not show

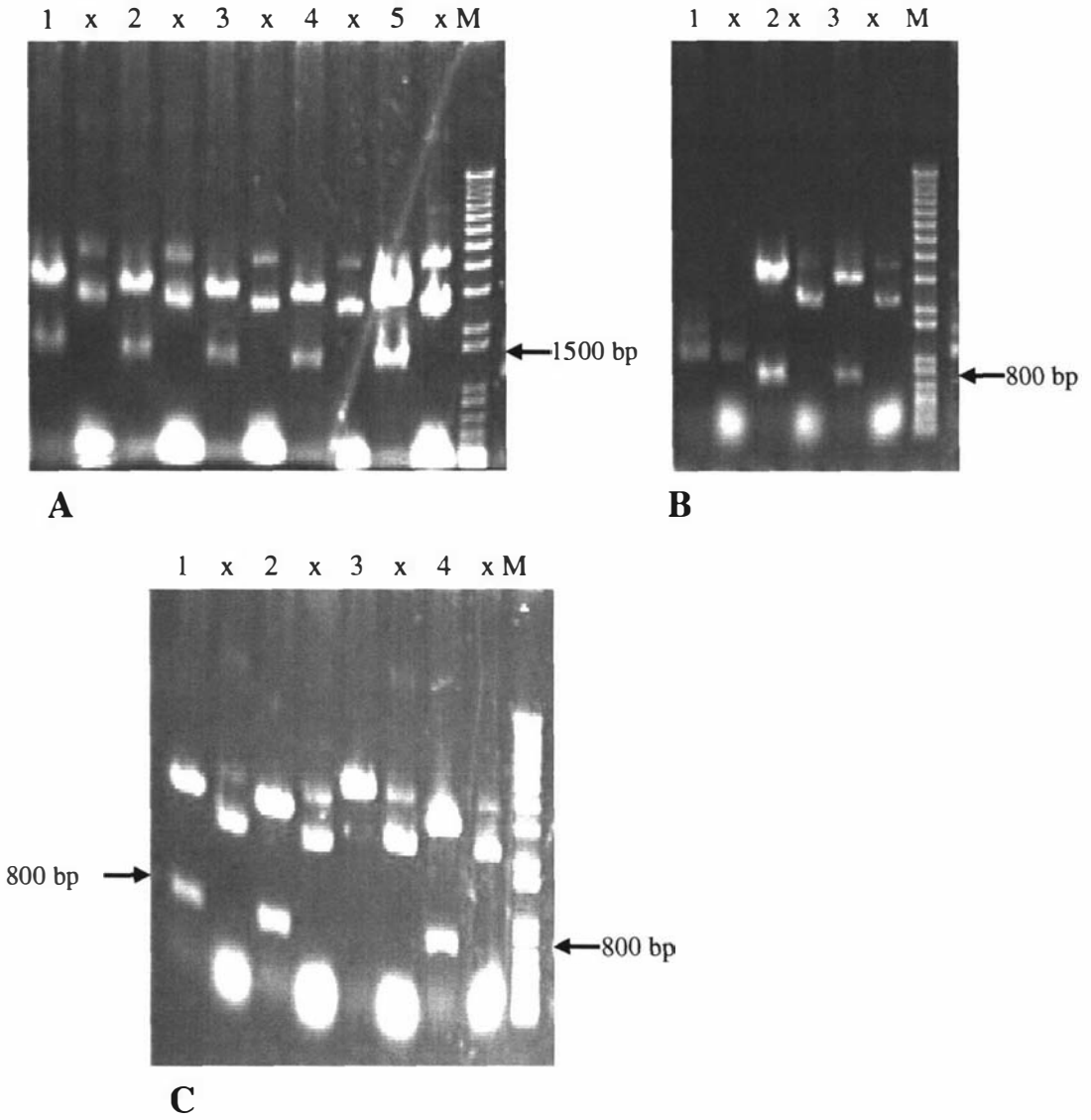

Figure 3.1.2 Restriction enzyme digestion screening of p-GEM plasmids containing putative *TR-ACO1* promoter inserts in *E. coli* cells

A. Screening of the L1 library (*Dra* I digestion) with putative 1500 bp inserts
B. Screening of the L2 library (*Eco* RV digestion) with putative 1600 bp inserts
C. Screening of the L2 library (*Eco* RV digestion) with putative 800 bp inserts

Products from *Eco* RI digests were separated on 0.8 % (w/v) agarose gel and visualized with ethidium bromide. The sizes of the inserts are indicated on the right. The numbers refer to colonies screened. X = undigested plasmid. M = commercially-available 1 Kb plus ladder.

***TR-ACO1*-L1 (1.44k)**

AAATATTATTCTTACTGCTTATTTTTTTCTTTTCAAAATGAAGGCCAGCAATTACTTTTTGTATTAATC
AATTTGGTAAATGACTGTTAGGATTATTTTTTGTTTTAATCAATTTGGGTGAGGATTTGAATTTATCTT
ACCGTTTTAATGGGAGAAAATAGTATTGGTTGAATGGAAATAATTATTTTGGATATGTTTTAATTTGTT
TTGATTGGAGGATTTGATTTGATTATAATGATTCCCTAGAATATTTTTTATTTGTAGTTATTTCAATGA
TTTGAAGTTAATGTATGATTTTTTATTTTTATTTTTTGGTTTACAAAGTACAGTATGATTTTTGTTCAA
CTGGCAAAAATTTGCCGAAATTGCAAGGCCGGACGTCATGACCGGGGTTCGAACCCCGGCTCTCTCACT
TGTGTTAGAATTTATCATATTTACTTTGCCAATTCTTCTATGTACCAAAAAAAAAGTACAGTATGATTT
TTGTTCCAATTTAAGTGGATTGATTTTTTACATTTGAATTTAATCCACATAAAATCTCATTATAAATTG
ATACATTAGATTTTTTTTTCTTTCACTACCAGTTTAATCTGGTTCGGTGGTCAGTTCTGACATCAAGTG
ATTCTAATCTCCTTCTGATCGCAGCTGCGGAAGTATCAAACTGTGATCCTCTCTACCAAACACCAATCA
TCACTTAACCCACTAACGATTTCTTGACACATCAAAATTCTATGCCAAGAGACTTTGGAACAAAATTTC
TTATATACTACTTTCTTAATTAGTTTTAATTAATAATAGATTTTATTCTAAGATTCACTGAGAGCCTTG
GAATAAAATTTTTATTATTTTTTACATTCTTTAGCCATTCCCTCAAGTTGCAGGCCTATAAATACATCC
ATTTGCATTGCACTTATAACACTCACACTACTCACATCATATACACTCTTTATTCACATATAACTAAAT
ATCAAAGTGAGTGAAAAGAAAGAAAATTGAAAGAAGCAAA**ATG**GAAAACTTTCCAATTGTTGACATGGG
GAAGCTTAACACAGAAGAGAGAAAATCAACCATGGAGAAGATCAAAGATGCTTGTGAGAACTGGGGTTT
CTTTGAGGTACAAACTCTTTATATATATAAAAATTTCTTATGTTTGGACTAACAATATCTTTAACAGAA
TCACAGTGTCTCATCGTAATTTTGACAAAATATCACTTCAGAGTTTAACAGAATCACAGTGTCTCATCG
TAATTTTGTCAAACTTATTGTGATTTTAAGGCTTTCTAATATTATTCTTTGTATTGTTTTGTGAAGTTG
GTGAACCATGGAATATCTATTGAGATGATGGACAAAGTGGAGAAGCTCACAAAAGATCACTACAAGAAG
TGTATGGAACAAAGGTTCAAAGAAAT**GGTTTCAAGCAAAGGTTTGGAGTGTGTTCAGT-3'**

Figure 3.1.3 Sequence of the putative *TR-ACO1* promoter from the L1 digestion library

An 1440 bp DNA sequence isolated and sequenced from the L1 library (*Dra* I digestion). The putative ATG is boxed, and the inner nested reverse primer used to amplify the putative promoter sequence (Fig 2.1.2 A) is underlined.

Sequences producing significant alignments:

Access number	Gene	Source	Score (bits)	e-value
gi|4704655	*TR-ACO1*	*Trifolium repens*	256	4e-65
gi|169040	*PE8*	*Phaseolus lunatus*	161	2e-36
gi|12802438	*VR-ACO1*	*Vigna radiata*	117	3e-23
gi|458337	*VR-ACO1*	*Vigna radiata*	111	2e-21
gi|13570025	*PP-ACO2*	*Prunus persica*	94	4e-16

Trifolium repens **stolon apex 1-aminocyclopropane-1-carboxylate oxidase (ACO1) mRNA, partial cds**

```
Length = 1177, Score = 256 bits (129), Expect = 4e-65, Identities = 131/132 (99%), Strand = Plus / Plus

Query: 623 agttggtgaaccatggaatatctattgagatgatggacaaagtggagaagctcacaaaag 682
           ||||||||||||||||||||||||||||||||||||||||||||||||||||||||||||
Sbjct: 26  agttggtgaaccatggaatatctattgagatgatggacaaagtggagaagctcacaaaag 85

Query: 683 atcactacaagaagtgtatggaacaaaggntcaaagaaatggtttcaagcaaaggtttgg 742
           |||||||||||||||||||||||||||| ||||||||||||||||||||||||||||||
Sbjct: 86  atcactacaagaagtgtatggaacaaaggttcaaagaaatggtttcaagcaaaggtttgg 145

Query: 743 agtgtgttcagt 754
           ||||||||||||
Sbjct: 146 agtgtgttcagt 157
```

Pea 1-aminocyclopropane-1-carboxylate oxidase mRNA, complete cds

```
Length = 1122, Score = 161 bits (81), Expect = 2e-36, Identities = 93/97 (95%), Strand = Plus / Plus

Query: 331 ctttccaattgttgacatggggaagcttaacacagaagagagaaaatcaaccatggagaa 390
           |||||||||||||||||||||||||||||||||||| ||||||||||||||||||
Sbjct: 12  ctttccaattgttgacatggggaagcttaacacagaagacagaaaatcaaccatggagtt 71

Query: 391 gatcaaagatgcttgtgagaactggggtttctttgag 427
           |||||||||||| |||||||||||||||||||||||
Sbjct: 72  gatcaaagatgcctgtgagaactggggtttctttgag 108

Query: 628 gtgaaccatggaatatctattgagatgatggacaaagtggagaagctcacaaaagatcac 687
           ||||| ||||| ||||||||||||||||||| |  || |||||||| ||||| || |||
Sbjct: 112 gtgaatcatggtatatctattgagatgatggatacggttgagaagctgacaaaggaacac 171
```

Figure 3.1.4 Results from NCBI database BLAST-n analysis of the putative *TR-ACO1* sequence

Query = *TR-ACO1* sequence isolated in this thesis
Sbjct = *TR-ACO1* sequence (gi|4704655) or *PE8* sequence (gi|169040) in the database

any significant identity with other sequences in the database (data not shown).

3.1.1.4.2. GCG analysis of the TR-ACO1 sequence

The result of the alignment between the 3′ end of the *TR-ACO1* promoter sequence and the 5′ end of *TR-ACO1* gene sequence, indicates that a 197 bp intron is located 105 bp downstream from the translation start site (ATG). Immediately downstream of the ATG, a 78 bp sequence represents a novel sequence obtained upstream of that reported from the Genebank accession of *TR-ACO1* lodged by Hunter et. al. (1999) (GI 4704655) (Figure 3.1.5).

3.1.2. *TR-ACO2* promoter isolation

3.1.2.1 Amplification of the *TR-ACO2* promoter using Genome Walker™ PCR

Five libraries were amplified using the Genome Walker™ method with nested PCR primers. The primers used were nested forward primers based on the commercially-available 5′ adaptor sequence (AP-F1; AP-F2), and reverse primers based on the known 3′ sequence of the *TR-ACO2* gene (designated GW-ACO2-R1; GW-ACO2-R2, Section 2.8)(Figure 2.2). After two rounds of PCR, amplified products were present in two of the libraries. In L1 (*Eco* RV digested), 3500 bp and 1800 bp products were amplified, and 1600 bp and 700 bp products from the L2 (*Pvu* II digested) library (Figure 3.1.6).

3.1.2.2 Screening of the *TR-ACO2* promoter inserts in *E.coli*

The two amplified products from the L1, and the 1600 bp product from L2 libraries were purified, ligated into the p-GEM vector and transformed into *E. coli* strain DH-5α. After plating onto selection media, colonies were selected, the plasmid DNA isolated and then digested. Preliminary screening showed that seven colonies contained putative inserts were generated from the purified 1800 bp product of the L1 library (Figure 3.1.7 A), and colony #2 was chosen for further DNA sequencing. No inserts were obtained from the purified 3500 bp

TATAAATACATCCATTTGCATTGCACTTATAACACTCACACTACTCACATCA

TATACACTCTTTATTCACATATAACTAAATATCAAAGTGAGTGAAAAGAAAG

AAAATTGAAAGAAGCAAA**ATG**GAAAACTTTCCAATTGTTGACATGGGGAAGC

TTAACACAGAAGAGAGAAAATCAACCATGGAGAAGATCAAAGATGC**TTGTGA**

GAACTGGGGTTTCTTTGAG*gtacaaactctttatatatataaaaatttctta*

tgtttggactaacaatatctttaacagaatcacagtgtctcatcgtaatttt

gacaaaatatcacttcagagtttaacagaatcacagtgtctcatcgtaattt

tgtcaaacttattgtgattttaaggctttctaatattattctttgtattgtt

*ttgtga***AGTTGGTGAACCATGGAATATCTATTGAGATGATGGACAAAGTGGA**

GAAGCTCACAAAAGATCACTACAAGAAGTGTATGGAACAAAGGTTCAAAGAA

ATGGTTTCAAGCAAAGGTTTGGAGTGTGTTCAGT

Figure 3.1.5 Structure of the 3' region of the 1440 bp p*TR-ACO1* sequence

The comparison between the 5' end of the *TR-ACO1* partial genomic sequence isolated in this thesis (bold) shows 100 % identity with *TR-ACO1* (GI4704655). The upper dots represent novel sequence obtained in this study (78 bp) that is not included in the Genebank sequence of the *TR-ACO1* cDNA. The grey highlighted lower case *italics* is the first intron sequence. The lower dots indicate the inner nested reverse primer used to amplify the sequence. The ATG is bold and underlined. The upstream sequence from ATG sequence is only partially shown in this figure.

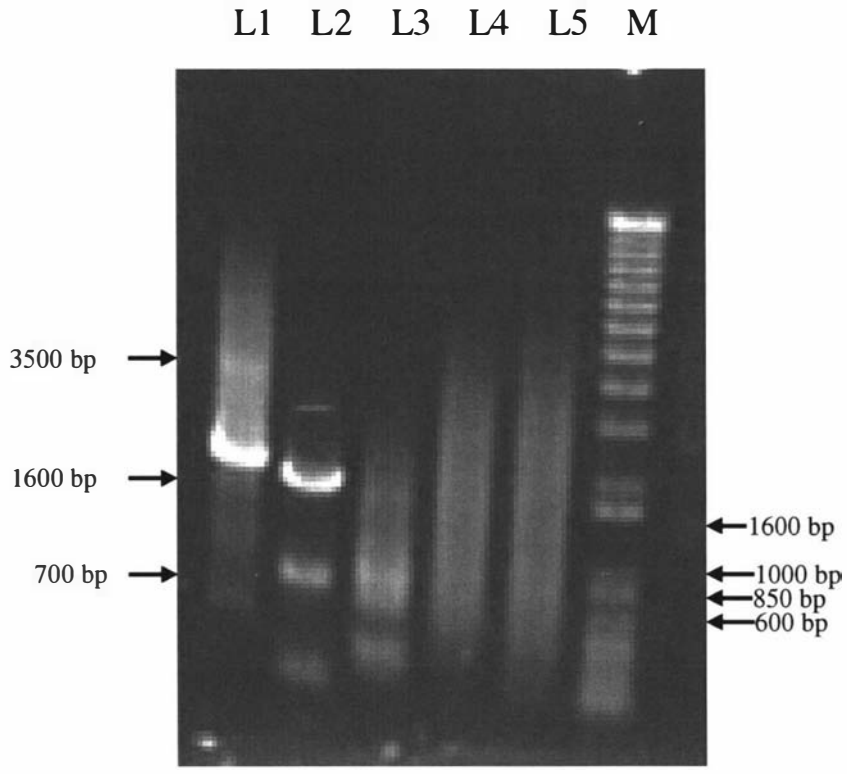

Figure 3.1.6 *TR-ACO2* promoter isolation using PCR

PCR-generated DNA fragments, using the GW-ACO2-R1 and AP-F1 primers for round one, and the GW-ACO2-R2 and AP-F2 primers for round two. PCR products were separated by electrophoresis on a 0.75 % (w/v) agarose gel and visualized with ethidium bromide. The relative sizes of the DNA ladder are indicated on the right.

L1: Two rounds of PCR amplification from a *Eco* RV digested library
L2: Two rounds of PCR amplification from a *Pvu* II digested library
L3: Two rounds of PCR amplification from a *Stu* I digested library
L4: Two rounds of PCR amplification from a *Sma* I digested library
L5: Two rounds of PCR amplification from a *Nae* I digested library

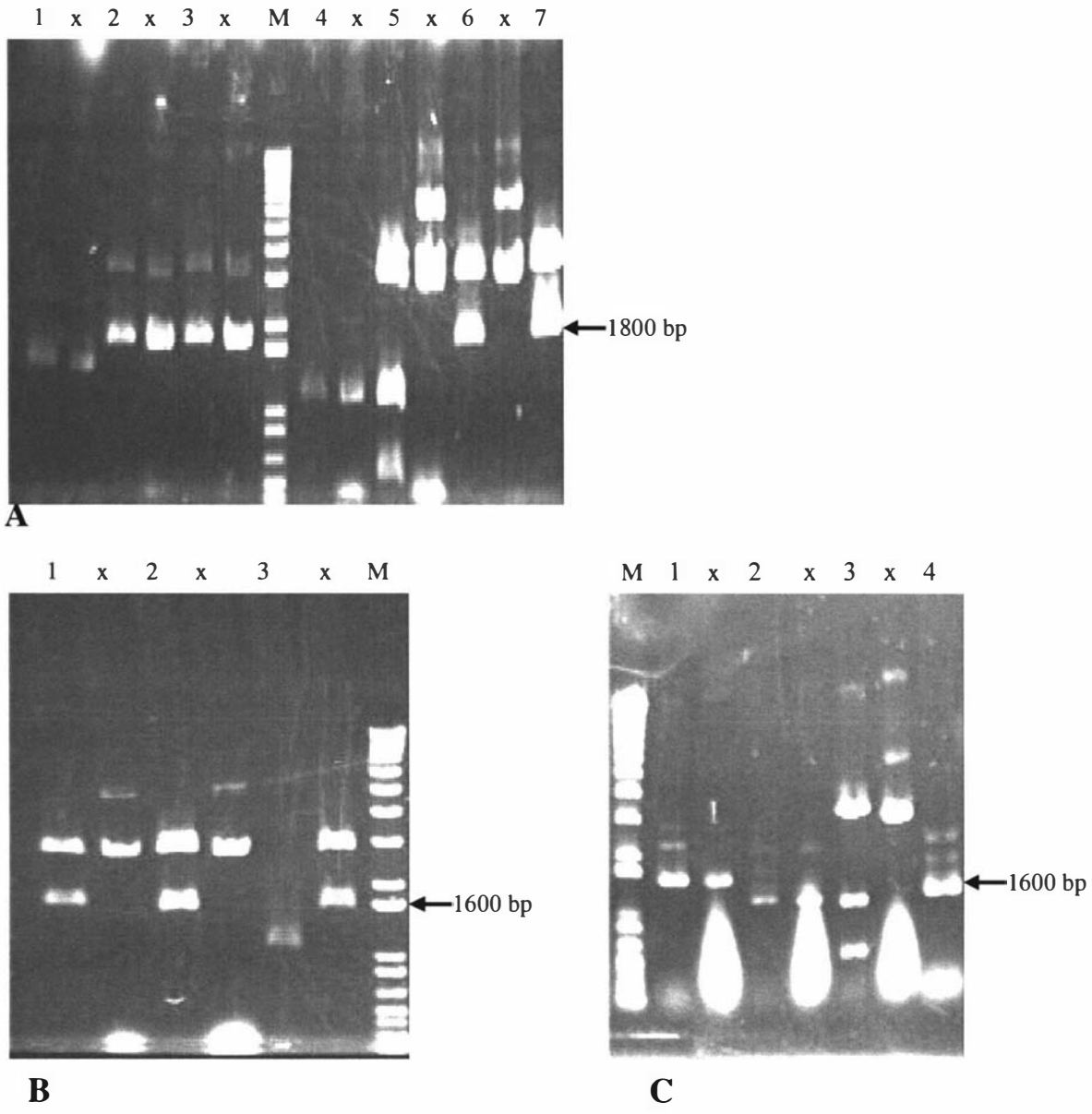

Figure 3.1.7 Restriction enzyme digestion screening of p-GEM plasmids containing putative *TR-ACO2* promoter inserts in *E. coli* cells

A. Screening of the L1 library (*Eco* RV digestion) with putative 1800 bp inserts
B. Screening of the L1 library (*Eco* RV digestion) with putative 3500 bp inserts
C. Screening of the L2 library (*Pvu* II digestion) with putative 1600 bp inserts

Products from *Eco* RI digests were separated on 0.8 % (w/v) agarose gel and visualized with ethidium bromide. The sizes of the inserts are indicated on the right. The numbers refer to colonies screened. X = undigested plasmid. M = commercially-available 1 Kb plus ladder.

product from the L1 library. Three colonies containing 1600 bp inserts were obtained, but these were not sequenced (Figure 3.1.7 B). Three colonies with putative 1600 bp inserts were obtained from the L2 library, and colony #2 was chosen for DNA sequencing (Figure 3.1.7 C).

3.1.2.3 Sequencing of the putative *TR-ACO2* promoter

The results of DNA sequencing showed that a 1750 bp insert was obtained from the original 1800 bp product from the L1 library (Figure 3.1.7 A) and no sequence was obtained from the original 1600 bp purified product from the L2 library. Therefore, the 1750 bp sequence was used for further analysis (Figure 3.1.8).

3.1.2.4 Confirmation of putative *TR-ACO2* promoter sequence

3.1.2.4.1. TR-ACO2 sequence analysis using BLAST-n

The alignment results from the NCBI BLAST-n database indicated that a 305 bp sequence was closely related to the *TR-ACO2* sequence isolated from white clover (Hunter et al., 1999). At least 80 different ACC oxidase genes were aligned, and highly conserved first intron and 5′ and 3′ splice sites can be detected in the *TR-ACO2* sequence (data not shown). Unlike *TR-ACO1*, the sequence with highest significant alignment is a cDNA sequence from *Medicago truncatula* (*MT-ACCO*), the next is white clover (*TR-ACO2),* and then a cDNA sequence from *Prunus persica* (*PP-ACO1*) (Figure. 3.1.9). A 187 bp sequence from the *TR-ACO2* isolated from this thesis is shown to have 89 % identity with the *M. truncatula* sequence (GI 17342710), while a 110 bp sequence from the database *TR-ACO2* (GI 4704657) is shown to have 96 % identity. In contrast with the reading frame, the upstream sequence from the putative ATG codon also show a 83 bp sequence alignment with the *MT-ACCO* sequence in the database.

***TR-ACO2*-L1 (1.75kb)**

ACCAGCATCTACCAAAAGTGTTTTGTCGCGGCCATTTTCGCGGTCGCGGACTTTTATTTGAAACCTTATTACTGTC
ATGTGATAGTGCCTTTTCATTAATGTTGTGATTCTGTCTTTTAATTTCTTTAATTAACATCAATATTGATTTATTT
ATTTTGATAGAGATTAACATCAATGTTGATTGTTGTGATTCTGTTTTTTAATTTCATTAATTCGTCACTATTACTA
TCACACTACAAAAATTTGCTCATTAGCCACGGTTATGTTTTTCTTTTTTGAAAGAATTAGCCACGGTTATGTTGAC
TGTGTCTGAATTGTATGTTTGCCACGGTTCTAAGCGTGGCTATAATATAATGATCATATATGTGATAGTGTATTAG
TGTTTTTTCATTTTATTTCATTTATTTATTTAATATTTTGTTATTATATATGCAGTTCTTTTACATCAATTCATAT
TTAAATTGCAAGAACATTGCTAAGGGCATTCAAACACCGTTCATGAAACTCACATAGTACTGTCTTTGCCAAAACT
CGCATATTAAATACATATTCCTATTACGTAATAATAATTCAATATATATTATTACTACTTTAGTTTAAAAAATATT
ATAGTCATTACTAATTTTTGAAATAAAAAAATATGCATCCACTAGTCCATGGTCCTAGATCCACCATTGTATATAAG
TATTTGTATGAATTTATGTATAAAGTATTTGGAATGAATTATTTTCTAAATTTTCTATTTTGTTAATGTTACTTTG
TTTATCAACTATGAAATTGGAAAATTATATAACGATTTAATGTAAACGATTTAATAACAGTTGAATCAGTTCGACC
GGTTGACTCTTGGACCAGTGACCACACCAATTCGAGTTCGGTGGTTTATACTATGTTAGAATGTGCGTCCAAAAAA
CATTTTCGTTTGGGAAATGCGAGTTCGAGGCTCCTTCTTAAACATCATTTTCAAATGCATTTAAAAAATGTTAAAT
AAAATAGAGAACAAATAGAGGTTGCGGCAGCCTTAGAAGTTGAATTTGGTCAAATGTTCAAGAGGAAAAACCAGCC
ATCAAGTAGGGCCAACCCTATGCCCAGTGTTTTTGACAAATCAACCAAAAGAACCCAAAATAAACACAAGCTTCTG
ATTAGAACTATTAATAATAAACAAAGAAAATTAAGCTGAACAAATCATACTATTAAAATATAAAATATATTCAATT
AGATTTAAAATAATAATAAGTTGTCTATTTGGTCTTGTGATGTAAAGGTCTATAAATACAACCTTCTAAGGAACTC
TAATATTCATCATAAAGCAAGCAACCTACAATAAACTTGGAGAAAGAAAAGCATACAAAAGAGTTCAAGTTAAGAG
TTTGTTTGAGAGATATGGAGAACTTCCCAATCATCAACTTAGAAAACCTCAATGGTGAGGAGAGAAAAGCTACCAT
GGAAAAAATCAAGGATGCTTGTGAAAACTGGGGATTCTTTGGGGTACCTAATGATCTCAATAAATAAAAGTTTTTT
TTCTTTTCAAATAAGTTTCTACATTGGCCTCTAAATCTGTATTCATATTTGTTTGTTTTTTTTTTCTGTAGCTGGT
GAATCATGGCATATCTCATGACTTAATGGACACTGTGGAGAGGTTGACAAAAGAACACTACAGAATATGTATGGAA
CAAAGATTCAAGGATTTGGTGGCCAAC-3′

Figure 3.1.8 Sequence of the putative *TR-ACO2* promoter from the L1 digestion library

An 1750 bp DNA sequence isolated and sequenced from the L1 library (*Eco* RV digestion). The putative ATG is boxed, and the inner nested reverse primer used to amplify the putative promoter sequence (Fig 2.1.7 A) is underlined.

Sequences producing significant alignments:

Access number	Gene	Source	Score (bits)	E-value
gi|17342710	*MT-ACCO*	*Medicago truncatula*	198	6e-48
gi|4704657	*TR-ACO2*	*Trifolium repens*	188	6e-45
gi|7108576	*PP-ACO1*	*Prunus persica*	109	5e-21
gi|16588827	*PP-ACO1*	*Prunus persica*	107	2e-20
gi|452670	*PAO1*	*Prunus persica*	107	2e-20

Medicago truncatula **1-aminocyclopropanecarboxylic acid oxidase mRNA, complete cds** Length = 1279

Score = 198 bits (100), Expect = 6e-48, Identities = 168/187 (89%), Gaps = 4/187 (2%), Strand = Plus / Plus

```
Query: 162 tcataaagcaagcaacctacaataaacttggagaaagaaaagcatacaa-aagagttc-- 218
           |||||||||| ||||||||||||||||||||||||||||||||||||| |||||||
Sbjct: 1   tcataaagca-gcaacctacaataaacttggagaaagaaaagcatacaacaagagttttt 59
Query: 219 aagttaagagtttgtttgagagatatggagaacttcccaatcatcaacttagaaaacctc 278
           |||||||||  || | | | | ||||||| | ||||||||| ||||||||||||||||
Sbjct: 60  aagttaagaaattctattaaaaatatggatagcttcccaattatcaacttagaaaacctg 119
Query: 279 aatggtgaggagagaaaagctaccatggaaaaaatcaaggatgcttgtgaaaactgggga 338
           |||||||| |||||||||||||| ||||| ||||||||||||||||||||||||||||
Sbjct: 120 aatggtgatgagagaaaagctactatggagaaaatcaaggatgcttgtgaaaactgggga 179
Query: 339 ttctttg 345
           |||||||
Sbjct: 180 ttctttg 186
Query: 450 agctggtgaatcatggcatatctcatgacttaatggacactgtggagaggttgacaaaag 509
           |||||||||||||||||| |||||||||||||||||||||||||||||| || ||||
Sbjct: 187 agctggtgaatcatggcatacctcatgacttaatggacactgtggagaggttaaccaaag 246
Query: 510 aacactacagaatatgtatggaacaaagattcaagga 546
           |||||||||| | ||| ||||||||||||||||||||
Sbjct: 247 aacactacaggaaatgcatggaacaaagattcaagga 283
```

Trifolium repens **mature green leaf 1-aminocyclopropane-1-carboxylate oxidase (ACO2) mRNA, partial cds**

Length = 1114, Score = 188 bits (95), Expect = 6e-45, Identities = 106/110 (96%), Strand = Plus / Plus

```
Query: 450 agctggtgaatcatggcatatctcatgacttaatggacactgtggaaaggttgacaaaag 509
           ||||||||||||||||||||||||||||||||||||||||||||||||||||||||||||
Sbjct: 26  agctggtgaatcatggcatatctcatgacttaatggacactgtggaaaggttgacaaaag 85
```

Figure 3.1.9 Results from NCBI database BLAST-n analysis of the putative *TR-ACO2* sequence

Query = *TR-ACO2* sequence isolated in this thesis
Sbjct = *MT-ACCO* sequence (gi|17342710) and *TR-ACO2* sequence (gi|4704657) in the database

3.1.2.4.2. GCG analysis of the TR-ACO2 promoter sequence

The result of the alignment between the 3′ end of the *TR-ACO2* promoter sequence and the 5′ end of the *TR-ACO2* gene sequence reveals a 104 bp intron located 103 bp downstream from the translation start site (ATG). Immediately downstream of the ATG, a 78 bp sequence represents novel sequence obtained upstream of that reported from the Genebank accession of *TR-ACO2* lodged by Hunter et. al. (1999) (GI 4704657) (Figure 3.1.10).

3.1.3. *TR-ACO3* promoter isolation

3.1.3.1 Amplification of the *TR-ACO3* promoter using Genome Walker™ PCR

Five libraries were amplified using the Genome Walker™ method with nested PCR primers. The primers used were nested forward primers based on the commercially-available 5′ adaptor sequence (AP-F1; AP-F2), and reverse primers based on the known 3′ sequence of the *TR-ACO3* gene (designated GW-ACO3-R1; GW-ACO3-R2, Section 2.8)(Figure 2.2). After two rounds of PCR, amplified products were present in three libraries. A 800 bp product was amplified from the L1 (*Eco* RV digested) library, 700 bp and 1600 bp products were amplified from the L2 (*Pvu* II digested) library, and 1600 bp and 3000 bp products were amplified from the L3 (*Stu* I digested) library (Figure 3.1.11).

3.1.3.2 Screening of the *TR-ACO3* promoter inserts in *E.coli*

The two amplified products of the L3 library were purified, ligated into the p-GEM vector and transformed into *E. coli* strain DH-5α. After plating onto selection media, colonies were selected, the plasmid DNA isolated and then digested. Preliminary screening showed that three colonies contained putative 1600 bp inserts from the (3000 bp) L3 library (Figure 3.1.12 A) and colony #2 was chosen for further DNA sequencing. Also, two colonies containing

AGATTTAAAATAATAATAAGTTGTCTATTTGGTCTTGTGATGTAAAGGTCTA

TAAATACAACCTTCTAAGGAACTCTAATATTCATCATAAAGCAAGCAACCTA

CAATAAACTTGGAGAAAGAAAAGCATACAAAAGAGTTCAAGTTAAGAGTTTG

TTTGAGAGAT**ATG**GAGAACTTCCCAATCATCAACTTAGAAAACCTCAATGGT

GAGGAGAGAAAAGCTACCATGGAAAAAATCAAGGATGCT**TGTGAAAACTGGG**

GATTCTTTG*gggtacctaatgatctcaataaataaaagtttttttctttc*

aaataagtttctacattggcctctaaatctgtattcatatttgtttgttttt

*ttttctgt***AGCTGGTGAATCATGGCATATCTCATGACTTAATGGACACTGT**

GGAAAGGTTGACAAAAGAACACTACAGAATATGTATGGAACAAAGATTCAAG

GATTTGGTGGCCAAC

Figure 3.1.10 Structure of the 3' region of the 1750 bp p*TR-ACO2* sequence

The comparison between the 5' end of the *TR-ACO2* partial genomic sequence isolated in this thesis (bold) shows 100 % identity with *TR-ACO2* (GI4704657). The upper dots represent novel sequence obtained in this study (78 bp) that is not included in the Genebank sequence of the *TR-ACO2* cDNA. The grey highlighted *italics* lower case is the first intron sequence. The lower dots indicate the inner nested reverse primer used to amplify the sequence. The ATG is bold and underlined. The upstream sequence from ATG sequence only partially shown in this figure.

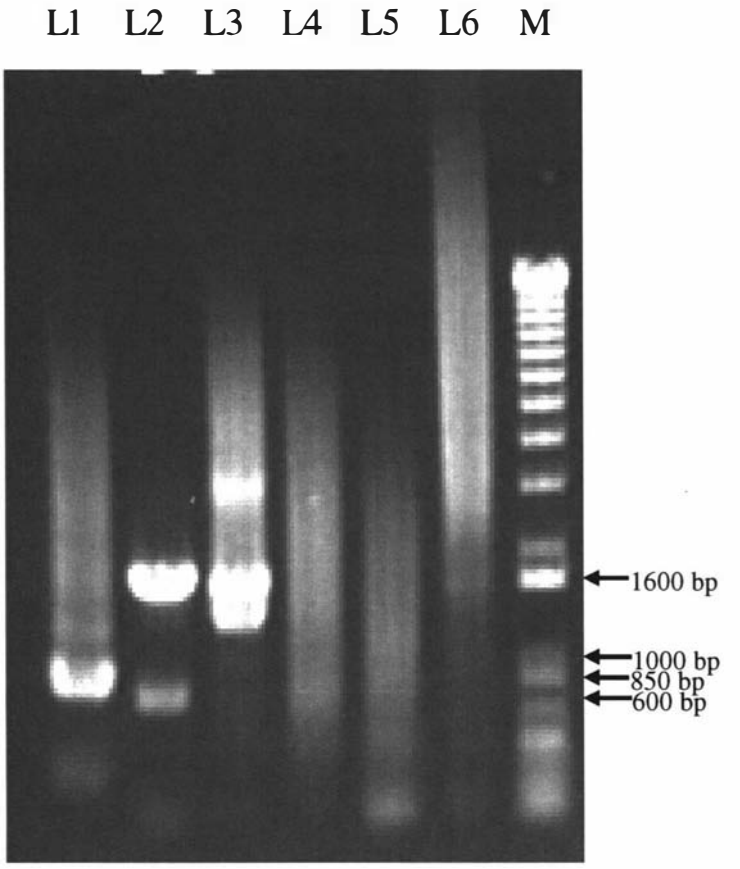

Figure 3.1.11 *TR-ACO3* promoter isolation using PCR

PCR-generated DNA fragments, using the GW-ACO3-R1 and AP-F1 primers for round one, and the GW-ACO3-R2 and AP-F2 primers for round two, to amplify putative *TR-ACO3* promoter fragments. PCR products were separated by electrophoresis on a 0.75 % (w/v) agarose gel and visualized with ethidium bromide. The relative sizes of the DNA ladder are indicated on the right.

L1: Two rounds of PCR amplification from a *Eco* RV digested library
L2: Two rounds of PCR amplification from a *Pvu* II digested library
L3: Two rounds of PCR amplification from a *Stu* I digested library
L4: Two rounds of PCR amplification from a *Sma* I digested library
L5: Two rounds of PCR amplification from a *Nae* I digested library
L6: Two rounds of PCR amplification from a *Dra* I digested library

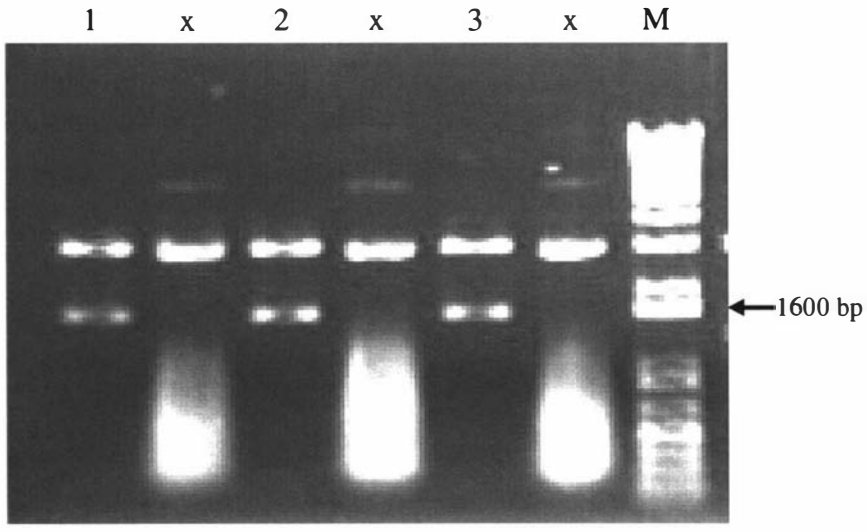

A

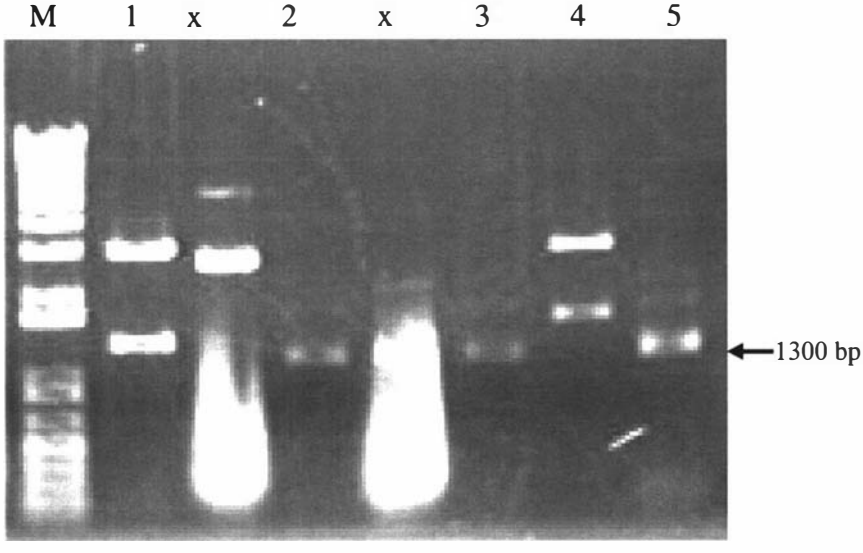

B

Figure 3.1.12 Restriction enzyme digestion screening of p-GEM plasmids containing putative *TR-ACO3* promoter inserts in *E. coli* cells

A. Screening for L3 library (*Stu* I digestion) with putative 1600 bp inserts
B. Screening for L3 library (*Stu* I digestion) with putative 1300 bp inserts

Products from *Eco* RI digests were separated on 0.8 % (w/v) agarose gel and visualized with ethidium bromide. The sizes of the inserts are indicated on the right. The numbers refer to colonies screened. X = undigested plasmid. M = commercially-available 1 Kb plus ladder.

putative 1300 bp inserts were identified from the (1600 bp) L3 library (Figure 3.1.12 B) and colony #1 was chosen for DNA sequencing.

3.1.3.3 Sequencing of the putative *TR-ACO3* promoters

The results of DNA sequencing showed a 1566 bp insert was obtained from the original 1600 bp purified product of the L3 library, and a 1264 bp insert from the original 1300 bp purified product. These two sequences were 85 % identical (Figure 3.1.13 and 3.1.14). Since both were isolated from the same library (Figure 3.1.11 L3), but from different sized products using the Genome Walker™ procedure, they were both used for further experiments (and designated *TR-ACO3-1* (1566 bp) and *TR-ACO3-2* (1264 bp)).

3.1.3.4 PCR extension of the *TR-ACO3* promoters

The 1264 bp sequence was considered to be too truncated for further study. Thus another set of primers (designated GW-ACO32-ext R1; GW-ACO32-ext R2 Section 2.2) were designed to extend the sequence using the GenomeWalker™ libraries as template. Using nested PCR, several smeared lower molecular weight bands were obtained from the six original libraries (Figure 3.1.15). Several of these bands were ligated into p-GEM vectors, transformed into *E. coli*, and colonies only obtained from the *ca.* 500 bp purified band isolated from L6. After selection, plasmid isolation and digestion, three colonies containing putative 500 bp inserts from L6 was obtained (Figure 3.1.16). One of these colonies (# 1) was sequenced, and a 390 bp extension sequence was identified that extended the 5′ end of the 1264 bp *TR-ACO3-2* sequence to make a 1654 bp sequence for further analysis (Figure 3.1.17).

3.1.3.5 Confirmation of the putative *TR-ACO3* promoter sequences

***TR-ACO3*-1 (1.56kbp)**

CCTACATGTCTTAAACCTACTGTATCTTAAAATCTAAAAAGTCAATTTTTTTAGGATAAGTAGGCTTATACCCCCC
TGTAATGTAGGCAAGTTTTGTTTTCCCCCTGTAATTTTTTTTTTTGTGACTCGCCCTTTGCAATGTTGAATATTTTT
TTTCCCAGTTCATTTTACCCCATGTAATGTTGGCCTTTACTCCCCTGCAAGGGGTAAAAATGAACTAAAAGAGAAA
AAAATCAACATTGCAAGGGGCAAGTCAGACAAAAAAAAATTATAGGGGGAAAACCAAAACTCGCCCATATTAAGGG
GATATTAACCTATTTACCCCATTTTTTATTAGACGGCTCACAAGTGCACTTAATCCAATTTAATACCATACAAAGG
TACCATTAATGAGCACTTCATTTCTCACATATATTCTACAGAAGCTCAAGTCATTCCGTACAAGAAAGCATATAAG
TAATTAAGAAACAAATGTAACATAAACCTGTCATTCTGTCCCAACTTTTCTCCAATACAAAGATGCTATAATTTTG
GAAGTGCTGAGTTCAAAAGAAAATTATGTTGGAAGTAAATGGAGTTGTTATGTTCCTTCCTAGAAGTTACCTTTAT
AGTATATCATATGACCCCAAAATAAATGTCACTTCACAACTCAATAACTCATAAGAGAAAAGTAAATTCCAGAATT
GATAGATAGAGGTGGCAGCTTGTATTGTACTGTTTTGGTCAAATTTTTAAAAGGAGAAAAGAAATCAGCCACCAAG
TGGGTCCATAACTTACACAAAGTTCACAGACAATTCAAATACGGAACCAAAATAAATCATGGCTGTGATTTGTATT
AAAAGTAAAGATAAAACATAGACATGCAAATATTGAACAAGGATTCTTCTTTTAGTGATTGGTCCACATCATATCT
AGGTCTATGGAATTAGATTCATGTTATAATTGCATCCTACAATTACAACTCTCAACCATTCGATCTTAAATGATGA
TTGAGATCATTTTACTATGTGAATTGACAGTGATCTAGACCGTCCGATTTCGAATTAACAGTCGAGATTTATTAAT
ACGTGAAACTATGTGAAAGTTGAAACGACAGGTAATCTTTGATTCCGGTCTATAAATACCATGCTGCCTAACTCCA
ACATGCATAAATCAAAAGAGCAATAGGAAGATAGAAACTAGAAAGGGAGTTACCTTGAGTTTAAGAAATGATGATG
AACTCCCCAATTATCAGCTTGGAGAGACTCAATGGTGTGGAGAGAAAAGATACCATGGAGAAAATAAAGGATGCTT
GTGAGAATTGGGGATTCTTTGAGGTACTTCAGGAACACAATAAAAAAACTTTTTACTACAACTTTAATTTATACAA
TACATTTCCCTCTAAATATCTATTCATGTTAGTTGTTCATGTTACTTTCTTGGTTTAACTATTCTTATTCTTTGCT
TTCAAAAATCTAGCTGGTGAATCATGGCATACCTCATGACCTTATGGACACATTGGAGAGATTGACCAAAGAGCAC
TACAGGAAATGCATGG**AGCAGAGGTTTAAGGAATTGGTATCAAGCA**

Figure 3.1.13 Sequence of the putative *TR-ACO3-1* promoter from the L3 digestion library

An 1566 bp DNA sequence isolated and sequenced from the L3 library (*Stu* I digestion). The putative ATG is boxed, and the inner nested reverse primer used to amplify the putative promoter sequence (Fig 2.1.12 A) is underlined.

***TR-ACO3*-2 (1.24kbp)**

CCTGCGTGTCTAAAAGCTATCTTAAAATCTAAACAATCAAATTTTTTTTATTAGACGGTTCACAAGTGCACTTAAT
CCAATTTCATATACCATACAAAGGTACCATTAATGAGCACTTCATTTCTCACATATTCTATAGAAGCTCAAGTCAT
TCCGTACAAGAAAGCATAGTAAGTAATTTAAGAACAAATGCAACATAAATCTGTCATTCTGTCCCAACTTTTCTCC
AATACAAAGATGCTATAATTTTGGAAGTGCCGAGTCAAAAAGAAAATTATGTTGGAAGTGCATGGGAGTTGTTTAT
GTTCCCTCCTAGAAGTTACCTTTATATCATATGACCCCAAAATAAATGTCACAACTCAATAACTCGTAAGAGAAAA
GTAAATTCCAGAATTGATAGATAGAGGTGGCAGTTTGTATTGTACTGTTTTGGTCAAATTTTTAAAAGGAGAAAAG
AAATCAGCCACCAAGTGGGTCCATAACTTACACAAAGTTGATAGACAATTCAAATACGGAACCAAAATAAATCATA
TGGCTGTGATTTGTATTAAAAGTAAAGGATAAAACATAGAACATGCAAAAATTGAACAAAGTATTCTTTTTTAGTG
ATTGGGCCCTCATTAATATCCTAGGGGCTATGGGAACTATATTCATGTTTATAAACTGGGGTGTTCCGCGTTCATG
TAATTACAGGCACTTCAGCTGTCTGATTCTAGAATGGACAGCTGAGATTCGTTTTATTATGTGAATTGGACGGTGA
TCTAGACCGTTCGATTTTTGAATTAACAGTCGAGATTTATTAATACGTGAAACTATGTGAAAGTTGAAACAACAGG
TAATCTTTGATTCCTAGGTCTATAAATACCATGCTGCCTAACTCCAACATGCATAAAGCAAAAGAGCAATAGGAAG
ATAGAAACTAGAAAGAGAGTTACTTTGAGTTTAAGTTATGATGATGAACTTCCCGATTATCAGCTTAGAGAGACTC
AATGGTGTGGAGAGAAAAGATACCATGGCGAAAATAAAAGATGCTTGTGAAAATTGGGGATTCTTTGAGGTACTTC
AAGAATACATAATAAAATGTTTTATGCTACAACTTTGATTTATACAATACATTTCCCTCTAAATATCTATTCATGT
TACTTTCTTGGTTTAACGATTCTTATTGTTTGCTTTCAAAAATCCAGCTGGTGAATCATGGCATACCTCATGACCT
TATGGACACATTGGAGAGATTGACCAAAGAGCACTACAGGAAATGCATGG**AGCAGAGGTTTAAGGAATTGGTATCA**
AGCA

Figure 3.1.14 Sequence of the putative *TR-ACO3-2* promoter from the L3 digestion library

An 1264 bp DNA sequence isolated and sequenced from the L3 library (*Stu* I digestion). The putative ATG is boxed, and the inner nested reverse primer used to amplify the putative promoter sequence (Fig 2.1.12 A) is underlined.

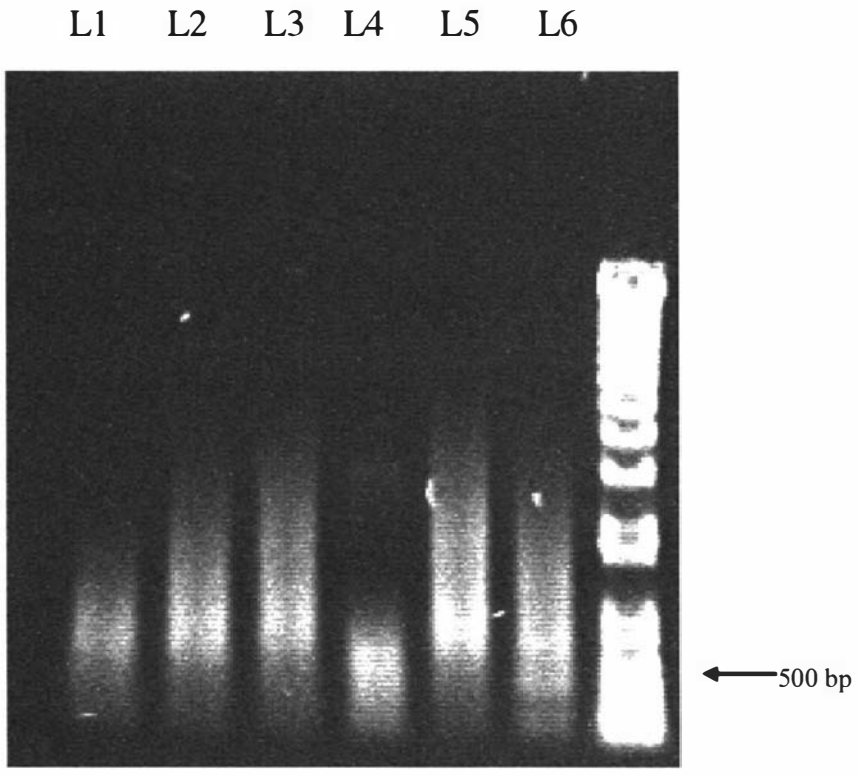

Figure 3.1.15 *TR-ACO3-2* promoter extending isolation using PCR

PCR-generated DNA fragments, using the GW-ACO32-extR1 and AP-F1 primers for round one, and the GW-ACO32-extR2 and AP-F2 primers for round two, to amplify putative extending *TR-ACO3-2* promoter fragments. PCR products were separated by electrophoresis on a 0.75 % (w/v) agarose gel and visualized with ethidium bromide. The relative size of the DNA ladder is indicated on the right.

L1: Two rounds of PCR amplification from a *Dra* I digested library
L2: Two rounds of PCR amplification from a *Eco* RI digested library
L3: Two rounds of PCR amplification from a *Pvu* II digested library
L4: Two rounds of PCR amplification from a *Stu* I digested library
L5: Two rounds of PCR amplification from a *Sma* I digested library
L6: Two rounds of PCR amplification from a *Nae* I digested library

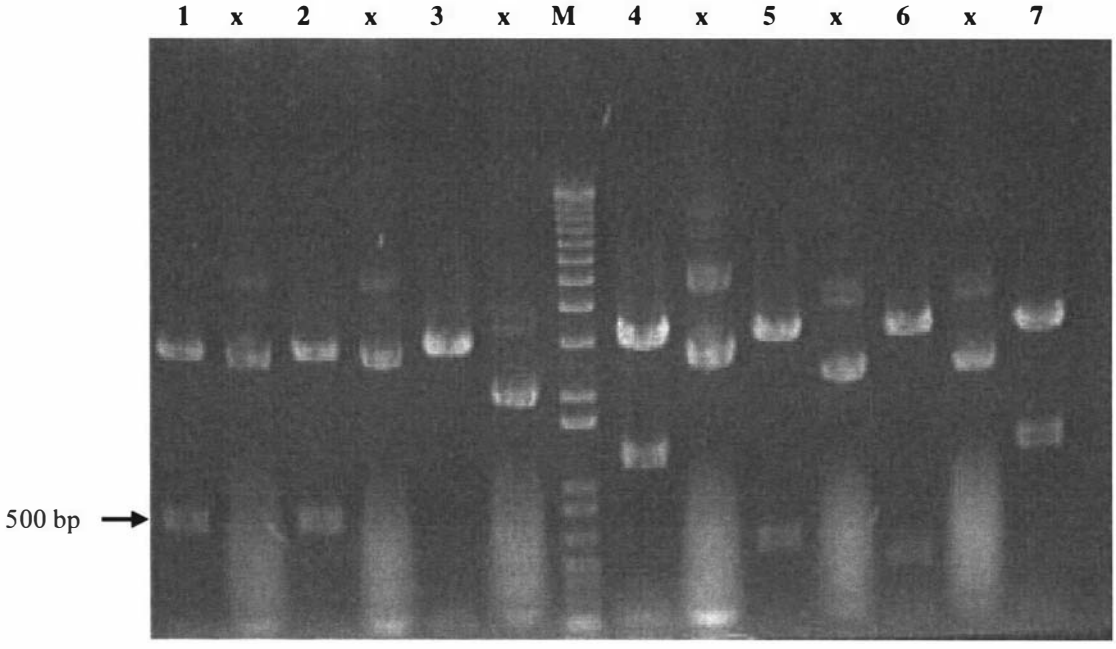

Figure 3.1.16 Restriction enzyme digestion screening of p-GEM plasmids containing putative *TR-ACO3-2* extension promoter inserts in *E. coli* cells

Screening of the L6 library (*Nae* I digestion) for putative 500 bp inserts. Products from the *Eco* RI digested were separated on 0.8 % (w/v) agarose gel and visualized with ethidium bromide. The size of the inserts are indicated on the left. The numbers refer to colonies screened. X = undigested plasmid. M = commercially-available 1 Kb plus ladder.

***TR-ACO3*-2-EXT (1.24+0.4kbp)**

AAACTGATCCCACTAACCCACAAAAATTGAGTTAAAAATAGGGGAAAATAATACGACTCACTATAGGGCACGCGTG
GTCGATGACCCGGGCTGGTAAATTCTCTCAAAGCGTTAACCATGTCTGGTATGCCTTTTTCTGTTGTTTTTTTATT
TTTACCAGCCCTACGACTCACTATAGGGCACGCGTGGTCGACGGCCCGGGCTGGTAAACATAAACGAATTGATTAA
ACAGAAATTGTTTTCAATCTGTTTAAACGACTCACTATAGGGCACGCGTGGTCGACGGCCCGGGCTGGTAAACATA
AACGAATTGATTAAACAGAAATTGTTTTCAATCTGTTTAAACGACTCACTATAAGGCACGCGTGGTCGACCGCCCG
GGCTGGTcctgcgtgtctaaaagctatcttaaaatctaaacaatcaaatttttttattagacggttcacaagtgc
acttaatccaatttcATATACCATACAAAGGTACCATTAATGAGCACTTCATTTCTCACATATTCTATAGAAGCTC
AAGTCATTCCGTACAAGAAAGCATAGTAAGTAATTTAAGAACAAATGCAACATAAATCTGTCATTCTGTCCCAACT
TTTCTCCAATACAAAGATGCTATAATTTTGGAAGTGCCGAGTCAAAAAGAAAATTATGTTGGAAGTGCATGGGAGT
TGTTTATGTTCCCTCCTAGAAGTTACCTTTATATCATATGACCCCAAAATAAATGTCACAACTCAATAACTCGTAA
GAGAAAAGTAAATTCCAGAATTGATAGATAGAGGTGGCAGTTTGTATTGTACTGTTTTGGTCAAATTTTTAAAAGG
AGAAAAGAAATCAGCCACCAAGTGGGTCCATAACTTACACAAAGTTGATAGACAATTCAAATACGGAACCAAAATA
AATCATATGGCTGTGATTTGTATTAAAAGTAAAGGATAAAACATAGAACATGCAAAAATTGAACAAAGTATTCTTT
TTTAGTGATTGGGCCCTCATTAATATCCTAGGGGCTATGGGAACTATATTCATGTTTATAAACTGGGGTGTTCCGC
GTTCATGTAATTACAGGCACTTCAGCTGTCTGATTCTAGAATGGACAGCTGAGATTCGTTTTATTATGTGAATTGG
ACGGTGATCTAGACCGTTCGATTTTTGAATTAACAGTCGAGATTTATTAATACGTGAAACTATGTGAAAGTTGAAA
CAACAGGTAATCTTTGATTCCTAGGTCTATAAATACCATGCTGCCTAACTCCAACATGCATAAAGCAAAAGAGCAA
TAGGAAGATAGAAACTAGAAAGAGAGTTACTTTGAGTTTAAGTTATGATGATGAACTTCCCGATTATCAGCTTAGA
GAGACTCAATGGTGTGGAGAGAAAAGATACCATGGCGAAAATAAAAGATGCTTGTGAAAATTGGGGATTCTTTGAG
GTACTTCAAGAATACATAATAAAATGTTTTATGCTACAACTTTGATTTATACAATACATTTCCCTCTAAATATCTA
TTCATGTTACTTTCTTGGTTTAACGATTCTTATTGTTTGCTTTCAAAAATCCAGCTGGTGAATCATGGCATACCTC
ATGACCTTATGGACACATTGGAGAGATTGACCAAAGAGCACTACAGGAAATGCATGG**AGCAGAGGTTTAAGGAATT**
GGTATCAAGCA

Figure 3.1.17 Sequence of the putative *TR-ACO3-2* extension from the L6 digestion library

A 471 bp DNA sequence isolated and sequenced from the L6 library (*Not* I digestion). The 3′ end of the overlapping sequence is highlighted in lower case. The extended sequence is underlined, and the inner nested reverse primer used to amplify the putative promoter sequence is boxed. The remaining sequence is the original isolated *TR-ACO3-2* sequence.

3.1.3.5.1. TR-ACO3-1 and TR-ACO3-2 sequence analysis using BLAST-n

The alignment indicated that a 355 bp sequence from both *TR-ACO3-1* and *TR-ACO3-2* was most closely related to *TR-ACO3* from white clover. At least 105 different ACC oxidase genes were aligned, and a highly conserved first intron and 5′ and 3′ splice sites were also present in the *TR-ACO3-1* and *TR-ACO3-2* sequences (data not shown). Excluding the white clover *TR-ACO3* sequence isolated by Hunter et al (1999), the second most identical sequence to both *TR-ACO3-1* and *TR-ACO3-2* was as cDNA, *MT-ACCO* from *M. truncatula*, and then the third from *Phaseolus lunatus* (*PL-ACO1*) (Figure 3.1.18). A 111 bp and a 17 bp sequence that are identical in both *TR-ACO3-1* and *TR-ACO3-2* sequences is shown aligned to *TR-ACO3* from database (GI 4704659) and *M. truncatula* (GI 17342710). The upstream sequence from the putative ATG does not show any identity with other sequence in the database.

3.1.3.5.2. GCG analysis of the TR-ACO3-1 (1566 bp) and the TR-ACO3-2 (1654 bp) promoter sequences

The result of the alignment between the 3′ end of the *TR-ACO3-1* and *TR-ACO3-2* promoter sequences and the 5′ end of the *TR-ACO3* gene sequence, reveals a 142 bp intron in *TR-ACO3-1* and a 131 bp intron in *TR-ACO3-2*, both located 105 bp downstream from the putative translation site (ATG). Immediately downstream of the ATG, a 84 bp sequence represents novel sequence obtained upstream of that reported from the Genebank sequence accession *TR-ACO3* lodged by Hunter et. al. (1999) (Figure 3.1.19). A comparison of *TR-ACO3* with the *TR-ACO3-1* and *TR-ACO3-2* sequences reveals 94 % identity over the exon 1 sequences (105 bp), and 94 % identity over the 84 bp novel sequence.

In both *TR-ACO3-1* and *TR-ACO3-2,* one of three consecutive ATG codons may represent the

Sequences producing significant alignments:

Access number	Gene	Source	Score (bits)	E-value
gi|4704659	*TR-ACO3*	*Trifolium repens*	220	2e-54
gi|17342710	*MT-ACCO*	*Medicago truncatula*	111	1e-21
gi|18157332	*PL-ACO1*	*Phaseolus lunatus*	109	5e-21
gi|3037046	*PV-ACO1*	*Phaseolus vulgaris*	96	7e-17
gi|9857251	*PAO1*	*Diospyros kaki*	92	1e-15

Trifolium repens **senescent leaf 1-aminocyclopropane-1-carboxylateoxidase (ACO3) mRNA, partial cds**

Length = 1164, Score = 220 bits (111), Expect = 2e-54, Identities = 111/111 (100%), Strand = Plus / Plus

Query: 468 agctggtgaatcatggcatacctcatgaccttatggacacattggagagattgaccaaag 527

Sbjct: 26 agctggtgaatcatggcatacctcatgaccttatggacacattggagagattgaccaaag 85

Query: 528 agcactacaggaaatgcatggagcagaggtttaaggaattggtatcaagca 578

Sbjct: 86 agcactacaggaaatgcatggagcagaggtttaaggaattggtatcaagca 136

Score = 37.1 bits (18), Expect = 3.6, Identities = 18/18 (100%), Strand = Plus / Plus

Query: 310 aattggggattctttgag 327

Sbjct: 10 aattggggattctttgag 27

Medicago truncatula **1-aminocyclopropanecarboxylic acid oxidase mRNA, complete cds**

Length = 1279, Score = 111 bits (56), Expect = 1e-21, Identities = 89/100 (89%), Strand = Plus / Plus

Query: 468 agctggtgaatcatggcatacctcatgaccttatggacacattggagagattgaccaaag 527

Sbjct: 187 agctggtgaatcatggcatacctcatgacttaatggacactgtggagaggttaaccaaag 246

Query: 528 agcactacaggaaatgcatggagcagaggtttaaggaatt 567

Sbjct: 247 aacactacaggaaatgcatggaacaaagattcaaggaatt 286

Figure 3.1.18 Results from NCBI database BLAST-n analysis of the putative *TR-ACO3-1* and *TR-ACO3-2* sequences

Query = *TR-ACO3-1* and *TR-ACO3-2* sequences isolated in this thesis
Sbjct = *TR-ACO3* sequence (gi|4704659) and *MT-ACCO* sequence (gi|17342710) in the database

TR-ACO3-1

ACATGCATAAATCAAAAGAGCAATAGGAAGATAGAAACTAGAAAGGGAGTTACCTTGAGTTTA

AGAA**ATGATGATG**AACTCCCCAATTATCAGCTTGGAGAGACTCAATGGTGTGGAGAGAAAAGA

TACCATGGAGAAAATAAAGGATGCTTGTGAG**AATTGGGGATTCTTTGAG***GTACTTCAGGAACA*

CAATAAAAAAACTTTTTACTACAACTTTAATTTATACAATACATTTCCCTCTAAATATCTATT

CATGTTAGTTGTTCATGTTACTTTCTTGGTTTAACTATTCTTATTCTTTGCTTTCAAAAATCT

*AG***CTGGTGAATCATGGCATACCTCATGACCTTATGGACACATTGGAGAGATTGACCAAAGAGC**

ACTACAGGAAATGCATGGAGCAGAGGTTTAAGGAATTGGTATCAAGCA

TR-ACO3-2

TAGGAAGATAGAAACTAGAAAGAGAGTTACTTTGAGTTTAAGTTATGATGATGAACTTCCCGA

TTATCAGCTTAGAGAGACTCAATGGTGTGGAGAGAAAAGATACCATGGCGAAAATAAAAGATG

CTTGTGAA**AATTGGGGATTCTTTGAG***GTACTTCAAGAATACATAATAAAATGTTTTATGCTAC*

AACTTTGATTTATACAATACATTTCCCTCTAAATATCTATTCATGTTACTTTCTTGGTTTAAC

*GATTCTTATTGTTTGCTTTCAAAAATCCAG***CTGGTGAATCATGGCATACCTCATGACCTTATG**

GACACATTGGAGAGATTGACCAAAGAGCACTACAGGAAATGCATGGAGCAGAGGTTTAAGGAA

TTGGTATCAAGCA

Figure 3.1.19 Structure of the 3´ region of the *TR-ACO3-1* and the *TR-ACO3-2* sequences

The comparison between the 5´ end of the *TR-ACO3-1* and *TR-ACO3-2* partial genomic sequence isolated in this thesis (bold) both show 100 % identity with *TR-ACO3* (GI4704659). The upper dots represent novel sequence obtained in this study (84 bp) that is not included in the Genebank sequence of the *TR-ACO3* cDNA. The grey highlighted *italics* upper case is the first intron sequence. The lower dots indicate the inner nested reverse primer used to amplify the sequence. The three possible ATGs are bold and underlined. The upstream sequence from ATG sequence only partial shown in this figure.

translation start. Alignment of ACO genes from other species suggests that the second ATG is the translation start since this puts a proline residue at amino acid position 5. This proline at position 5 is conserved in many ACO genes that have been sequenced (Figure 3.1.20). Further, downstream of the second ATG, both *TR-ACO3* sequences align with a cDNA of the *P. lunatus, P. vulgaris* and *M. truncatula* sequences. Finally, designation of the middle ATG as the translation start is also supported by alignment in which the 5′ and 3′ splice sites for intron 1 that are also conserved over other ACO sequences (Figure 3.1.20).

3.1.4. Confirmation of promoter sequences using Southern analysis

Using each promoter sequence as a probe, Southern analysis revealed that p*TR-ACO1,* p*TR-ACO2,* p*TR-ACO3-1* and p*TR-ACO3-2* all hybridized to one or more DNA fragments from the digested genome of white clover, and that the size of these fragments differed.

For p*TR-ACO1*, the promoter probe hybridized to two fragments of different sizes (2.5 kb and 4.2 kb) in the *Eco* RI digestion. In the *Bam* HI digestion, the probe hybridized to two fragments of 1 kb and 3.5 kb, while in the *Hin*d III digestion, the promoter hybridized to one big mass of 9.5 kb. For p*TR-ACO2*, the promoter probe hybridized to two fragments of different size (5 kb and 4 kb) in the *Eco* RI digestion. In the *Xba* I digestion, the probe hybridized to two fragments of 6 kb and 10 kb, while in the *Bam* HI digestion, the promoter hybridized to two fragments of 4.5 kb and 9.5 kb. For p*TR-ACO3-1,* the promoter hybridized to a single fragment of 6.5 kb in the *Eco* RI digestion. In the *Hind* III digestion, the probe hybridized to one fragment of 10 kb, while in the *Bam* HI digestion, the promoter hybridized to one band of 7.5 kb. For p*TR-ACO3-2,* the promoter probe hybridized to only one fragment of 3.5 kb in the *Eco* RI digestion. In the *Hind* III digestion, the probe hybridized to one fragment of 4 kb, while in the *Bam* HI digestion, the promoter hybridized to a single fragment of 3 kb.

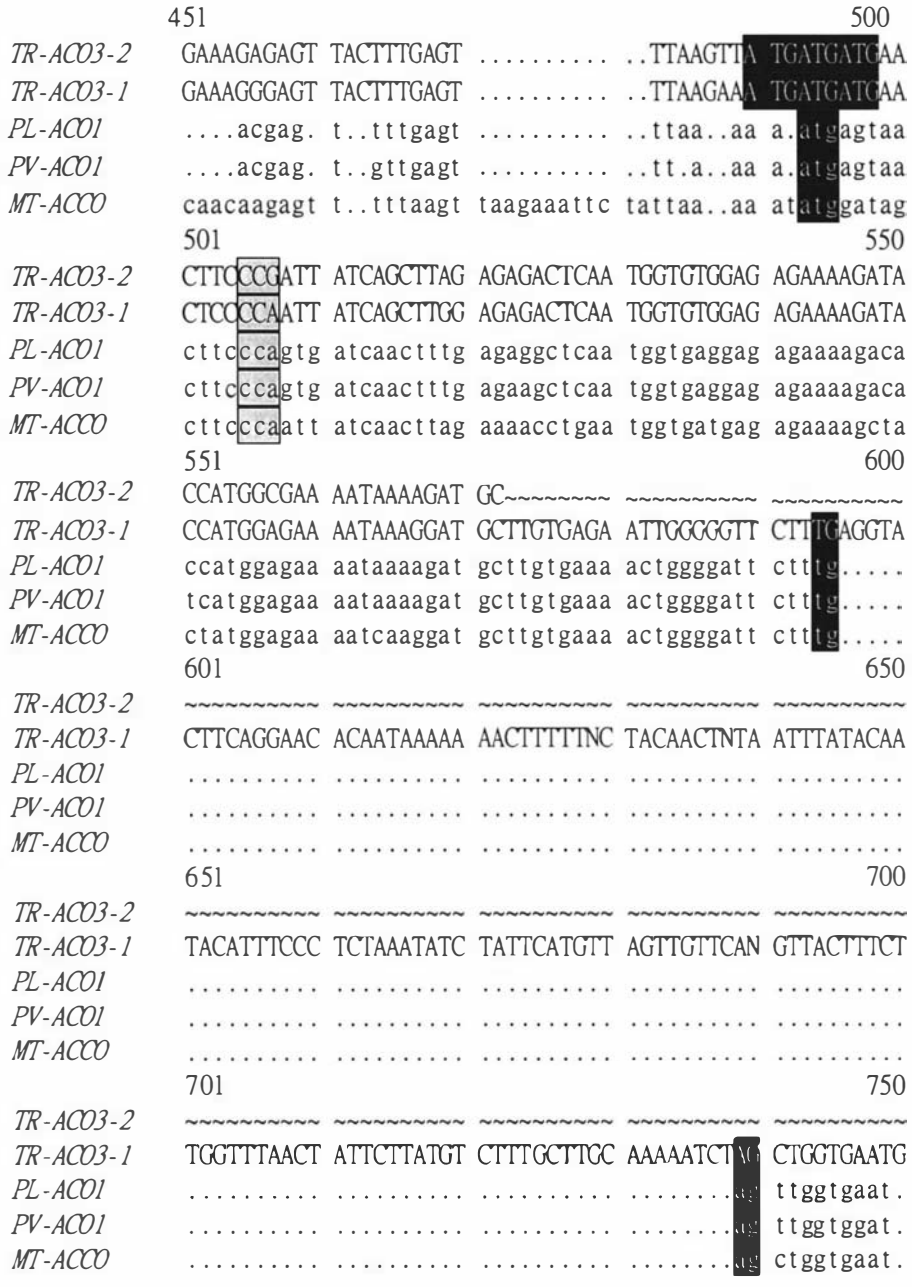

Figure 3.1.20 The 5' end coding sequence alignment of the *TR-ACO3-1* and the *TR-ACO3-2* with selected other species

The putative translation start site is located at 493-495 bp. The three ATGs are highlighted at 490-497 bp in the *TR-ACO3-1* and *TR-ACO3-2* sequences. The ATG codon in the other species is highlighted. The 5' excision site of intron 1 is highlighted at 594/595 bp and the 3' excision site at 739-740 bp. The boxed and shaded grey codon at 505-507 bp codes for proline at position 5 of the ACC oxidase protein

Southern analysis using the 3′ UTR specific probe from the *TR-ACO3* gene identified by Hunter et al (1999) revealed that the probe hybridized to fragments of 3.5 kb and 6 kb in the *Eco* RI digestion, a 7.5 kb fragment in the *Hind* III digestion, and a 6.5 kb fragment in the *Bam* HI digestion (Figure 3.1.21).

3.1.5. Genomic sequence isolation to characterise the *TR-ACO* gene family

To further characterize each *TR-ACO* gene, genomic DNA was used as template for PCR. The forward primers (designated TR1-genome-F; TR2-genome-F etc.) were based on the first intron sequence of each *TR-ACO* gene, and the reverse primer (designated TR1-genome-R; TR2-genome-R etc.) was located to the 3′ end of each *TR-ACO* coding sequence.

3.1.5.1 Isolation of the *TR-ACO1* genomic sequence

After PCR amplification using TR1-genome-F and TR1-genome-R as primers, a product of 1650 bp was obtained (Figure 3.1.22-A). After sequencing and comparison with the already known exon-1 and intron-1 sequences identified by the GenomeWalker™ method, the analysis indicated that the *TR-ACO1* gene contains four exons and three introns. Exon-1 comprises 105 bp, exon-2 comprises 225 bp, exon-3 comprises 335 bp, and exon-4 comprises 289 bp. Intron-1 comprises 197 bp, intron-2 comprises 491 bp, and intron-3 comprises 583 bp long (Figure 3.1. 23).

3.1.5.2 Isolation of the *TR-ACO2* genomic sequence

After PCR amplification using TR2-genome-F and TR2-genome-R as primers, a product of 1150 bp was obtained (Figure 3.1.22-B). After sequencing and comparison with the *TR-ACO2* coding sequence, the analysis indicated that the *TR-ACO2* gene contains four exons and three introns. Exon-1 comprises 103 bp, exon-2 comprises 230 bp, exon-3 comprises 331 bp, and exon-4 comprises 277 bp. Intron-1 comprises 104 bp, intron-2 comprises 514 bp, and intron-3

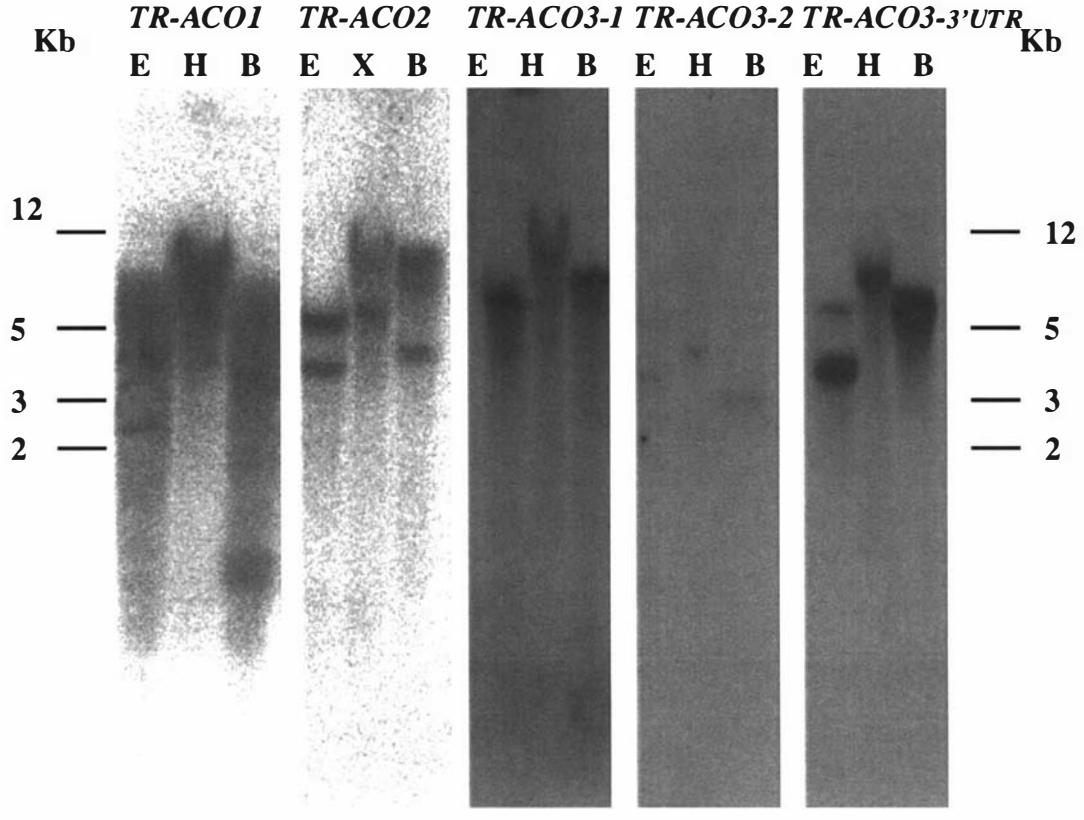

Figure 3.1.21 Southern blot analysis of *TR-ACO* genes

TR-ACO1: Membrane probed with α-^{32}P-dCTP labeled *TR-ACO1* promoter probe
TR-ACO2: Membrane probed with α-^{32}P-dCTP labeled *TR-ACO2* promoter probe
TR-ACO3-1: Membrane probed with α-^{32}P-dCTP labeled *TR-ACO3-1* promoter probe
TR-ACO3-2: Membrane probed with α-^{32}P-dCTP labeled *TR-ACO3-2* promoter probe
*TR-ACO3-3*UTR: Membrane probed with α-^{32}P-dATP labeled 3'UTR of *TR-ACO3* (Hunter et al. 1999)

Membranes were washed at high stringency (0.1X SSPE, 0.1 % SDS at 65°C) to remove non-specific binding. E = DNA digested with *Eco* RI, H = DNA digested with *Hind* III, B = DNA digested with *Bam* HI, X = DNA digested with *Xba* I. Molecular weight markers (kb) are indicated on both sides.

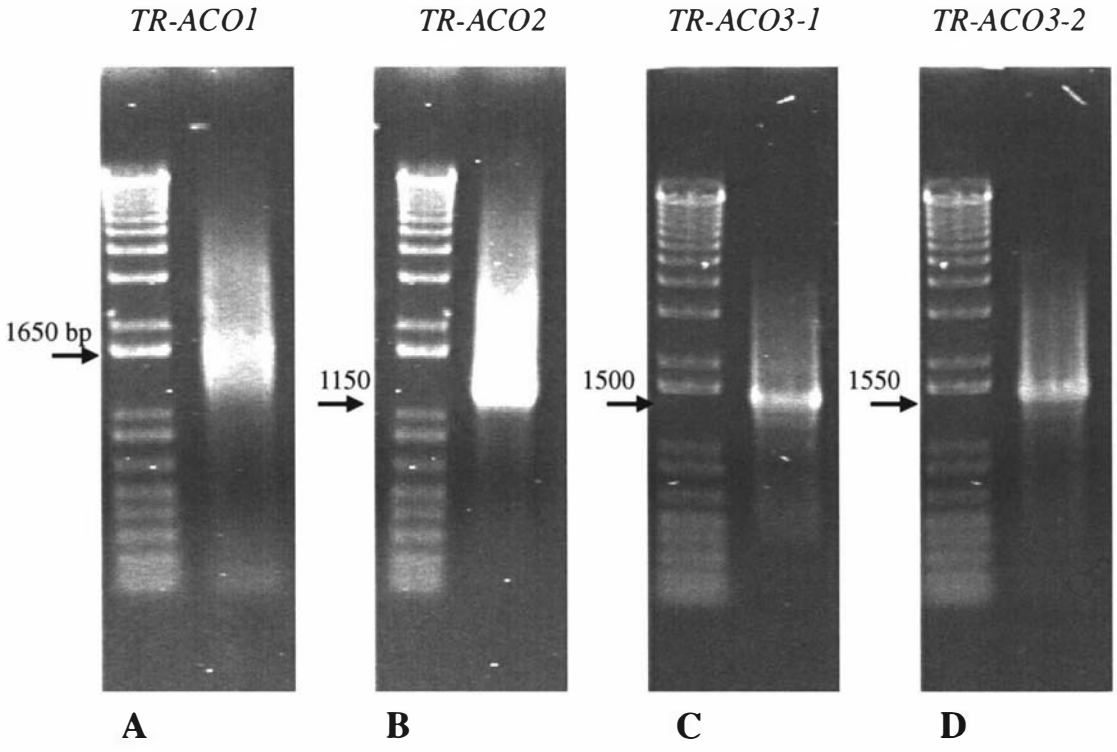

Figure 3.1.22 *TR-ACO* genomic sequence isolation using PCR

A. PCR-generated putative *TR-ACO1* DNA fragments, using the TR1-genome-F and TR1-genome-R primers

B. PCR-generated putative *TR-ACO2* DNA fragments, using the TR2-genome-F and TR2-genome-R primers

C. PCR-generated putative *TR-ACO3-1* DNA fragments, using the TR31-genome-F and TR31-genome-R primers

D. PCR-generated putative *TR-ACO3-2* DNA fragments, using the TR32-genome-F and TR32-genome-R primers

PCR products were separated by electrophoresis on a 0.75 % (w/v) agarose gel and visualized with ethidium bromide. The relative sizes are calculated from the DNA ladder and are indicated on the left.

Figure 3.1.23 Structure of *TR-ACO1* genomic sequence (2225 bp)

The grey highlighted and bold upper case represent the exon sequences. The *italics* and underlined upper case represent the intron sequences.

Exon-1

5'--ATGGAGAACTTCCCAATCATCAACTTAGAAAACCTCAATGGTGAGGAGAGAAAAGCTACC
ATGGAAAAAATCAAGGATGCTTGTGAAAACTGGGGATTCTTTG*GGGTACCTAATGATCTCAAT*
*AAATAAAAGTTTTTTTTCTTTTC*AAATAAGTTTCTACATTGGCCTCTAAATCTGTATTCATAT
*TTGTTTGTTTTTTTTTTCTGT*AGCTGGTGAATCATGGCATATCTCATGACTTAATGGACACTG

Exon-2

TGGAGAGGTTGACAAAAGAACACTACAGAATATGTATGGAACAAAGATTCAAGGATTTGGTGG
CCAACAAAGGACTAGAGGCTGTTCAAACTGAGGTCAAAGACATGGACTGGGAGAGTACCTTCC
ACTTGCGTCACCTACCTGAGTCAAACATTTCAGAGGTCCCTGATCTCACTGATGAATACAGG*T*
TACACAACATATCTAACATTTACATTGCCTACCATATAAGTTATCACTCTTATCACACACAAA
TAATTTGTTCAATTTGCAAAACAAAAAGGTCACATATTTCCTTTTAATTTTAAACATTGTTCC
ATTCATTTTTTAGCGTCCTTCTTTCTTTCTCCCTATTACTTTATAATATTATTATCTACATAA
CACCAAAAGAAGATTTTAATACCAACATTACATTACTCCGGAAGAAATTCTACTCTCATAACA
*TTTTTAAATAAATTCTCATGTATTATTCTTATAAT*AAAAAAACATTGTTAGAAAAAGCTACTC
*TACTAATAGTGGATAAGTAACCCGATCTTGTGTTGCGTGAGTGTGGGGC*ATCCGAAAAACCAA
CTAGCATCTCCCATCTATTACCTGGGATAGAGAGAGTGATGATCTCAAAAATAGGAGATAAAA
CAATCAATTTCAGAAACTATAAATTTCAGTTTCGTATGAGATTCTTAATTATACAAGATAATG
*ATGCACGGA*AAAGCAATGAAGGAATTTGCTTTGAAGCTAGAGAAACTAGCAGAGGAGCTGCTA

Exon-3

GACTTATTATGTGAGAATCTTGGACTAGAAAAGGGATACCTCAAAAAAGCCTTTTATGGATCA
AAGGGACCAACTTTTGGCACCAAGGTTGCAAACTACCCTCCATGCCCAAAACCAGACCTTGTA
AAAGGTCTCCGAGCACACACCGATGCCGGTGGAATAATCCTCCTTTTCCAAGATGACAAAGTC
AGTGGCCTTCAGCTTCTCAAAGATGGTAAATGGGTAGATGTTCCTCCCATGCATCATTCCATT
GTCATCAACCTTGGTGACCAACTCG*AAGTATAAAAAAAATTATTCCTTCTAAATTCATATTGAC*
ATTTTCACAAACATGTAAAATGCAAAAAAACCTGATTCATGAAAAACATTATCTTTGTTTATC
AGGTAATAACAAATGGTAAGTACAAGAGTGTGGAACATCGTGTGATAGCACAAAGTGATGGAA

Exon-4

CAAGAATGTCCATAGCTTCATTCTACAATCCTGGTAGTGATGCTGTTATCTATCCAGCAACAA
CATTGATTGAAGAGAATAATGAAGTTTACCCAAAATTTGTTTTTGAAGATTACATGAATCTTT
ATGCTGGATTAAAGTTTCAAGCTAAAGAACCAAGATTTGAAGCATTTAAGGAATCATCAAATG
TTAAACTTGGTCCAATTGCAACAGT–3'

Figure 3.1.24 Structure of *TR-ACO2* genomic sequence (1660 bp)

The grey highlighted and bold upper case represent the exon sequences. The *italics* and underlined upper case represent the intron sequences.

comprises 101 bp long (Figure 3.1. 24).

3.1.5.3 Isolation of the *TR-ACO3-1* genomic sequence

After PCR amplification, using TR31-genome-F and TR31-genome-R as primers a product of 1500 bp was obtained (Figure 3.1.22-C). After sequencing and comparison with the *TR-ACO3-1* coding sequence, the analysis indicated that the *TR-ACO3-1* gene contains four exons and three introns in its gene structure. Exon-1 comprises 105 bp, exon-2 comprises 224 bp, exon-3 comprises 334 bp, and exon-4 comprises 254 bp. Intron-1 comprises 142 bp, intron-2 comprises 259 bp, and intron-3 comprises 354 bp long (Figure 3.1. 25).

3.1.5.4 Isolation of the *TR-ACO3-2* genomic sequence

After PCR amplification using TR32-genome-F and TR32-genome-R as primers, a product of 1550 bp was obtained (Figure 3.1.22-D). After sequencing and comparison with the *TR-ACO3-2* coding sequence, the analysis indicated that the *TR-ACO3-2* gene contains four exons and three introns in its gene structure. Exon-1 comprises 105 bp, exon-2 comprises 224 bp, exon-3 comprises 334 bp, and exon-4 comprises 254 bp. Intron-1 comprises 131 bp, intron-2 comprises 273 bp, and intron-3 comprises 354 bp long (Figure 3.1. 26).

Since the exon sequences of *TR-ACO3-2* are identical to those deposited in the Genebank accession as *TR-ACO3* (Hunter et. al. 1999) (data not shown), and to draw a distinction between *TR-ACO3-1* and *TR-ACO3-2*, *TR-ACO3-2* is renamed *TR-ACO3* and *TR-ACO3-1* is renamed *TR-ACO4*. The evidence that these represent distinct genes is evaluated in the Discussion section.

3.1.6. Comparison of the genome structure and identity of the *TR-ACO* gene family

The genome structures of each *TR-ACO* gene is summarized as Figure 3.1.27, and the identities of the four *TR-ACO* genes are compared over the whole genomic sequence and for

Exon-1

5'--ATGATGATGAACTCCCCAATTATCAGCTTGGAGAGACTCAATGGTGTGGAGAGAAAAGATA
CCATGGAGAAAATAAAGGATGCTTGTGAGAATTGGGGATTCTTTGAG*GTACTTCAGGAACACAAT*
AAAAAAACTTTTTACTACAACTTTAATTTATACAATACATTTCCCTCTAAATATCTATTCATGTT
*AGTTGTTCATGTTACTTTCTTGGTTTAACTATTCTTATTCTTTGCTTTCAAAAATCTAG***CTGGTG**

Exon-2

AATCATGGCATACCTCATGACCTTATGGACACATTGGAGAGATTGACCAAAGAGCACTACAGGAA
ATGCATGGAGCAGAGGTTTAAGGAATTGGTATCAAGCAAAGGCTTAGATGCTGTCCAAACTGAGG
TCAAAGATATGGATTGGGAAAGTACCTTCCATGTTCGACATCTTCCTGAATCAAACATTTCAGAG
CTCCCTGATCTCAGTGATGAATAC*AGGTTACACAAAACAAACATTATGATATCACAACACTGCAT*
AACATATATAATATTTAGCACAAAACAAAAATTAATTAACCCAAAATTTCCCCCACCATTTTGGT
TGCATGAATGGATATAAAGAGAGGTTCCATACAAATAGGATAAGAAGTTAAGTTTGAGCATATTT
CTTTTCCTAATTTAATAATGGAAATTTCGCCTTTTCTTTTTTTTTTTGCTTTGACATGACATTTC
*TTATCTTAAGGATAATATAAGAC***AGGAAGGTGATGAAGGAATTTTCTGTTAGGGAAGAGAACCTA**
ACAGATTAGCTTTTGGACTTGTTATGAGAGAATCTTGGACTTGAAAAAGGTTACCTCGGAAAGGC
CTTCTATGGATCAAGAGGACCTACTTTCGGCACCAAGGTACCCCACTACCCTCCATGCCCTAATC
CTGAGGTGGGGAAGGGTCTCCCCGCTCACACCGATTCCGGTGGGATCTTCCTTCTCTTCCAAGAA

Exon-3

GACAAAGGCAGCGGCCTTCATCTACTCAGAGACGACGAGCGGATCGCTCCTCCCCCAATGCTTCA
CTCCTTTGAAGTCAACCTTCGTGATCAGCTCG*AGGTAAATTAATTTTCATTCCAATCTTCACCTT*
GAGTAAAAAATTTCTCAATACCCTAATATTGAAAGAACCCCAACCTTAAGTCATGAATTTCCTTT
TCTTGTGTTCCTTTACCCCTTAAAAGGGGATAAAGGTTTAGGGTTCTTTTGAACCTTGTGCCCCA
ATTTAAGTTCCACCTTGTGCCAAGGGTTCCATAACCAAAAATTATTAAGGGGACCAAAATTTTAA
GTCCTTAATCCCCCAATTATTTTAAGGTTATATATGAAAATGATAGGAACTATTTTACATAGACA
*TTTTCACAAACAAGTTATGTGCAAAAATCATGAAACTTTATTAACACTTTTTGATAAAAAC***AGGT**

Exon-4

AATAACAAATGGTAAATATAAGAGTGTGGAGCACCGTGTGATAGCACAAACAAATGGAACAAGAA
TGTCTATAGCATCATTCTACAACCCTGGAAGTGATGCTGTAATCTACCCTGCTCCAGAATTGTTG
GAAAAAGAAACAGAGGAAAAAACCAATGTGTATCCTAAATTTGTGTTTGAAGAGTACATGAAGAT
CTATGCTGCTTTGAAATTTCAAGCTAAGGAACCAAGATTTGAAGCACTGAAAGCA–3'

Figure 3.1.25 Structure of *TR-ACO3-1* genomic sequence (1676 bp)

The grey highlighted and bold upper case represent the exon sequences. The *italics* and underlined upper case represent the intron sequences.

Exon-1

5′--ATGATGATGAACTTCCCGATTATCAGCTTAGAGAGACTCAATGGTGTGGAGAGAAAAGATA
CCATGGCGAAAATAAAAGATGCTTGTGAAAATTGGGGATTCTTTGAG*GTACTTCAAGAATACATA*
ATAAAATGTTTTATGCTACAACTTTGATTTATACAATACATTTCCCTCTAAATATCTATTCATGT
*TACTTTCTTGGTTTAACGATTCTTATTGTTTGCTTTCAAAAATCCAGC*TGGTGAATCATGGCATA

Exon-2

CCTCATGACCTTATGGACACATTGGAGAGATTGACCAAAGAGCACTACAGGAAATGCATGGAGCA
GAGGTTTAAGGAATTGGTATCAAGCAAAGGCTTAGATGCTGTCCAAACTGAGGTCAAAGATATGG
ATTGGGAAAGTACCTTCCATGTTCGACATCTCCCTGAATCAAACATTTCAGAGCTCCCTGATCTC
AGTGATGAATAC*AGGTCAGTTGGTTACAAAAAAACAAACATTATGATATCACAACATTGCATAAC*
AAATATAAAATTTAGCAAAAAATCACTCATAATTGACACAAAATTTTCCTCACCCATTTGAGTTG
CATAAATGGATATAAAGAGAGGTTCCATACATATAGGATAAAAAATAAAGTTTGAGCGTATATCT
CTCCATATATATAATTTATGTAGGTACCTATAAAAGCCATATATATCTTTCTTTGGCATGACTCT
*CACTTTTTTATGGTTATTATTAAGC*AGGAAGGTGATGAAGGAATTTTCTTTGAGGTTAGAGAAGC
TAGCAGAAGAGCTTTTGGACTTGTTATGTGAGAATCTTGGACTTGAAAAAGGTTACCTCAAAAAG
GCCTTCTATGGATCAAGAGGACCAACTTTCGGCACCAAGGTAGCCAACTACCCTCAATGCCCTAA
TCCAGAGCTGGTGAAGGGTCTCCGTGCTCACACCGATGCCGGTGGGATCATCCTTCTCTTCCAGG

Exon-3

ATGACAAAGTCAGCGGCCTTCAGCTACTCAAAGACGACGAGTGGATCGATGTTCCCCCAATGCGT
CACTCCATTGTTGTCAACCTTGGTGACCAGCTCG*AGGTAAATTAACTCTCATTTCCATTCTCAAC*
CTGAGTAAAAAATTTCATAATAACCTTATATTGAAAGAAACACAAACATAAGTCCTCGATTTACT
TTTCATGTGATACTCTAGCACCTGATAGAGGATTAACGATTATGGATCCTCTGCAGCACGTTTCA
CAATGTAAGATGCAACATGCTGCAAAGGATCCATAAACAAGATATACTTATGTGACCAAAAATAT
TAGACACTAATACCACAAATCATCTGAGGTTATATATGAAAATGATAGGAACTATTTTACTTAGA
*CATTTTCACAAACAAGTTATGTGCAAAAATCATGAAACTTTATTAACACTTTTTGATAAAAAC*AG
GTAATAACAAATGGTAAATATAAGAGTGTGGAGCACCGTGTGATAGCACAAACAAATGGAACAAG

Exon-4

AATGTCTATAGCATCATTCTACAACCCTGGAAGTGATGCTGTAATCTACCCTGCTCCAGAATTGT
TGGAAAAAGAAACAGAGGAAAAAACCAATGTGTATCCTAAATTTGTGTTTGAAGAGTACATGAAG
ATCTATGCTGCTTTGAAATTTCAAGCTAAGGAACCAAGATTTGAAGCACTGAAAGCA—3′

Figure 3.1.26 Structure of *TR-ACO3-2* genomic sequence (1678 bp)

The grey highlighted and bold upper case represent the exon sequences. The *italics* and underlined upper case represent the intron sequences.

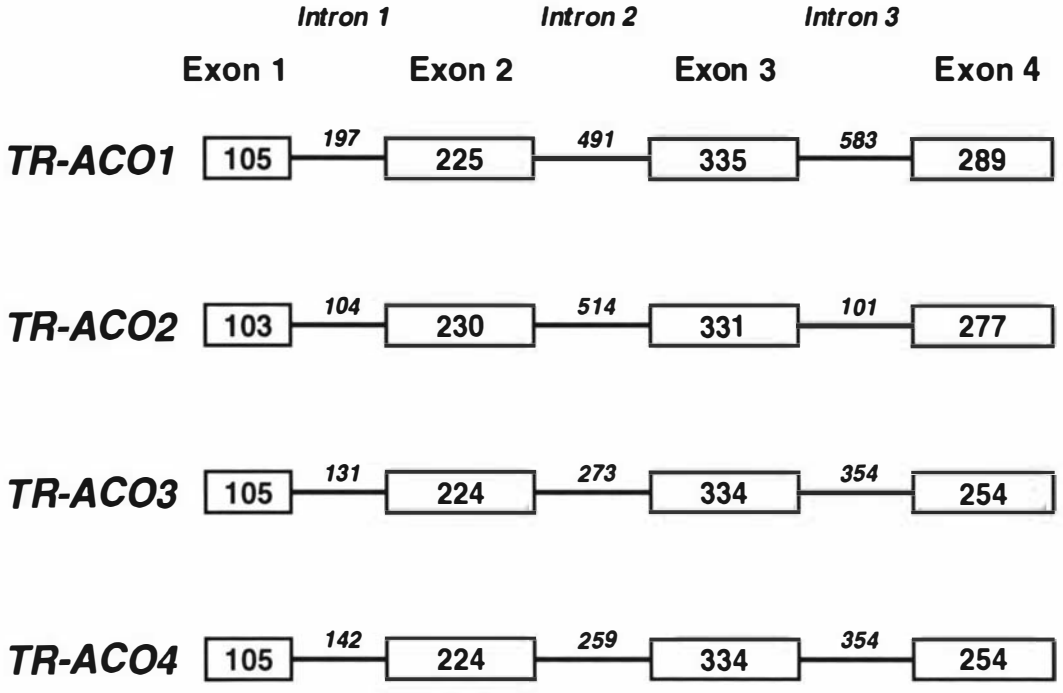

Figure 3.1.27 Gene structure of *TR-ACO1, TR-ACO2, TR-ACO3* and *TR-ACO4*

The genomic structure of each TR-ACO gene member is indicated. The boxes indicate the exon sequences and the numbers represent DNA sequence length in base pairs. The bold lines between the boxes represent the intron sequences, and the numbers indicate DNA length in base pairs

A

Genome	*TRACO1*	*TRACO2*	*TRACO3*	*TRACO4*
TRACO1	---	49 %	52 %	51 %
TRACO2	49%	---	58 %	58 %
TRACO3	52 %	58 %	---	87 %
TRACO4	51%	58 %	87 %	---

B

EXON-1	*TRACO1*-EX 1	*TRACO2*-EX 1	*TRACO3*-EX 1	*TRACO4*-EX 1
TRACO1-EX 1	---	75 %	69 %	71 %
TRACO2-EX 1	75 %	---	81 %	81 %
TRACO3-EX 1	69 %	81 %	---	94 %
TRACO4-EX 1	71 %	81 %	94 %	---

C

EXON-2	*TRACO1*-EX 2	*TRACO2*-EX 2	*TRACO3*-EX 2	*TRACO4*-EX 2
TRACO1-EX 2	---	70 %	72 %	72 %
TRACO2-EX 2	70 %	---	82 %	82 %
TRACO3-EX 2	72 %	82 %	---	99 %
TRACO4-EX 2	72 %	82 %	99 %	---

D

EXON-3	*TRACO1*-EX 3	*TRACO2*-EX 3	*TRACO3*-EX 3	*TRACO4*-EX 3
TRACO1-EX 3	---	78 %	77 %	71 %
TRACO2-EX 3	78 %	---	84 %	75 %
TRACO3-EX 3	77 %	84 %	---	89 %
TRACO4-EX 3	71 %	75 %	89 %	---

E

EXON-4	*TRACO1*-EX 4	*TRACO2*-EX 4	*TRACO3*-EX 4	*TRACO4*-EX 4
TRACO1-EX 4	---	74 %	62 %	62 %
TRACO2-EX 4	74 %	---	69 %	69 %
TRACO3-EX 4	62 %	69 %	---	100 %
TRACO4-EX 4	62 %	69 %	100 %	---

Table 3.1.1 Identity of intron and exon sequences among *TR-ACO1*, *TR-ACO2*, *TR-ACO3* and *TR-ACO4*

A. Identity values over the whole genomic sequence
B. Identity values over the first exon sequence
C. Identity values over the second exon sequence
D. Identity values over the third exon sequence
E. Identity values over the forth exon sequence

each of the exon sequences (Table 3.1.1).

3.2 Bioinformatic analysis of the *TR-ACO1, TR-ACO2, TR-ACO3-1,* and *TR-ACO3-2* promoters

3.2.1. Analysis of potential regulatory binding sites

The putative promoter sequences from the four ACO genes of white clover were used to interrogate two databases, PLACE (plant *cis*-acting regulatory DNA elements; http://www.dna.affrc.go.jp) and Mat Inspector (http://www.genomatix.de) to identify putative 6 bp to 18 bp transcription factor binding domains (TFBDs). These range from 80 % identity (over 16 bp to 18 bp) to 100 % identity over the 6 bp. For the purpose of this analysis, the sequences upstream of the putative ATG site were used such that a 1006 bp sequence for *TR-ACO1,* a 1510 bp sequence for *TR-ACO2*, a 1350 bp sequence for *TR-ACO3*, and a 1250 bp sequence for *TR-ACO4* were examined. The putative domains were divided into three broad groups (designated class I, class II and class III). Class I comprises binding domains that are associated with hormonal or environmental cues, and include domains shared by other genes for which transcription has been shown to be induced by either environmental or hormonal cues. Examples of TFBDs in this class include a low temperature response element (L-Temp-RE), an abscisic acid (ABA) response element (ABA-RE), an indole-3-acetic acid (IAA) response element (IAA-RE also known as Aux-RE), a sucrose response element (Sucrose-RE), a salicylic acid (SA) response element (SA-RE), and a light response element (Light-RE). This later domain is similar to a TFBD designated as RUBISCO, as the domain has similarity with a light-responsive element in the small subunit gene of the RUBISCO (RBCS) promoter of *A. thaliana*. TFBDs in class I also contain motifs that are either targets for hormonally-induced transcription factors including a gibberellin acid (GA)-induced transcription factor (GA-Myb), a domain that is similar to a GA-Myb domain but occurs in a

cysteine proteinase gene induced in barley (Cysteine). As well, class I comprises TFBDs that occur on other genes that are induced by hormones, eg. α-amylase (α-amyl), β-amylase (β-amyl), and an endosperm-specific *Nap A* (Endos). TFBDs in class II include domains for transcription factors MADS, AGAMOUS (AG), AGAMOUS-LIKE3 (AGL-3) that are induced by developmental cues, and domains in class III comprise either domains that are shared in other genes in which transcription is induced by ethylene (ERE, GCC box) or are binding sites for wounding-induced transcriptional factors (W-boxes).

3.2.1.1 Identification of transcription factor binding domains in the *TR-ACO1* promoter

In the *TR-ACO1* promoter sequence, six class I domains were observed, including motifs identified in the promoters of α- and β-amylase genes (α-amyl) (β-amyl) and an endosperm-specific storage gene, *napA* (Endos), as well as a low temperature response element (L-temp-RE), a GA-induced myb-protein binding domain (GA-Myb), and an ABA response element (ABA-RE). Five class II domains were detected including two *Agamous* (AG), an *AG-like 3* (AGL3), and two MADS-box protein binding domains (MADS). In addition, three class III domains were observed including two ethylene response elements (EREs), and a wounding response domain (W-box) (Figure 3.2.1). These domains are grouped as clusters, with a major cluster comprising 6 domains (representing members of each class) located at *ca.* 570 to 700 bp upstream of the ATG codon (Figure 3.2.1).

3.2.1.2 Identification of transcription factor binding domains in the *TR-ACO2* promoter

The *TR-ACO2* promoter sequence contains twelve class I domains (three α-amyl elements, one β-amyl, one ABA-RE element, two salicylic acid response elements (SA-RE), three IAA-response elements (IAA-RE)(IAA-RE2), one light response element (Light-RE), and one sucrose response element (Sucrose). In addition, the promoter contains six class II

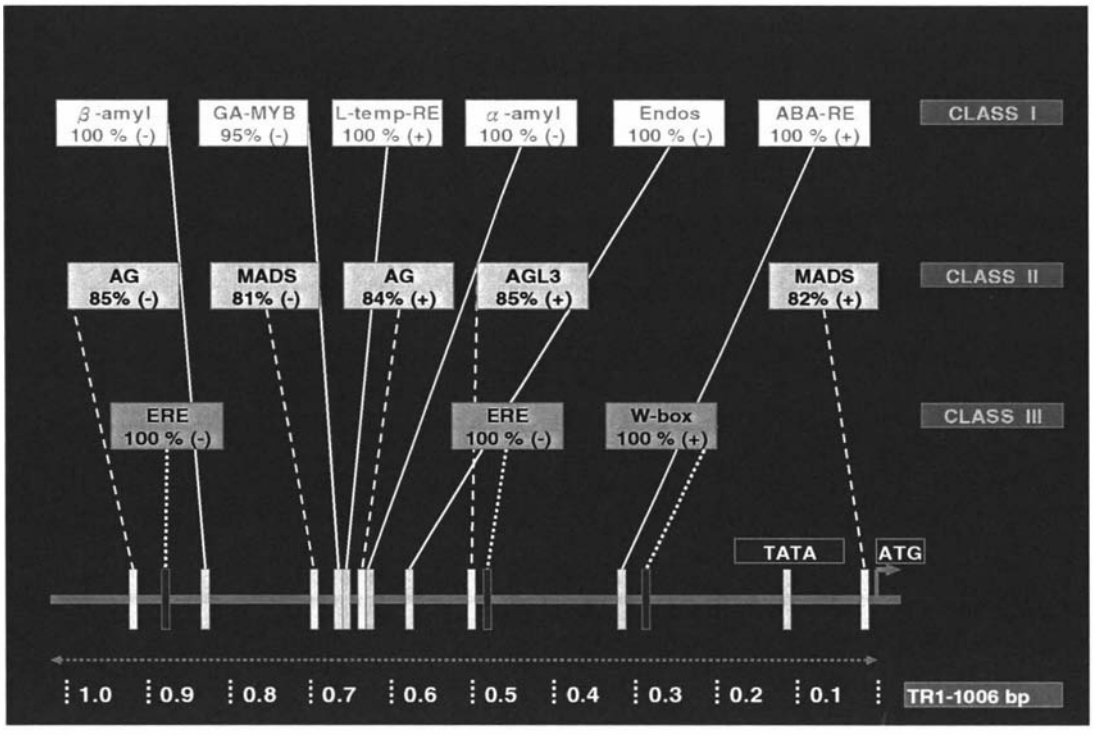

Figure 3.2.1 Identification of putative transcription factor binding domains in the *TR-ACO1* promoter sequence

The numbers at the base of the figure represent the distance in kb upstream from the ATG codon. The location of each element is indicated in boxed form. The percentage values associated with some TFBDs refer to the percentage identity with the 16 to 18 bp domains identified by MatInspector, and (+) or (-) denotes a match on the sense (5′ to 3′) or anti-sense (3′ to 5′) strand, respectively. TFBDs with 100 % values associated are wholly identical over the 6 to 8 bp sequences contained in the PLACE database. The major function and reference for each TFBD is indicated as follows:

ABA-RE= ABA response element; CAAACACC; (Choi,et al 2000)
AG=*Agamous* binding element (MADS-box protein); ttTGCCaaaactcgcata; (Huang, et al1993)
AGL3=*Agamous-like 3* binding element; tgttCCAAtttaagtgga; (Huang, et al 1995)
α-amyl= cis-element of α-amylase genes TGACGT; (Yamauchi, et al 2001)
β-amyl= cis-element of β-amylase genes TACTATT; (Ishiguro, et al 1994)
Endos= cis-element of storage protein (*napA*); CAAACAC; (Stalberg, et al 1996)
ERE=ethylene response element; AWTTCAAA; (Itzhaki, et al 1994)
GA-Myb= GA regulated myb gene; gccaGTTG; (Gubler, et al 1999)
L-temp-RE= low temperature response element; CCGAAA; (Bunn, et al 1998)
MADS= floral meristem identity protein; aattcaAAAAtcgaac; (Riechmann, et al 1996)
W-box=wound response element; TTGAC; (Yu, et al 2001)

domains including four MADS-box domains, one AGL3 domain and one L1-layer specific element (SAM), and five class III domains including one ERE, one ethylene-response GCC-box, and three W-box elements (Figure 3.2.2). Again, a major cluster of 5 domains representing members of each class is located 600bp to 650 bp upstream of ATG codon, with three other clusters comprising three domains located at *ca.* 370 bp, *ca.* 950 bp and *ca.* 1380 bp upstream of the ATG codon (Figure 3.2.2).

3.2.1.3 Identification of transcription factor binding domains in the *TR-ACO3* promoter

The *TR-ACO3* promoter contains six class I domains including a light-responsive element identified in the gene encoding the small sub-unit of RUBISCO (RUBISCO), one SA-RE element, two ABA-RE and two IAA-RE2 elements, three class II domains (two AGL3 and one MADS-box), and five class III domains (two EREs, one GCC-box and two W-box elements) (Figure 3.2.3). A main cluster of 6 domains is located at *ca.* 350 bp to 520 bp upstream of the ATG codon, with another cluster of three domains located at *ca.* 620 bp to 700 bp upstream of the ATG codon (Figure 3.2.3).

3.2.1.4 Identification of transcription factor binding domains in the *TR-ACO4* promoter

The *TR-ACO4* promoter sequence is quite similar to the *TR-ACO3* promoter and contains five class I domains [one Light-RE, one IAA-RE2, one ABA-RE element, a light-responsive element identified in the small sub-unit of RUBISCO (RuBiSCO), and an element identified as a GA-Myb binding domain in a cysteine proteinase gene of barley (Cysteine)], two class II domains (two AGL3 elements), and six class III elements (three W-boxes, two GCC-boxes and one ERE domain) (Figure 3.2.4). Two clusters of 4 domains are located at *ca.* 400 bp to 540 bp and at *ca.* 860 bp to 980 bp upstream of the ATG codon, while a second cluster of three domains is located *ca.* 1100 bp to 1200 bp upstream of the ATG codon (Figure 3.2.4).

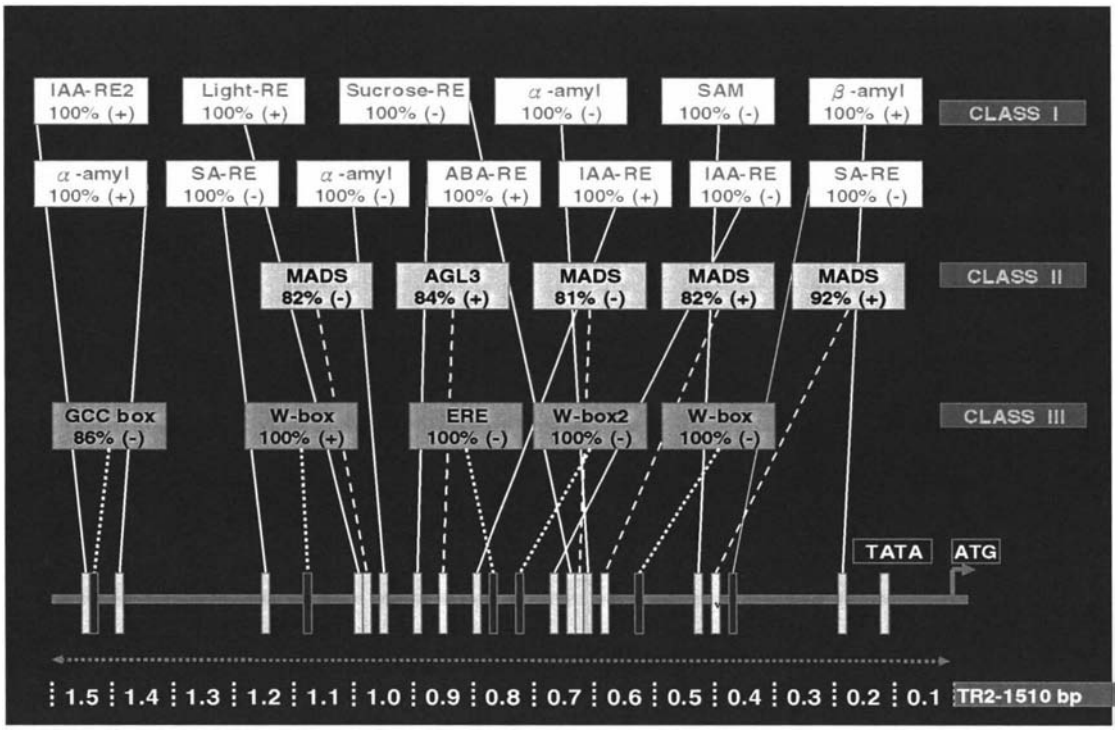

Figure 3.2.2 Identification of putative transcription factor binding domains in the *TR-ACO2* promoter sequence

The numbers at the base of the figure represent the distance in kb upstream from the ATG codon. The location of each element is indicated in boxed form. The percentage values associated with some TFBDs refer to the percentage identity with the 16 to 18 bp domains identified by MatInspector, and (+) or (-) denotes a match on the sense (5′ to 3′) or anti-sense (3′ to 5′) strand, respectively. TFBDs with 100 % values associated are wholly identical over the 6 to 8 bp sequences contained in the PLACE database. The major function and reference for each TFBD is indicated as follows:

ABA-RE= ABA response element; CAAACACC; (Choi, et al 2000)

AGL3=*Agamous-like 3* binding element; tgttCCAAtttaagtgga; (Huang, et al 1995)

α-amyl= cis-element of α-amylase genes TGACGT; (Yamauchi, et al 2001)

β-amyl= cis-element of β-amylase genes TACTATT; (Ishiguro, et al 1994)

ERE=ethylene response element; AWTTCAAA; (Itzhaki, et al 1994)

GCC-box= ethylene response element; AGCCGCC; (Hao, et al 1998)

IAA-RE=auxin response element; ACTTTA; (Baumann, et al 1999)

IAA-RE2= auxin response element; CATATG; (Xu, et al 1997)

Light-RE2=light regulate element; tttagGATAagtaggc; (Teakle, et al 2002)

L-temp-RE= low temperature response element; CCGAAA; (Bunn, et al 1998)

MADS= floral meristem identity protein; aattcaAAAAtcgaac; (Riechmann, et al 1996)

SA-box-2= Salicylic acid response element; TGACG; (Katagiri, et al 1990)

SAM/L1= L1 layerof SAM specific element; TAAATGYA; (Abe, et al 2001)

Sucrose-RE= sucrose response element; AATAGAAAA; (Grierson, et al 1994)

W-box=wound response element; TTGAC; (Yu, et al 2001)

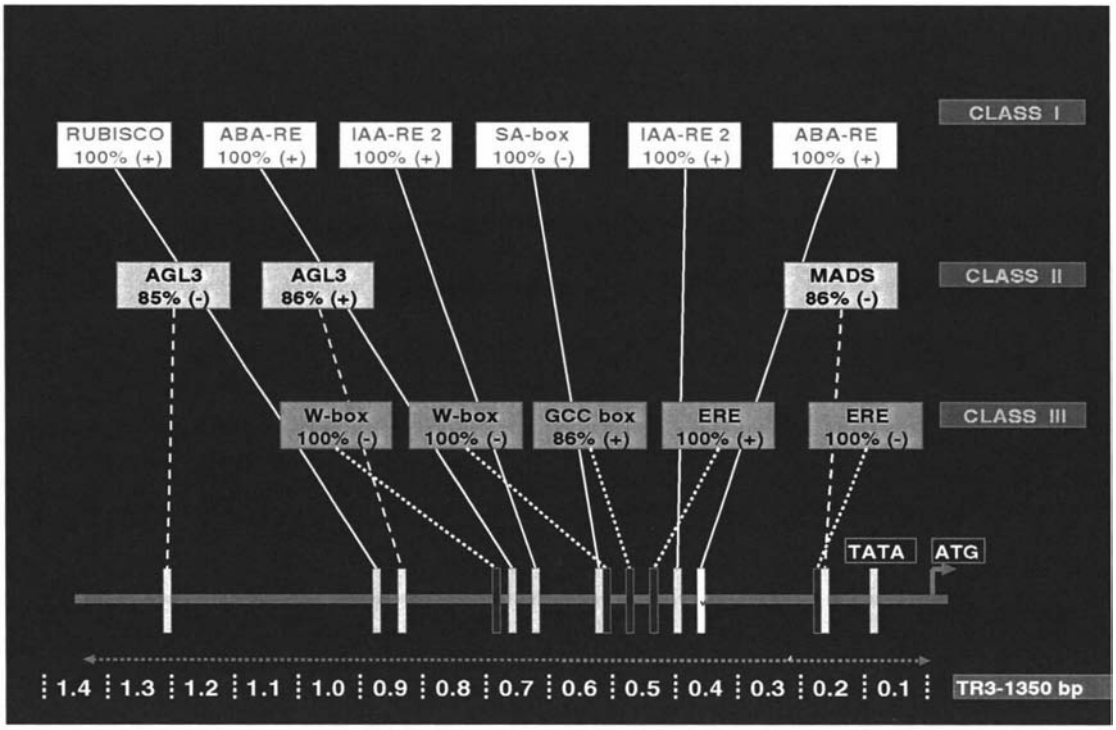

Figure 3.2.3 Identification of putative transcription factor binding domains in the *TR-ACO3* promoter sequence

The numbers at the base of the figure represent the distance in kb upstream from the ATG codon. The location of each element is indicated in boxed form. The percentage values associated with some TFBDs refer to the percentage identity with the 16 to 18 bp domains identified by MatInspector, and (+) or (-) denotes a match on the sense (5′ to 3′) or anti-sense (3′ to 5′) strand, respectively. TFBDs with 100 % values associated are wholly identical over the 6 to 8 bp sequences contained in the PLACE database. The major function and reference for each TFBD is indicated as follows:

ABA-RE= ABA response element; CAAACACC; (Choi, et al 2000)
AGL3=*Agamous-like 3* binding element; tgttCCAAtttaagtgga; (Huang, et al 1995)
ERE=ethylene response element; AWTTCAAA; (Itzhaki, et al 1994)
GCC-box= ethylene response element; AGCCGCC; (Hao, et al 1998)
IAA-RE2= auxin response element; CATATG; (Xu, et al 1997)
MADS= floral meristem identity protein; aattcaAAAAtcgaac; (Riechmann, et al 1996)
RUBISCO= cis-element of RuBiSCO; AATCCAA; (Donald, et al 1990)
SA-box=salicylic acid response element; TTGACC; (Chen, et al 2000)
W-box=wound response element; TTGAC; (Yu, et al 2001)

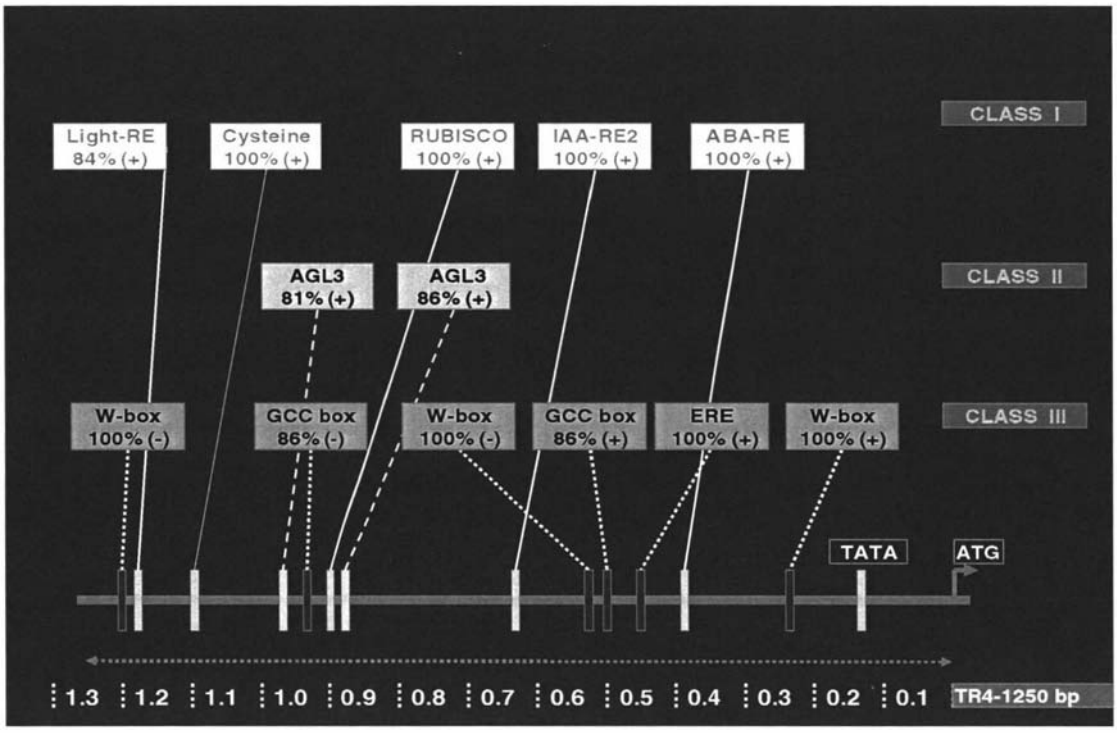

Figure 3.2.4 Identification of putative transcription factor binding domains in the *TR-ACO4* promoter sequence

The numbers at the base of the figure represent the distance in kb upstream from the ATG codon. The location of each element is indicated in boxed form. The percentage values associated with some TFBDs refer to the percentage identity with the 16 to 18 bp domains identified by MatInspector, and (+) or (-) denotes a match on the sense (5′ to 3′) or anti-sense (3′ to 5′) strand, respectively. TFBDs with 100 % values associated are wholly identical over the 6 to 8 bp sequences contained in the PLACE database. The major function and reference for each TFBD is indicated as follows:

ABA-RE= ABA response element; CAAACACC; (Choi, et al 2000)
Cysteine= cis-element of cysteine proteinase; TTTTTTCC; (Cercos, et al 1999)
ERE=ethylene response element; AWTTCAAA; (Itzhaki, et al 1994)
GCC-box= ethylene response element; AGCCGCC; (Hao, et al 1998)
IAA-RE2= auxin response element; CATATG; (Xu, et al 1997)
Light-RE-2=light regulate element; tttagGATAagtaggc; (Teakle, et al 2002)
MADS= floral meristem identity protein; aattcaAAAAtcgaac; (Riechmann, et al 1996)
RUBISCO= cis-element of RuBiSCO; AATCCAA; (Donald, et al 1990)
W-box=wound response element; TTGAC; (Yu, et al 2001)

3.2.1.5 Comparison of the transcription factor binding domains in the *TR-ACO* promoters

In terms of class I transcription factor binding domains, the *TR-ACO1* promoter contains six elements, the *TR-ACO2* promoter contains 12 elements, the *TR-ACO3* promoter has six elements, and the *TR-ACO4* promoter has five elements. For the class II transcription factor binding domains, the *TR-ACO1* promoter contains five elements, the *TR-ACO2* promoter has six elements, the *TR-ACO3* promoter has three elements, and the *TR-ACO4* promoter only has two elements. In terms of the numbers of class III transcription factor binding domains, the *TR-ACO1* promoter contains three elements, the *TR-ACO2* promoter has five elements, the *TR-ACO3* promoter has five elements, and the *TR-ACO4* promoter has six elements (Figure 3.2.5).

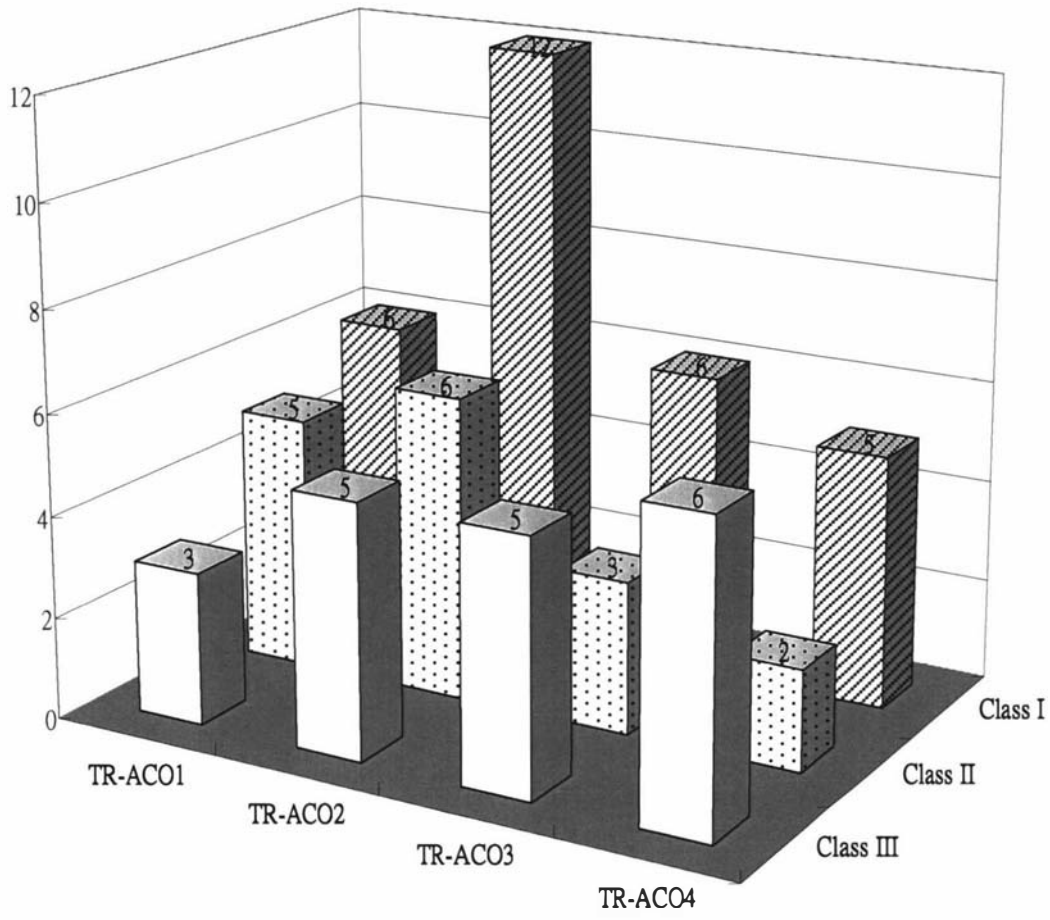

Figure 3.2.5 Comparison of the number of transcription factor binding domains in each class for each of the *TR-ACO* promoter sequences

Values on the Y axis represent the numbers of transcription factor binding domains for each gene in each class
The X axis indicates each *TR-ACO* promoter sequence
The Z axis represents the different classes of transcription factor binding domains

3.3 Analysis of the *TR-ACO1*, *TR-ACO2*, *TR-ACO3*, and *TR-ACO4* promoter activity *in vivo*

3.3.1. Construction of the plant transformation vectors

3.3.1.1 Vector modification and isolation

The pRD-410 vector obtained originally for use in this study contained the GUS reporter gene fused with the 35S CaMV promoter. Thus it was necessary to remove the 35 CaMV sequence and replace it with each of the *TR-ACO* promoter sequences. To do this, pRD-410 was transformed into the *E.coli* strain DH-5α, colonies isolated, plasmids purified, and then digested with *Hind* III and *Bam* HI. After separation of the fragments using agarose gel electrophoresis, colonies #5 and #6 contained plasmids with one 12 kb band and one 820 bp band (Figure 3.3.1; the 820 bp band is difficult to visualise after ethidium bromide staining). Since the size of 35S CaMV promoter is 820 bp, and the linearised vector is *ca.* 12 kb long, the 12 kb band was purified further for cloning.

3.3.1.2 Isolation of promoter sequences using PCR

To insert the promoter sequences into pRD-410, PCR was used to amplify the 5′ UTR of each *TR-ACO* gene and each promoter sequence. In common with the bioinformatics analysis, the sequence upstream of the each promoter sequence had been analyzed previously to determine whether internal *Hin*d III or *Ba*m HI sites were present. If not, *Hin*d III and *Bam* HI sites were added to the PCR primers used to amplify each promoter sequence.

Since the *TR-ACO3* promoter comprises two separate sequences (the 1264 bp and the 390 bp obtained by PCR extension) (section 3.1.3.4), *Hin*d III and *Bam* HI sites were added to the end of each DNA fragment.

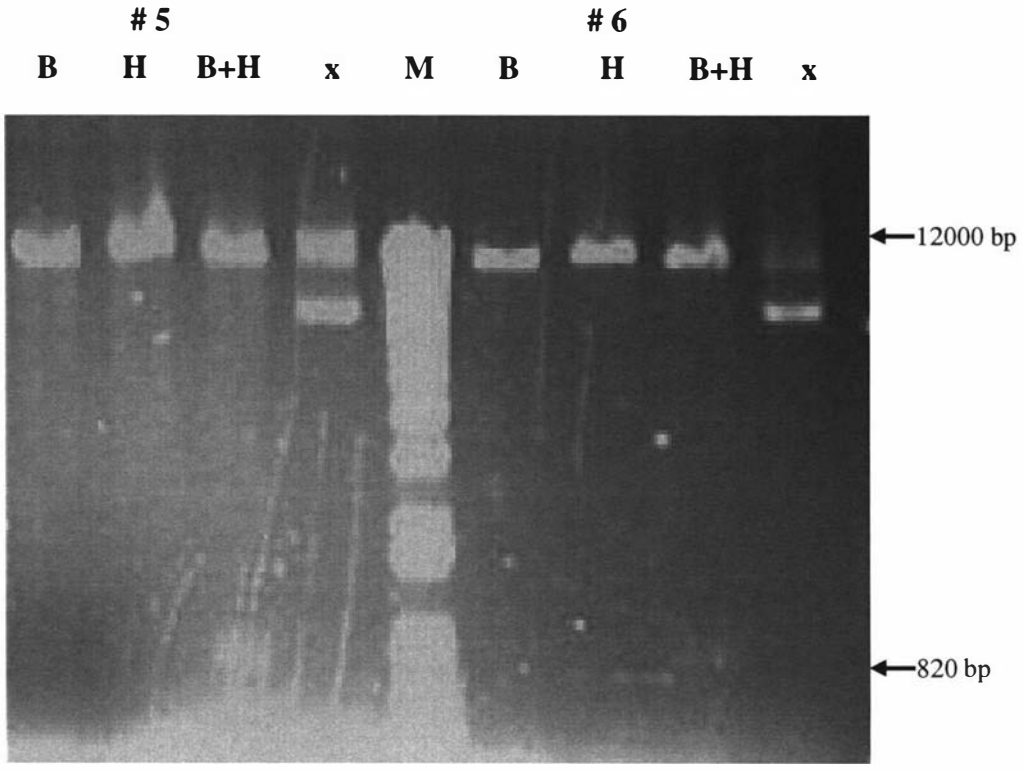

Figure 3.3.1 Restriction digestion of the pRD-410 vector

Products from enzyme digestions were separated on a 0.6 % (w/v) agarose gel and visualized with ethidium bromide. The sizes of the fragments are indicated on the right. The numbers refer to colonies screened. B = *Bam* HI digested; H = *Hind* III digested; B+H = both *Bam* and *Hin*d III digested; X = undigested plasmid. M = commercially-available 1 Kb plus DNA ladder.

After PCR amplification, each product was digested with *Hind* III and *Bam* HI, and all of the products amplified were of the expected sizes (Figure 3.3.2). The *TR-ACO1* product was *ca.* 1000 bp (predicted size 1006 bp), the *TR-ACO2* product was *ca.* 1500 bp (predicted size 1510 bp), the *TR-ACO3* had one fragment of *ca.* 500 bp (predicted size 453 bp) and another of *ca.* 900 bp (predicted size 900 bp), and the *TR-ACO4* product was *ca.* 1300 bp (predicted size 1250 bp).

3.3.1.3 Transformation of *E.coli* with the plant transformation vectors

The isolated DNA fragments (section 3.3.1.2) were ligated into a linearised p-RD410 plasmid from which the 35S CaMV promoter had been removed (section 3.3.1.1). The ligated and circularised plasmids were then transformed into *E.coli* strain DH-5α and selected colonies digested with *Bam* HI and *Hind* III to screen for inserts of the expected size.

For p*TR-ACO1*, five colonies had inserts of *ca.* 1000 bp (Figure 3.3.3-A; #4, #5, #6, #7, #8), and colony # 8 was chosen for plasmid isolation. For p*TR-ACO2*, only one colony (#9) had an insert of the expected size (*ca.*1500 bp) (Figure 3.3.3-B) and so colony # 9 was used for plasmid isolation. For p*TR-ACO3*, plasmid isolated from only one colony (# 2) had an insert of the expected size (*ca.* 1350 bp) from 200 colonies screened (Figure 3.3.3-C), and so colony # 2 was used for vector isolation. For p*TR-ACO4*, six colonies (#1, #2, #3, #4, #5, #6) contained plasmids that had inserts of *ca.* 1250 bp (Figure 3.3.3-D), and colony # 5 was chosen for further plasmid isolation.

3.3.1.4 Transformation of pRD-410 into *Agrobacterium tumefaciens*

Plasmids containing the *TR-ACO* promoters fused with the GUS reporter gene were isolated (section 3.3.1.3), and transformed into the disarmed *Agrobacterium tumefaciens* strain

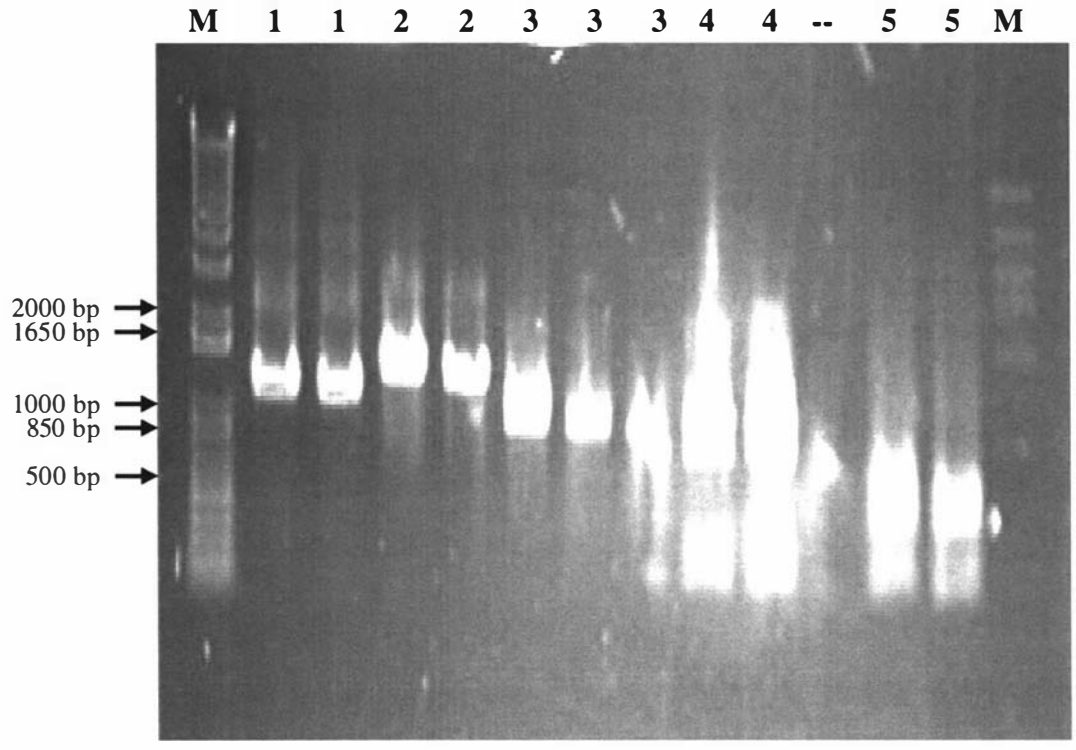

Figure 3.3.2 Isolation of promoter sequences using PCR

Generation of putative promoter sequences by PCR using p-GEM vectors as template. PCR products were separated by electrophoresis on a 0.75 % (w/v) agarose gel and visualized with ethidium bromide. The total reaction mix for each PCR was loaded over two lanes. The relative sizes are indicated on the left. M = 1kb plus ladder, -- = blank lane.

Lane-1=putative *TR-ACO4* promoter sequence as a PCR product generated using TR4-cloneF and TR4-cloneR primers
Lane-2=putative *TR-ACO2* promoter sequence as a PCR product generated using TR2-cloneF and TR2-cloneR primers
Lane-3=putative *TR-ACO1* promoter sequence as a PCR product generated using TR1-cloneF and TR1-cloneR primers
Lane-4=putative *TR-ACO3* (900 bp) promoter sequence as a PCR product generated using TR3-1-cloneF and TR3-1-cloneR primers
Lane-5=putative *TR-ACO3* (453 bp) promoter sequence as a PCR product generated using TR3-2-cloneF and TR3-2-cloneR primers

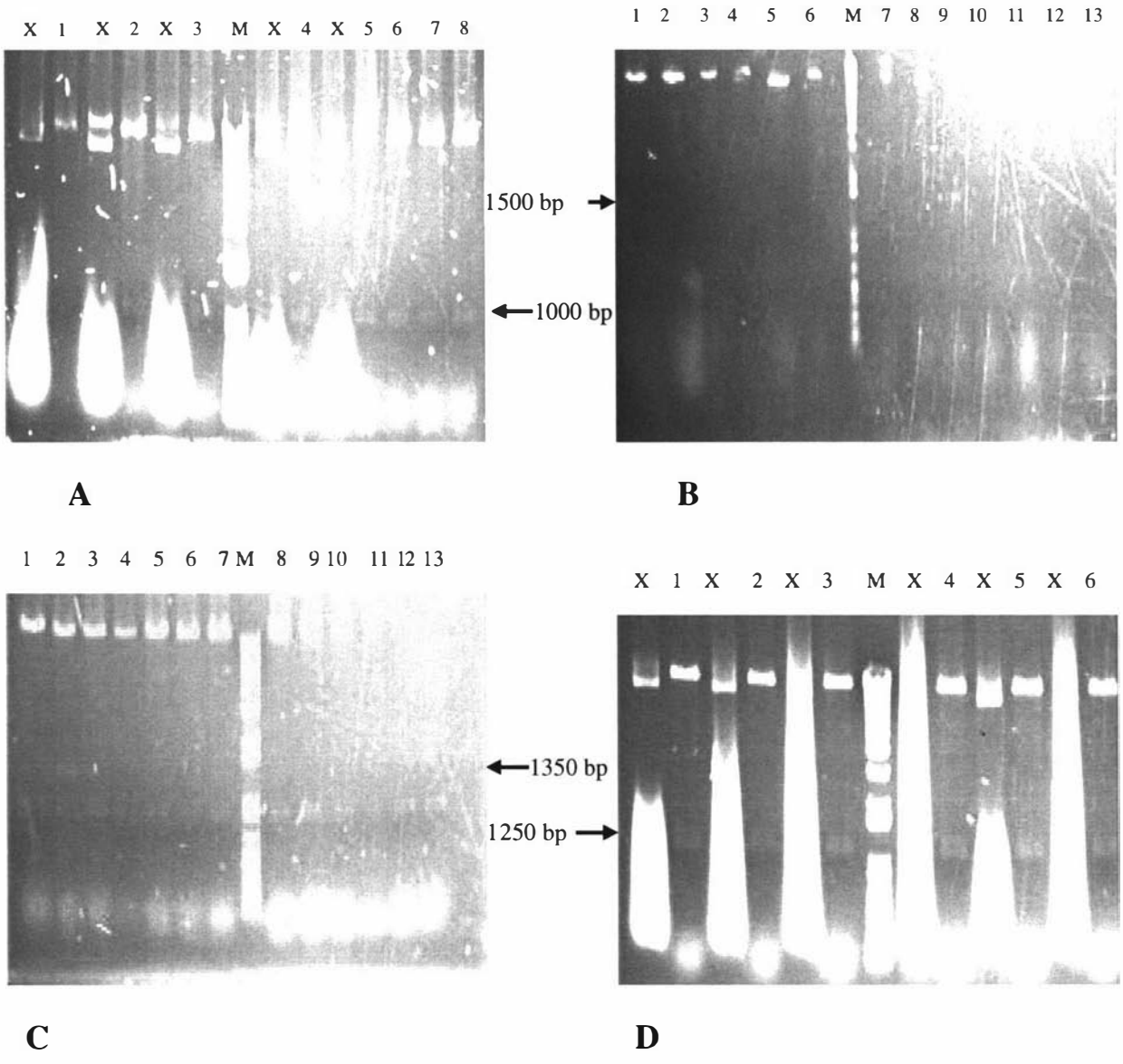

Figure 3.3.3 Screening of pRD-410 plasmids with putative *TR-ACO* promoter inserts using restriction enzyme digestion

A. Screening of putative *TR-ACO1* promoter inserts (1006 bp)
B. Screening of putative *TR-ACO2* promoter inserts (1510 bp)
C. Screening of putative *TR-ACO3* promoter inserts (1350 bp)
D. Screening of putative *TR-ACO4* promoter inserts (1250 bp)

Products from *Bam* HI and *Hin*d III double digests were separated on a 0.8 % (w/v) agarose gel and visualized with ethidium bromide. The sizes of the inserts were indicate on the sides. The numbers refer to colonies screened. X = undigested plasmid. M = 1 Kb plus ladder.

LBA4404 using electroporation (section 2.11.3). PCR or restriction enzyme digestion were then used to screen the transgenic strains.

PCR screening of three putative p*TR-ACO1*-containing plasmids colonies using a reverse primer designed from the 5′ region of the GUS gene (designated GUS-R), and a forward primer designed from the 3′ end of the *NPT II* gene (designated NPT-F), amplified a product of *ca.* 2500 bp (the expected size) (Figure 3.3.4). Some colonies were also screened using primers designed within the *TR-ACO1* promoter (designated TR1-clone-F and TR1-clone-R), and these amplified a product of *ca.* 1000 bp (expected size 1006 bp) (Figure 3.3.4). Thus the 1000 bp band was isolated for DNA sequencing. The sequence result aligned with the original *TR-ACO1* promoter sequence with 100% identity (data not shown).

Eight colonies containing the p-RD410 plasmids harbouring the putative *TR-ACO2* promoter were isolated from *A. tumefaciens* transformants, and digested with *Hind* III and *Bam* HI. Colonies #1 and #8 contained plasmids with an insert of *ca.* 1500 bp fragment (expected size 1510 bp) (Figure 3.3.5-A). PCR was used to re-screen colony # 8, and the sizes of the amplified product coincided with the predicted sizes using the GUS reverse primer (GUS-R) and a forward primer from the 5′ end of *TR-ACO2* promoter sequence (designated TR2-internal-F) (Fig. 3.3.5-B; lane-b, 1550 bp). A product of 2900 bp was also amplified but its identity is not known. A product of 2900 bp was also noted in lane-c, but again its identity is not expected. Using the GUS primer (GUS-R) and a forward primer from the 3′ end of the *NPT II* gene (NPT-F) (Figure 3.3.5-B; lane-d, 2900 bp). A *ca.* 1500 bp product (expected size 1550 bp), amplified with the GUS primer and the promoter sequence primer, was sequenced and shown to be identical to the putative *TR-ACO2* promoter (data not shown).

Plasmids isolated from three of the *TR-ACO3* colonies were screened using PCR and all of them had the predicted product sizes when using the GUS reverse primer (GUS-R) and the 5′ end of the *TR-ACO3* promoter as the forward primer (designated TR3-clone-F) (1450 bp), and using the 3′ end of promoter as the reverse primer (designated TR3-clone-R) and the *NPT*

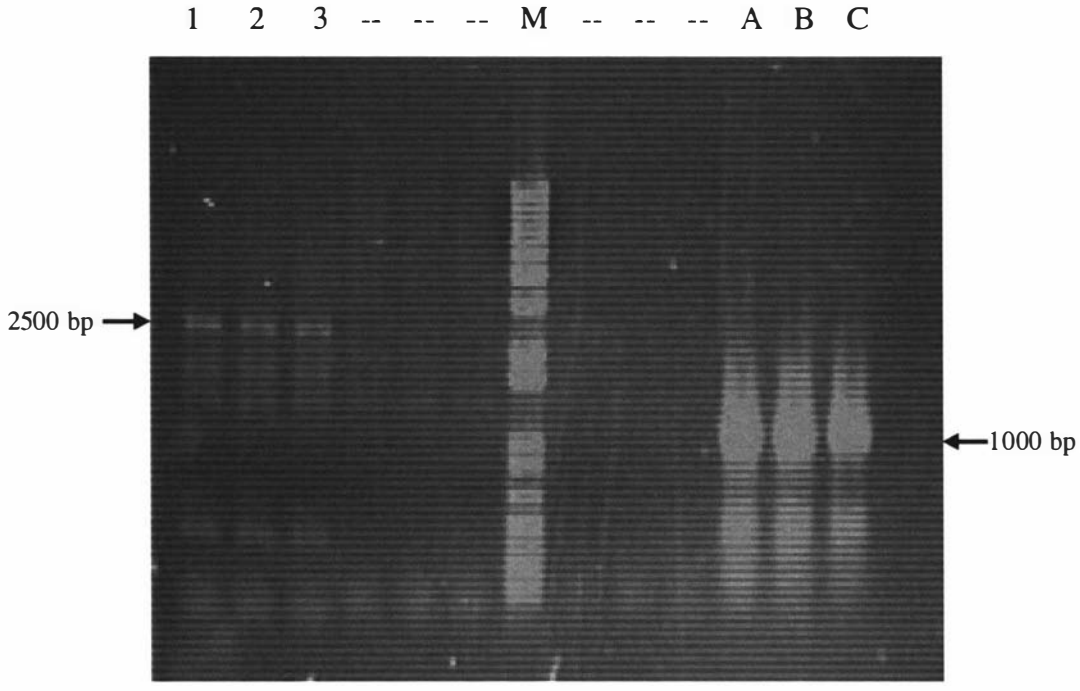

Figure 3.3.4 PCR screening and confirmation of the p*TR-ACO1::GUS* transformation into *Agrobacterium* cells

Screening for colonies containing plasmids with positive inserts by PCR using GUS-R and NPT-F primers (lanes 1-3), and confirmation of positive colonies by PCR using TR1-clone-F and TR1-clone-R primers (lanes A-C). The PCR products were separated by electrophoresis on a 0.75 % (w/v) agarose gel and visualized with ethidium bromide. The sizes of the relative fragments are indicated on both side. M = 1kb plus ladder, -- = blank lanes

Land 1: screening of isolated plasmid from colony #1 by PCR using the GUS-R and NPT-F primers
Land 2: screening of isolated plasmid from colony #2 by PCR using the GUS-R and NPT-F primers
Land 3: screening of isolated plasmid from colony #3 by PCR using the GUS-R and NPT-F primers
Land A: plasmid isolated from colony #1 screened by PCR using the TR1-clone-F and TR1-clone-R primers
Land B: plasmid isolated from colony #2 screened by PCR using the TR1-clone-F and TR1-clone-R primers
Land C: plasmid isolated from colony #3 screened by PCR using the TR1-clone-F and TR1-clone-R primers

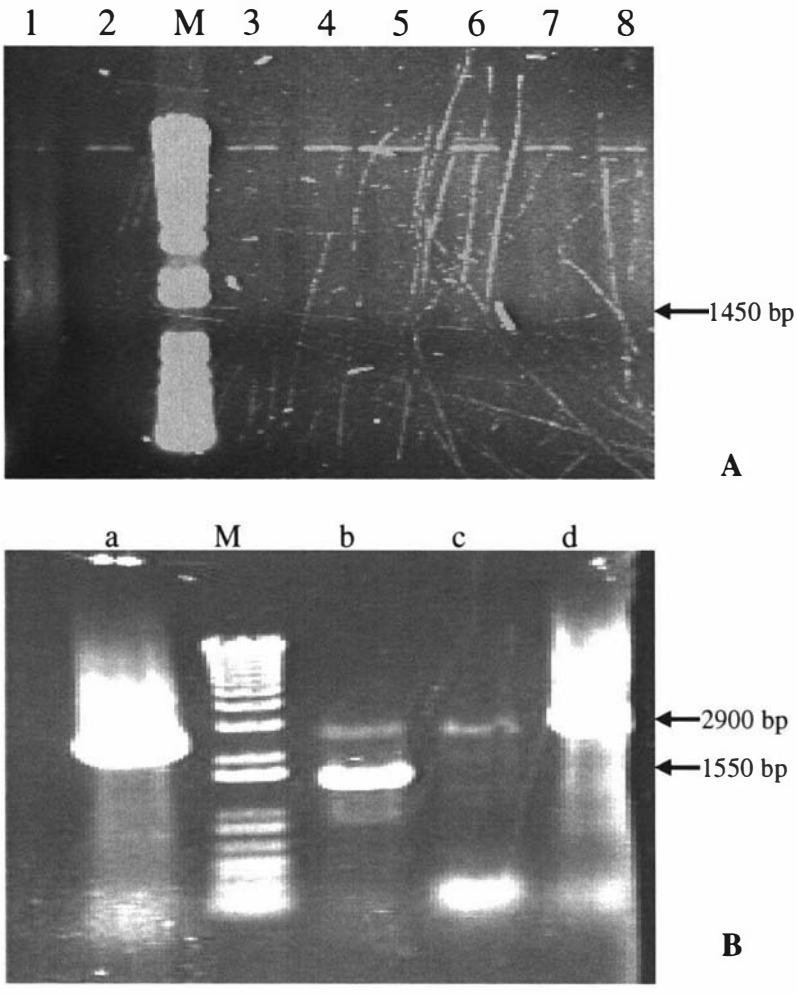

Figure 3.3.5 Restriction enzyme digestion screening and confirmation using PCR, of p*TR-ACO2::GUS* transformation into *Agrobacterium* cells

Screening for colonies containing plasmids with positive inserts using *Hin*d III and *Bam* HI digestion (A), and confirmation of colonies containing plasmids with positive inserts in (A) by PCR (B).

(A) Restriction enzyme digestion screening

Products were separated by electrophoresis on a 0.75 % (w/v) agarose gel, and visualized with ethidium bromide. The sizes of the relative fragments are indicated on the right. The lane numbers indicate colony numbers. M = 1kb plus ladder.

(B) Confirmation using PCR

Lane-a= p-RD410 vector only as template; PCR using GUS-R and NPT-F primers

Lane-b=plasmid isolated from colony # 8 as template; PCR using GUS-R and TR2-internal-F primers

Lane-c= plasmid isolated from colony # 8 as template; PCR using NPT-F and TR2-internal-R primers

Lane-d= plasmid isolated from colony # 8 as template; PCR using GUS-R and NPT-F primers

II primer (NPT-F) as the forward (2600 bp) (Figure 3.3.6). Sequence analysis also indicated that the promoter sequence is 100 % identical to the p*TR-ACO3* sequence (data not shown).

Three colonies containing p-RD410 plasmids harbouring the putative *TR-ACO4* promoter were isolated from *A. tumefaciens* transformants, and digested with *Hind* III and *Bam* HI. Colonies #1, #2, and #3 contained plasmids with an insert of the expected size (1350 bp) (Figure 3.3.7-A). PCR was used to re-screen colonies, and the sizes of the amplified product coincided with the predicted sizes using the GUS reverse primer (GUS-R) and a forward primer from the 5′ end of *TR-ACO4* promoter sequence (designated TR4-internal-F) (1350 bp), and using the 3′ end of promoter as the reverse primer (designated TR4-clone-R) and the *NPT II* primer (NPT-F) as the forward (2600 bp) (Figure 3.3.7-B). The 1350 bp product amplified with the GUS primer and the promoter sequence primer was sequenced and shown to be identical to the putative *TR-ACO4* promoter (data not shown).

3.3.2. Analysis of GUS expression in transgenic tobacco

3.3.2.1 Southern blot analysis

Using a GUS specific probe (Section 2.12.2)(Figure 2.9), Southern analysis revealed that selected transgenic tobacco lines harbouring p*TR-ACO1::GUS,* p*TR-ACO2::GUS,* p*TR-ACO3::GUS* and p*TR-ACO4::GUS* contained either one or two copies of the promoter::GUS construct in the diploid tobacco genome.

In the p*TR-ACO1::GUS* transgenic lines, in line # 1, the GUS probe hybridized to one fragment in the *Hind* III and *Bam* HI digested lanes, while no hybridization was observed in the *Eco* RI digested lane. In line #7, the GUS probe hybridized to two fragments in the *Hind* III digested lane, three fragments in the *Bam* HI and *Eco* RI digested lanes. Whereas, in line #11 two fragments were detectable in each of the *Hind* III, *Bam* HI and *Eco* RI digested lanes (Figure 3.3.8).

In the p*TR-ACO2::GUS* transgenic lines, Southern analysis showed in line #2 that the GUS

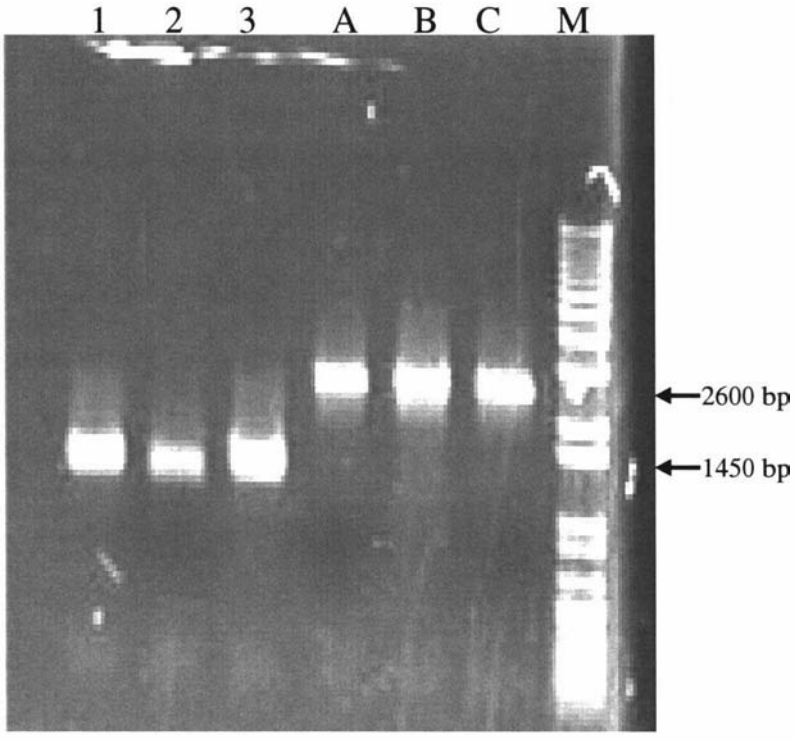

Figure 3.3.6 PCR screening and confirmation of the p*TR-ACO3::GUS* transformation into *Agrobacterium* cells

Screening for colonies containing plasmids with positive inserts by PCR using GUS-R and TR3-clone-F primers (lanes 1-3) and confirmation of positive colonies by PCR using TR3-clone-R and NPT-F primers (lanes A-C). The PCR products were separated by electrophoresis on a 0.75 % (w/v) agarose gel a visualized with ethidium bromide. The relative sizes within the DNA ladder are indicated on the left. M = 1kb plus ladder, -- = blank lanes

Land 1: screening of isolated plasmid from colony #1 by PCR using the GUS-R and TR3-clone-F primers
Land 2: screening of isolated plasmid from colony #2 by PCR using the GUS-R and TR3-clone-F primers
Land 3: screening of isolated plasmid from colony #3 by PCR using the GUS-R and TR3-clone-F primers
Lane A: plasmid isolated from colony #1 screened by PCR using the NPT-F and TR3-clone-R primers
Lane B: plasmid isolated from colony #2 screened by PCR using the NPT-F and TR3-clone-R primers
Lane C: plasmid isolated from colony #3 screened by PCR using the NPT-F and TR3-clone-R primers

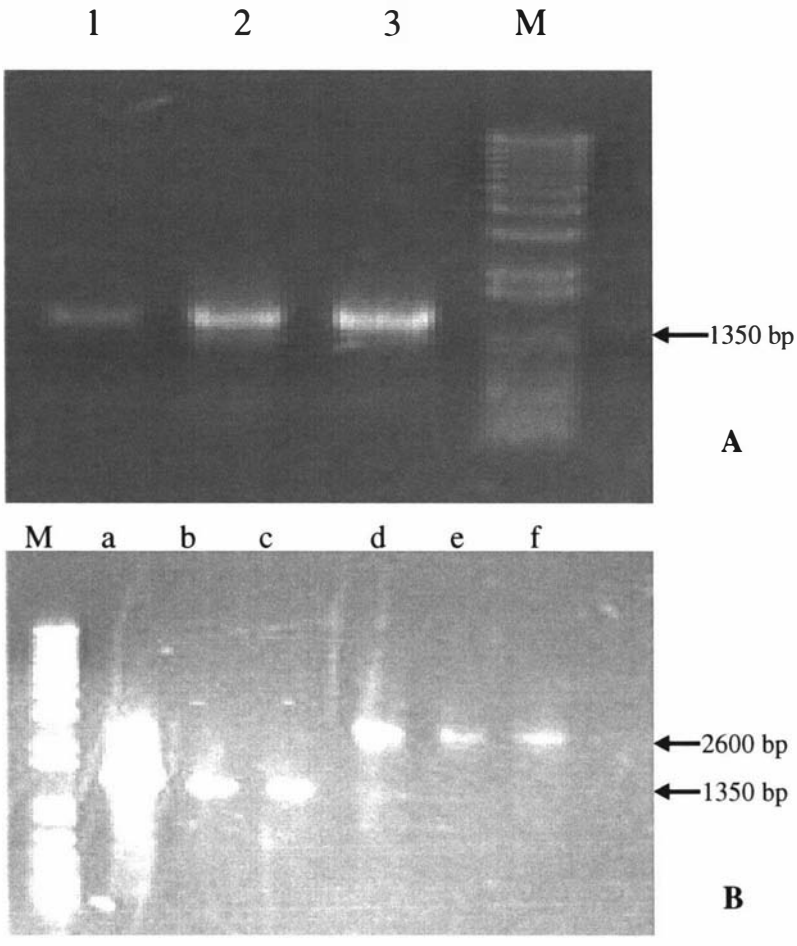

Figure 3.3.7 Restriction enzyme digestion screening and confirmation using PCR, of p*TR-ACO4::GUS* transformation into *Agrobacterium* cells

Screening for colonies containing plasmids with positive inserts using *Hind* III and *Bam* HI digestion (A), and confirmation of positive colonies in (A) by PCR (B).

(A) Restriction enzyme digestion screening

Products were separated by electrophoresis on a 0.75 % (w/v) agarose gel and visualized with ethidium bromide. The sizes of the relative fragments are indicated on the right. The lane numbers indicate the screening colonies. M = 1kb plus ladder.

(B) Confirmation using PCR

Lane-a=plasmid isolated from colony # 1as temple; PCR using GUS-R and TR4-internal-F primers
Lane-b=plasmid isolated from colony # 2 as temple; PCR using GUS-R and TR4-internal-F primers
Lane-c =plasmid isolated from colony # 3 as temple; PCR using GUS-R and TR4-internal-F primers
Lane-d =plasmid isolated from colony # 1 as temple; PCR using NPT-F and TR4-internal-R primers
Lane-e =plasmid isolated from colony # 2 as temple; PCR using NPT-F and TR4-internal-R primers
Lane-f =plasmid isolated from colony # 3 as temple; PCR using NPT-F and TR4-internal-R primers

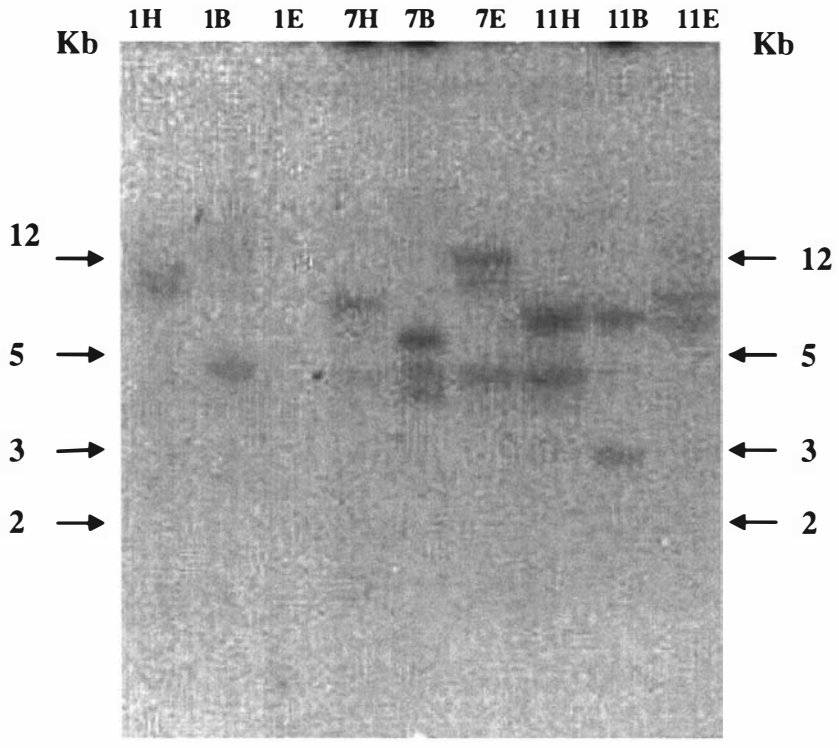

Figure 3.3.8 Screening, using Southern analysis, of putative p*TR-ACO1::GUS* transgenic tobacco plant lines

The membrane was probed with a [α-^{32}P]-dCTP-labeled GUS gene probe, and washed at high stringency (0.1X SSPE, 0.1 % SDS at 65°C) to remove non-specific binding. The numbers represent the selected transgenic plant lines. E = DNA digested with *Eco* RI, H = DNA digested with *Hind* III, B = DNA digested with *Bam* HI. Molecular weight markers are indicated on both sides.

probe did not hybridize to any fragment in the *Hind* III digested lane, but hybridized to two fragments in the *Bam* HI digested lane, and to one fragment in the *Eco* RI digested lane. In line #7, the GUS probe hybridized to two fragments in the *Hind* III, *Bam* HI and *Eco* RI digested lanes. In line #8, the GUS probe hybridized to three fragments in the *Hind* III digested lane, one fragment in the *Bam* HI digested lane, and one fragment in the *Eco* RI digested lane. (Figure 3.3.9).

In the p*TR-ACO3::GUS* transgenic lines, in line #4 the GUS probe hybridized to two fragments in the *Hind* III digested lane, one fragment in the *Bam* HI digested lane, and one fragment in the *Eco* RI digested lane. In line #13 the GUS probe hybridized to one fragment detectable in each of the *Hind* III, *Bam* HI and *Eco* RI digested lanes. The hybridization pattern from line #13 is similar to line #4 with two fragments in the *Hind* III digested lane, one fragment in the *Bam* HI and *Eco* RI digested lanes. (Figure 3.3.10).

In the p*TR-ACO4::GUS* transgenic lines, in line #14 the GUS probe hybridized to two fragments in the *Hind* III and *Eco* RI digested lanes, and one fragment in the *Bam* HI digested lane. In line #17, the GUS probe hybridized to three fragments in the *Hind* III digested lane, two fragments in the *Eco* RI digested lane, and no hybridization was observed in the *Bam* HI digested lane. In line #18, no hybridization was observed in the *Hind* III and *Bam* HI digested lane, but two fragments in the *Eco* RI digested lane were observed (Figure 3.3.11).

3.3.2.2 Primary GUS staining pattern in the p*TR-ACO1::GUS* transformed tobacco plants

Twenty potentially independent lines of p*TR-ACO1::GUS* transformed tobacco plants were screened by GUS staining when they had obtained *ca.* 10 cm in height. Six plants had detectable GUS staining in the apical bud tissues, while in one plant (line # 3) GUS staining was detected in the young root tissue, but not in the terminal apical bud (data not shown). Three of these positive plants lines (# 1, # 7, and # 11) were selected for Southern analysis to

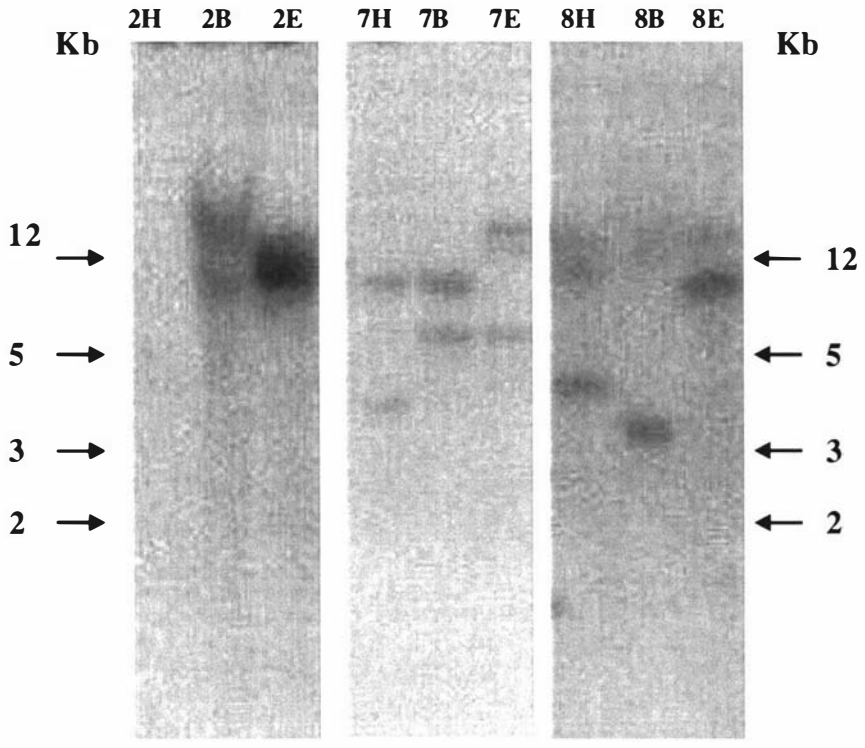

Figure 3.3.9 Screening, using southern analysis, of putative p*TR-ACO2::GUS* transgenic tobacco plant lines

The membrane was probed with a [α-^{32}P]-dCTP-labeled GUS gene probe, and washed at high stringency (0.1X SSPE, 0.1 % SDS at 65°C) to remove non-specific binding. The numbers represent the selected transgenic plant lines. E = DNA digested with *Eco* RI, H = DNA digested with *Hind* III, B = DNA digested with *Bam* HI. Molecular weight markers are indicated on both sides.

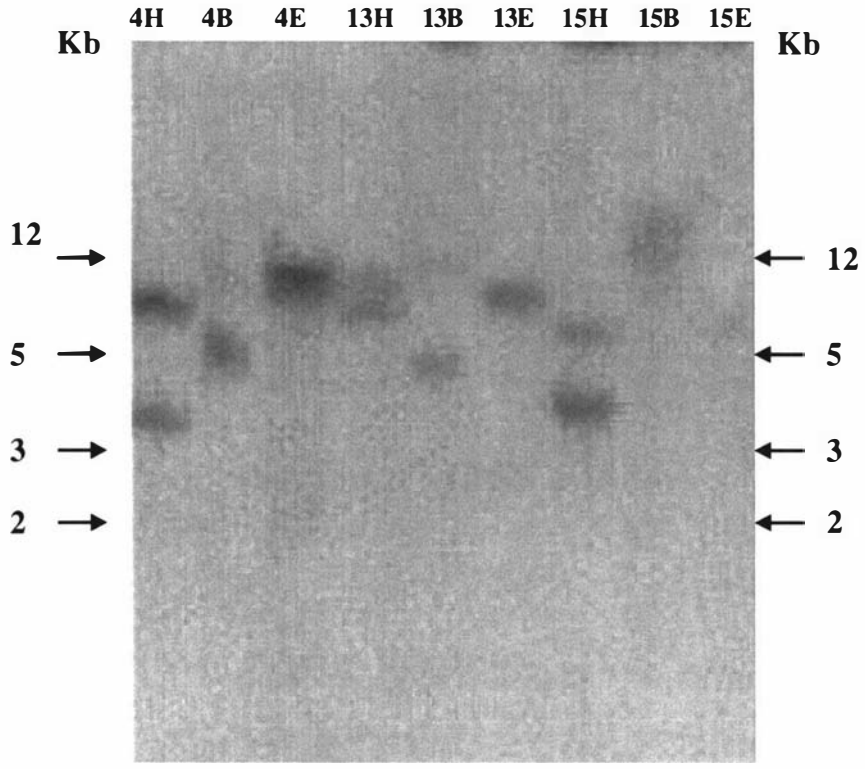

Figure 3.3.10 Screening using Southern analysis, of putative p*TR-ACO3::GUS* transgenic tobacco plant lines

The membrane was probed with a [α-^{32}P]-dCTP-labeled GUS gene probe, and washed at high stringency (0.1X SSPE, 0.1 % SDS at 65°C) to remove non-specific binding. The numbers represent the selected transgenic plant lines. E = DNA digested with *Eco* RI, H = DNA digested with *Hind* III, B = DNA digested with *Bam* HI. Molecular weight markers are indicated on both sides.

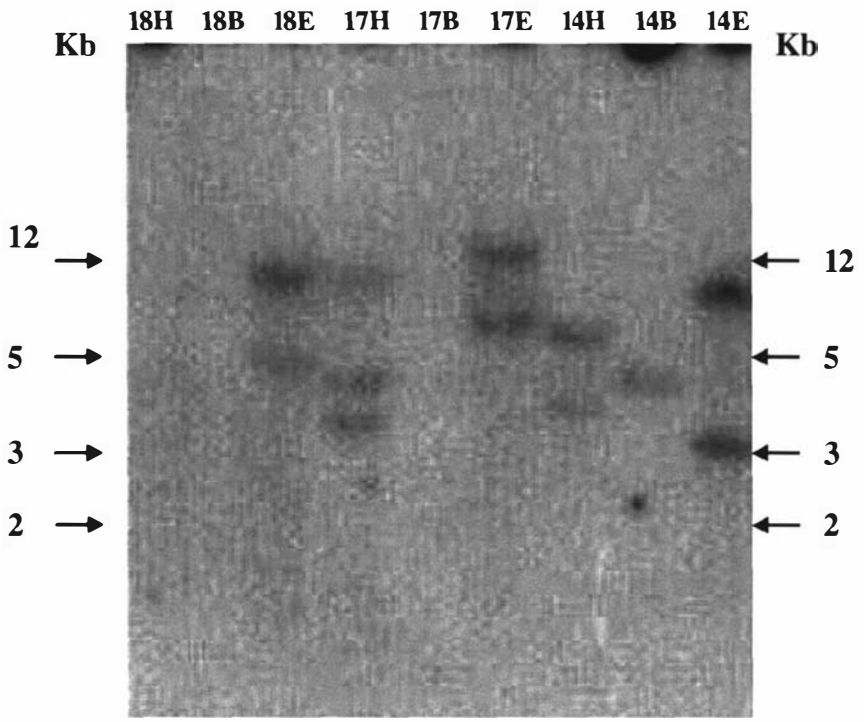

Figure 3.3.11 Screening using Southern analysis, of putative p*TR-ACO4::GUS* transgenic tobacco plant lines

The membrane was probed with a [α-^{32}P]-dCTP-labeled GUS gene probe, and washed at high stringency (0.1X SSPE, 0.1 % SDS at 65°C) to remove non-specific binding. The numbers represent the selected transgenic plant lines. E = DNA digested with *Eco* RI, H = DNA digested with *Hind* III, B = DNA digested with *Bam* HI. Molecular weight markers are indicated on both sides.

confirm that they were independent lines and determine the copy number of the inserted GUS gene (see Section 3.3.2.1). When these three plants grew to 40 cm in height (designated the mature green leaf stage), leaf tissues at different stages of development were analyzed for GUS staining. The results showed that all of these three plants displayed GUS staining only at the terminal apical bud and in the axillary buds, while GUS staining was not observed in the leaf tissue at any stage of development. The intensity of GUS staining in the axillary buds ranged from a higher level observed in buds in the axils of the younger leaves (leaves # 1 to # 3) to a lower intensity of staining observed in buds in the axils of the older leaves (leaves # 8 to # 10). No staining could be observed in the axils of the oldest leaves (leaves # 11 and # 12) (Figure 3.3.12-A).

When these plants grew to over 60 cm in height with more yellowing leaves, the GUS staining pattern was assessed again. To assist in assessing leaf development in these transformants, and in the p*TR-ACO2::GUS,* p*TR-ACO3::GUS* and p*TR-ACO4::GUS* transformants, chlorophyll content was determined in wild-type plants that had reached a similar size (Figure 3.3.16). In the p*TR-ACO1* transformants, the axillary buds in the axils of youngest leaves (leaves # 1 and # 2) did not show any GUS staining, and then staining increased in intensity (leaves # 3 to # 10) followed by a decrease in intensity (leaves # 11 and # 12). At the leaf developmental stages in which the highest GUS staining was observed in the axils (leaves # 4 to # 7), faint GUS staining can be observed in the vascular cells of the leaf petiole (Figure 3.3.12-B).

3.3.2.3 Primary GUS staining pattern in the p*TR-ACO2::GUS* transformed tobacco plants

Twenty potentially independent lines of tobacco putatively containing the p*TR-ACO2::GUS* construct were screened by GUS staining once they had attained 10 cm in height. Only three plants lines (# 2, # 7, and # 8) displayed GUS staining on the leaf discs. These plants were

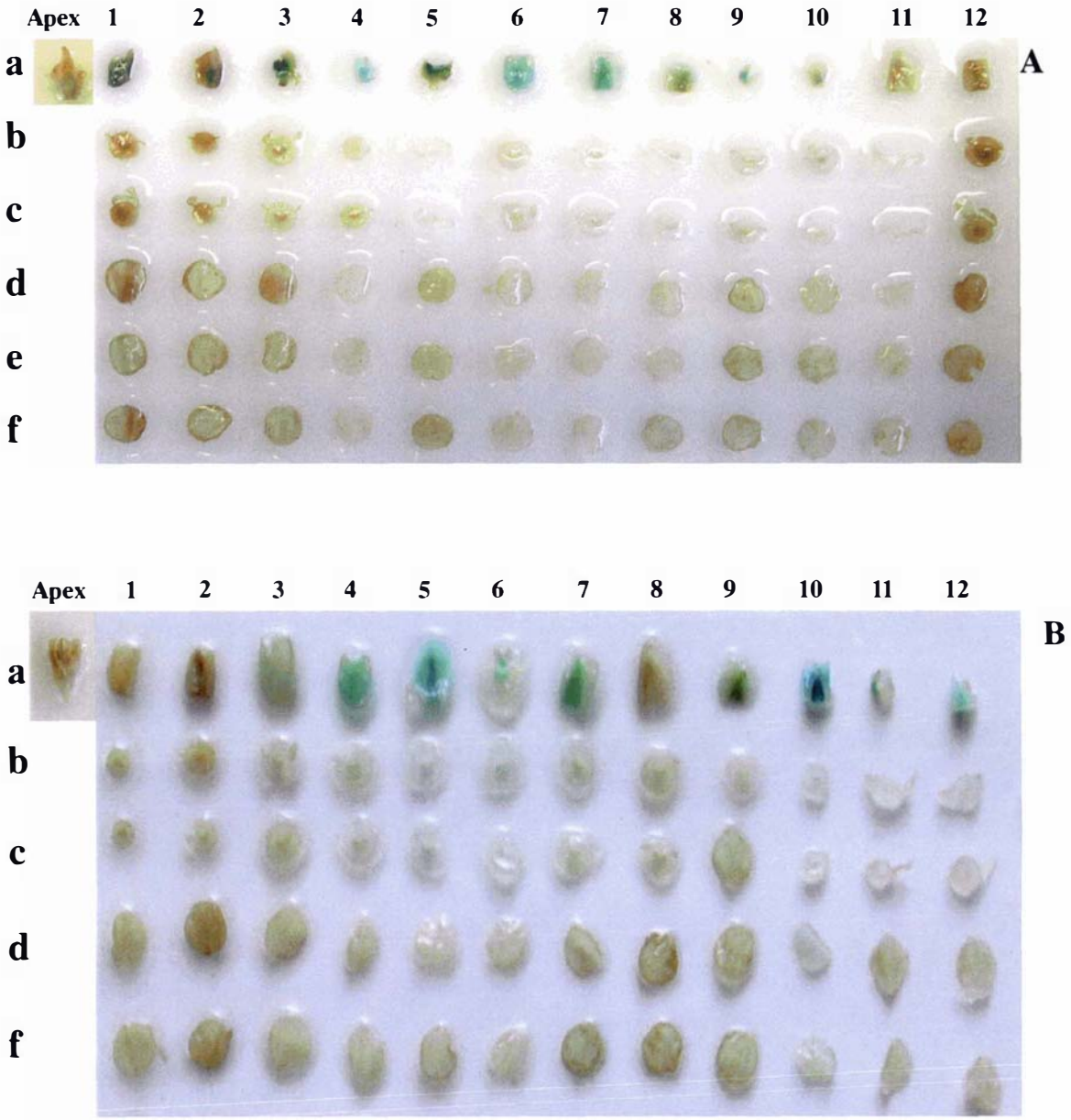

Figure 3.3.12 GUS staining analysis of leaf tissues excised from p*TR-ACO1::GUS* transformed tobacco lines

A. Transgenic line #1 of p*TR-ACO1::GUS* construct at the mature green leaf stage
B. Transgenic line #1 of p*TR-ACO1::GUS* construct at the senescence stage

Tissues, as indicated, were stained by X-Gluc and de-stained through an ethanol series. The numbers represent the node number, starting from the terminal apical bud. a = axillary/ apical bud, b = proximal section of the petiole, c = distal section of the petiole, d= proximal lamina, e = middle lamina, f = distal lamina

grown further and Southern blot analysis used to confirm each as an independent line and to determine the number of copies of GUS inserts (Section 3.3.2.1). Once these plants were at 40 cm in height (mature-green leaf stage) their leaf tissues were analyzed for the pattern of GUS staining. Results showed that GUS staining in axillary buds appeared from leaf # 2 to leaf # 10 (Figure 3.3.13-A-a). After leaf # 10, no axillary buds were observed in the leaf axils. A very low intensity of GUS staining was observed in the petiole tissue at the mature green leaf stage (leaves # 3 to # 10), but with higher intensity staining in senescent leaves (leaves # 11 to # 13) (Figure 3.3.13-A-b). The GUS staining in leaf midribs started at the late mature-green leaf stage (leaves # 6 to # 10) and increased in intensity until the senescent leaf stage (leaves #11-#13) (Figure 3.3.13-A-c). GUS staining in leaf lamina tissue was observed from leaf # 8 and increased in intensity until leaf #13 (Figure 3.3.13-A-d).

When these plants grew to over 60 cm in height with more yellowing leaves, GUS staining showed more intensity and appeared earlier in development, and chlorophyll content used to assess leaf development (Figure 3.3.16). The GUS staining in axillary buds, started to appear from leaf # 5 to leaf # 7 (Figure 3.3.13-B-a). After leaf # 7, no axillary buds were observed in the leaf axils. A high intensity of GUS staining was observed in petioles at the mature green leaf stage (leaves # 4 to # 7) and this increased in intensity in senescent leaves (leaves # 8 to # 12) (Figure 3.3.13-B-b). GUS staining was observed in leaf midribs from early mature-green leaves (leaf # 3) and then increased in intensity until the late senescent leaf (leaf # 12) (Figure 3.3.13-B-c). The GUS staining in leaf lamina tissue displayed a similar pattern to that observed in midribs (Figure 3.3.13-B-d).

3.3.2.4 Primary GUS staining pattern in the p*TR-ACO3::GUS* transformed tobacco plants

Twenty five potentially independent lines putatively harbouring p*TR-ACO3::GUS* constructs were screened by GUS staining when plants were at a young stage (10 cm in height). Fifteen

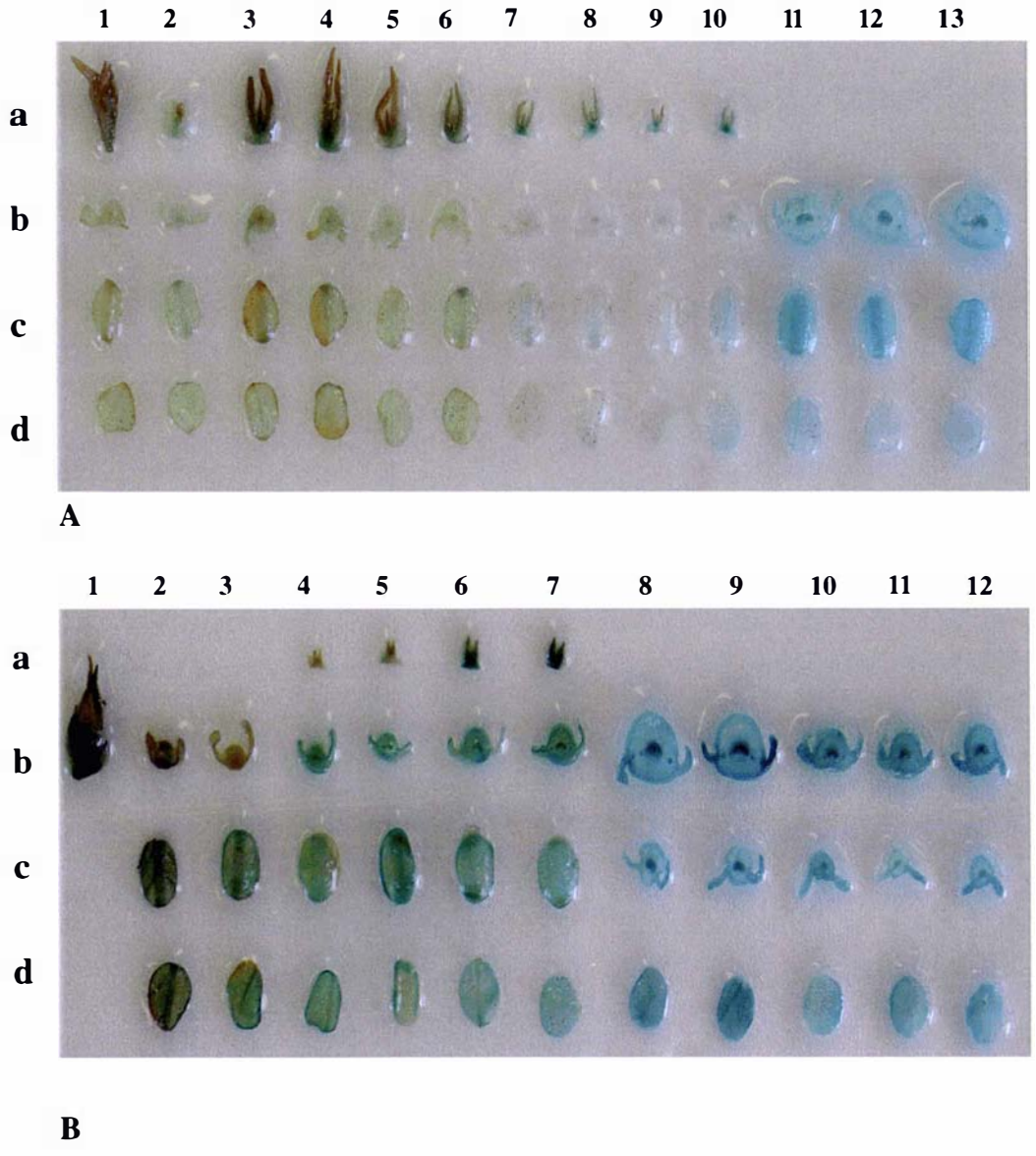

Figure 3.3.13 GUS staining analysis of leaf tissues excised from p*TR-ACO2::GUS* transformed tobacco lines

A. Transgenic line #2 of p*TR-ACO2::GUS* construct at the mature green leaf stage
B. Transgenic line #2 of p*TR-ACO2::GUS* construct at the senescence stage

Tissues, as indicated, were stained by X-Gluc and de-stained through an ethanol series. The numbers represent the node number, starting from the terminal apical bud. a = axillary bud, b = distal petiole, c = distal midrib, d = middle lamina

plants displayed blue staining on leaf discs. Three of these positive plants lines (# 4, # 13, and # 15) were selected for Southern analysis to confirm that these were individual lines and to determine the copy number of inserted GUS genes (Section 3.3.2.1). When these three plants had grown to the mature green leaf stage (around 40 cm in height), leaf tissues were analyzed for the pattern of GUS staining. The results showed that GUS staining in axillary buds, appeared from leaf # 5 and increased in intensity until leaf # 15, and then decreased in the oldest leaf (# 16) (Figure 3.3.14-A-a). In petiole tissue, GUS staining was observed throughout from the young leaf (leaf # 2) and increasing through to the senescent leaf (leaf # 16) (Figure 3.3.13-A-b, c). The GUS staining in leaf midribs also began at the young leaf (leaf # 2) and increased in intensity through to the senescent leaf (leaf # 16). (Figure 3.3.13-A-d,e). GUS staining in leaf lamina tissue was observed only in the proximal lamina in the vascular tissue. The intensity of blue colour observed from leaf # 2 increased to leaf # 12, and then decreased until leaf #16 (Figure 3.3.14-A-f). No staining was observed in the middle or proximal lamina (Figure 3.3.14-A-g, h).

When these plants grew to over 60 cm in height and increased numbers of yellowing leaves, GUS staining was more intense and the staining pattern was altered. The GUS staining in axillary buds started to appear from leaf # 2 and increased in intensity until leaves # 9 to # 13, after which it decreased at the yellowing leaves (leaves # 14 to # 16) (Figure 3.3.14-B-a). Staining in the petiole tissue was observed from leaf # 3 to leaf # 16. The highest intensity of staining was observed in leaves # 7 to # 11, and in leaf # 14. (Figure 3.3.14-B-b, c). In leaf lamina tissue, GUS staining was evident in the early mature-green leaf (leaf # 4) and increased in intensity through to the senescent leaf stage (leaf # 15) but had disappeared by leaf # 16. Also, from leaf # 8 to leaf #16, dense GUS staining appeared at the cut edges of the leaf lamina (Figure 3.3.14-B-f, g).

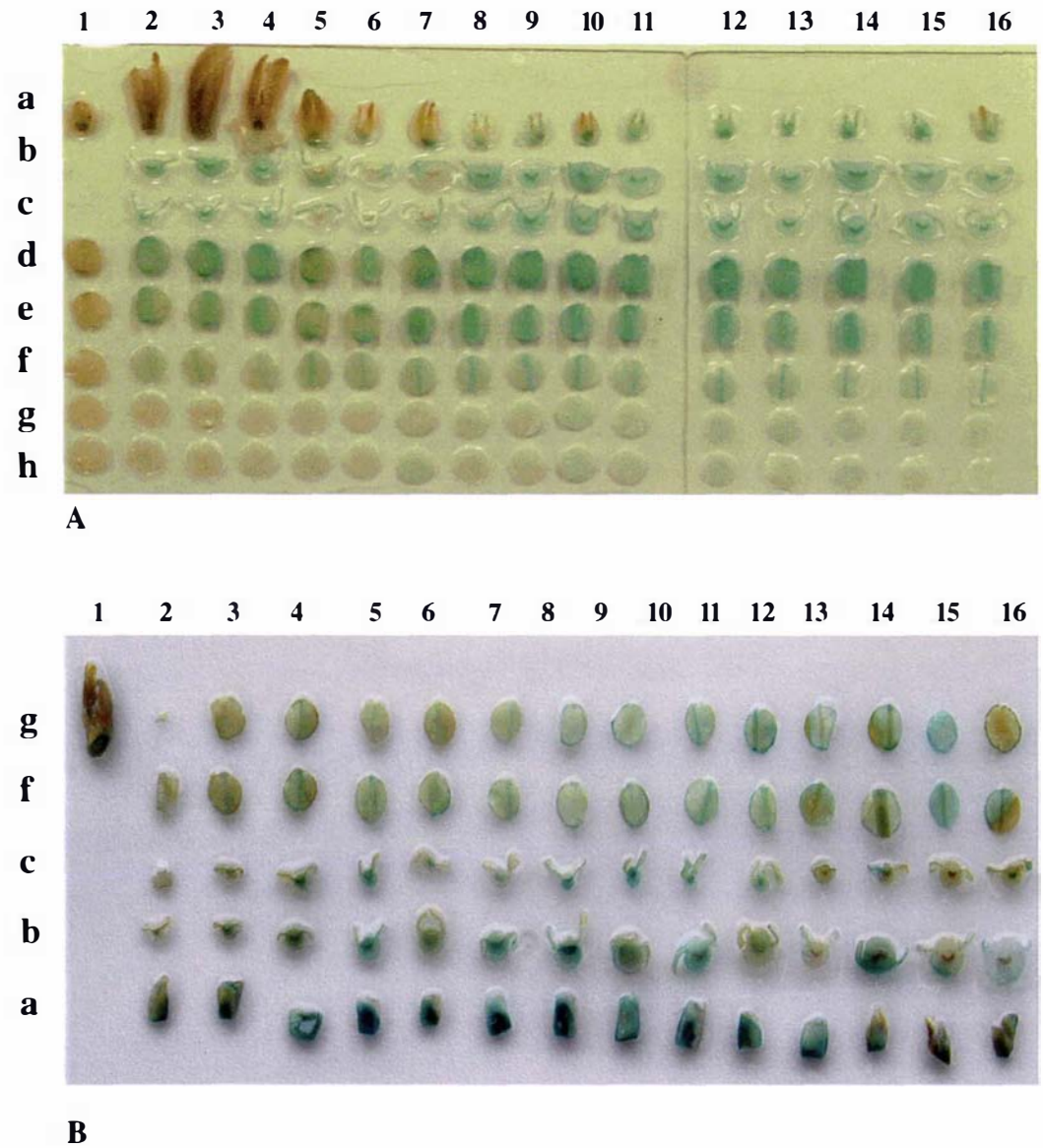

Figure 3.3.14 GUS staining analysis of leaf tissues excised from p*TR-ACO3::GUS* transformed tobacco lines

A. Transgenic line #13 of p*TR-ACO3::GUS* construct at the mature green stage
B. Transgenic line #13 of p*TR-ACO3::GUS* construct at the senescent stage

Tissues, as indicated, were stained by X-Gluc and de-stained through an ethanol series. The numbers represent the node number starting from the terminal apical bud. a = axillary bud, b = proximal petiole, c = distal petiole, d = proximal midrib, e = distal midrib, f = proximal lamina, g = middle lamina, h = distal lamina

3.3.2.5 Primary GUS staining pattern in the p*TR-ACO4::GUS* transformed tobacco plants

Thirty potentially independent lines putatively harbouring the p*TR-ACO4::GUS* construct were screened by GUS staining at the young leaf stage (10 cm in height). Twenty two plants displayed GUS staining on leaf discs. Three of these positive plants lines (# 14, # 17, and # 18) were selected for Southern blot analysis to confirm that they were independent lines and to determine the copy number of the inserted GUS gene (Section 3.3.2.1). These three plants grew to around 40 cm in height (mature-green leaf stage), and their leaf tissues were analyzed for the pattern of GUS staining. The results showed that all three plants displayed intense GUS staining in the axillary buds, leaf petioles, midribs, and leaf lamina. When compared with the results of GUS staining of the selected p*TR-ACO3::GUS* transformants, the blue colour was significantly denser in the p*TR-ACO4::GUS* plants. The intensity of GUS staining in leaf tissues increased from young leaf tissue arising from the terminal bud to the mature green leaf tissue towards the base. (Figure 3.3.15-A). The results showed that GUS staining in axillary buds started to appear from leaf # 1 and increased in intensity until leaf # 11 (Figure 3.3.15-A-a). The GUS staining in petiole tissue was observed throughout the developmental sequence, from the youngest leaf (leaf # 1) through to the senescent leaf stage (leaf # 11) (Figure 3.3.15-A-b, c). The GUS staining in leaf midribs also started in the youngest leaf (leaf # 1) and increasd in intensity through to the senescent leaf stage (leaf # 11). (Figure 3.3.15-A-d,e). The GUS staining in the leaf lamina tissues was observed in the proximal lamina tissue from leaf # 1 to leaf # 11, but in the middle and distal lamina tissues, the GUS staining started at leaf # 3, and increased in intensity to leaf # 11 but staining was a lower intensity when compared with that observed in the proximal lamina. Also, in the proximal lamina of leaves # 1 and # 2, GUS staining appeared at the cut edge (Figure 3.3.15-A-f, g, h).

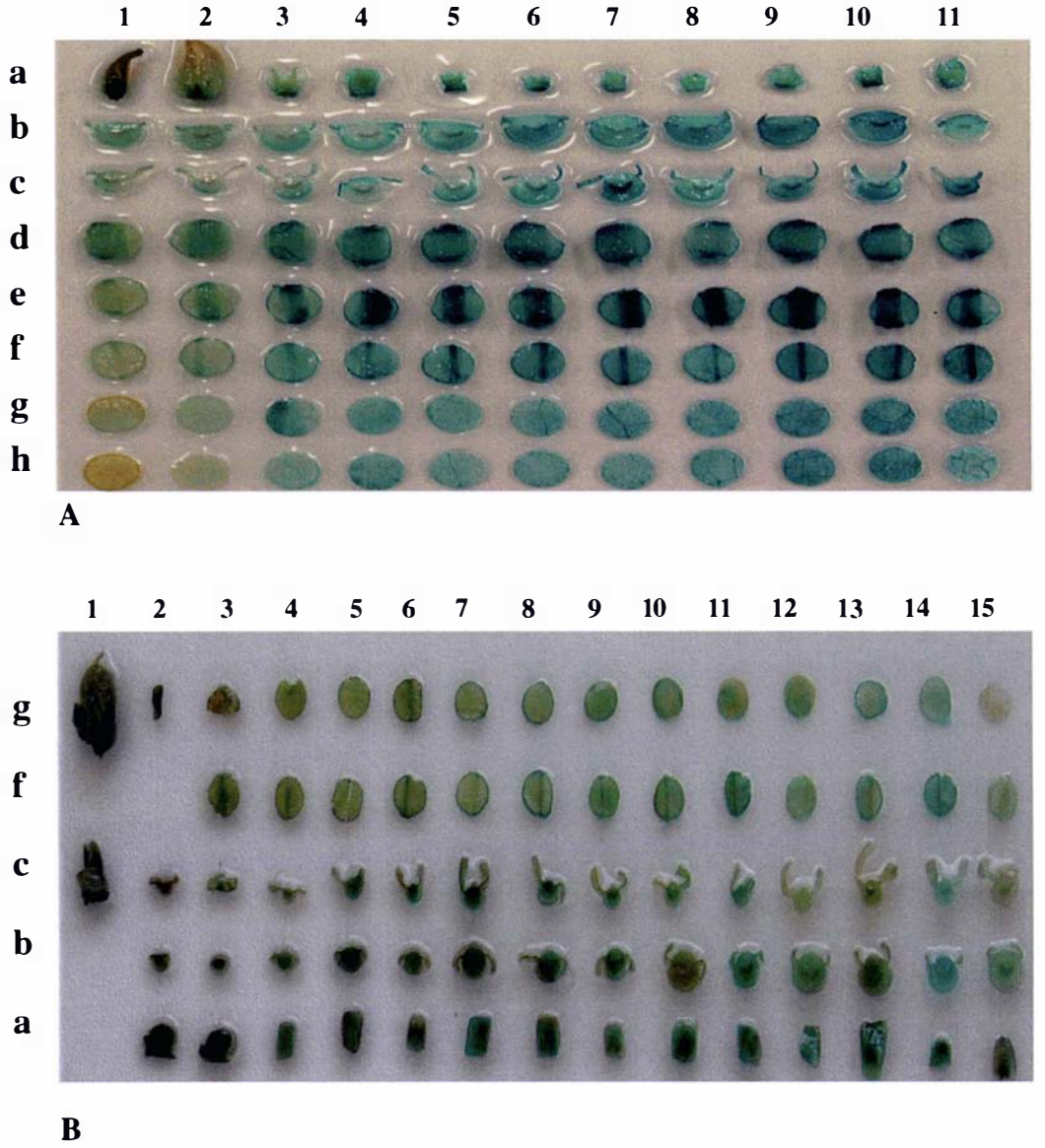

Figure 3.3.15 GUS staining analysis of leaf tissues excised from p*TR-ACO4::GUS* transformed tobacco lines

A. Transgenic line #14 of p*TR-ACO4::GUS* construct at the mature green leaf stage
B. Transgenic line #14 of p*TR-ACO4::GUS* construct at the senescent stage

Tissues, as indicated, were stained by X-Gluc and de-stained through an ethanol series. The numbers represent the node number, starting from the terminal apical bud. a = axillary bud, b = proximal petiole, c = distal petiole, d = proximal midrib, e = distal midrib, f = proximal lamina, g = middle lamina, h = distal lamina

When these plants grew to over 60 cm in height so they had greater numbers of yellowing leaves, a less intense GUS staining and different staining pattern was observed. The GUS staining in axillary buds appeared from leaf # 4 and increased in intensity until leaves # 10 to # 14, and then decreased in the oldest leaf (leaf # 15) (Figure 3.3.15-B-a). Staining in petiole tissue can be observed from leaf # 3 to leaf # 15. The highest intensity can be detected in leaves # 7 to # 11, and in leaf # 14. (Figure 3.3.15-B-b, c). GUS staining in leaf lamina tissue started in an early mature-green leaf (leaf # 3), increased in intensity until late senescent leaf stage (leaf # 14), and then decreased and had disappeared in leaf #15. Also, from leaf # 7 to leaf # 14, GUS staining appeared at the cut edges of the leaf lamina (Figure 3.3.15-B-f, g).

3.3.2.6 Changes in total chlorophyll concentration during leaf ontogeny in tobacco

To assist in assessing leaf development, total chlorophyll content (as chlorophyll *a* + *b*) was determined in wild-type plants that had reached *ca.* 60 cm in size (Figure 3.3.16). At each developmental stage (over 18 leaves), leaves from three individual wild-type tobacco lines were used for total chlorophyll determination. The chlorophyll concentration in the first leaf (designed newly initiated (leaf # 1)) is very low (52 μg/g Fw) when compared with the other leaves. After this, the concentration increases until leaf # 7 (1605 μg/g Fw), which is at the young mature-green leaf stage. But for the following leaves (# 8 to # 10), the concentrations decreased until reaching 839 μg/g Fw. In this range, the leaves are in the mature green leaf stages. From leaves # 11 to # 13, the chlorophyll concentrations decreased slowly. In these leaves, the colour started to yellow at the edge of lamina. After leaf # 13, the chlorophyll concentrations decreased until the deep yellow senescent leaf stage (leaf # 18) was reached, with a concentration of 138 μg/g Fw (Figure 3.3.16).

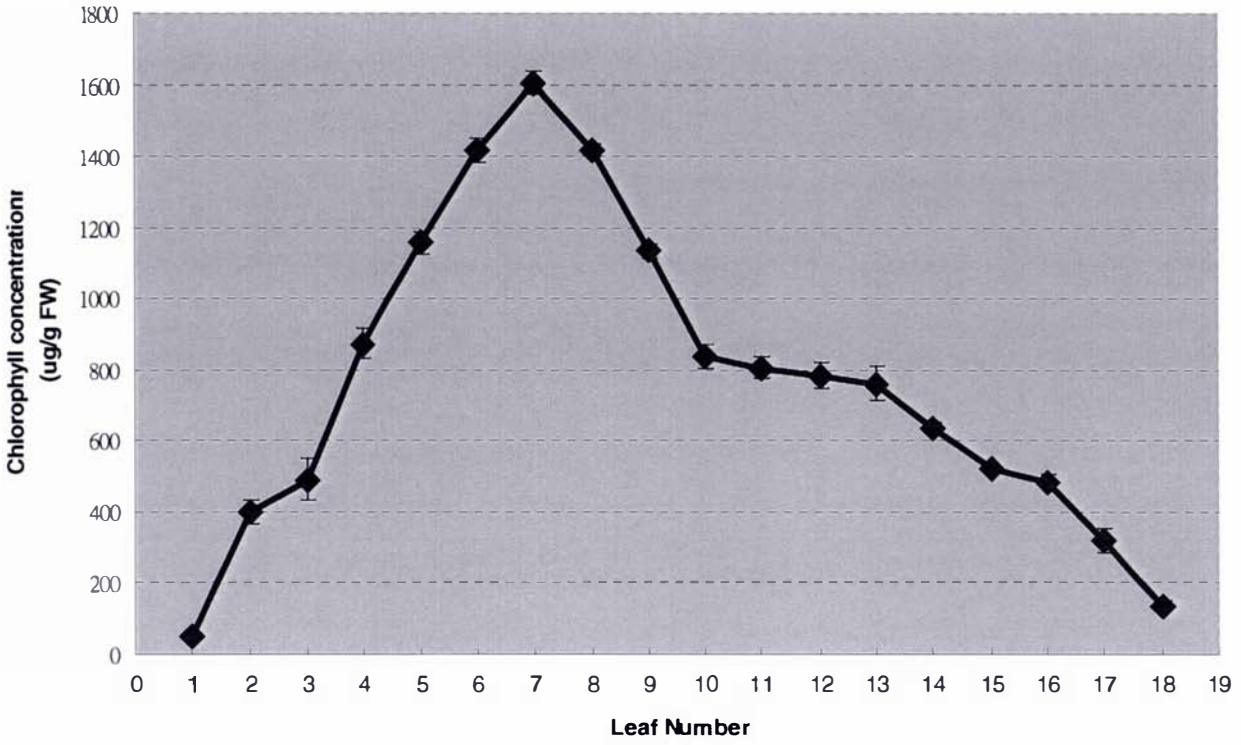

Figure 3.3.16 Changes total in chlorophyll concentration during leaf ontogeny in tobacco

At each leaf number, the data is the mean for each leaf sample from three individual wild-type tobacco lines. Error bars = ± 1 sem for 3 plant lines.

3.3.3. Analysis of GUS expression in transgenic white clover

3.3.3.1 Southern blot analysis

By using a GUS specific probe (Section 2.12.2)(Figure 2.9), Southern analysis revealed that selected transgenic white clover lines harbouring p*TR-ACO1::GUS,* p*TR-ACO2::GUS,* p*TR-ACO3::GUS* and p*TR-ACO4::GUS* contained either one or two copies of the p*TR-ACO::GUS* insert in their genome.

In the p*TR-ACO1::GUS* transgenic lines, in line #1 the GUS probe hybridized to two fragments in the *Hind* III, *Bam* HI and *Eco* RI digested lanes. In line # 3, the GUS probe hybridized to two fragments in the *Hind* III and *Bam* HI digested lanes, and one fragment in the *Eco* RI digested lane. In line #11, one fragment is detectable in the *Hind* III and *Bam* HI digested lanes, and two fragments in the *Eco* RI digested lanes (Figure 3.3.17).

In the p*TR-ACO2::GUS* transgenic lines, Southern analysis showed that in line #1, the GUS probe hybridized to two fragments in the *Hind* III and *Bam* HI digested lanes, and to three fragments in the *Eco* RI digested lane. In line #12, the GUS probe hybridized to one fragment in the *Hind* III, *Bam* HI and *Eco* RI digested lanes, and in the line #19, the GUS probe hybridized to two fragments in each of the *Hind* III, *Bam* HI and *Eco* RI digested lanes (Figure 3.3.18).

In the p*TR-ACO3::GUS* transgenic lines, in line #1 the GUS probe hybridized to one fragment in the *Hind* III and *Bam* HI digested lanes, and two fragments in the *Eco* RI digested lane. In line #2, the GUS probe hybridized has two fragments detectable in each of the *Hind* III, *Bam* HI and *Eco* RI digested lanes, and in line #6, the GUS probe hybridized to two fragments in the *Hind* III and *Eco* RI digested lanes, and one fragment in the *Bam* HI digested lane. (Figure 3.3.19).

In the p*TR-ACO4::GUS* transgenic lines, in line #1 the GUS probe hybridized to two

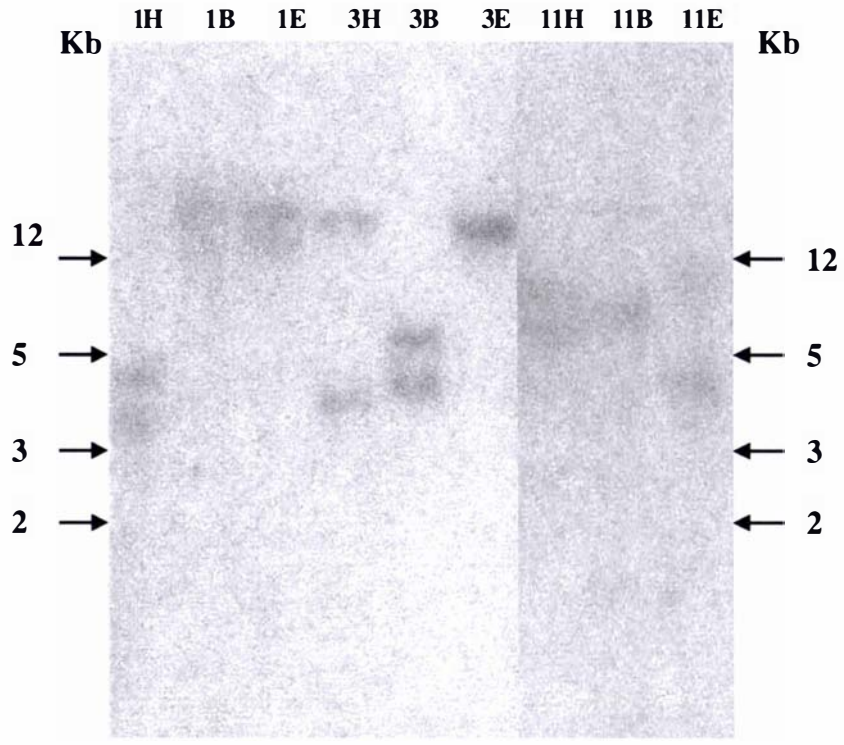

Figure 3.3.17 Screening, by Southern analysis, of transgenic white clover transformed with the p*TR-ACO1::GUS* construct

The membrane was probed with a [α-^{32}P]-dCTP labeled GUS gene probe, and washed at high stringency (0.1X SSPE, 0.1 % SDS at 65°C) to remove non-specific binding. The numbers represent the selected transgenic plant lines. E = DNA digested with *Eco* RI, H = DNA digested with *Hind* III, B = DNA digested with *Bam* HI. Molecular weight markers are indicated on both sides.

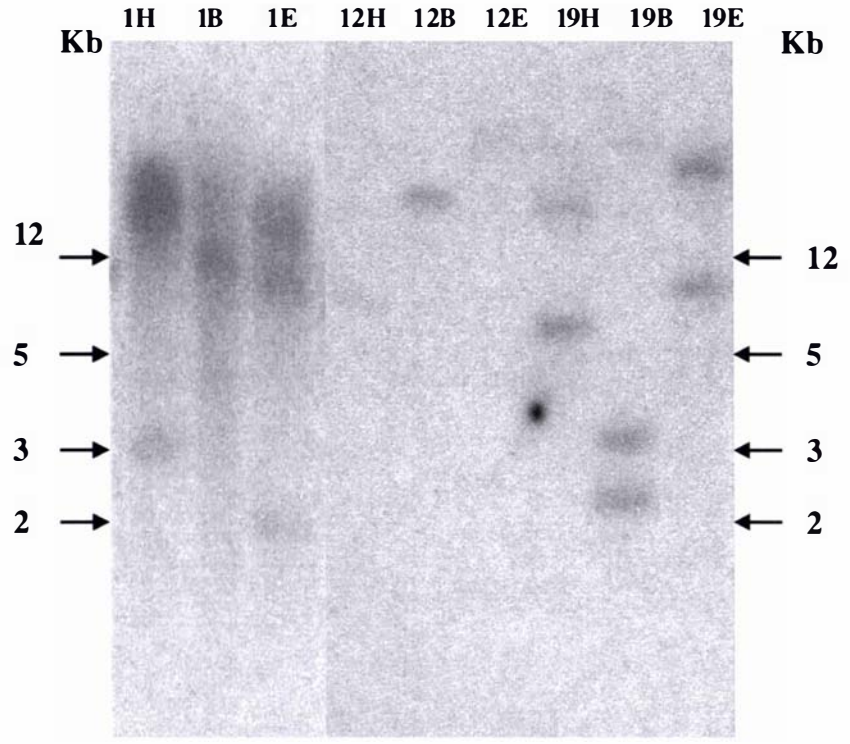

Figure 3.3.18 Screening, by Southern analysis, of transgenic white clover transformed with the p*TR-ACO2::GUS* construct

The membrane was probed with a [α-^{32}P]-dCTP labeled GUS gene probe, and washed at high stringency (0.1X SSPE, 0.1 % SDS at 65°C) to remove non-specific binding. The numbers represent the selected transgenic plant lines. E = DNA digested with *Eco* RI, H = DNA digested with *Hind* III, B = DNA digested with *Bam* HI. Molecular weight markers are indicated on both sides.

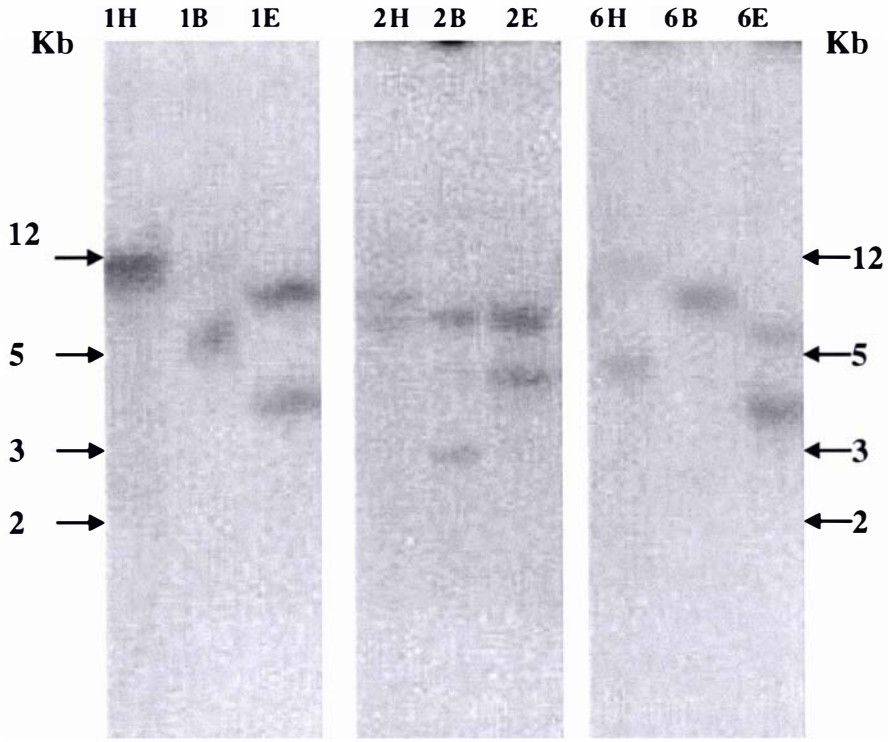

Figure 3.3.19 Screening, Southern analysis, of transgenic white clover transformed with the p*TR-ACO3::GUS* construct

The membrane was probed with a [α-^{32}P]-dCTP labeled GUS gene probe, and washed at high stringency (0.1X SSPE, 0.1 % SDS at 65°C) to remove non-specific binding. The numbers represent the selected transgenic plant lines. E = DNA digested with *Eco* RI, H = DNA digested with *Hind* III, B = DNA digested with *Bam* HI. Molecular weight markers are indicated on both sides.

fragments in the *Hind* III, *Bam* HI and *Eco* RI digested lanes. In line #22, the GUS probe hybridized to two fragments in the *Hind* III digested lane, and to three fragments in the *Bam* HI and *Eco* RI digested lanes. In line #26, the probe hybridized to two fragments in the *Hind* III digested lane, and to three fragments in *Bam* HI and *Eco* RI digested lanes (Figure 3.3.20).

3.3.3.2 Changes in chlorophyll concentration during leaf ontogeny in white clover

To determine the relationship between the developmental stage of each leaf (node) and the p*TR-ACO::GUS* expression pattern, the total chlorophyll content (chlorophyll *a* + *b*) of each leaf was measured (Figure 3.3.21). The chlorophyll concentration in the first two leaves (# 1 and # 2) was lower (290-330 μg/g Fw) when compared with all the other leaves, but by leaf # 3, the chlorophyll concentration had increased to 1400 μg/g Fw. After that stage, the chlorophyll concentration slowly increased from leaf # 3 to leaf # 6 to reach a peak at 1700 μg/g Fw to form the mature-green leaf stage. From this peak (leaves # 5 and # 6), the chlorophyll concentration decreased, so that at leaf # 9 (a yellowing leaf) a concentration of 350 μg/g Fw was measured.

3.3.3.3 Primary GUS staining patterns in the p*TR-ACO1::GUS* transformed white clover plants

Twenty five potentially independent lines of white clover putatively transformed with the p*TR-ACO1::GUS* construct were screened by GUS staining once they had developed 3 to 4 trifoliate leaves. Nineteen plants displayed a blue colour within the apical structure. Three of those positive plant lines (# 1, # 3, and # 11) were selected for subsequent Southern analysis (section 3.3.3.1) to confirm that they did represent independent lines and to determine the copy number of the inserted GUS gene (Figure 3.3.17). When these three plants had developed stolons comprising 7 to 9 leaves, three different stolons, from the same plant were analyzed for the pattern of GUS staining and a representative stolon from each line is shown

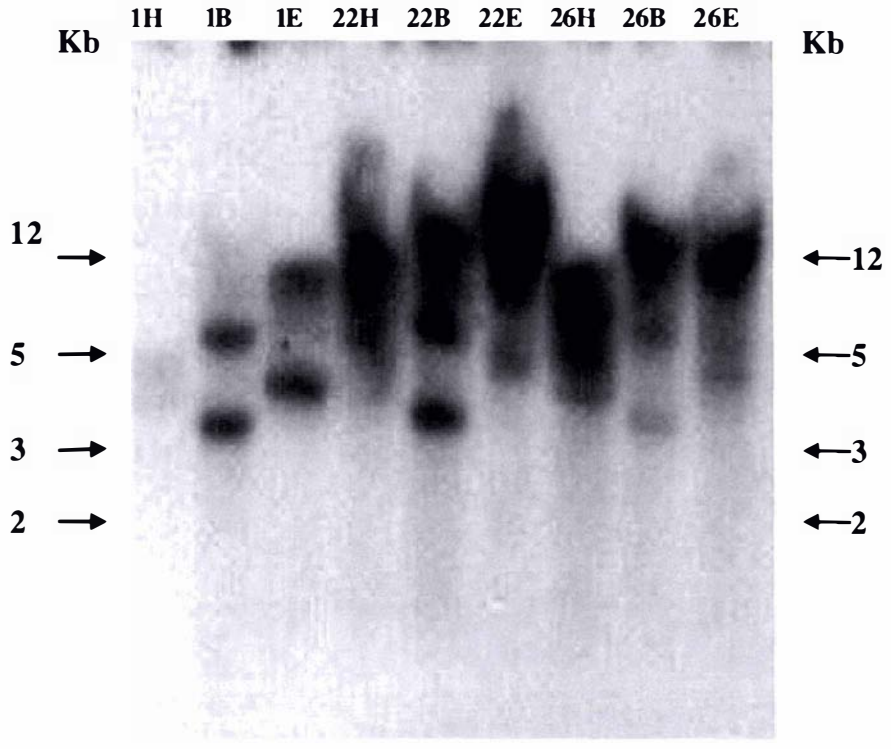

Figure 3.3.20 Screening, by Southern analysis, of transgenic white clover transformed with the p*TR-ACO4::GUS* construct

The membrane was probed with a [α-^{32}P]-dCTP labeled GUS gene probe, and washed at high stringency (0.1X SSPE, 0.1 % SDS at 65°C) to remove non-specific binding. The numbers represent the selected transgenic plant lines. E = DNA digested with *Eco* RI, H = DNA digested with *Hind* III, B = DNA digested with *Bam* HI. Molecular weight markers are indicated on both sides.

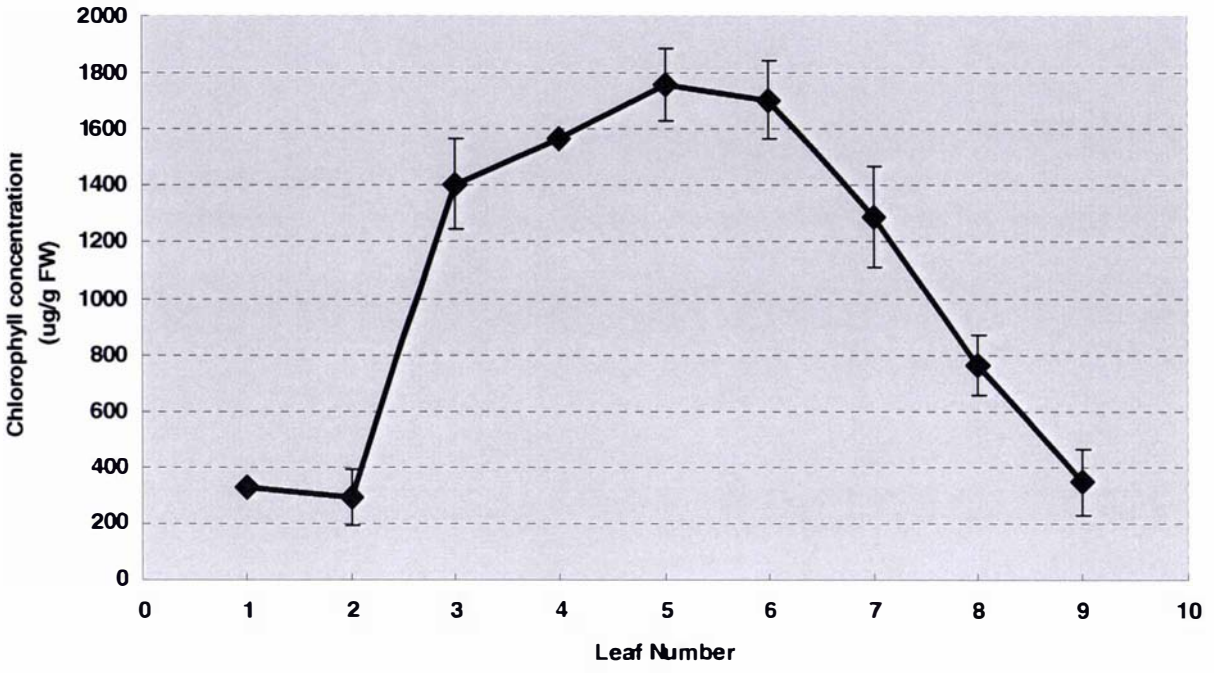

Figure 3.3.21 Changes in total chlorophyll concentration during leaf ontogeny in white clover

At each leaf number, the data is the mean for each leaf sample from three individual white clover stolons. Error bars = ± 1 sem for 3 plant lines.

in Figure 3.3.22. In these stolons, staining was generally more pronounced in the apical structure and axillary buds when compared with the petiolule and leaf lamina. In terms of leaf ontogeny, staining was highest generally in the apical structure and in the axillary buds subtending from the younger nodes, and least in the newly senescent plant parts (Figure 3.3.22).

The GUS staining in the axillary bud/ stolon segments of line # 1, was intense from leaf # 1 to leaf # 7, with staining most concentrated in leaf # 1, # 2 and # 7 (Figure 3.3.22-A-a). In the trifoliate leaves, GUS staining was observed in the petiolules with highest intensity at leaf # 1 and then intensity decreased along to leaf # 6. Staining then increased in leaf # 7 (Figure 3.3.22-A-b). The GUS staining in leaf lamina tissue was observed in leaf # 2, # 4 and leaf # 6, with the highest intensity of staining in leaf # 2 (Figure 3.3.22-A-c). In the petiole segment, no staining could be observed (Figure 3.3.22-A-d).

In line # 3, GUS staining in the axillary bud/ stolon segments began at leaf # 1 and increased in intensity until leaf # 8 (Figure 3.3.22-B-a). In the trifoliate leaves, GUS staining was observed mainly in the petiolules, and started to increase from leaf # 2 to leaf # 4 and then decreased to leaf # 8 (Figure 3.3.22-B-b). GUS staining in leaf lamina tissue was observed from leaf # 3 to leaf # 6. Leaf #8 also showed some trace of GUS staining but the highest intensity of staining appeared in leaf #4 (Figure 3.3.22-B-c). In petiole segments, GUS staining appeared from leaf # 2 to leaf # 7 but not in #8, with staining most concentrated at leaf # 2, # 3 and # 4 (Figure 3.3.22-B-d).

In line # 11, the GUS staining in the axillary bud/ stolon segments was intense at leaf #1 and # 2, and then decreased to leaf # 8 (Figure 3.3.22-C-a). In the trifoliate leaves, GUS staining was observed mainly in the petiolules, with highest intensity in leaf # 1, after which it decreased until leaf # 6, before it increased in leaf # 7 (Figure 3.3.22-C-b). GUS staining in the leaf lamina tissue was observed in leaves # 1, # 2 and leaf # 4, with the highest intensity of GUS staining in leaf # 2 (Figure 3.3.22-C-c). In petiole segments, GUS staining was

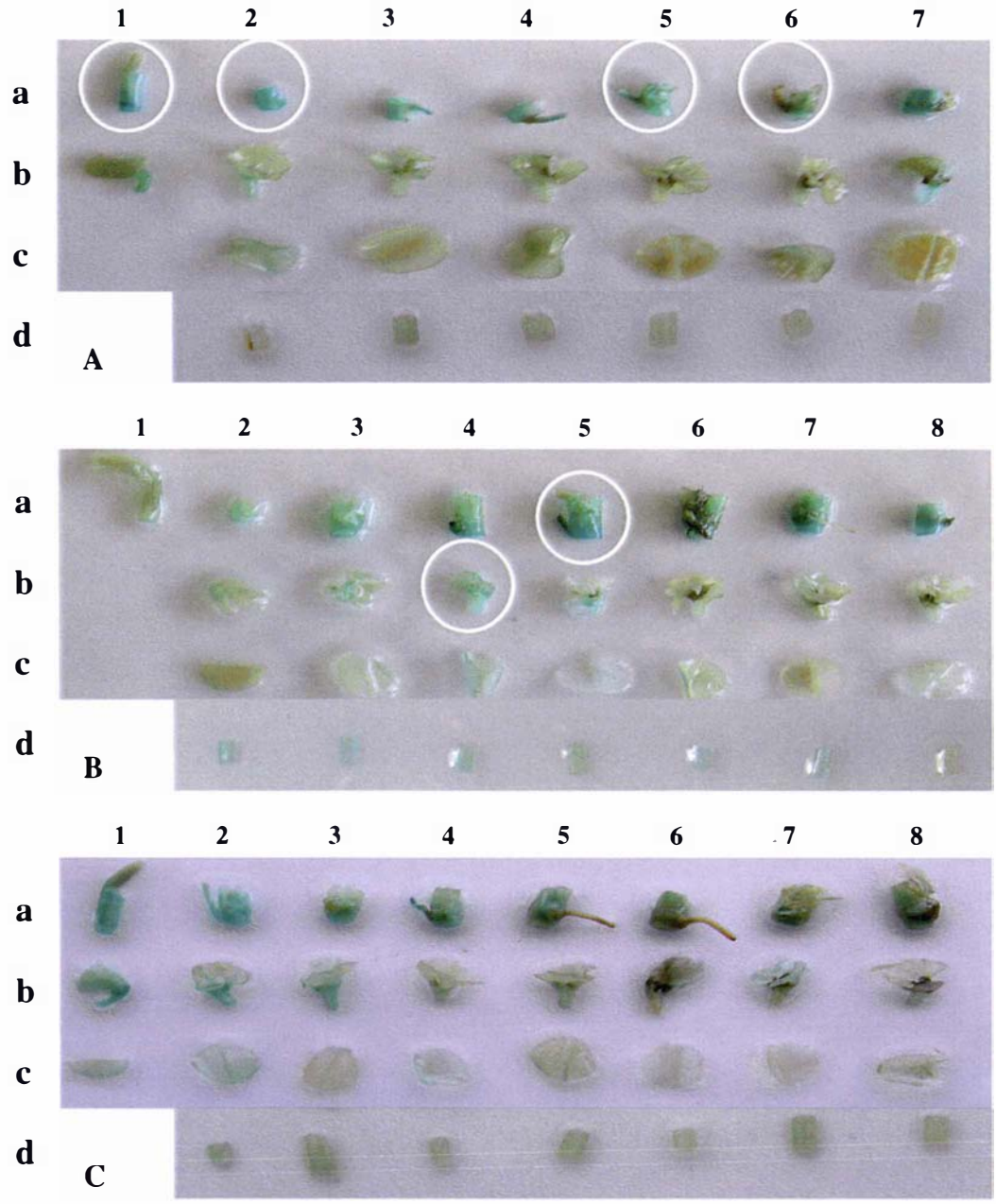

Figure 3.3.22 GUS staining analysis of three lines of white clover transformed with the p*TR-ACO1::GUS* construct

A. Selected tissues of transgenic line # 1
B. Selected tissues of transgenic line # 3
C. Selected tissues of transgenic line # 11
The selected plant tissues were stained by X-Gluc, and then de-stained through an ethanol series. The numbers at the top of each plate represent the node number. a = axillary bud, b = petiolule, c = lamina, d = middle section of leaf petiole
The circles refer to stained tissue used for subsequent cellular analysis of GUS staining (refer Fig 3.3.26)

detected in leaves # 2 ,# 3 and leaf # 7 with the highest intensity of staining concentrated at leaf # 2 (Figure 3.3.22-C-d).

3.3.3.4 Primary GUS staining patterns in the p*TR-ACO2::GUS* transformed white clover plants

Twenty five potentially independent lines of white clover putatively transformed with the p*TR-ACO2::GUS* construct were screened by GUS staining once they had developed 3 to 4 trifoliate leaves. Twenty two plants displayed a blue colour within the apical structure. Three of those positive plant lines (# 1, # 12, and # 19) were selected for Southern blot analysis (Section 3.3.3.1) to confirm that they were independent lines and to determine the copy number of inserted GUS gene (Figure 3.3.18). When these three plants had developed stolons comprising 7 to 9 leaves, three different stolons from same plant were analyzed for the pattern of GUS staining and the staining of tissues from a representative stolon from each line is shown as Figure 3.3.23. In terms of an overall picture, staining was more pronounced in the axillary buds and in the petiolule tissue when compared with the leaf lamina and petiole. In terms of leaf ontogeny, staining was higher in the newly-initiated and mature-green tissues and then gradually decreased in the senescent plant parts (Figure 3.3.23).

The GUS staining in the axillary bud/ stolon segments of line # 1, started to appear from leaf # 1 and increased in intensity to leaf # 8 (Figure 3.3.23-A-a). In the trifoliate leaves, GUS staining was observed in the petiolules, and staining intensity increased from leaves # 2 to # 4 before declining to leaf # 8 (Figure 3.3.23-A-b). GUS staining in leaf lamina tissues can be observed in leaves # 3 to # 8, but the highest intensity of staining appeared in leaves # 7 and # 8 (Figure 3.3.23-A-c). In the petiole segments, GUS staining was apparent from leaf # 2 to leaf # 6, with the most intense staining concentrated at leaves # 3 and # 4 (Figure 3.3.23-A-d). In line # 12, GUS staining in the axillary bud/ stolon segments started to appear from leaf # 1 and was observed through to leaf # 8 with the highest intensity in # 4 and # 5 (Figure

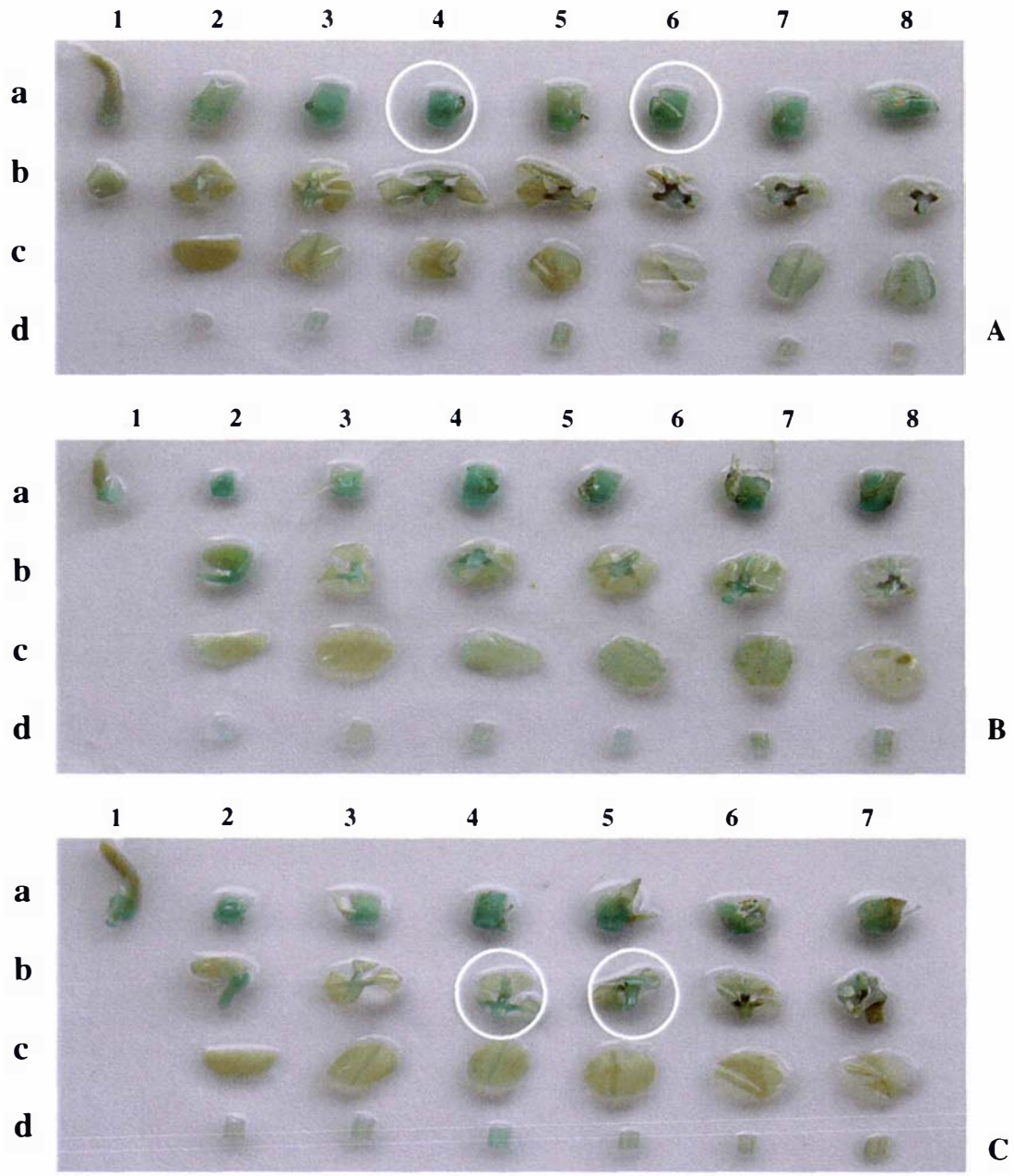

Figure 3.3.23 GUS staining analysis of three lines of white clover transformed with the p*TR-ACO2::GUS* construct

A. Selected tissues of transgenic line # 1
B. Selected tissues of transgenic line # 12
C. Selected tissues of transgenic line # 19
The selected plant tissues were stained by X-Gluc, and then de-stained through an ethanol series. The numbers at the top of each plate represent the node number. a = axillary bud, b = petiolule, c = lamina, d = middle section of leaf petiole
The circles refer to stained tissue used for subsequent cellular analysis of GUS staining (refer Fig 3.3.27)

3.3.23-B-a). In the trifoliate leaves, GUS staining was observed mainly in the petiolules, with intense staining in leaf # 2 to leaf # 7 but less in leaf # 8 (Figure 3.3.23-B-b). The GUS staining in the leaf lamina tissues can be observed in leaves # 4 to # 7, with leaf # 2 showing some trace of GUS staining, but the most intense staining was observed in leaf # 5 (Figure 3.3.23-B-c). In petiole segments, GUS staining appeared from leaves # 4 to # 8, as well as being detectable in leaf # 2. The most intense staining is observed in leaves # 4 and # 5 (Figure 3.3.23-B-d).

In line #19, GUS staining in the axillary bud/ stolon segments starts with intense staining from leaves # 1 to # 5, before a decline in staining intensity to leaf # 7 (Figure 3.3.23-C-a). In the trifoliate leaves, GUS staining was observed mainly in the petiolules, with the most intense staining from leaf # 2 to leaf # 5 (Figure 3.3.23-C-b). GUS staining in leaf lamina tissues was observed in leaf # 3 and leaf # 4, but it was only at a trace level (Figure 3.3.23-C-c). In petiole segments, GUS staining appeared from leaf # 2 to leaf # 5, with the most intense staining at leaf # 4 (Figure 3.3.23-C-d).

3.3.3.5 Primary GUS staining patterns in the p*TR-ACO3::GUS* transformed white clover plants

Fifteen potentially independent lines of white clover putatively transformed with the p*TR-ACO3::GUS* construct were screened by GUS staining once they had developed 3-4 trifoliate leaves. Nine plants displayed a blue colour within the young leaf tissue. Three of those positive plant lines (# 1, # 2, and # 6) were selected for subsequent Southern analysis (section 3.3.3.1) to confirm that they were independent lines and to determine the copy number of the inserted GUS gene (Figure 3.3.19). When these three plants had developed stolons comprising 7 to 11 leaves, three different stolons, from same plant were analyzed for the pattern of GUS staining and a representative stolon from each line is shown as Figure 3.3.24. In general terms, in these stolons, staining was more pronounced in the nodes when

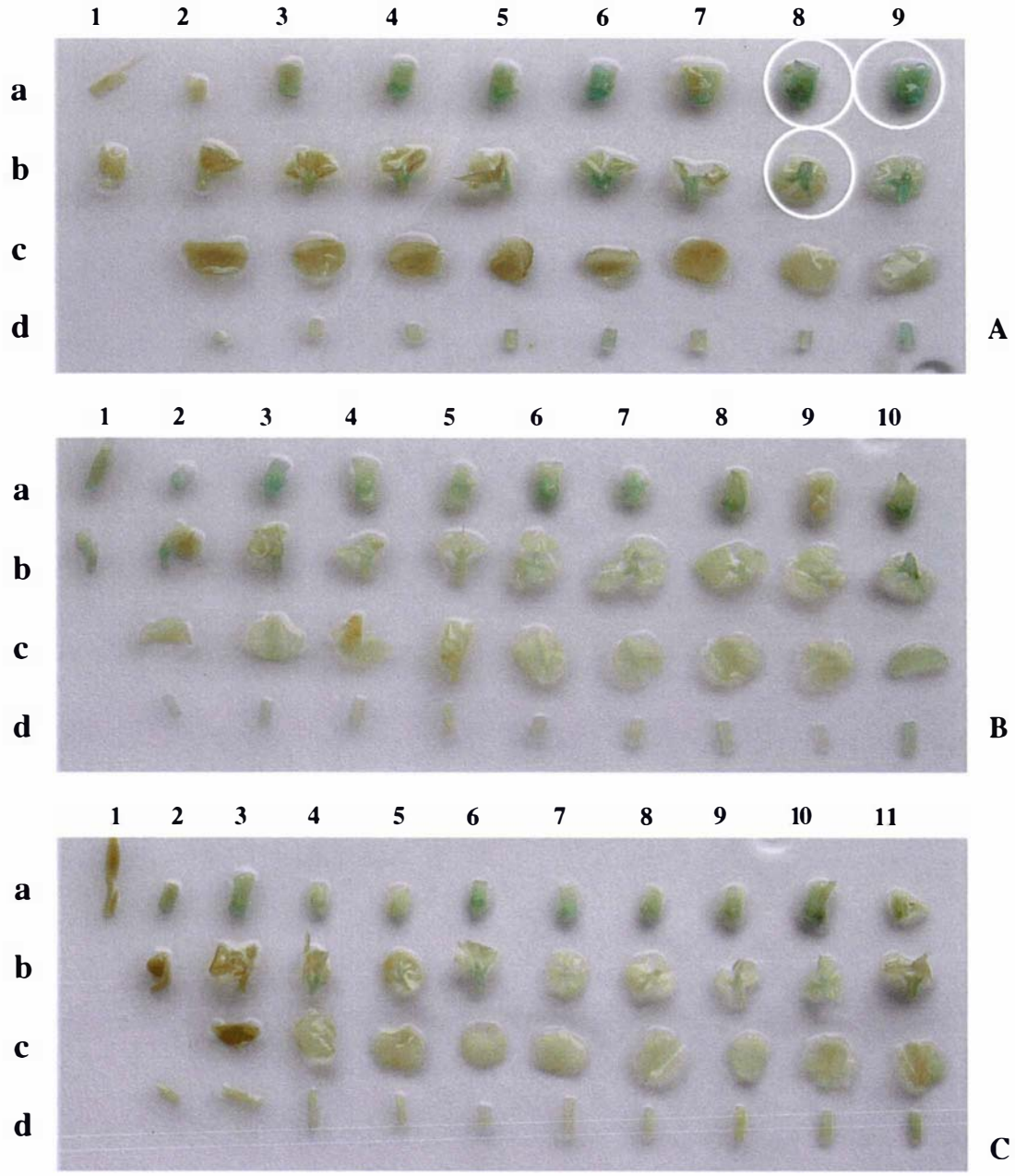

Figure 3.3.24 GUS staining analysis of three lines of white clover transformed with the p*TR-ACO3::GUS* construct

A. Selected tissues of transgenic line # 1
B. Selected tissues of transgenic line # 2
C. Selected tissues of transgenic line # 6
The selected plant tissues were stained by X-Gluc, and then de-stained through an ethanol series. The numbers at the top of each plate represent the node number. a = axillary bud, b = petiolule, c = lamina, d = middle section of leaf petiole
The circles refer to stained tissue used for subsequent cellular analysis of GUS staining (ref Fig 3.3.28)

compared with the petiolule, leaf lamina and petiole. In terms of leaf ontogeny, a general trend was that staining was more pronounced in the older tissues (Figure 3.3.24).

GUS staining in the axillary bud/ stolon segments of line # 1, started to appear from leaf # 3 and increased in intensity to leaf # 9 with the highest intensity in node # 6, # 8 and # 9 (Figure 3.3.24-A-a). In the trifoliate leaves, GUS staining was observed in the petiolules and started to increase in intensity from leaf # 3 to leaf # 9 with the highest intensity from leaves # 6 to # 9 (Figure 3.3.24-A-b). GUS staining in leaf lamina tissues was not observed in all leaf samples (Figure 3.3.24-A-c). In petiole segments, GUS staining was observed in leaves # 6, # 8 and # 9, with the most staining intense staining at leaf # 9 (Figure 3.3.24-A-d).

In line # 2, GUS staining in the axillary bud/ stolon segments started to appear from leaf # 1 and increased in intensity to leaf # 7, and then decreased in staining intensity in leaves # 8 and # 10 (Figure 3.3.24-B-a). In the trifoliate leaves, GUS staining was observed mainly in the petiolules. Staining was observed from leaf # 1 to leaf # 4 and from leaves # 6 to # 10, with the highest intensity of staining observed in leaves # 2, # 3 and # 10 (Figure 3.3.24-B-b). The GUS staining in leaf lamina tissues was also not observed in all samples (Figure 3.3.24-B-c). In petiole segments, GUS staining was detected in leaves # 2, # 3 and # 10 (Figure 3.3.24-B-d).

In line # 6, GUS staining in the axillary bud/ stolon segments appeared from leaf # 2 to # 11, with most of the staining was concentrated in leaves # 3, # 6 and # 7. (Figure 3.3.24-C-a). In the trifoliate leaves, GUS staining was observed mainly in the petiolules. The staining was detected from leaf # 4 to leaf # 7 and in leaves # 10 and # 11 (Figure 3.3.24-C-b). GUS staining in leaf lamina tissues was not observed in all samples (Figure 3.3.24-C-c). In petiole segments, GUS staining only appeared in leaf # 11, and at a very low level (Figure 3.3.24-C-d).

3.3.3.6 Primary GUS staining patterns in the p*TR-ACO4::GUS* transformed white clover plants

Forty potentially independent lines of white clover putatively transformed with the p*TR-ACO4::GUS* construct were screened by GUS staining once they had developed 3-4 trifoliate leaves. Thirty three plants displayed a blue colour within the young leaf tissue. Three of those positive plants (#1, #22, and #26) were selected for subsequent Southern analysis (section 3.3.3.1) to confirm that they did represent independent lines and to determine the copy number of the inserted GUS gene (Figure 3.3.20). When these three plants had developed stolons comprising 7 to 9 leaves, three different stolons, from same plant were analyzed the GUS expression pattern. In these stolons, staining was more pronounced in the node than in the petiolule, leaf lamina or petiole. In terms of leaf ontogeny, staining was generally higher in the mature green and senescent tissues (Figure 3.3.25).

GUS staining in the axillary bud/ stolon segments of line # 20 appeared from leaf # 1 and increased in staining intensity to leaf # 5, after which the intensity of staining remained constant (Figure 3.3.25-A-a). In the trifoliate leaves, GUS staining was first observed (at trace levels) in the petiolule from leaf # 1, and then staining increased in intensity to leaf # 3, and then staining was maintained through to leaf # 8 (Figure 3.3.25-A-b). GUS staining in leaf lamina tissues was observed in leaves # 2 to # 4 and leaf # 8 (Figure 3.3.25-A-c). In petiole segments, GUS staining can be observed in leaves # 2, # 3 and leaf # 5 to leaf # 8. The most intense staining is observed at leaf # 9 (Figure 3.3.25-A-d).

In line # 22, GUS staining in axillary bud/ stolon segments appeared from leaf # 1 to leaf # 9, with the most intense staining observed in leaves # 4, # 6,# 7 and # 8 (Figure 3.3.25-B-a). In the trifoliate leaves, GUS staining was observed mainly in the petiolules of leaves # 1 to # 9 with the most intense staining observed in leaf # 2, after which staining intensity decreased toward to leaf # 9 (Figure 3.3.25-B-b). GUS staining in leaf lamina tissues was not observed in all leaf samples (Figure 3.3.25-B-c). In petiole segments, GUS staining also was not

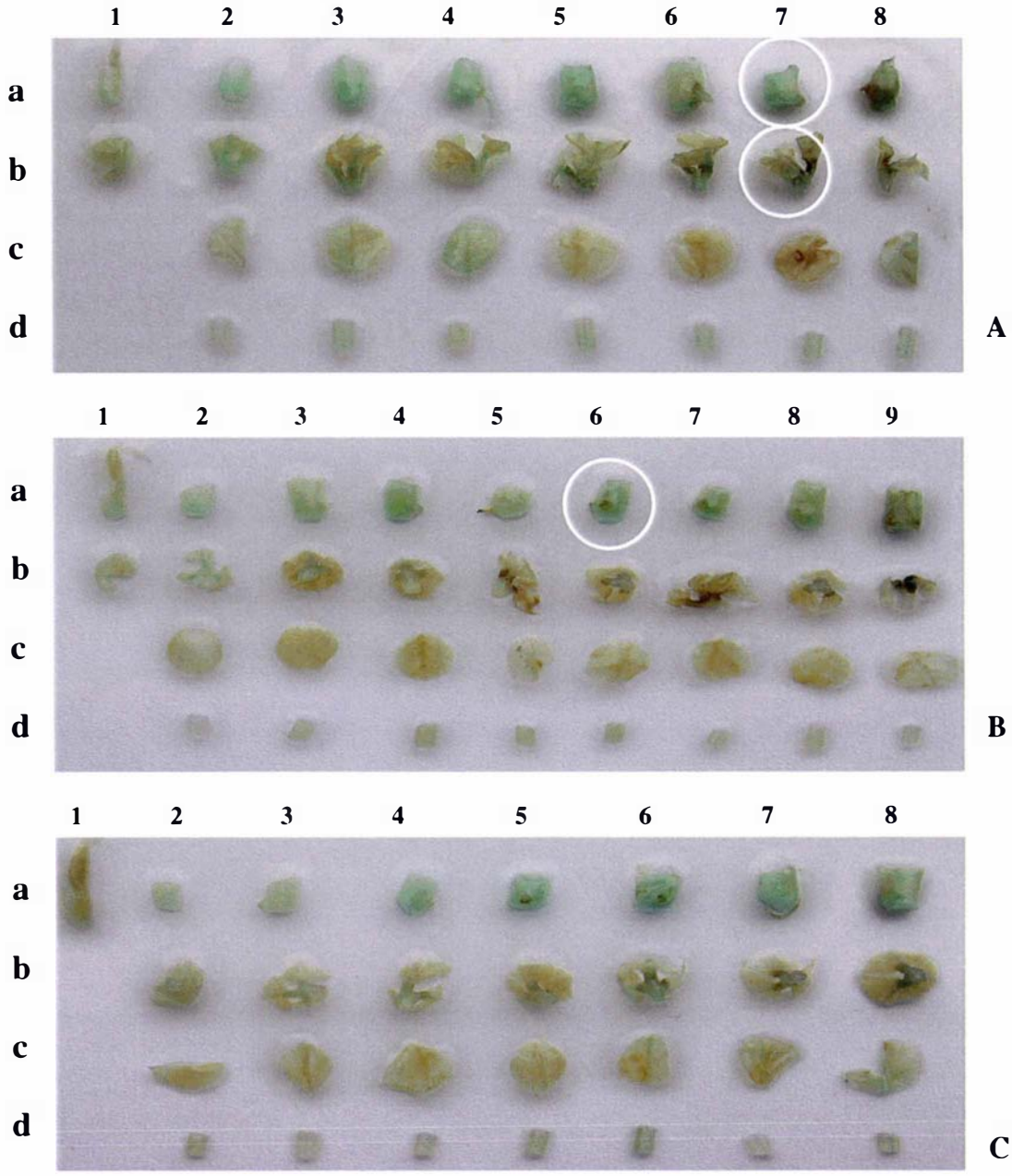

Figure 3.3.25 GUS staining analysis of three lines of white clover transformed with the p*TR-ACO4::GUS* construct

A. Selected tissues of transgenic line # 1
B. Selected tissues of transgenic line # 22
C. Selected tissues of transgenic line # 26
The selected plant tissues were stained by X-Gluc, and then de-stained through an ethanol series. The numbers at the top of each plate represent the node number. a = axillary bud, b = petiolule, c = lamina, d = middle section of leaf petiole
The circles refer to stained tissue used for subsequent cellular analysis of GUS staining (refer Fig 3.3.29)

detected in all leaf samples (Figure 3.3.25-B-d).

In line # 26, GUS staining in the axillary bud/ stolon segments increased in intensity from leaves # 2 to # 5 and then remained more constant through to leaf # 8 (Figure 3.3.25-C-a). In the trifoliate leaves, GUS staining was observed mainly in the petiolules. Staining was detected from leaf # 1 to leaf # 8, but was most intense at leaves # 6 to # 8 (Figure 3.3.25-C-b). The GUS staining in leaf lamina tissues was observed in leaf # 6 to # 8, and was most intense in leaf # 8 (Figure 3.3.25-C-c). In petiole segments, GUS staining appeared in leaves # 6 and # 8 (Figure 3.3.25-C-d).

3.3.3.7 Cellular expression pattern of GUS staining in white clover transformed with the p*TR-ACO1::GUS* construct

For p*TR-ACO1*, the highest intensity of staining in the apical structure of the stolon is observed in the ground meristem tissue and in the developing leaves (Figure 3.3.26-A). At a higher magnification of the apical structure, a much lower intensity of GUS staining is observed in the SAM dome and in newly initiated leaf primordia (Figure 3.3.26-B). In a longitudinal section through a young node (node # 2), the highest intensity of GUS staining is observed in the stolon tissue and included the cortical tissue, vascular tissue and pith (Figure 3.3.26-C). In the axil, staining was more intense in the ground meristem tissue, but was much lower in the SAM region, leaf primordia and in the subtending sheath tissue (Figure 3.3.26-D). In a longitudinal section through older node tissue (node # 6), the intensity of staining was not as marked as that observed in the tissues comparising a young node. However, in common with the young node tissue, highest staining intensity was observed in the stolon tissue and in particular was associated with the vascular tissue. In this node, both the axillary bud and the developing nodal root were observed. In the axillary bud, the ground meristem (basal) tissues display the highest staining intensity, with a much lower intensity observed in the SAM. However, for the root initial, a higher intensity of staining was observed in epidermal/ outer

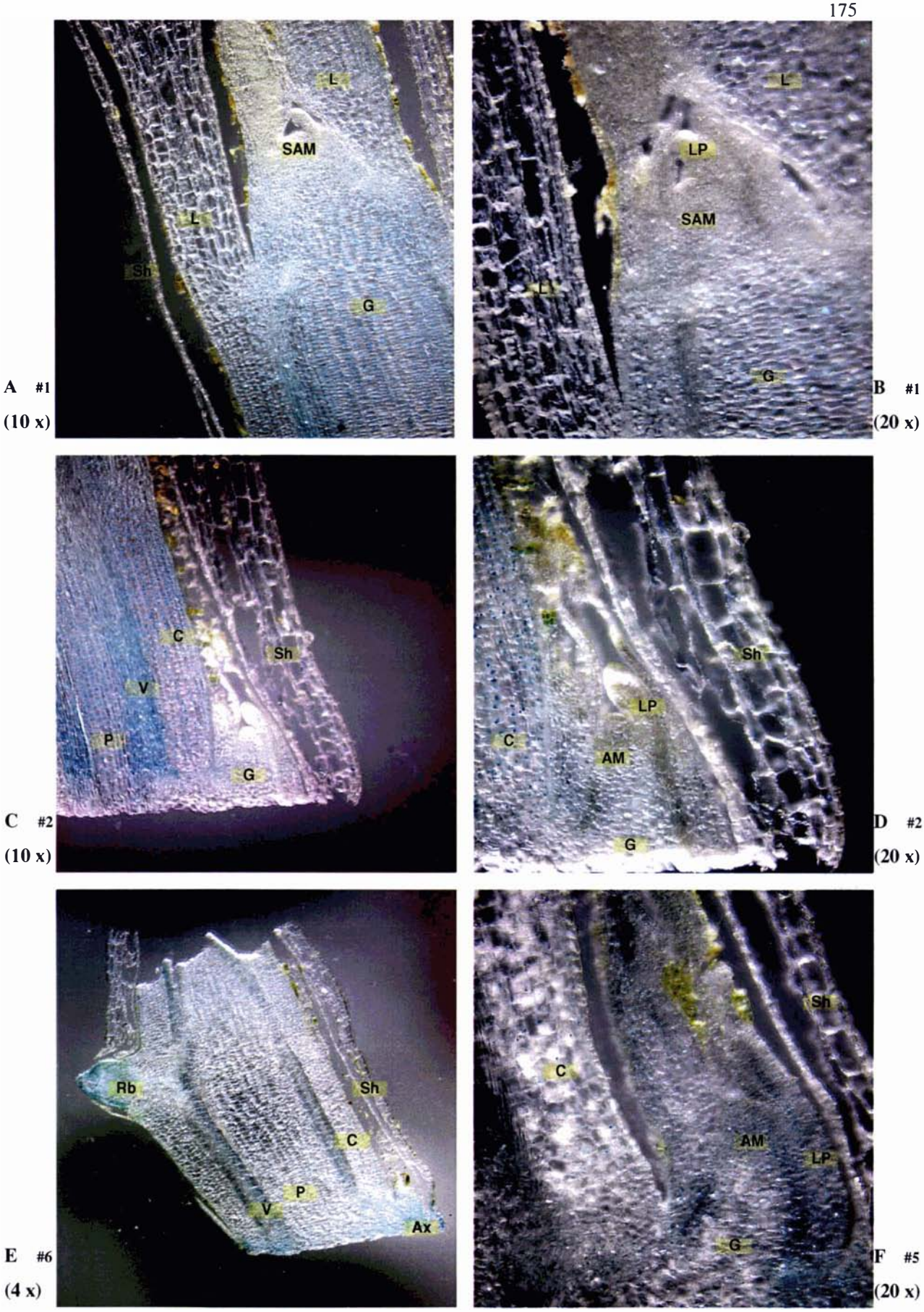

Figure 3.3.26 GUS-staining of selected tissues of p*TR-ACO1::GUS* transformed white clover (Legend details see overpage)

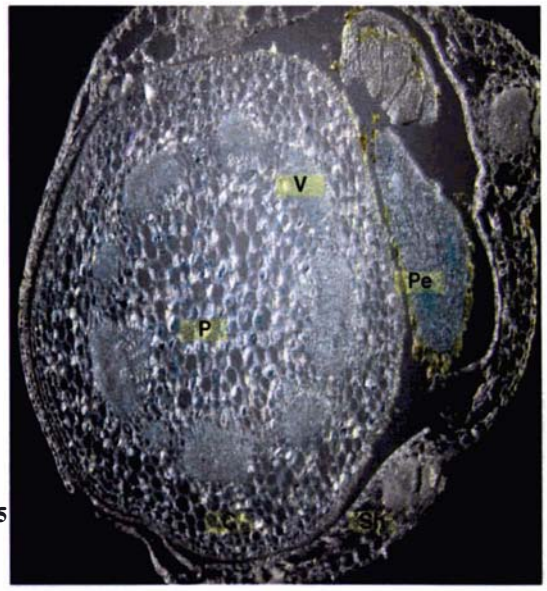

G #5
(4 x)

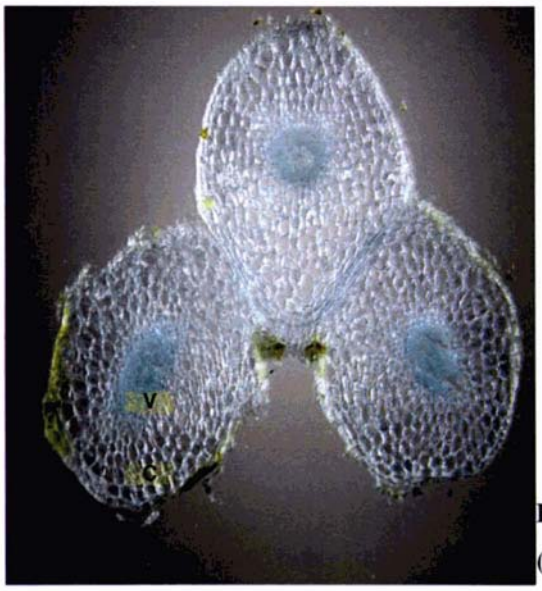

H #4
(10 x)

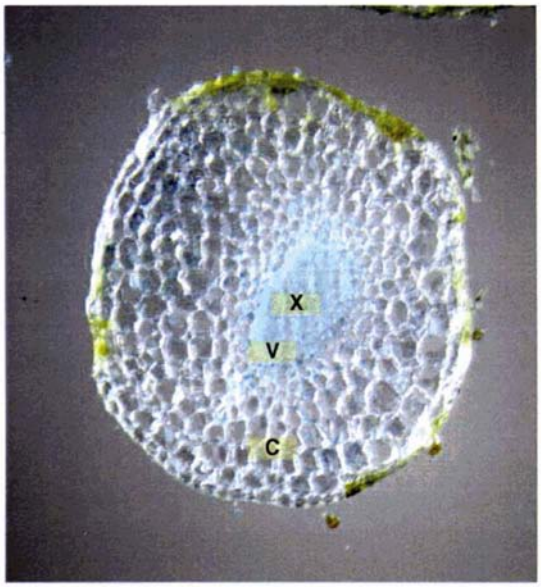

I #4
(20 x)

Figure 3.3.26 GUS-staining of selected tissues of p*TR-ACO1::GUS* transformed white clover

Tissues were stained by X-Gluc and de-stained through an ethanol series. The samples were fixed in paraffin chips and sectioned to 15-20 µm

A- B. Longitudinal section of the apical structure of the stolon

C-D. Longitudinal section through an axillary bud subtending from node # 2

E- F. Longitudinal section of axillary bud from node # 5 and # 6

G. Transverse section of an internode between node # 5and # 6

H-J. Transverse section of the petiolule from leaf # 4

Sh= sheath, SAM= shoot apical meristem, AM= apical meristem, L= leaf, LP= leaf primordium, C= cortex, G= ground meristem, P= pith, V= vascular bundle, Ax= axillary bud, Rb= root bud, Pe= petiole, X= xylem

cortex region as compared with that in the ground meristem tissue (Figure 3.3.26-E, F). In a transverse section of node # 5, higher intensity of staining was observed in the subtending petiole as compared with that in the main stolon. In the main stolon, staining was observed in the vascular tissue, pith and cortex. Very little staining was observed in the vascular bundles in the sheath enclosing the main stolon (Figure 3.3.26-G). In the petiolule tissue from a leaf excised from node # 4, staining was observed in all cell types present in cross-section, although the highest intensity of staining was in the vascular strand, with less staining evident in the central xylem tissue (Figure 3.3.26-H, I). The number of tissue dissections examined and the consistency of staining is displayed in Table 3.3.1.

3.3.3.8 Cellular expression pattern of GUS staining white clover transformed with the p*TR-ACO2::GUS* construct

For the p*TR-ACO2::GUS* transformed plants, a longitudinal section through a young/ mature node (node # 4) reveals that GUS staining was mostly localized in the stolon tissue, and included the cortical cells, pith and the vascular tissue, but was less intense in the sheath (Figure 3.3.27-A). At higher magnification, staining was again more intense in the ground tissue of the axillary bud and cortex of the stolon as compared with that in the SAM, and in the newly initiated leaf promordia (Figure 3.3.27-B). In a transverse section of the node (node # 6), higher intensity of staining was observed in the subtending petiole than in the main stolon, with staining highest in the vascular tissue of the petiole. Much less staining was observed in the vascular bundles in the sheath. In the main stolon, staining is highest in the vascular bundles, but is also detectable in the pith and cortex (Figure 3.3.27-C). At higher magnification of the vascular tissue, staining was observed in the phloem tissue, in the vascular cambium and in the differentiating fibres that form a cap of cells internal to the xylem elements (Figure 3.3.27-D). In the transverse section of the petiolule tissue excised from node # 5, GUS staining was most intense in the parenchyma cells associated with the

A

Section tissues	Stages	Leaf number	*TR-ACO1*	*TR-ACO2*	*TR-ACO3*	*TR-ACO4*
Apical bud/ axillary bud	Y	(# 1-# 2)	**9** (3G; 3C,3C,3C)	--	--	
	M	(# 3-# 6)	**6** (3G; 2C,2C,2C)	**5** (3G; 2C,1C,1C)	--	**5** (3G; 2C,2C,1C)
	S	(# 7-# 9)	**5** (3G; 2C,2C,1C)	--	**5** (3G; 2C,2C,1C)	**10** (3G; 4C,3C,3C)
Stolon/node	Y	(# 1-# 2)	-	--	**1** (1G; 1C)	**2** (2G; 1C,1C)
	M	(# 3-# 6)	**2** (2G; 1C,1C)	**10** (3G;4C,3C,3C)	--	**1** (1G; 1C)
	S	(# 7-# 9)	**1** (1G; 1C)	**2** (2G; 1C,1C)	**5** (3G; 2C,2C,1C)	**8** (3G; 3C,3C,2C)
Petiolule	Y	(# 1-# 2)	**2** (2G; 1C,1C)	--	--	**1** (1G; 1C)
	M	(# 3-# 6)	**2** (2G; 1C,1C)	**8** (3G; 3C,3C,2C)	--	**2** (2G; 1C,1C)
	S	(# 7-# 9)	**3** (2G; 2C,1C)	**3** (3G; 1C,1C,1C)	**5** (3G; 2C,2C,1C)	**9** (3G; 3C,3C,3C)

B

Section tissues	Stages	Leaf number	*TR-ACO1*	*TR-ACO2*	*TR-ACO3*	*TR-ACO4*
Apical bud/ axillary bud	Y	(# 1-# 2)	**9** (7)	--	--	
	M	(# 3-# 6)	**6** (6)	**5** (5)	--	**5** (4)
	S	(# 7-# 9)	**5** (5)	--	**5** (5)	**10** (10)
Stolon/node	Y	(# 1-# 2)	-	--	**1** (1)	**2** (2)
	M	(# 3-# 6)	**2** (2)	**10** (9)	--	**1** (1)
	S	(# 7-# 9)	**1** (1)	**2** (2)	**5** (5)	**8** (8)
Petiolule	Y	(# 1-# 2)	**2** (2)	--	--	**1** (1)
	M	(# 3-# 6)	**2** (2)	**8** (8)	--	**2** (2)
	S	(# 7-# 9)	**3** (3)	**3** (3)	**5** (5)	**9** (9)

Table 3.3.1 Numbers of sections examined by GUS staining (A), and consistency of staining of transgenic white clover lines (B)

A. The section tissues indicate the dissected tissues which were examined in this thesis. The stages represent the leaf growth along stolon as different developmental stages, Y= newly initiated stage, M= mature-green stage, S= senescence stage. The leaf number indicates the tissues selected, under each developmental stage. The numbers (in bold) under each gene represent the frequency of tissue dissection from different stolons. The following numbers in parenthesis represent the total number of genotypes sampled (as x G); followed by the number of vegetative clones sampled from each genotype (as y C).

B. The numbers under each gene represents the frequency of tissue dissection from different stolons. The number in parenthesis represents the number of sections that displayed the consensus pattern of staining that is represented as Fig 3.3.26 (*TR-ACO1*), Fig 3.3.27 (*TR-ACO2*), Fig 3.3.28 (*TR-ACO3*), Fig 3.3.29 (*TR-ACO4*).

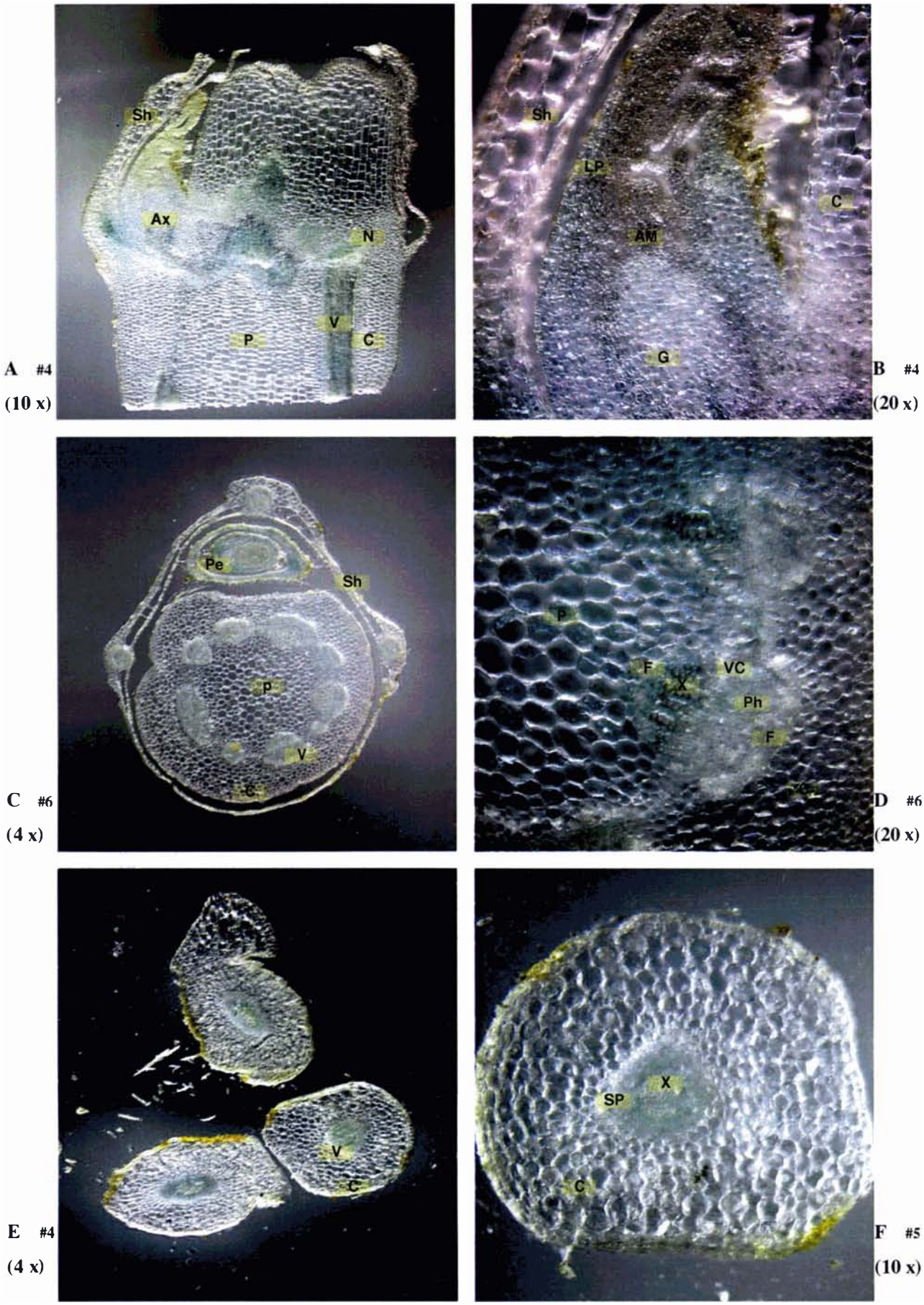

Figure 3.3.27 GUS-staining of selected tissues of p*TR-ACO2::GUS* transformed white clover (Legend details see overpage)

Figure 3.3.27-Legend GUS-staining of selected tissues of p*TR-ACO2::GUS* transformed white clover

Tissues were stained by X-Gluc, and de-stained through an ethanol series. The samples were fixed in paraffin chips and sectioned to 15-20 µm

A-B . Longitudinal section of axillary bud from node # 4
C-D. Transverse section of an internode between node # 5 and # 6
E-F . Transverse section of petiolule from leaf # 4 and # 5

Sh= sheath, G= ground meristem, AM= apical meristem, LP= leaf primordium, C= cortex, P= pith, V= vascular bundle, Ax= axillary bud, Pe= petiole, VC= vascular cambium, SP= sclerenchyma and phloem, X= xylem, Ph= phloem, F= fibres, N= node

vascular tissue, although staining was also be observed in the more highly vacuolate cells of cortex (Figure 3.3.27-G, H). The number of tissue dissections examined and the consistency of staining is displayed in Table 3.3.1.

3.3.3.9 Cellular expression pattern of GUS staining white clover transformed with the p*TR-ACO3::GUS* construct

In longitudinal sections of a mature node/ node at the onset of senescence (Node # 8), GUS staining was observed in both the cortical cells and the vascular tissue, with the highest intensity of staining localised in the cortical cells below the axillary bud, and in the vascular tissue in the sheath (Figure 3.3.28-A). At higher magnification, staining in the SAM of the axillary bud and in the newly initiated leaf primordia was very much lower than in the ground meristem cells. Staining was also observed in the leaf tissue (Figure 3.3.28-B, C). In a transverse section of the node (node # 5), higher intensity of staining was observed throughout the vascular bundles in the main stolon and in the enclosing sheath, than in the pith or cortex of the main stolon (Figure 3.3.28-D). In transverse sections of the petiolule from node # 8, the intensity of staining was highest in the sclerenchymatous sheath of cells associated with the vascular tissue although the central vascular tissue xylem and the cortex were stained at lower intensity (Figure 3.3.28-E, F). The number of tissue dissections examined and the consistency of staining is displayed in Table 3.3.1.

3.3.3.10 Cellular expression pattern of GUS staining white clover transformed with the p*TR-ACO4::GUS* construct

In longitudinal sections of a mature node/ node at the onset of senescence (node # 7), staining in the SAM of the axillary bud and in the newly initiated leaf primordia was almost absent as compared with ground pith cells, but staining was observed in the sheath and leaf tissue (Figure 3.3.29-A, B). In a transverse section of the internode (node # 6), higher intensity of staining was observed throughout the vascular bundles in the main stolon, with much less

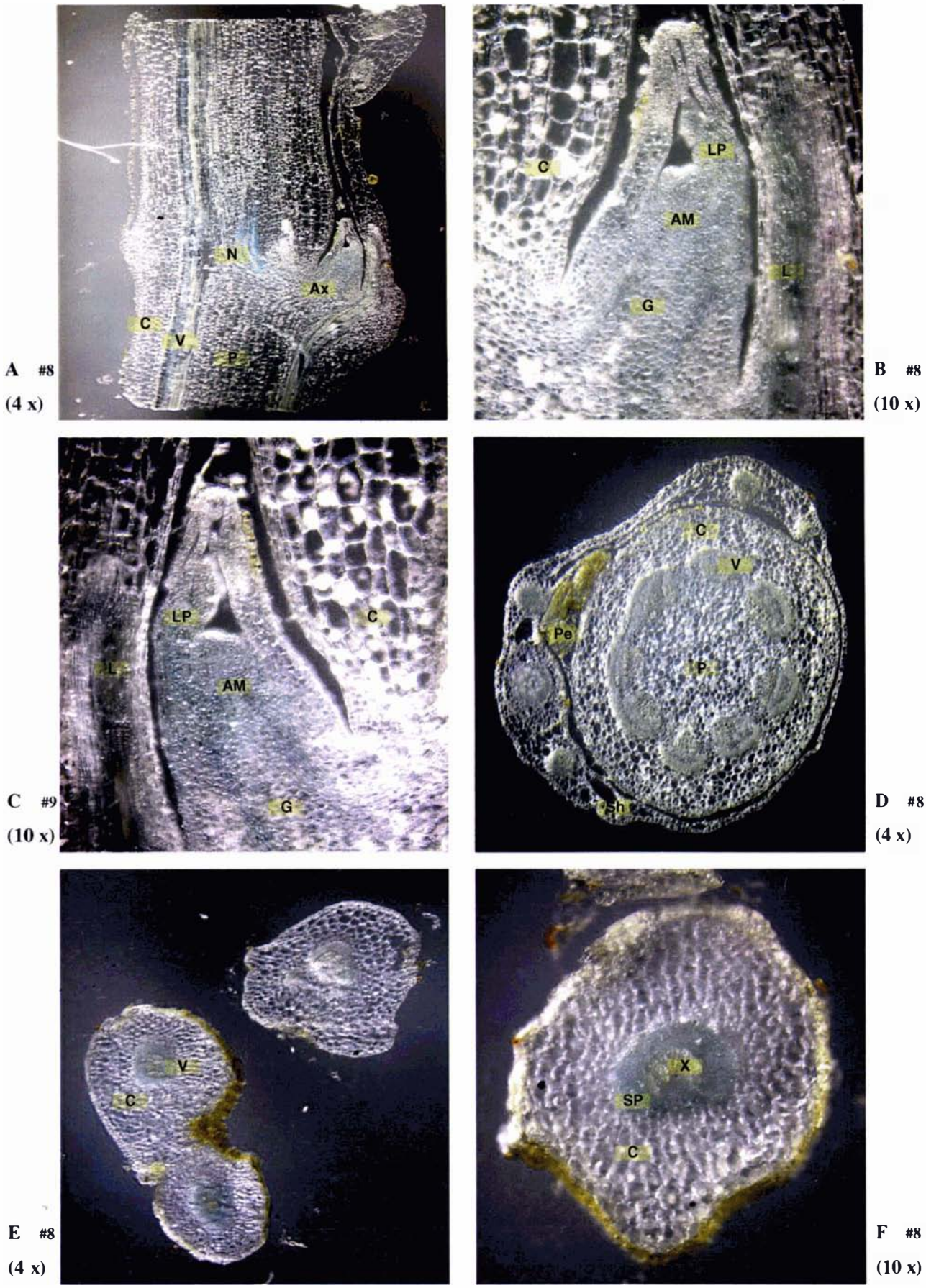

Figure 3.3.28 GUS-staining of selected tissues of p*TR-ACO3::GUS* transformed white clover (Legend details see overpage)

Figure 3.3.28-legend GUS-staining of selected tissues of p*TR-ACO3::GUS* transformed white clover

Tissues were stained by X-Gluc and de-stained through an ethanol series. The samples were fixed in paraffin chips and sectioned to 15-20 µm

A-C. Longitudinal section of axillary bud from node # 8 and # 9
D . Transverse section of an internode between node # 8 and # 9
E-F . Transverse section of petiolule from leaf # 8

Sh= sheath, G= ground meristem, AM= apical meristem, L= leaf, LP= leaf primordium, C= cortex, P= pith, V= vascular bundle, Ax= axillary bud, Pe= petiole, VC=vascular cambium, SP= sclerenchyma and phloem, X= xylem, Ph= phloem, F= fibres, N= node

A #7
(4 x)

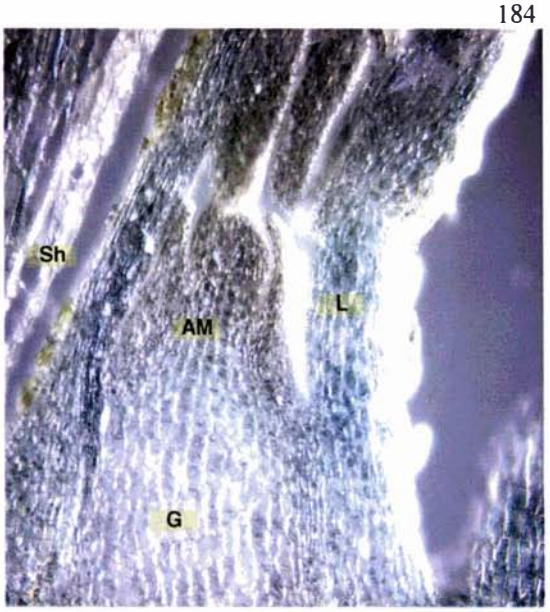

B #7
(20 x)

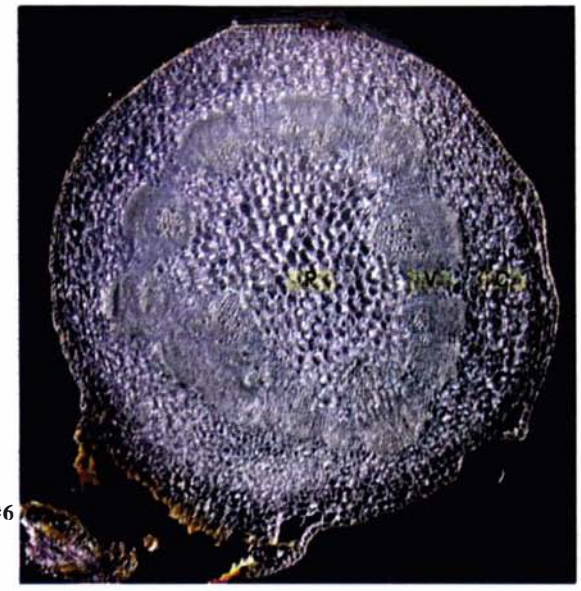

C #6
(4 x)

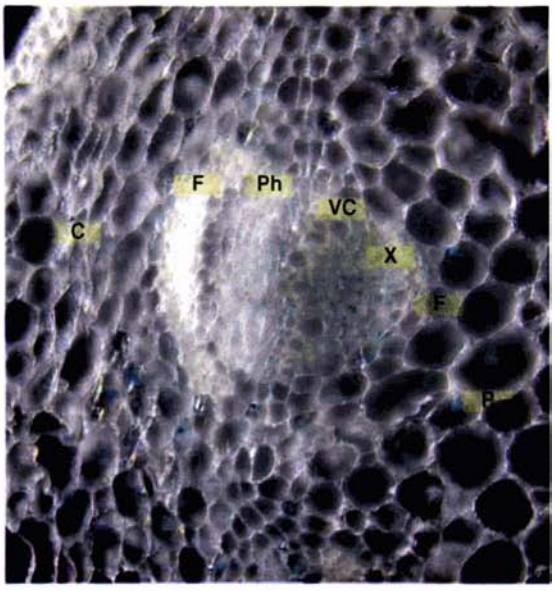

D #6
(20 x)

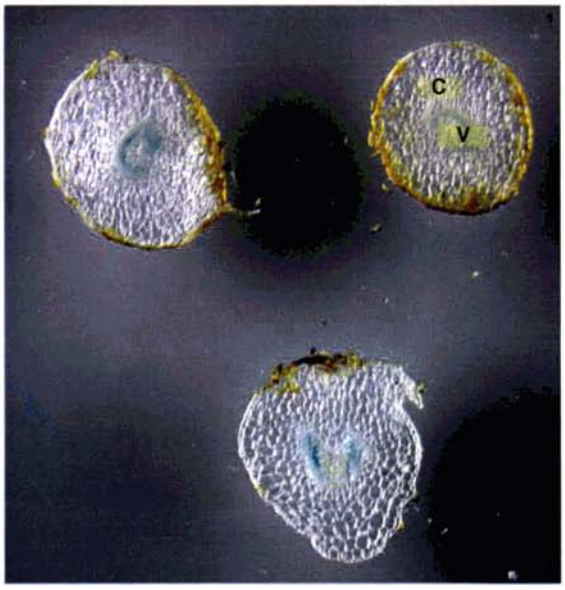

E #7
(4 x)

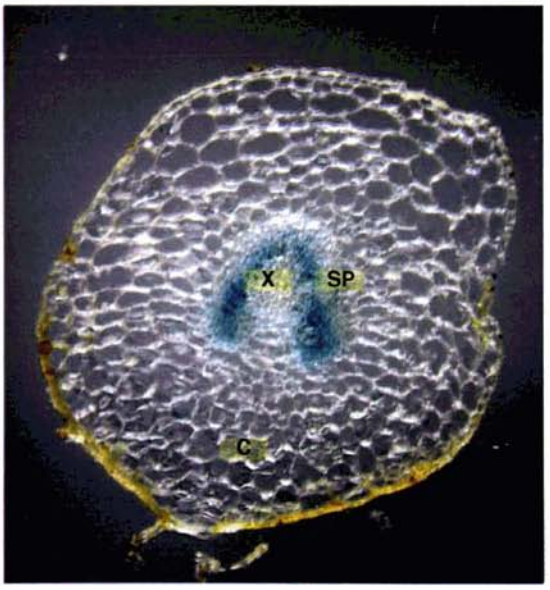

F #7
(10 x)

Figure 3.3.29 GUS-staining of selected tissues of p*TR-ACO4::GUS* transformed white clover (Legend details see overpage)

Figure 3.3.29-legend GUS-staining of selected tissues of p*TR-ACO4::GUS* transformed white clover

Tissues were stained by X-Gluc and de-stained through an ethanol series. The samples were fixed in paraffin chips and sectioned to 15-20 µm

A-B. Longitudinal section of axillary bud from node # 7
C-D. Transverse section of an internode between node # 6 and # 7
E-F. Transverse section of petiloule from leaf # 7

Sh= sheath, G= ground meristem, AM= apical meristem, L= leaf, C= cortex, P= pith, V= vascular bundle, Ax= axillary bud, VC=vascular cambium, SP= sclerenchyma and phloem, X= xylem, Ph= phloem, F= fibres, N= node

evidence of staining observed in the pith or cortex of the main stolon (Figure 3.3.29-C). At higher magnification, staining was highest in the vascular cambium tissue, and in the fibre cells internal to the xylem vessels. No staining was observed in the phloem or fibre cells external to the phloem (Figure 3.3.29-D). In transverse sections of the petiolule from node # 7, the intensity of staining was, again, highest in the sclerenchymatous sheath of cells associated with the vascular tissue, but was hardly detectable in the cortex (Figure 3.3.29-E, F). The number of tissue dissections examined and the consistency of staining is displayed in Table 3.3.1.

3.3.4. *In situ* hybridization studies of *TR-ACO* expression in white clover

3.3.4.1 Cellular expression pattern of *TR-ACO1*

The expression pattern determined using *in situ* hybridization was broadly similar to that determined in the p*TR-ACO1::GUS* transgenic plants. However, in the apical structure, hybridization was most readily detected in the shoot apical meristem (SAM), leaf primordium, developing leaves, and in the ground meristem. In the SAM, staining was detected as large blue colour spots in most cells of the SAM, the leaf primordium, and in the first and the second developing leaves. However, below the corpus of the SAM and unlike the GUS staining, the ground meristem tissue did not show any significant evidence of blue staining (Figure 3.3.30-A, B, C).

In the axillary bud structure (node # 3), *TR-ACO1* expression is similar to that of the SAM pattern, with the blue staining detectable in most cells of the leaf primordium and apical meristem (AM). In the ground meristem, blue staining was detectable in most cells (Figure 3.3.30-D, E) when compared with the negative control samples (Figure 3.3.30-F).

In a transverse section of the stolon internode (node # 3), staining can be detected in the pith, cortex, and vascular bundles (Figure 3.3.30-G). At higher magnification, cells in the pith

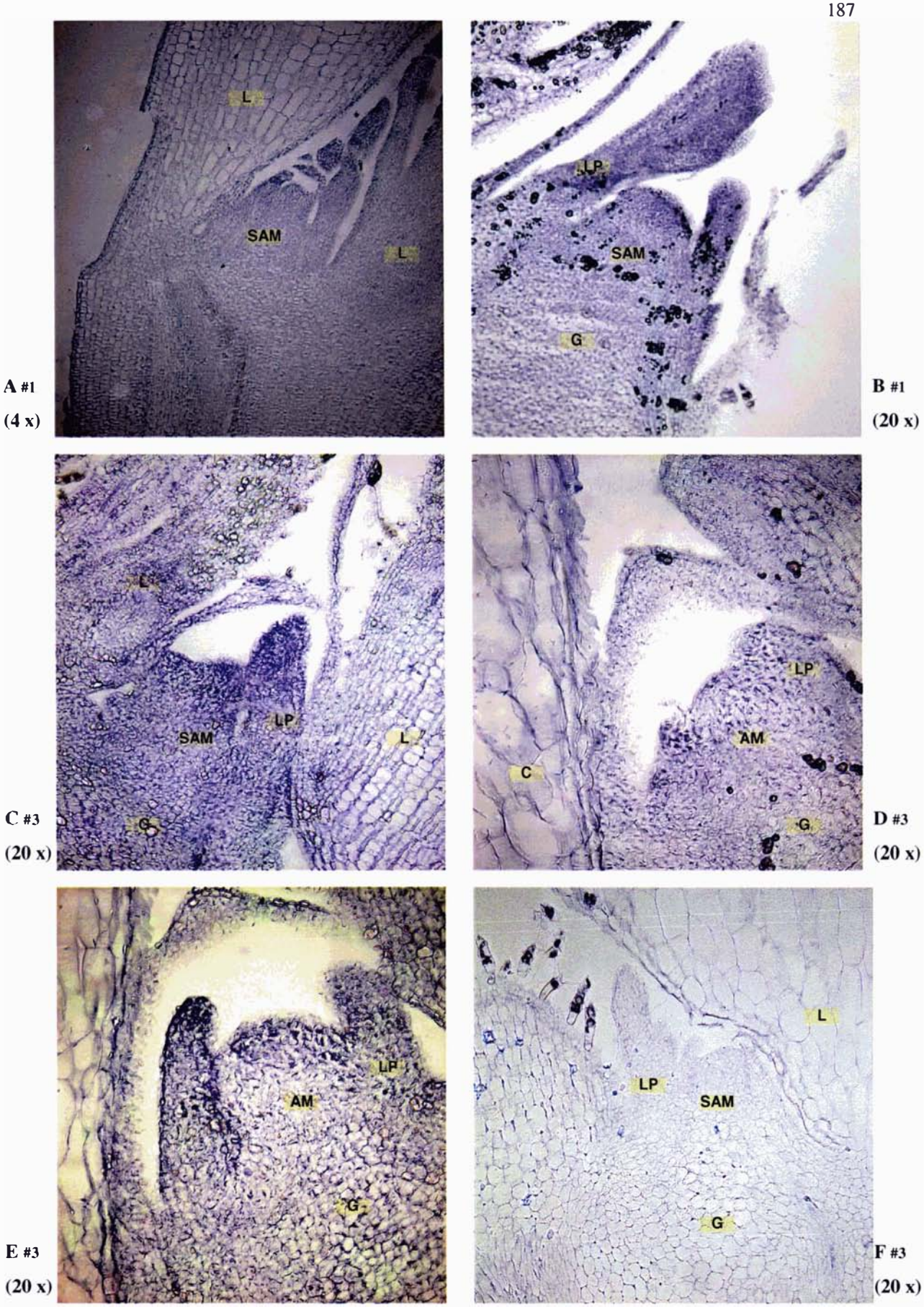

Figure 3.3.30 ***In situ*** **hybridization analysis of white clover tissues by 3´-UTR specific probe of** ***TR-ACO1*** (Legend details see over page)

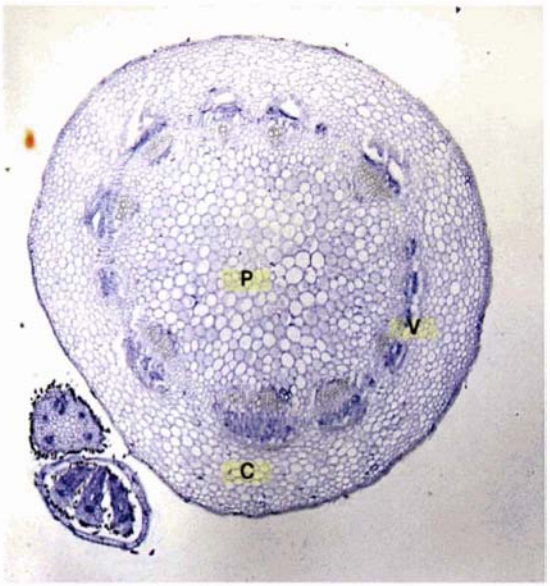

G #3
(4 x)

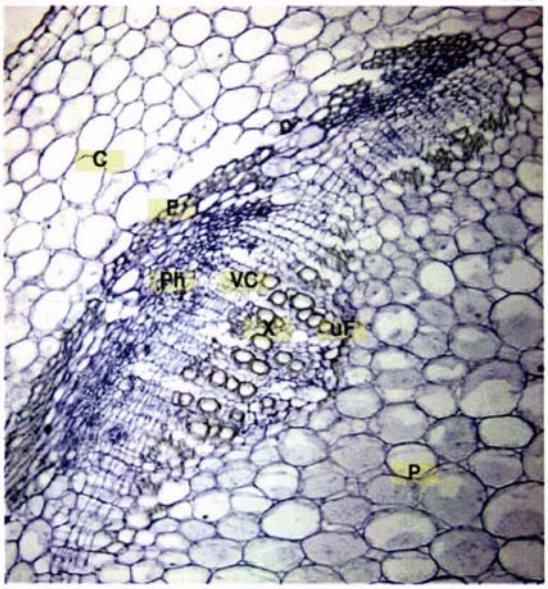

H #3
(20 x)

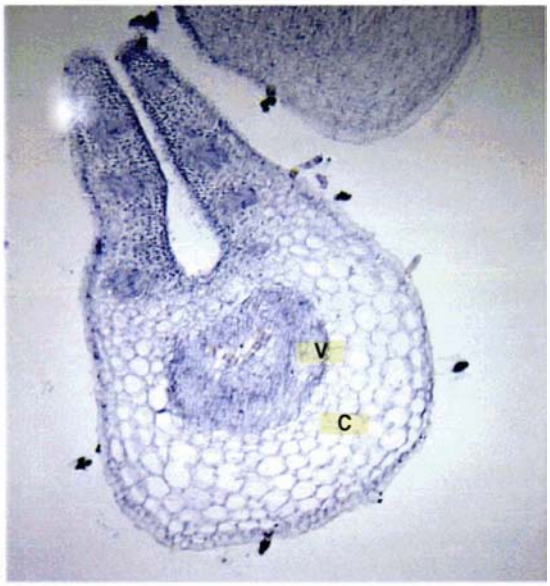

I #3
(10 x)

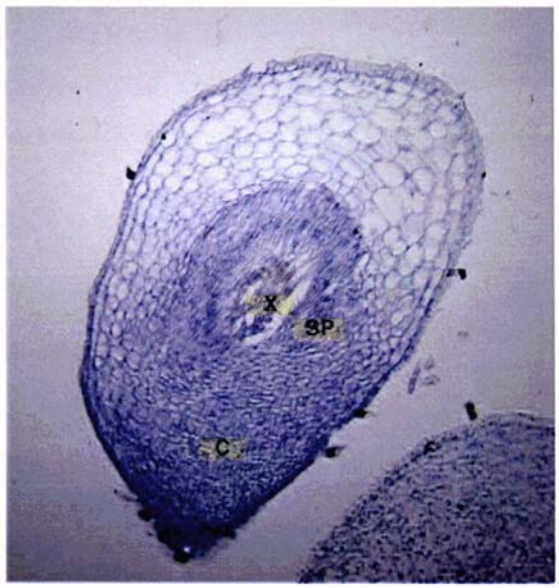

J #3
(10 x)

Figure 3.3.30 ***In situ*** **hybridization analysis of white clover tissues by 3´-UTR specific probe of** ***TR-ACO1***

Wild-type tissues were fixed and sectioned into 15-20 µM. The hybridization and washes were at high stringency condition and the slides were stained by BCIP/NBT and de-stained in TE buffer.

A-C. Longitudinal section of the apical structure of the stolon
D-E. Longitudinal section of an axillary bud subtending node # 3
F . Negative control (sense probe) on longitudinal section of apical bud (# 3)
G-H. Transverse section of stolon internode proximal to node # 3
I - J . Transverse section of the petiolule of leaf # 3
Sh= sheath, G= ground meristem, SAM= shoot apical meristem, AM= apical meristem, L= leaf, LP= leaf primordium, C= cortex, P= pith, V= vascular bundle, Ax= axillary bud, Pt= petiole, VC=vascular cambium, SP= sclerenchyma and phloem, X= xylem, Ph= phloem, F= fibres, uF= undifferentiated fibres, N= node

displayed more intense staining than cells of the cortex (Figure 3.3.30-H). In contrast, staining of the epidermal cells was hardly detectable. In the vascular bundles, most colour was concentrated in the fibre parenchyma cells associated with the xylem and the phloem. (Figure 3.3.30-G, H).

In the petiolule (node # 3), a faint blue colour was observed in the parenchyma cells of the cortex, but more dense blue spots were concentrated in the vascular bundle. In the bundle, the deepest blue colour can be detected in the sclerenchymatous cells surrounding the central xylem (Figure 3.3.30-I, J).

3.3.4.2 Cellular expression pattern of *TR-ACO3*

The expression patterns of *TR-ACO3* determined by *in-situ* hybridization also coincided broadly with that revealed using GUS staining of p*TR-ACO3::GUS* transgenic plants. In the apical structure, a faint blue colour of hybridization was observed in the shoot apical meristem (SAM), leaf primordium, developing leaves, and ground meristem (Figure 3.3.31-A). Higher magnification of the shoot apical meristem, revealed dense blue staining in the first and secondary layers of cells of SAM and leaf primordium, and less dense staining of most cells of newly initiated leaf (Figure 3.3.31-B).

In the axillary bud structure (node # 7), the staining in the stolon was detectable only faintly in the pith and cortex. A more dense blue colour was concentrated in the vascular traces and the axillary bud and leaf primordium (Figure 3.3.31-C). At higher magnification, more dense blue staining was detected in the SAM and leaf primordium cells (Figure 3.3.31-D) than was detected in the negative control samples (Figure 3.3.31-E).

In the stolon (node # 8), the blue colour was most dense in the cells of the vascular bundle, and was hardly detectable in the pith and cortex cells (Figure 3.3.31-F). At higher magnification of the vascular bundle, the main cell types in which putative *TR-ACO3* expression was observed were the fibre parenchyma cells, cambium cells and fibre cells

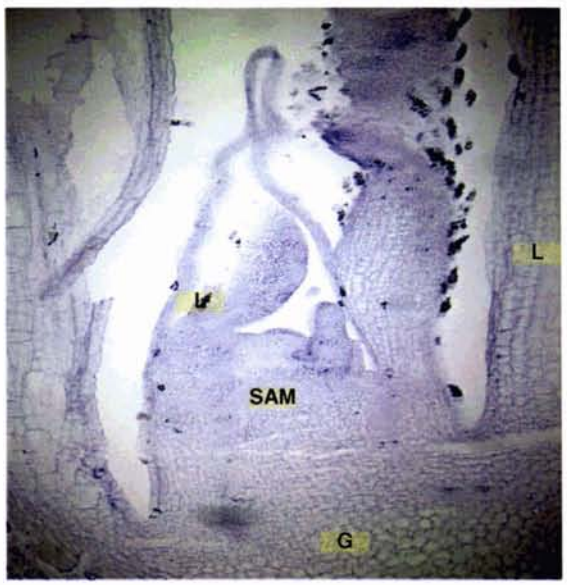

A #1
(10 x)

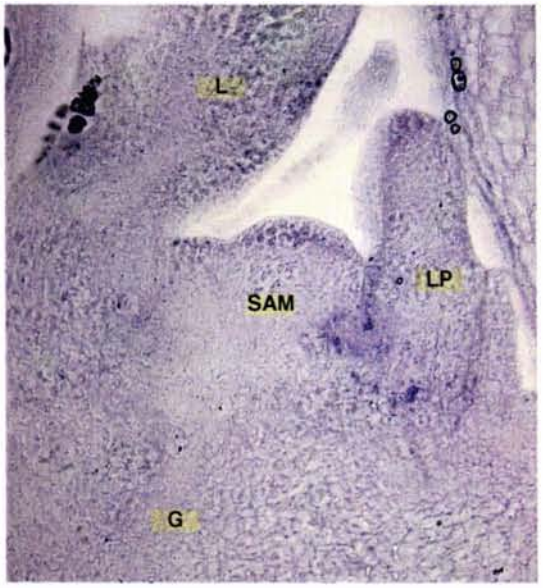

B #1
(20 x)

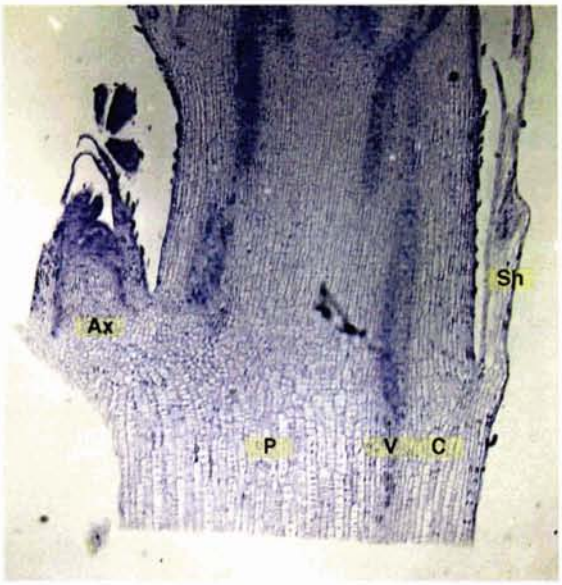

C #7
(4 x)

D #7
(10 x)

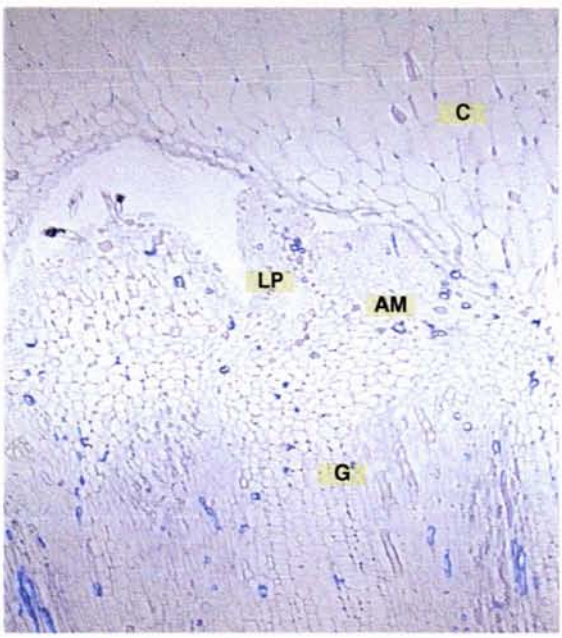

E #7
(20 x)

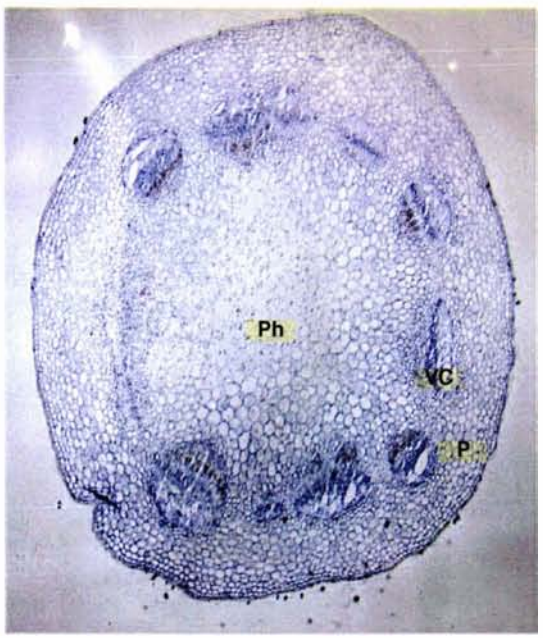

F #8
(4 x)

Figure 3.3.31 ***In situ*** **hybridization analysis of white clover tissues by 3´-UTR specific probe of** ***TR-ACO3*** (Legend details see overpage)

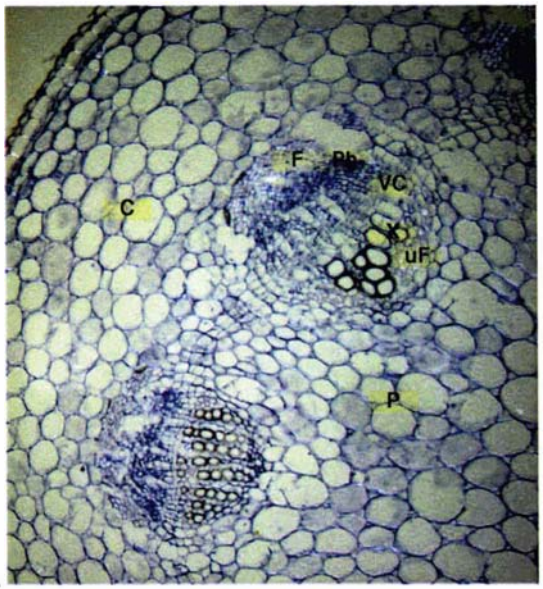

G #8
(20 x)

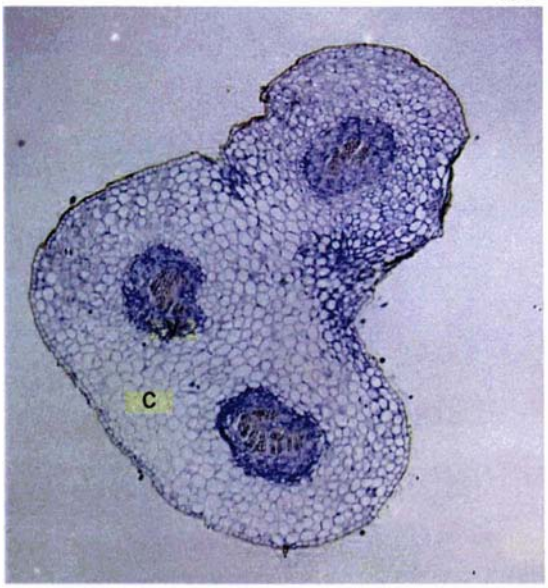

H #8
(4 x)

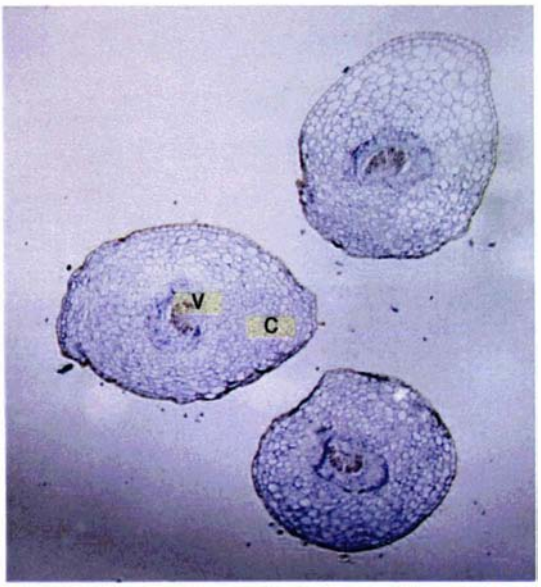

I #8
(10 x)

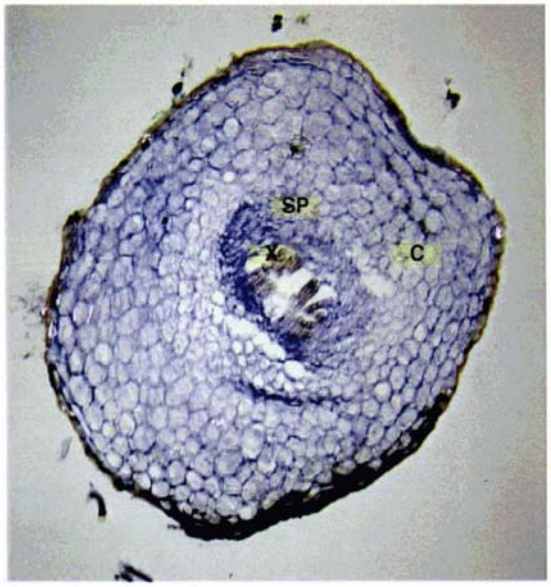

J #8
(10 x)

Figure 3.3.31 ***In situ*** **hybridization analysis of white clover tissues by 3´-UTR specific probe of** ***TR-ACO3***

Wild-type tissues were fixed and sectioned into 15-20 µM. The hybridization and washes were at high stringency condition and the slides were stained by BCIP/NBT and de-stained in TE buffer.

A-B. Longitudinal section of the apical structure of the stolon

C-D. Longitudinal section of an axillary bud subtending node # 7

E . Negative control (sense probe) on longitudinal section of axillary bud (# 7)

F-G. Transverse section of stolon internode between node # 7 and # 8

H-J. Transverse section of the petiolule of leaf # 8

Sh= sheath, G= ground meristem, SAM= shoot apical meristem, AM= apical meristem, L= leaf, LP= leaf primordium, C= cortex, P= pith, V= vascular bundle, Ax= axillary bud, Pt= petiole, VC=vascular cambium, SP= sclerenchyma and phloem, X= xylem, Ph= phloem, F= fibres, uF= undifferentiated fibres, N= node

internal to the xylem (Figure 3.3.31-F, G).

In the petiolule (node # 8), the blue colour was most concentrated in the vascular bundle, but staining was also evident in the cortex. In the bundle, the deepest blue colour was detected in the sclerenchymatous cells that surround the phloem and xylem (Figure 3.3.31- H, I, J).

Chapter 4 Discussion

4.1 Isolation of promoter sequences

4.1.1. Determination of criteria for promoter selection

Amplification of each promoter sequence was achieved using the Genome Walker™ method (Section 2.7). The results indicated that the length of most isolated sequences ranged from *ca.* 500 bp to 1750 bp, and the maximum length of sequences derived from each gene are 1264 bp (p*TR-ACO3-2*), 1440 bp (p*TR-ACO1*), 1566 bp (p*TR-ACO3-1*) and 1750 bp (p*TR-ACO2*). Since the p*TR-ACO3-1* and p*TR-ACO3-2* sequences were isolated from the same digested library (*Stu*I), and was based on the *TR-ACO3* cDNA, sequence comparison showed high identity over the coding sequence and the 5′-UTR regions. Therefore, to get more information in order to separate the two sequences, another amplification was performed from p*TR-ACO3-2*. A *ca.*500 bp fragment was thus obtained giving a 1654 bp sequence in total for p*TR-ACO3-2*. After alignment of each sequence with the original cDNA, more than 1000 bp upstream from the translation start codon (ATG) was identified. For example, p*TR-ACO1* is 1006 bp, p*TR-ACO2* is 1510 bp, p*TR-ACO3-2* is 1350 bp, and p*TR-ACO3-1* is 1250 bp.

In comparison with expression experiments using ACC oxidase promoters from other species, variable 5′ flanking sequences are used for ranging from several hundred base pairs to around two thousand base pairs. For example, in melon, a 726 bp sequence was isolated from *CM-ACO1* and a 2260 bp sequence was isolated from *CM-ACO3,* and each promoter directed tissue-specific expression and stimuli-specific response patterns (Lasserre et al., 1997). In tomato, a 1922 bp, a 493 bp, and a 221 bp 5′ flanking sequence from *LE-ACO1* was fused with the GUS reporter gene and transformed into tomato. The analysis showed that the 493 bp fragment is sufficient to direct tissue-specific expression when compared with the endogenous expression pattern of *LE-ACO1* (Blume and Grierson, 1997). In apple, 450 bp, 1159 bp, and

1966 bp sequences of the *AP4* ACC oxidase were fused with the GUS gene and transformed into tomato to assay the expression pattern. The results indicated that the 450 bp fragment was sufficient to drive GUS expression, and both longer fragments (1159 bp and 1966 bp) did not show any difference in the pattern of expression (Atkinson et al., 1998). Therefore, since the length of the 5´ flanking sequence isolated from each *TR-ACO* genes in this thesis are over 1000 bp, it puts them in the middle of p*AP4* series (1159 bp) and they are longer than the *CM-ACO1* (726 bp) sequence used. Thus they were used as further transformation assays and sequence analysis in this thesis.

4.1.2. Frequency of panhandle structures

During the isolation of the promoter sequences, many large DNA fragments were amplified from most digested libraries (section 3.1.1, 3.1.2, and 3.1.3). After sequencing, most of these were shown to be non-specific DNA fragments. This is because the gene specific primers designed originally had relatively low T_m values, and a feature of the GenomeWalker™ kit is that panhandle structures can form. If the annealing temperature falls to 68°C, non-primer binding fragments will anneal to both ends of the adaptors to form a panhandle loop structure. If both adaptor primers anneal to the fragments before the panhandle structure is formed, non-targeted sequences will be amplified. That may be the reason why every library had smearing or other very faint bands after electrophoresis. As the original three cDNA sequences isolated from Hunter et al. (Hunter et al., 1999) were used to design primers, it was difficult to design gene-specific primers at the 5′ end with a high T_m. As a consequence, many non-specific fragments were detected during amplification.

4.2 Confirmation of isolated sequences as *TR-ACO* promoters

4.2.1. Overlapping sequences

To confirm that the sequences isolated were *TR-ACO* promoters, two levels of analysis were carried out. The first level was to use a BLAST-n search to align similar sequences of other species in the Genebank database. From this analysis, it may be possible get a broad view of sequence structure, and the relationship to ACC oxidase genes of different species. As a second level, analysis was through the use of GCG or other programme tools to pairwise the known *TR-ACO* gene coding sequence and the isolated promoter sequence. From this analysis it should be possible to confirm the overlapping coding sequences with the known cDNA sequences and then determine the location of the intron sequences.

For the *TR-ACO1* promoter, the BLAST-n search revealed that the 5´ end regulatory sequence upstream of the translation start codon (ATG) site did not show any sequence identity, but downstream of the ATG codon, more than 90 bp shared high identity. This implies that the *TR-ACO1* promoter sequence may be an unique sequence, and its regulation mechanism might differ from other ACC oxidase genes. It also implies that there are only a few ACC oxidase promoter sequences that have been cloned and deposited in the Genebank database. Indeed, there are only 25 ACO promoter sequences from 12 different plant species that have been cloned thus far. In the gene coding sequence, the most identical sequence is the *TR-ACO1* partial CDS deposited by Hunter et.al.(1999), and then the pea *PE8* (GI|169040) and mung bean *VR-ACO1* (Kim and Yang, 1994)(section 3.1.1.4). These results reveal that the *TR-ACO1* gene might be related to other legumes.

Another benefit of the Genebank sequence alignment is that some ACO genes comprise cDNA sequences, while others are genomic sequences, and so when these sequences were

aligned with the existing cDNA sequence, a gap is observed suggesting the position of the first intron. For *TR-ACO1,* the first intron is located between the reverse primer and the ATG codon, and the introns differ in sequence between ACO genes of different species. For most ACO genes, the distance from the ATG codon to the first intron is about 105 bp long, so the cloned *TR-ACO1* promoter sequence not only provided the first intron sequence data, but also provided the 5′-UTR sequence that was not determined by the RT-PCR approach employed by Hunter et al. (1999).

Using BLAST-n analysis, the *TR-ACO1* translation start site (ATG) has also been located 432 bp upstream of the 3′-reverse primer sequence used in the GenomeWalker cloning. Sequencing and pairwire analysis reveals that the first intron of *TR-ACO1* is located 105 bp downstream of the ATG site, and the first two bases in the intron are GU and the last two are AG, which are consensus boundary sequences for intron splicing (Sharp, 1994).

From the GCG programme, pairwise results reveal that the sequence downstream from intron-I comprises 130 bp and is 100 % identical to the known *TR-ACO1* codon sequence. Another 27 bp upstream from the intron is also identical to the known coding sequence. Together both sequences comprise 14% of the total known coding sequence of *TR-ACO1*. Since this region is specific to *TR-ACO1,* and distinct from the *TR-ACO2* and *TR-ACO3* genes, it adds to the confirmation that the isolated 5′ flanking sequence is derived from the *TR-ACO1* gene.

For *TR-ACO2*, in common with *TR-ACO1*, BLAST-n searching of the Genebank database using the 5′-regulatory sequence upstream of the translation start codon (ATG) site did not show any sequence similarity with other sequence in the database. However, downstream of the ATG codon, there were more than 80 sequences that shared high identity. Again, this may imply that the *TR-ACO2* promoter sequence is a unique sequence, and its regulatory mechanisms may differ from the other ACC oxidase genes.

When aligning with gene coding sequences of other ACO genes, the most identical sequence is *Medicago truncatula MT-ACCO* (GI|17342710), then the *TR-ACO2* cDNA (Hunter et al., 1999) and then an ACO from peach fruit, *PP-ACO1* (Ruperti et al., 2001). Again, *via* comparison with these 80 sequences (as both cDNA and genomic sequences), a gap appeared in the alignment to indicate the position of the first intron. Again, this sequence differed from other ACO genes, and the distance from the ATG codon to the first intron splice site was 103 bp long.

Using BLAST-n, the *TR-ACO2* translation start site (ATG) has also been located 317 bp downstream of the 3′-reverse primer sequence used in the GenomeWalker cloning. Sequencing and pairwise analysis reveals that the first intron of *TR-ACO2* is located 103 bp downstream of the ATG site, and the first two bases in the intron are GG and the last two are GT, which are consensus boundary sequences for intron splicing (Sharp, 1994).

Pairwise analysis also reveals that the sequence downstream from the first intron comprises 110 bp and is 100 % identical to the known *TR-ACO2* coding sequence. Another 22 bp upstream from the intron is also identical to the known coding sequence. Together both sequences comprise 14% of total known coding sequence of *TR-ACO2*, and since this region is specific to *TR-ACO2,* and distinct from the *TR-ACO1* and *TR-ACO3* genes it again supports the assertion that the isolated 5′ flanking sequence is derived from the *TR-ACO2* gene.

Because the *TR-ACO3-1* and *TR-ACO3-2* promoter sequences were isolated from same library it implies that two distinct *TR-ACO3*-like genes and promoter sequences occur in the white clover genome. This maybe because there are two alleles from the same gene or a new *TR-ACO* gene has been isolated. Sequence comparison revealed that the coding sequences share highly identity, but the promoter sequences were distinct.

A BLAST-n comparison of the *TR-ACO3-1* and *TR-ACO3-2* sequences with others in the database revealed no identity with the other ACO sequences upstream of the ATG site,

including each other. In the coding sequence downstream of the ATG codon, there were more than 100 sequences that had some sequence identity. The sequence with highest percentage identity to either *TR-ACO3-1* or *TR-ACO3-2* coding sequences was the *TR-ACO3* partial CDS deposited by Hunter et al. (1999), and then *MT-ACCO* from *Medicago truncatula* (GI|17342710) and *PL-ACO1* from lima bean (GI|18157332). Comparison with these sequences against the cDNA sequence identified a gap indicating the first intron of both *TR-ACO3-1* and *TR-ACO3-2*. Another significant feature is the translation start site has a triple ATG codon in both *TR-ACO3-1* and *TR-ACO3-2*. This phenomenon is not observed in any other ACO sequences identified by BLAST searching.

To confirm which ATG is the translation start site, a comparison with other ACO genes suggests that the second ATG may be the start codon, because the most identical ACO genes to *TR-ACO3-1* and *TR-ACO3-2* including *M. truncatula* (*MT-ACCO*), *P. lunatus* (*PL-ACO1*), and *P. vulgaris* (*PV-ACO1*), have the ATG site located 105 bp upstream of the first intron boundary. Also for *TR-ACO1* and *TR-ACO2*, the second ATG site is located 105 bp upstream from the first intron boundary. A further comparison of amino acid sequence initiated from the second ATG places a proline residue at amino acid position +5. This proline at position 5 is conserved in all the ACO genes sequenced initially (Kadyrzhanova et al., 1997), and therefore, the second ATG is suggested to be the translation start site for both *TR-ACO3-1* and *TR-ACO3-2*. This analysis may also suggest that the structure of 5′ end of the coding sequence of legume ACOs will always have a 105 bp coding sequence as the first exon, and then have a diverse length (100 bp ~200 bp) within the first intron.

Using the GCG programme pairwise analysis, the ATG start site of *TR-ACO3-1* and *TR-ACO3-2* is shown to be located 356 bp and 344 bp upstream respectively of the 3′-reverse primer sequence using the GenomeWalker cloning approach. Sequencing and pairwise analysis reveals that the first intron of both *TR-ACO3-1* and *TR-ACO3-2* is located 105 bp downstream of the ATG site. The first two bases in the intron are GT and the last two are AG,

which are consensus boundary sequences for intron splicing (Sharp, 1994). The sequence downstream from the intron comprises 109 bp and for both *TR-ACO3-1* and *TR-ACO3-2* is 100 % identical to the known *TR-ACO3* cDNA sequence. The 24 bp upstream from the intron of *TR-ACO3-2* is also identical to the known *TR-ACO3* cDNA coding sequence, but the *TR-ACO3-1* has one bp difference to the known coding sequence. Together both sequences comprise 14 % of total known coding sequence of *TR-ACO3*. Since this region is specific to both *TR-ACO3-1* and *TR-ACO3-2,* and also distinct from the *TR-ACO1* and *TR-ACO2* genes it helps to confirm that one of the isolated sequences is derived from the *TR-ACO3* gene, and the second is a possibly new *TR-ACO* gene or another allele of the *TR-ACO3.* However, the very diverse sequence of the promoter regions of *TR-ACO3-1* and *TR-ACO3-2* support the view that these are distinct genes.

4.2.2. Confirmation by Southern analysis

Southern analysis using the 5´ flanking sequences of *TR-ACO1* and *TR-ACO2* as probes, identified two fragments in each digested lane, although one large molecular mass fragment appeared in the *Hind* III digest when probed with *TR-ACO1,* suggesting that this may be due to incomplete digestion. When probing with the 5´ flanking sequences of *TR-ACO3-1* and *TR-ACO3-2* only one fragment was hybridized to in each digested lane. Because these probes are specific, it suggests that in the white clover genome, *TR-ACO1* and *TR-ACO2* occur as at least two copies and may be located on different genomes, but only one copy of *TR-ACO3-1* or *TR-ACO3-2* occur on each genome. White clover has an allotetraploid genome, but the origin of the two diploid genomes in white clover is uncertain. The current view is that they arose from hybridization of the diploid species *T. nigrescens* and the autotetraploid species *T. uniflorum* (Badr et al., 2002). Therefore, the two copies of *TR-ACO1* and *TR-ACO2* may represent identical copies in both genomes as part of this hybridization process. In this regard, it is of interest that both *TR-ACO3-1* and *TR-ACO3-2* appear as single copies suggesting that

each gene occurs in only one of the two genomes. To resolve this further, Southern analysis with the putative diploid progenitors of *T. repens* will be necessary, and these species include *T. nigrescens*, *T. occidentale*, *T. uniflorum* and *T. ambiguum* (Baker and Williams, 1987).

It is also worth noting that the hybridization pattern obtained when using the *TR-ACO3-1* 5´ regulatory sequence as probe differed from that using the *TR-ACO3-2* probe. This is further evidence that these two sequences represent two genes.

4.3 Gene structure of the *TR-ACO* genes

4.3.1. Occurrence of exons and introns

All four of the isolated *TR-ACO* genes share the same gene structure. That is, each gene contains four exons interspersed with three intron sequences. In broad terms, the length of each exon is similar in size, but each intron sequence displays a different size.

A comparison of average peptide number over 23 ACC oxidases revealed a value of 314 a.a. (Kadyrzhanova et at, 1997). The amino acid residue number calculated from the four *TR-ACO* genes range from 306 a.a. (*TR-ACO3-1* and *TR-ACO3-2*), 313 a.a. (*TR-ACO2*) to 317 a.a. (*TR-ACO1*). Therefore, the similar exon lengths among these genes reveal that the ACC oxidase protein structure is conserved in white clover, when compared with ACC oxidase proteins from other species.

The conservation in gene structure is not only displayed in white clover, but can also be observed in other species. In comparison with other published accounts of ACC oxidase gene structures, the occurrence of 4 exons interspersed with 3 introns has been observed in melon (*CM-ACO1*) (Lasserre et al., 1996), peach (*PP-ACO1*) (Ruperti et al., 2001) and in petunia (*PH-ACO1, PH-ACO3* and *PH-ACO4*) (Tang et al., 1993). It should be noted that other members of the melon gene family (*CM-ACO2, CM-ACO3)* and peach (*PP-ACO2)* comprise 2 introns interspersing 3 exons (Lasserre et al., 1996; Ruperti et al., 2001).

The examination of the structure of the genes also allows more comparison between

TR-ACO3-1 and TR-ACO3-2. The two genes share high identity in the coding sequences with *TR-ACO3,* but both intron sequences and promoter sequences display low identity with each other. However, comparison of the exon sequences show that exon # 1 and exon # 3 are 94% and 89 % identical (section 3.1.6), but only the *TR-ACO3-2* sequence is wholly identical to the *TR-ACO3* sequence identified by Hunter et al (1999). Thus *TR-ACO3-2* is renamed *TR-ACO3* and *TR-ACO3-1* is renamed *TR-ACO4.*

It should be noted that in this thesis the genomic sequences for each gene have been compared up to the stop codon, and this has not extended into the 3′ UTR region of the gene. In the study by Hunter et al. (1999), 3′-RACE was used to isolate the 3′ UTR sequences of *TR-ACO1*, *TR-ACO2* and *TR-ACO3.* However, as the primer sequence used was based within exon-4 and this exon sequence is identical in both *TR-ACO3* and *TR-ACO4*, it is now not certain whether the 3 ´ UTR reported for *TR-ACO3* in Hunter et al (1999) is *TR-ACO3* or *TR-ACO4.* Indeed, the Southern data reported in this thesis (Figure 3.1.21) makes it possible that the *TR-ACO3* 3 ´ UTR region used in expression studies reported by Hunter (1999) is associated with *TR-ACO4* (i.e. *TR-ACO3-1* in this thesis). However, until the 3 ´ -UTR sequences have been isolated from both *TR-ACO3* and *TR-ACO4* and the Southern analysis repeated, this can only be a suggestion.

4.4 Expression analysis of the *TR-ACO* promoters

4.4.1. Bioinformatic analysis

The regulation of gene expression at the transcriptional level is mostly controlled by transcription factors. These proteins recognize, and bind to, specific domains on the promoter sequence to enhance or to inhibit the activities of RNA polymerase II. Thus through the analysis for specific domains within promoters it might be possible to gain information on the controls of specific ACO gene expression.

As the initial analysis of the four ACO gene 5′ flanking sequences, an analysis *in silico* was

performed using database identification of putative transcription factor binding domains. This analysis gave information on both the broad categories of factors that may regulate the expression of each gene, but also gave a more specific indication of the nature of these developmental and environmental cues.

4.4.2. Trends of p*TR-ACO*-directed expression established using TFBD analysis

In summary, there are three classes of TFBDs dispersed in the four promoter sequences. From the overview of each sequence, the *TR-ACO1* and both *TR-ACO3* and *TR-ACO4* sequences appear to contain a variation in the proportion of classes. The *TR-ACO1* sequence contains only a minimal number of ethylene-related signals (class III) but it does have a high number of development-related domains (class II). In contrast, the *TR-ACO3* and *TR-ACO4* promoter sequences contain a higher number of ethylene-related domains, but have a minimal number of developmentally-related domains. This suggests that *TR-ACO1* expression is regulated more by developmental signals and less from the ethylene-associated signals, whereas both *TR-ACO3* and *TR-ACO4* expression is controlled more by the ethylene-related signals and less by developmental signals. These observations broadly match the northern data reported for *TR-ACO* gene expression during leaf ontogeny. In these, *TR-ACO1* is expressed in the apical structure and in axillary buds whereas *TR-ACO3* expression is predominantly in the senescent leaves (Hunter et al., 1999).

Another interesting phenomenon is the TFBDs identified in the *TR-ACO2* promoter sequence. An overview of the TFBDs in this sequence suggests that the total number of elements in the *TR-ACO1* and both *TR-ACO3* and *TR-ACO4* sequences does not exceed the number of TFBD domains that occur in *TR-ACO2*. The *TR-ACO2* sequence has the same number of developmentally-related classes (class II) as *TR-ACO1,* but it also has the same number of ethylene-related classes (class III) as both of *TR-ACO3* and *TR-ACO4* promoters. The number

of the hormone-related and environmentally-related signals (class I) in the *TR-ACO2* promoter is nearly twice that of *TR-ACO1*, *TR-ACO3* and *TR-ACO4* promoters. This implies that the *TR-ACO2* promoter sequence is regulated by a broad range of stimuli, and at different developmental stages. This broad pattern correlates with the northern blot data which shows that *TR-ACO2* expression can be detected from newly initiated through to mature green leaves (Hunter et al., 1999) but expression is also regulated by environmental stimuli such as ethylene and ageing, and displays a circadian pattern of expression (Hunter et al., 1999).

4.4.3. *TR-ACO* gene expression and the distribution of TFBD classes in each 5′ flanking sequence

A more detailed analysis of some of the more significant TFBDs from each sequence reveals that the *TR-ACO1* promoter contains TFBDs that suggests these genes are regulated by developmental signals particularly expressed in young tissues. High numbers of MADS-box family binding domains occur in the p*TR-ACO1* sequence, and these proteins have been well characterized as factors that regulate plant development in *Arabidopsis*, especially in floral tissue (Riechmann et al., 1996) and fruit ripening (Vrebalov et al., 2002). One member, AG (*Agamous*) has been shown to be an important transcription factor for regulating floral tissue (sepal and petal) development (Huang et al., 1993). Another family member, AGL3 (*Agamous-like 3*), is expressed in all above-ground vegetative organs, and has been implicated as being involved in the regulation of developmental genes in many cells (Huang et al., 1995). In addition to these developmental class II cues, a number of hormonal and environmental (Class I) boxes that occur in the p*TR-ACO1* are involved in germination or seedling emergence. For example, the α-amylase and β-amylase gene-specific-expression domains. These have been found in genes expressed during rice germination (Yamauchi, 2001) and in potato tuber development (Ishiguro and Nakamura, 1994). Further, an endosperm-specific domain is found in many genes encoding storage proteins, including seeds of rape (*Brasica*

napus) (Stalberg et al., 1996). The occurrence of these putative TFBDs with the *TR-ACO1* promoter is interesting since the expression of *TR-ACO1* in 16 hr imbibed seeds of white clover has been observed (Jaya, 2003).

For *TR-ACO2*, one interesting TFBD is the light-response element. This has been identified in the light-regulated photosystem I gene (*PSA*) in tobacco (Nakamura et al., 2002). The identification of this element may be significant as there is some evidence that the expression of *TR-ACO2* is under circadian control (Hunter, 1998). In these experiments, highest *TR-ACO2* expression was observed at 1:30 PM and the lowest at 7:30 PM as determined by northern analysis.

The other significant TFBDs are the ethylene response elements. One is the ERE-box, as described in the p*TR-ACO1* analysis, which is involved in the ethylene up-regulated expression of E4 gene in tomato ripening (Itzhaki et al., 1994). This element has also been found in the melon *ACO-1* gene promoter which has also shown to be induced by ethylene (Bouquin et al., 1997). The second domain is the GCC box, which is conserved in a number of ethylene-responsive defense genes, such as the class I chitinase gene, and the pathogenesis-related genes (PR) (Hao et al., 1998). Both of these ethylene response elements occur in the *TR-ACO2* promoter suggesting that *TR-ACO2* is regulated by ethylene. There is good experimental support for this, since treatment of white clover leaf tissue with ethylene induced the expression of *TR-ACO2* in mature green leaves (Hunter, 1998)(Scott, R.W., 2004, *pers. comm.*).

In both the p*TR-ACO3* and p*TR-ACO4* sequences, the interesting elements are the wounding-response element (W-box) and a tissue ageing associated element (Cysteine). The W-boxes can be recognized by a large family of zinc-finger transcription factors, and their main function is to regulate the response to wounding and pathogen attack (Yu et al., 2001). A W-box may also be involved in the onset of leaf senescence and have also been shown to be expressed constitutively throughout all plant tissues (Ulker and Somssich, 2004). The

cysteine proteinase specific expression domain (Cysteine), has been found to be conserved in most cysteine proteinase promoters including *SAG-12* from *Arabidopsis*, and other plants (eg. barley and rape) (Cercos et al., 1999). Since cysteine proteinases are highly expressed during senescence, and are involved in protein degradation including RuBiSCO, and other chloroplast proteins, the occurrence of this domain may be directly linked to *TR-ACO3* and *TR-ACO4* expression, and the senescence process. It has been shown that ageing of leaf tissue (eg. by detachment) and wounding of white clover leaves results in the induction of *TR-ACO3* expression (Hunter, 1998), and this might support the appearance of these elements in the p*TR-ACO3* and p*TR-ACO4* sequences.

Some other hormone-response elements also may be important factors in these sequences. For example, the auxin-response element (Aux-RE) has been identified in many genes from different plant species (Baumann et al., 1999), the expression of which are involved in cell division and extension, root formation, shoot apical dominance, leaf tropisms and senescence (Berleth et al., 2004). One such gene, the *NPH4* gene of *Arabidopsis*, which contains the IAA-box in its promoter, is expressed in hypocotyl bending but this response has been shown to involve both auxin and ethylene (Harper et al., 2000). The occurrence of these hormone related boxes in the *TR-ACO* promoters also highlights the concept of hormonal cross-talk (Voesenek et al., 2003) and that the expression of each *TR-ACO* gene will be regulated by more than one hormone working together.

4.4.4. TFBD analysis in other ACO promoter sequences

Promoter analysis has also been undertaken for ACO gene from other multi-gene families. For example, the promoter from the melon *CM-ACO1* and *CM-ACO3* genes have been fused with the GUS reporter gene and transformed into tobacco. The results showed that the *CM-ACO1* driven GUS activity increased sharply with the onset of leaf chlorophyll breakdown, whereas GUS expression driven from the *CM-ACO3* promoter was higher in

mature green leaves and declined at the onset of senescence. This expression pattern is consistent with the expression patterns observed from northern analysis. Further, GUS expression from the senescence-associated *CM-ACO1* promoter can be also be induced by ethylene, wounding, heavy metal ($CuSO_4$) factors, and pathogen infection. Therefore, the senescence tissue specific *CM-ACO1* promoter can be highly induced by most stress factors including pathogen infections whereas the green-tissue-specific *CM-ACO3* promoter only has basal stress responses, and can not be induced by pathogen attraction. When the *CM-ACO1* promoter is examined for the occurrence of TFBDs, in common with the *TR-ACO3* and *TR-ACO4* promoters, ethylene response and W-boxes are prevalent with two ethylene response elements (EREs) and seven wounding response elements (WUN) identified. In addition other stress-associated TFBDs have been identified, with two drought response elements (DREs) and three elicitor response elements (PI, ELI, BRE). These elements have not been identified in the *TR-ACO3* promoter, but may be present on the promoter, and require a different programme to identify them. In contrast, the *CM-ACO3* promoter sequence contains seven stigma/style specific elements (SLG13 box), two flower-specific Myb binding elements (H-box), three DREs and two heavy metal response element (MTRE) (Lasserre et al., 1997). The developmentally regulated TFBDs also occur in *TR-ACO2*, but not the DREs or the MTREs. Again, these elements may be present on the promoter, and require a different programme to identify them.

Similar experiments have also been undertaken in the peach ACO family where the *PP-ACO1* and *PP-ACO2* promoters have been fused to the GUS gene and transformed into tomato. The results showed that GUS expression driven from *PP-ACO1* promoter was mainly expressed throughout most stages of leaf development and in wounded senescent leaves, whereas the *PP-ACO2* promoter was only active in senescent leaves, but not in response to wounding (Rasori et al., 2003). In a more detailed analysis of the *PP-ACO1* promoter sequence, putative TFBDs included one primary ethylene response element (PERE), one secondary ethylene

response element (SERE), one putative repressor region (N-), an enhancer element (CATT-box) and two auxin response elements (Aux-RE). Again, the ethylene response elements are shared by all the *TR-ACO* promoters, but the putative repressor region (N-) was not searched for.

Together these observations suggest that the tissue-specific and response-specific patterns of ACO gene expression including the *TR-ACO* genes can be predicted by the TFBDs domains that occur in the promoter sequences. How the transcription factor binding domains leads to tissue-specific expression still not clear, but for those stress factors (eg. pathogens, wounding) and the other hormones response factors (eg. IAA, ethylene), identification of the TFBDs is becoming more reliable.

4.4.5. Strategies to test the function of the TFBDs

There are more than one hundred TFBDs distributed among the four *TR-ACO* promoter sequences, and while it is possible to speculate on their function, it is necessary to directly test this in the future. For the hormone- and environmentally-related class I and the ethylene-related class III TFBDs, the various candidate signals can be applied to transgenic plants transformed with each promoter fused to a reporter gene (eg. GUS or GFP). Certain concentrations of hormones (eg. IAA, C_2H_4, ABA, GA, or SA) can then be applied to these transgenic plants and reporter gene activity changes recorded. For the developmentally-related class (class II) cues, PCR methods can be used to mutate certain elements, and the mutant construct transformed back to model plants to determine their developmental changes. In the analysis of the *PP-ACO1* promoter, the SERE and N- elements have been deleted, and GUS activity slightly increased but not in response to ethylene treatment (Rasori et al., 2003). Thus a similar analysis can be undertaken on the EREs in the *TR-ACO* promoters.

To examine the significance of clusters, 5´-end deletion assays can also be used and the truncated promoter (fused to a reporter gene) transformed into model plants to determine any change in promoter function.

4.5 Analysis of *TR-ACO* promoter-directed expression using GUS reporter transcripted fusions

4.5.1. Transgenic tobacco as the genetic background

From the results of Southern analysis, most transgenic tobacco lines contained two copies of each promoter fused with the GUS sequence, and hybridization pattern obtained confirmed that these are individual transgenic lines. In addition, the expression pattern of each construct in the different plant lines examined was consistent. For example, *TR-ACO1* lines # 1 (data shown), #7, and #11 lines, all displayed GUS expression predominantly in the apical and axillary buds, and the *TR-ACO2* lines #2 (data shown), #7, and #8 displayed GUS expression predominantly in the petiole and senescent leaves. For the *TR-ACO3* lines #4, #13 (data shown), and #15, GUS staining was highest in the green to yellow leaves, petiole and axillary buds, while the *TR-ACO4* lines #14 (data shown), #17, and #18 showed a similar pattern, but with increased staining density when compared with the *TR-ACO3* lines. These data suggests that two copies of the inserts has not resulted in any gene silencing in the transgenic tobacco plants examined (Bastar et al., 2004), and the *TR-ACO* promoters are recognized by specific binding factors in the heterologous background.

As described in section 3.3.2, the results of GUS staining for most of the transgenic tobacco lines harbouring the p*TR-ACO1::GUS* construct shows expression in the apical terminal bud and in axillary buds. This is similar to the northern blot data observed for clover leaves (Hunter et al., 1999). The staining of GUS in most axillary buds as well as the terminal bud suggests that both tissues may share similar controls in terms of regulation of ethylene

biosynthesis. This may also suggest that ethylene may play a similar role in both the terminal and axillary buds.

The *TR-ACO1* promoter is derived from the white clover genome, but when the promoter sequence is expressed in the heterologous host (i.e. tobacco), a similar pattern of expression is observed. This suggests that the transcription factors in the apical bud or axillary bud tissues may have similar functions, and that the TFBDs are conserved in both tobacco and white clover. For example, the MADS-box transcription factors have been reported to be highly conserved in their sequences and their binding domains among many plant species (Riechmann and Meyerowitz, 1997). These TFBDs, at least, may be part of the explanation of a conserved tissue-specific expression pattern between clover and tobacco.

GUS staining in most of the transgenic tobacco lines transformed with the p*TR-ACO2::GUS* construct revealed promoter-directed expression in mature-green to senescent leaves. This expression pattern differs from northern blot data of white clover leaves (Hunter et al., 1999), in which *TR-ACO2* is expressed highly in the newly initiated leaf tissues, and then decreases into the mature green leaves. In fact, the expression of *TR-ACO2* in tobacco is very similar to the pattern of *TR-ACO3* gene expression pattern in clover as shown by northern blot analysis. The difference in expression directed by the p*TR-ACO2* between clover and tobacco can be possibly explained by the different host plants suggesting that the regulatory mechanisms governing expression in these tissues differ. Such differences in promoter driven expression in heterologous hosts has also been found when the *PP-ACO2* gene from peach (Rasori et al., 2003) is expressed in tomato. In tomato, expression of *PP-ACO2* can be detected in vascular bundles of developing and ripe fruit, the senescent leaf blade, and in fruit and leaf abscission zones. Whereas, in peach, the *PP-ACO2* mRNA is detected only in immature fruit, and the epicotyls and roots of the seedlings. Therefore, the heterologous host may contain different transcription factors expressed at different developmental stages when compared with the

natural background. For *TR-ACO2*, expression in transgenic tobacco resulted in expression directed in both mature-green and senescent tissue suggesting that the *TR-ACO2* promoter sequence is a clover-specific promoter sequence, and its TFBDs and specific transcription factors are specific to this species.

The *TR-ACO3* promoter-directed expression pattern in tobacco begins in the newly initiated leaves, carries through to the newly senescent leaves, and then decreases in the late senescent leaves. This expression pattern, with the exception of the intensity of GUS staining, is very similar to the expression pattern directed by the *TR-ACO4* promoter. During the senescence process, ethylene evolution increases as the leaf chlorophyll content decreases (Gan and Amasino, 1997), and it is known that ethylene can stimulate chlorophyllases and the expression of other proteinases that degrade cellular protein (Buchanan-Wollaston, 1997). Further, in broccoli and *Arabidopsis,* it has been shown that the ethylene concentration increases with leaf yellowing (Gong and Mattheis, 2003; Todorov et al., 2003). Also, in melon, the expression of *CM-ACO1* increases when the leaf chlorophyll content decreases (Lasserre et al., 1997). Further, when ACO genes are transformed into tomato or *Arabidopsis* plants in the anti-sense orientation, leaf senescence is delayed (Grbic and Bleecker, 1995; John et al., 1997). Thus an increase in expression directed by the *TR-ACO3* and *TR-ACO4* (and *TR-ACO2*) promoters during the senescence process, as observed in the transgenic tobacco plants, is consistent with these observations.

When comparing the expression pattern of both the *TR-ACO3* and *TR-ACO4* promoters, the tissue and cellular specific patterns are the same, but the *TR-ACO4* promoter directs stronger expression (as determined by a visual assessment of the relative intensity of GUS staining). Although both promoter sequences contain a similar number of TFBDs, it maybe that the location of the TFBDs and/or the clustering explains this difference in intensity.

The pattern of expression directed by the *TR-ACO3* and *TR-ACO4* promoters during leaf senescence in tobacco suggests that these promoters respond to transcription factors that are similar to those that occur in white clover. While the expression of *TR-ACO3* in tobacco is in agreement with northern blot data from white clover leaves (Hunter et al., 1999), in which expression is highest in the senescent leaf tissues and decreases in younger leaves, northern analysis to determine the expression pattern of *TR-ACO4* has yet to be undertaken. However, a similar pattern of GUS staining directed by both p*TR-ACO3* and p*TR-ACO4* suggests that the expression pattern of *TR-ACO3* and *TR-ACO4* will be similar. It is known that some of the TFBDs are conserved in these promoters. For example, the W-box has been identified in tobacco, but this sequence is also conserved among other species including *Arabidopsis* and tomato (Chen and Chen, 2000; Robatzek and Somssich, 2002). These conserved sequences imply not only that the response binding factors are common, but also their expression patterns are similar. This may explain, therefore, why the *TR-ACO4* expression pattern during senescence is conserved between tobacco and white clover.

When the expression patterns driven by the *TR-ACO4* and *TR-ACO2* promoters are compared in tobacco, they both show a similar pattern of ontological expression. However, in the green leaf tissues, *TR-ACO4* expression is much higher when compared with *TR-ACO2*, but in the yellow leaves, *TR-ACO2* expression is higher than *TR-ACO4*. During necrosis, the *TR-ACO2* promoter is still active, but expression from the *TRACO4* promoter is reduced. Thus in common with *TR-ACO2*, the expression of *TR-ACO4* differs between clover and tobacco in the mature-green leaf tissue. This suggests that there are additional mechanisms that regulate ethylene production in mature green tissues, and that the binding factors differ for each promoter.

When the expression pattern directed from the *TR-ACO4* promoter is examined in more detail, two sites of GUS staining occur in leaf discs. One site is localized in the vascular tissues in the leaf (leaf, midrib and petiole) and the second at the edge of the disc. In the midrib tissues

at the magnification used, it is hard to detect any difference between vascular bundle and leaf lamina, but in the petiole of yellowing leaves, the intensity of GUS staining in the cortex cells is higher with respect to that observed in the vascular bundle (Figure 3.3.15). This pattern differs from the pattern of *TR-ACO2*-directed expression in yellowing leaves of tobacco (Figure 3.3.13-B), where more intense GUS staining is located in the vascular bundle and leaf lamina when compared with the cortical cells, and this is also noted in the petiole. Since the vascular tissue in the tobacco petiole may act as a conduit for nutrient remobilisation, this may suggest that the ethylene produced from *TR-ACO2* expression is associated with these processes during senescence, but the ethylene produced from *TR-ACO4* expression (as determined by *TR-ACO4* promoter activity) may be more involved with regulating necrosis in the lamina of the senescent leaves.

For *TR-ACO4*, dense GUS staining was also located at the edge of green leaf disc, suggesting that the *TR-ACO4* promoter can be induced by the wounding stimulus. It is known that *TR-ACO3* activity can be induced by wounding of white clover leaves (Hunter, 1998), and because this promoter sequence (with *TR-ACO4*) contains many wounding boxes, it is likely that wounding can stimulate expression. But this phenomenon appears to be limited more to the green leaf tissue, which suggests that the wounding response is also controlled by other developmental factors which are specific to the green leaf tissue.

4.5.2. Transgenic white clover as the genetic background

From the Southern analysis results in section 3.3.3, most transgenic white clover lines analysed contained two copies of each promoter fused with the GUS sequence, and the expression pattern of each construct in the individual plant lines differed. For example, in broad terms, the p*TR-ACO1* # 1, # 3, and # 11 lines, displayed GUS expression predominantly in the apical and axillary buds; the p*TR-ACO2* lines # 1, # 12, and # 19 displayed consistent GUS expression predominantly in mature-green tissues; *TR-ACO3* lines # 1, # 2, and # 6

showed dense GUS staining consistently in the older tissues, while the *TR-ACO4* lines # 1, # 22, and # 26 showed a similar pattern of expression, but with increased density when compared with the *TR-ACO3* lines. These data suggest that the selected transgenic plant lines display minimal or no transgenic position effects.

As described in results section 3.3.3.3, the transgenic white clover lines containing the p*TR-ACO1::GUS* construct lines showed highest density of GUS staining in the developing tissues. For example, in the newly-initiated trifoliate leaf, GUS staining can be detected in the whole of leaf (Figure 3.3.22; node 2), but gradually disappears starting from the lamina, then midrib, and then can only be detected in the petiolule tissues in leaves subtending from the ontologically older leaves. The most active period of cell growth (the log phase) occurs from the newly initiated leaf (#1 node) to the young green leaf (#3 and #4 nodes), and then after that the leaf size does not increase (Baker and Williams, 1987). Thus the expression pattern directed from the *TR-ACO1* promoter may be correlated to the growing pattern of the leaf suggesting that the *TR-ACO1* promoter responds to developmental cues in these tissues.

At least two other tissues display higher expression directed by the *TR-ACO1* promoter in the white clover shoot: the terminal bud and the axillary buds. The evolution of high levels of ethylene has been observed from the apical structure of white clover (Yoo, 1999), and is commonly observed during bud-break in deciduous tissue (Osborne, 1991). This suggests *TR-ACO1* expression may be tightly linked with branch development and bud dormancy mechanisms.

The second tissue with intense GUS staining is the petiolule tissue at the base of each trifoliate leaf. The main function of this tissue is to control leaf folding and un-folding in response to a diurnal rhythm (Baker and Williams, 1987). This mechanism has been reported to be driven by changes in turgor pressure in the petiolule cells, which efflux water from cells into the apoplast, in response to an accumulation of sucrose in the apoplast that has been unloaded from the phloem (Moysset et al., 1991; Morillon et al., 2001). During daylight, the

cells contain water that accompanies sucrose produced by photosynthesis which is transported across the cell wall and loaded into the phloem cells. During the evening, loading slows and so some unloaded sucrose accumulates in the cell wall, and results in water effluxing out the cytoplasm (Raven et al., 1999). Since the petiolule cells are located at the base of leaf lamina, the change in cell turgor triggers the nastic movement and it has been shown that ethylene is involved in the regulation of nastic movements (Cox et al., 2003; Voesenek et al., 2003; Wachter et al., 2003), but it is yet to be demonstrated whether the p*TR-ACO1* directs expression in a diurnal fashion.

Closer examination of these GUS-stained tissues using histological sections reveals that most cell types in the apical bud, axillary buds and the petiolule are stained. The exception is the apical meristem and the newly initiated leaf primordia in both the terminal bud and the axillary buds. However, the results of the *in situ* hybridization suggest that expression of *TR-ACO1* does occur in these cells (see later Discussion). The use of *in situ* hybridization also confirms that expression of *TR-ACO1* occurs in the vascular tissue, particularly the phloem (Figure 3.3.30, H) and in the cortex of the petiolule (Figure 3.3.30, J). In the example shown (Figure 3.3.30, J) cells at the adaxial side of the cortex have constricted to cause the tropic response. An apparent increase in the density of substrate deposition in the smaller cells may be due to a difference in cell number, but it does show that *TR-ACO1* may be involved in the tropic response. Together, these results supports the view that most (but not all) cells of leaf have the ability to convert ACC to ethylene (*i.e.* express and accumulate ACC oxidase).

The expression of the p*TR-ACO2::GUS* construct in transgenic white clover plants is described in section 3.3.3.4. The results show expression predominantly in the newly-initiated and mature-green leaves with lesser intensity of staining in the old tissues. For example, in the leaf lamina, GUS staining can only be detected from the young green leaf. GUS staining can not be detected in the newly initiated leaf, but gradually appears in the petiolule cells and then

the petiole and midrib and finally the whole leaf lamina (at node # 4). After the mature green leaf stage (node # 7), the intensity of GUS staining decreases as senescence ensues. Because this expression pattern correlates with leaf chlorophyll content (section 3.3.3.2), which is a good indicator of a photosynthetically competent leaf, it implies that the *TR-ACO2* promoter is active during leaf growth and the maintenance of leaf function.

In leaf tissues, intense GUS staining is again located in the petiolule tissues. In common with the discussion of *TR-ACO1*, the main function of this tissue is to control leaf folding and un-folding in response to a diurnal rhythm (Baker and Williams, 1987) and it suggests that the ethylene produced by *TR-ACO2* plays a similar role in this tissue as *TR-ACO1* in the younger tissues.

The other tissue with higher intensity of GUS staining is the stolon tissues particularly at the nodes (Figure 3.3.23; a). The pattern of expression directed by p*TR-ACO2* in this tissue differs from p*TR-ACO1* in that GUS staining in the *TR-ACO1::GUS* transgenics were concentrated in the axillary bud rather in the stolon, However, p*TR-ACO2* directed expression in both tissues, suggesting that the *TR-ACO2* promoter is also associated with metabolic cues and photosynthesis, and may be associated with sucrose loading and transport (Naik and Mohapatra, 2000). In support of this, the *TR-ACO2* promoter sequence contains more than six different metabolism-associated signals (eg. the Sucrose-box, β-and α-amylase-boxes).

Closer examination using histological analysis (Figure 3.3.27), again shows that many cell types are stained, with the exception of the apical meristem and very young leaf primordia. The large cortical cells in the sheath and the pith also appear not to be stained, but the vascular tissue is stained with more intensity. In common with the p*TR-ACO1*-directed pattern of expression, most cells express the gene and so may have the ability to convert ACC to ethylene. In addition to the apical cells, the larger, more vacuolated cells of pith and sheath do not stain. This may be due to developmental control or that the large vacuole dilutes out the cytoplasmic-based GUS signal.

As described in section 3.3.3.5, the p*TR-ACO3::GUS* transformed white clover lines all showed more intense GUS staining predominantly in the older leaf tissue including the axillary buds. For example GUS staining is very faint at the apical bud and in the young green leaves (#3), but gradually as the leaves mature, blue staining increased in the petiolule cells and in the petiole (Figure 3.3.24). In common with the analysis of the *TR-ACO4* promoter (see later), *TR-ACO3*-directed expression is consistent with the chlorophyll content which is highest in leaf numbers #4 and #5, after which it gradually decreases. This chlorophyll degradation pattern is consistent with visual yellowing that indicates the progress of senescence suggesting that the *TR-ACO3* promoter is a senescence-regulated sequence.

As described in section 3.3.3.6, the p*TR-ACO4::GUS* transgenic lines also directed a senescence-associated pattern of GUS staining. For example, GUS staining is very faint at the apical bud and in the young green leaves (node #5), but gradually as the leaves mature, blue staining increased in the petiolule cells and petiole tissues first, and then in the leaf lamina. In common with the analysis of the *TR-ACO3* promoter, *TR-ACO4*-directed expression is consistent with the chlorophyll content.

As discussed in section 3.2.1, analysis *in silico* of the *TR-ACO3* and *TR-ACO4* promoter sequences suggests regulation by senescence factors and this also coincides with the transgenic expression pattern *in vivo*. In general, the *TR-ACO3* and *TR-ACO4* promoters contain more senescence-related signals when compared with the *TR-ACO1* and *TR-ACO2* promoters, including the ethylene-related TFBDs (eg. GCC-box), and the ethylene-associated TFBDs (eg. W-box).

The expression pattern directed by both *TR-ACO3* and *TR-ACO4* was examined using histological analysis (Figure 3.3.28 and 3.3.29). In the axillary buds of older node tissue, the ground meristem tissue is stained, and in the node tissues the vascular tissue display intense staining. In these sections, it is harder to detect staining in the pith or cortical cells. In the

petiolule cells the phloem and sclerenchyma cells are stained, but less staining is observed in the cortical cells.

However, at higher magnification staining can be observed in the cortex and pith, and it may be that the very vasculated cells of the cortex and pith do not show the GUS staining very clearly, in comparison with the more dense cells of the phloem and vascular parenchyma.

An alterative view is that the ACC oxidase activity expressed in older tissue is concentrated in the vascular tissue (but not the xylem elements) and ACC moves through the vascular tissue. For example, the movement of ACC in the xylem sap has been shown in flooded tomato (Else et al., 1995). *In situ* hybridization studies (Figure 3.3.31) did show more dense hybridization in the phloem tissue, and in fibres (Figure 3.3.31; G, H, J). However, *in situ* hybridization also suggested that the petiolule cortex also expresses the *TR-ACO3* gene, and ethylene synthesized from the oxidase may mediate the nastic growth responses. *In situ* hybridization did not support *TR-ACO3* expression in the stolon cortex or pith.

A feature of the GUS staining directed by all four promoters, and the more limited *in situ* hybridization is that many cells in the vegetative tissues (stolon and leaf) display ACC promoter activity. If it is assumed that this promoter activity is transcribed and then translated into active enzyme, then most cells in these tissues can convert ACC to ethylene, and ACC oxidase does represent a constitutive step in the pathway. While expression from ACC oxidase promoters has been studied previously, more detailed histochemical analysis at the cell level in vegetative tissues is less common. Examination of GUS expression directed by the promoter of *LE-ACO1* in transgenic tomato conducted by Blume and Grierson (1997), revealed little evidence of staining in young petioles but more intense staining in petioles supporting senescent leaves. In these sections of the older tissue, staining was most pronounced in the phloem and in the sub-epidermal collenchyma cell layers. In other ACO promoter::GUS fusion studies, more specific patterns of cell or tissue staining have been observed. For example, when the *AP4* promoter of apple was fused to GUS and transformed

into tomato, the full-length promoter fragments (1966 bp and 1159 bp) drove GUS expression in the inner pericarp, vascular tissues and the seeds in fruit after breaker stage. However, no staining was observed in the outer pericarp and epidermis (Atkinson et al., 1998). In another study, Blume and Grierson (1997) showed that GUS staining directed by the full-length *LE-ACO1* promoter as the fruits matured showed even staining in the pericarp as well as the columella, whereas staining in the placental and locular tissue was less marked. A feature was the stronger but not exclusive staining in the outer pericarp associated with the vascular tissue. However, when seeds were examined, staining was detected exclusively in the endosperm. It maybe, therefore, that if promoter-directed expression was examined in seeds or floral tissue of white clover, then more specific patterns of GUS staining will be recognised.

In this thesis the level of GUS staining has not been quantified. Therefore, the relative intensity of expression driven by each promoter can not be compared. It is possible to quantify GUS expression using 4-methylumbelliferyl-β-$_D$-glucuronide (MUG) as substrate and some plant promoter studies have used this method (Blume and Grierson, 1997; Lasserre et al., 1997). However, the primary aim of this thesis was to examine the pattern of staining in cell types and tissues of different ontological status.

4.5.3. Assessment of the consistency of the GUS staining pattern

The use of promoter::GUS fusions is a powerful tool to dissect the pattern of gene expression in plant tissues. However, there are two commonly perceived drawbacks. The first is the question as to whether enough of the promoter sequence has been isolated to faithfully direct expression of the gene in a transgenic background. The second is whether position effects influence the pattern of expression of the reporter gene.

The length of *TR-ACO* promoters in this thesis was more than 1000 bp, and this compares well with other studies, particularly those that have used 5´ flanking sequence deletion

experiments which show that truncated lengths can drive the basic GUS expression pattern, and even tissue-specific expression patterns (Blume and Grierson, 1997; Lasserre et al., 1997; Atkinson et al., 1998). In this study, all the p*TR-ACO::GUS* transformants displayed a developmental pattern of expression that broadly correlated with the expression of the *TR-ACO* gene family. These patterns support the view that the 5´ flanking sequences do contain most of the *cis*-elements that are necessary to drive the basic and tissue-specific expression pattern of the GUS reporter gene in white clover.

Although the upstream 5´ flanking sequences contain most regulatory information, the downstream intragenic sequences may also play some important role in regulation. For example, northern analysis has shown that the rice α-tubulin gene (*Os-TUB A1)* is expressed specifically in young dividing tissues. However, when using the 5´ flanking sequence of the *Os-TUB A1* gene fused with the GUS gene in a transgenic background, expression was only detected in the mature tissues. However once the reporter fusion included the first intron sequence, then GUS expression can be detected in young dividing tissues with high activity (Jeon et al., 2000). In the p*TR-ACO1::GUS* transgenic plant lines, GUS staining can not be detected in the apical terminal bud in the SAM cells, while *in situ* hybridization analysis showed expression of *TR-ACO1* in the SAM cells (albeit at a low level). This maybe interpreted that not only the 5´ flanking sequence, but also the intragenic sequences are needed to control expression of the *TR-ACO* genes in certain cell types.

The second perceived drawback for the use of transgenic plants to study promoter activity is the concept of position effects. To reduce position effects and to obtain a consistent pattern of expression, sufficient numbers of transgenic lines need to be analyzed. From Southern analysis (section 3.3.3.1) all of the three selected transgenic lines from each gene transformation contained two to three copy numbers of the GUS gene insert. It might be expected that a higher number of gene inserts increase the chances of position effects. In this thesis at least 3 independent lines of white clover were examined (Table 3.3.1), and these

were selected from a larger pool of plants [*TR-ACO1* (18 plants); *TR-ACO2* (23 plants); *TR-ACO3* (27 plants); *TR-ACO4* (32 plants)]. Also, at least three vegetative stolons for GUS expression were selected from each plant. The data reported on the pattern of GUS staining, is consistent over these 3 independent replicates and 3 clonal replicates. This degree of replication provided a broad consensus of staining (Figure 3.3.12 to 3.3.15 and 3.3.22 to 3.3.25), although this was not perfect. As far as the author is aware, there is no definite number of sufficient transgenic lines, and it may be that more are required in transformed tetraploid species, when compared with transformed diploid species.

4.6 Summary and concluding remarks

In this thesis four ACC oxidase 5′ flanking (promoter) sequences have been isolated from the genome of white clover. In a previous study (Hunter et al., 1999), three ACO cDNAs were isolated by RT-PCR although Southern analysis data suggested that a fourth ACO gene was present. This fourth ACO gene was predicted to share significant homology in the open reading frame with *TR-ACO3,* but was distinct in the 3′-UTR region. In the present thesis, Southern analysis has confirmed the occurrence of four distinct genes, and comparison of the exon sequences with the *TR-ACO3* gene confirmed that the gene designated as *TR-ACO3* in this study (originally *TR-ACO3-2*) was the same as that identified by Hunter et al. (1999). Further, isolation and sequencing of genomic DNA has confirmed that the exon sequences of *TR-ACO3* share highly identity with the *TR-ACO4* exons, but the intron sequences are quite divergent, again supporting that this thesis has identified a fourth ACO gene in white clover.

Southern analysis has also revealed that two copies of *TR-ACO1* and *TR-ACO2* occur in the allotetraploid genome of white clover. The origin of the two diploid genomes in white clover is uncertain, with the current opinion being that they arose from hybridization of the diploid species *T. nigrescens* and the autotetraploid species *T. uniflorum* (Badr et al., 2002). The two copies of *TR-ACO1* and *TR-ACO2* may represent, therefore, identical copies in both genomes

as part of this hybridization process. It may be of significance that both *TR-ACO3* and *TR-ACO4* appear as single copies suggesting that each gene occurs in only one of the two genomes. If each gene does arise from only one of the parents, then Southern analysis of the likely progenitors of white clover with these probes may yield interesting results.

The identification of four ACO genes in white clover plant confirms that this is a small multi-gene family, and is consistent with findings in other plant species. The structure of the four ACO genes has also been examined, and each comprises 4 exons and 3 introns. Generally, the exons are broadly conserved in terms of size [exon 1 (103 – 105 bp), exon 2 (224 – 268), exon 3 (331 – 335 bp) and exon 4 (254 – 289)], but the introns varied greatly in terms of size. In comparison with other published accounts of ACC oxidase gene structures, the occurrence of 4 exons interspersed with 3 introns has been observed in other plant species.

As the initial analysis of the four ACO gene 5′ promoter sequences, an examination *in silico* was performed using database identification of putative transcription factor binding domains. This analysis provided both the broad categories of factors that may regulate the expression of each gene, but also gave more specific indication of the nature of these developmental and environmental cues.

For p*TR-ACO1,* in terms of class I, many of the motifs suggest a germination-associated role and it may be significant, therefore, that *TR-ACO1* is expressed in 16 hr-imbibed white clover seeds (Jaya, 2003). It is also well established that ethylene and ACC oxidase expression are associated with germinating seeds (Monoz De Rueda et al., 1995; Petruzzelli et al., 2000). Five motifs concerned with MADS or *AGAMOUS* genes were also identified suggesting a role in early organ or floral development, and two ethylene-response elements suggest that ethylene itself may regulate the expression of the gene. Previous northern analysis has shown that this gene is expressed in the apical structure and in the axillary bud tissues; tissues associated with high levels of ethylene production (Hunter et al., 1999; Yoo, 1999). It will be interesting, therefore, to examine the expression of this gene in floral tissues.

For p*TR-ACO2,* a significant number of class I genes was identified, particularly with respect to the potential role of other signalling cues in regulating gene expression (ABA, IAA, light, sucrose, salicylic acid). In other expression studies, it has been shown that *TR-ACO2* is expressed predominantly in mature green tissue, and is the predominant enzyme activity in these tissues, suggesting a role as the producer of 'house-keeping' ethylene, termed Type I ethylene. However, examination of the 5′ promoter sequence suggests that several external influences can also induce expression, and it has been shown that ethylene itself induces *TR-ACO2* expression, and the gene displays a circadian rhythm (Hunter, 1998).

Examination *in silico* of the *TR-ACO3* and *TR-ACO4* 5′ flanking sequences reveals a common spectrum of motifs. In contrast to p*TR-ACO1,* ethylene- and wound-associated domains are now more common when compared with the developmentally-associated class I domains. In studies with mature-green leaves, wounding and ageing, but not ethylene, has been shown to induce the expression of *TR-ACO3,* although it cannot be discounted that wounding will induce the expression of *TR-ACO3* in other tissues (Hunter, 1998; Yoo, 1999). No similar expression studies have yet to be carried out with *TR-ACO4.* However, the occurrence of p*TR-ACO3* (and p*TR-ACO4)*-directed GUS staining in the axillary bud tissue is also consistent with the occurrence of class II developmentally-regulated domains observed within the 5′ flanking sequences of these genes. A striking feature of this analysis, *in-silico*, was that the spectrum of TFBDs broadly coincided with the expression of each gene determined by northern analysis. Therefore, such examination of the spectrum of TFBDs can be used to predict the likely expression pattern of ACO genes.

To examine the tissue-specific nature of expression driven by each promoter during leaf development, GUS staining of the p*TR-ACO::GUS* transformants was used. In terms of the global pattern of expression, the *TR-ACO1* promoter sequence directed GUS expression in predominantly developing tissues (the stolon apical structure and the axillary buds). In the axillary buds, GUS staining was most intense in the ontological younger structures. In

contrast, the *TR-ACO3* and *TR-ACO4* promoter sequences directed expression in ontologically older tissues, including the axillary buds.

More detailed histochemical analysis was used to determine if the promoter sequences directed any cell-specific pattern of expression during leaf development. For this survey, sections were examined that displayed more intense GUS staining. A feature of this examination was that no definite pattern of cell-specific expression was observed. More intense GUS staining was observed in the vascular tissue of the stolon including the subtending provascular strands emerging from the shoot apical mersitem and the apical meristem in the axillary buds, as well as the central vascular tissue (stele) in the petiolules. However, in pith and cortical cells, close observation did reveal evidence for GUS staining. This was most notable in the p*TR-ACO1::GUS* and p*TR-ACO2::GUS* transformants, particularly in the ontologically younger tissues. In the ontological older tissue (examined in the p*TR-ACO3::GUS* and p*TR-ACO4::GUS* transformants) staining was less pronounced in the cortex and pith tissues, but was still evident in the vascular tissue.

Such observations, lead to the suggestion that the intensity of GUS staining may partly reflect cytoplasmic density, such that cells with large vacuoles appear to be lower accumulators of the enzyme. Alternatively, it may be that ACC oxidase accumulates, preferentially, in the vascular tissues (predominantly in the phloem tissue) and thus co-localises with a source of mobile ACC substrate (Else and Jackson, 1998).

Taken together, these results confirm that most cells during leaf development can potentially display the competence to convert ACC to ethylene as determined by the expression of ACC oxidase genes. Subsequent translational regulation will also provide a further tier of control. Further, this thesis has confirmed, with many others, that this competence to synthesise the hormone is directed *via* transcriptional regulation of the ACO gene family. However, in leaf development of white clover, at least, if can now be added that the primary cues for this transcriptional regulation are ontological in nature, rather than the signals that direct

cell-specific expression.

References

Abeles, F., Morgan, P., and Saltveit, M. (1992). Ethylene in plant biology. 2nd ed. Academic Press, California.

Alexander, L., and Grierson, D. (2002). Ethylene biosynthesis and action in tomato: a model for climacteric fruit ripening. Journal of Experimental Botany **53**, 2039-2055.

Amrhein, N., Schneebeck, D., Skorupka, H., Tophof, S., and Stockigt, J. (1981). Identification of a major metabolite of the ethylene precursor 1-aminocyclopropane-1-carboxylic acid in higher-plants. Naturwissenschaften **68**, 619-620.

Arimura, G., Ozawa, R., Nishioka, T., Boland, W., Koch, T., Kuhnemann, F., and Takabayashi, J. (2002). Herbivore-induced volatiles induce the emission of ethylene in neighboring lima bean plants. Plant Journal **29**, 87-98.

Atkinson, R. G., Bolitho, K. M., Wright, M. A., Iturriagagoitia-Bueno, T., Reid, S. J., and Ross, G. S. (1998). Apple ACC-oxidase and polygalacturonase: ripening-specific gene expression and promoter analysis in transgenic tomato. Plant Molecular Biology **38**, 449-460.

Badr, A., Sayed-Ahmed, H., El-Shanshouri, A., and Watson, L. (2002). Ancestors of white clover (*Trifolium repens L.*), as revealed by isozyme polymorphisms. Theoretical and Applied Genetics **106**, 143-148.

Baker, M., and Williams, W. (1987). White clover. CAB International, Oxon, UK.

Barry, C. S., Blume, B., Bouzayen, M., Cooper, W., Hamilton, A. J., and Grierson, D. (1996). Differential expression of the 1-aminocyclopropane-1-carboxylate oxidase gene family of tomato. Plant Journal **9**, 525-535.

Bastar, M. T., Luthar, Z., Skof, S., and Bohanec, B. (2004). Quantitative determination of mosaic GFP gene expression in tobacco. Plant Cell Reports **22**, 939-944.

Baumann, K., De Paolis, A., Costantino, P., and Gualberti, G. (1999). The DNA binding site of the Dof protein NtBBF1 is essential for tissue-specific and auxin-regulated expression of the *rolB* oncogene in plants. Plant Cell **11**, 323-334.

Baur, A. H., and Yang, S. F. (1972). Methionine metabolism in apple tissue in relation to ethylene biosynthesis. Phytochemistry **11**, 3207-3208.

Bekman, E. P., Saibo, N. J. M., Di Cataldo, A., Regalado, A. P., Ricardo, C. P., and Rodrigues-Pousada, C. (2000). Differential expression of four genes encoding

1-aminocyclopropane-1-carboxylate synthase in *Lupinus albus* during germination, and in response to indole-3-acetic acid and wounding. Planta **211**, 663-672.

Benichou, M., Martinezreina, G., Romojaro, F., Pech, J. C., and Latche, A. (1995). Partial-purification and properties of a 36-Kda 1-aminocyclopropane-1-carboxylate N-malonyltransferase from mung bean. Physiologia Plantarum **94**, 629-634.

Berleth, T., Krogan, N. T., and Scarpella, E. (2004). Auxin signals - turning genes on and turning cells around. Current Opinion in Plant Biology **7**, 553-563.

Bhowmik, P. K., and Matsui, T. (2004). Changes in the activity and expression of 1-aminocyclopropane-1-carboxylate (ACC) synthase, ACC oxidase, and phenylalanine ammonia-lyase in asparagus spears in response to wound-induced ethylene synthesis. Hortscience **39**, 1074-1078.

Bleecker, A. B. (1999). Ethylene perception and signaling: an evolutionary perspective. Trends in Plant Science **4**, 269-274.

Bleecker, A. B., Estelle, M. A., Somerville, C., and Kende, H. (1988). Insensitivity to ethylene conferred by a dominant mutation in *Arabidopsis thaliana*. Science **241**, 1086-1089.

Bleecker, A. B., and Kende, H. (2000). Ethylene: A gaseous signal molecule in plants. Annual Review of Cell and Developmental Biology **16**, 1-+.

Bleecker, A. B., Kenyon, W. H., Somerville, S. C., and Kende, H. (1986). Use of monoclonal-antibodies in the purification and characterization of 1-aminocyclopropane-1-carboxylate synthase, an enzyme in ethylene biosynthesis. Proceedings of the National Academy of Sciences of the United States of America **83**, 7755-7759.

Bleecker, A. B., and Patterson, S. E. (1997). Last exit: senescence, abscission, and meristem arrest in *Arabidopsis*. Plant Cell **9**, 1169-1179.

Blume, B., and Grierson, D. (1997). Expression of ACC oxidase promoter-GUS fusions in tomato and *Nicotiana plumbaginifolia* regulated by developmental and environmental stimuli. Plant Journal **12**, 731-746.

Boerjan, W., Bauw, G., Vanmontagu, M., and Inze, D. (1994). Distinct phenotypes generated by overexpression and suppression of S-adenosyl-L-methionine synthetase reveal developmental patterns of gene silencing in tobacco. Plant Cell **6**, 1401-1414.

Boller, T., Herner, R. C., and Kende, H. (1979). Assay for and enzymatic formation of an ethylene precursor, 1-aminocyclopropane-1-carboxylic acid. Planta **145**, 293-303.

Bouquin, T., Lasserre, E., Pradier, J., Pech, J. C., and Balague, C. (1997). Wound and ethylene induction of the ACC oxidase melon gene *CM-ACO1* occurs via two direct and independent transduction pathways. Plant Molecular Biology **35**, 1029-1035.

Bouzayen, M., Latche, A., Pech, J. C., and Marigo, G. (1989). Carrier-mediated uptake of 1-(malonylamino) cyclopropane-1-carboxylic acid in vacuoles isolated from *catharanthus roseus* cells. Plant Physiology **91**, 1317-1322.

Britsch, L., and Grisebach, H. (1986). Purification and characterization of (2S)-flavanone 3-hydroxylase from *Petunia hybrida*. European Journal of Biochemistry **156**, 569-577.

Brock, J. L., Hay, M. J. M., Thomas, V. J., and Sedcole, J. R. (1988). Morphology of white clover (*Trifolium repens* L.) plants in pastures under intensive sheep grazing. Journal of Agricultural Science **111**, 273-283.

Brougham, R., Ball, P., and Williams, W. (1978). Ecology and management of white clover-based pastures. Plant Relations in Pastures Wilson JR ed, CSIRO, Melbourne, 309-324.

Buchanan Wollaston, V. (1997). The molecular biology of leaf senescence. Journal of Experimental Botany **48**, 181-199.

Buchanan-Wollaston, V. (1997). The molecular biology of leaf senescence. Journal of Experimental Botany **48**, 181-199.

Burns, J. K., and Evensen, K. B. (1986). Ca-2+ effects on ethylene, carbon-dioxide and 1-aminocyclopropane-1-carboxylic acid synthase activity. Physiologia Plantarum **66**, 609-615.

Butcher, S., Fountain, D., and McManus, M. (1996). Leaf senescence and clonal growth of white clover. New Zealand Competitive Edge Joint Symposium, Lincoln University, NZ, 21-22.

Casas, J. L., Garciacanovas, F., Tudela, J., and Acosta, M. (1993). A kinetic-study of simultaneous suicide inactivation and irreversible inhibition of an enzyme - application to 1-aminocyclopropane-1-carboxylate (ACC) synthase inactivation by its substrate S-adenosylmethionine. Journal of Enzyme Inhibition **7**, 1-14.

Cercos, M., Gomez-Cadenas, A., and Ho, T. H. (1999). Hormonal regulation of a cysteine proteinase gene, *EPB-1*, in barley aleurone layers: *cis*- and *trans*-acting elements involved in the co-ordinated gene expression regulated by gibberellins and abscisic acid. Plant J **19**, 107-118.

Chae, H. S., Cho, Y. G., Park, M. Y., Lee, M. C., Eun, M. Y., Kang, B. G., and Kim, W. T. (2000). Hormonal cross-talk between auxin and ethylene differentially regulates the expression of two members of the 1-aminocyclopropane-1-carboxylate oxidase gene family in rice (*Oryza sativa* L.). Plant and Cell Physiology **41**, 354-362.

Chae, H. S., Faure, F., and Kieber, J. J. (2003). The *eto1*, *eto2*, and *eto3* mutations and cytokinin treatment increase ethylene biosynthesis in *Arabidopsis* by increasing the stability of ACS protein. Plant Cell **15**, 545-559.

Chang, C. (1996). The ethylene signal transduction pathway in *Arabidopsis*: An emerging paradigm. Trends in Biochemical Sciences **21**, 129-133.

Chang, C., Kwok, S. F., Bleecker, A. B., and Meyerowitz, E. M. (1993). *Arabidopsis* ethylene-response gene *Etr1* - similarity of product to 2-component regulators. Science **262**, 539-544.

Chang, C., and Shockey, J. A. (1999). The ethylene-response pathway: signal perception to gene regulation. Current Opinion in Plant Biology **2**, 352-358.

Chang, C., and Stadler, R. (2001). Ethylene hormone receptor action in *Arabidopsis*. Bioessays **23**, 619-627.

Chang, C. R., and Bleecker, A. B. (2004). Ethylene biology. More than a gas. Plant Physiology **136**, 2895-2899.

Chapman, D. F., and Robson, M. J. (1992). The physiological-role of old stolon material in white clover (*Trifolium-Repens* L). New Phytologist **122**, 53-62.

Chen, C., and Chen, Z. (2000). Isolation and characterization of two pathogen- and salicylic acid-induced genes encoding WRKY DNA-binding proteins from tobacco. Plant Mol Biol **42**, 387-396.

Chen, Y. F., Randlett, M. D., Findell, J. L., and Schaller, G. E. (2002). Localization of the ethylene receptor *ETR1* to the endoplasmic reticulum of *Arabidopsis*. Journal of Biological Chemistry **277**, 19861-19866.

Chen, Y. T., Lee, Y. R., Yang, C. Y., Wang, Y. T., Yang, S. F., and Shaw, J. F. (2003). A novel papaya ACC oxidase gene (*CP-ACO2*) associated with late stage fruit ripening and leaf senescence. Plant Science **164**, 531-540.

Chomczynski, P. (1992). One-hour downward alkaline capillary transfer for blotting of DNA and RNA. Analytical Biochemistry **201**, 134-139.

Cox, M. C. H., Millenaar, F. F., van Berkel, Y., Peeters, A. J. M., and Voesenek, L. (2003). Plant movement. Submergence-induced petiole elongation in *Rumex palustris* depends on hyponastic growth. Plant Physiology **132**, 282-291.

Datla, R. S. S., Hammerlindl, J. K., Panchuk, B., Pelcher, L. E., and Keller, W. (1992). Modified binaryplant transformation vectors with the wild-type gene encoding *Npt II*. Gene **122**, 383-384.

Destefanobeltran, L. J. C., Vancaeneghem, W., Gielen, J., Richard, L., Vanmontagu, M., and Vanderstraeten, D. (1995). Characterization of 3 members of the acc synthase gene family in *Solanum-tuberosum* L. Molecular & General Genetics **246**, 496-508.

Dominguez, M., and Vendrell, M. (1993). Ethylene biosynthesis in banana fruit - evolution of efe activity and ACC Levels in peel and pulp during ripening. Journal of Horticultural Science **68**, 63-70.

Dong, J. G., Fernandezmaculet, J. C., and Yang, S. F. (1992). Purification and characterization of 1-aminocyclopropane-1-carboxylate oxidase from apple fruit. Proceedings of the National Academy of Sciences of the United States of America **89**, 9789-9793.

Dupille, E., Rombaldi, C., Lelievre, J. M., Cleyetmarel, J. C., Pech, J. C., and Latche, A. (1993). Purification, properties and partial amino-acid-sequence of 1-aminocyclopropane-1-carboxylic acid oxidase from apple fruits. Planta **190**, 65-70.

Dupille, E., and Zacarias, L. (1996). Extraction and biochemical characterization of wound-induced ACC oxidase from citrus peel. Plant Science **114**, 53-60.

Ecker, J. R. (2004). Reentry of the ethylene MPK6 module. Plant Cell **16**, 3169-3173.

Else, M. A., Hall, K. C., Arnold, G. M., Davies, W. J., and Jackson, M. B. (1995). Export of abscisic-acid, 1-aminocyclopropane-1-carboxylic acid, phosphate, and nitrate from roots to shoots of flooded tomato plants - accounting for effects of xylem sap flow-rate on concentration and delivery. Plant Physiology **107**, 377-384.

Else, M. A., and Jackson, M. B. (1998). Transport of 1-aminocyclopropane-1-carboxylic acid (ACC) in the transpiration stream of tomato (*Lycopersicon esculentum*) in relation to foliar ethylene production and petiole epinasty. Australian Journal of Plant Physiology **25**, 453-458.

Espartero, J., Pintortoro, J. A., and Pardo, J. M. (1994). Differential accumulation of S-adenosylmethionine synthetase transcripts in response to salt stress. Plant Molecular Biology **25**, 217-227.

Fernandez Maculet, J. C., and Yang, S. F. (1992). Extraction and partial characterization of the ethylene-forming enzyme from apple fruit. Plant Physiology **99**, 751-754.

Finlayson, S. A., Lee, I. J., Mullet, J. E., and Morgan, P. W. (1999). The mechanism of rhythmic ethylene production in sorghum. The role of phytochrome B and simulated shading. Plant Physiology **119**, 1083-1089.

Finlayson, S. A., Liu, J. H., and Reid, D. M. (1996). Localization of ethylene biosynthesis in roots of sunflower (*Helianthus annuus*) seedlings. Physiologia Plantarum **96**, 36-42.

Fluhr, R., and Mattoo, A. K. (1996). Ethylene - Biosynthesis and perception. Critical Reviews in Plant Sciences **15**, 479-523.

Gamble, R. L., Coonfield, M. L., and Schaller, G. E. (1998). Histidine kinase activity of the ETR1 ethylene receptor from *Arabidopsis*. Proceedings of the National Academy of Sciences of the United States of America **95**, 7825-7829.

Gan, S. S., and Amasino, R. M. (1997). Making sense of senescence - Molecular genetic regulation and manipulation of leaf senescence. Plant Physiology **113**, 313-319.

Gao, Z. Y., Chen, Y. F., Randlett, M. D., Zhao, X. C., Findell, J. L., Kieber, J. J., and Schaller, G. E. (2003). Localization of the Raf-like kinase CTR1 to the endoplasmic reticulum of *Arabidopsis* through participation in ethylene receptor signaling complexes. Journal of Biological Chemistry **278**, 34725-34732.

Gepstein, S., Sabehi, G., Carp, M. J., Hajouj, T., Nesher, M. F. O., Yariv, I., Dor, C., and Bassani, M. (2003). Large-scale identification of leaf senescence-associated genes. Plant Journal **36**, 629-642.

Gomez Lim, M. A., Valdeslopez, V., Cruzhernandez, A., and Saucedoarias, L. J. (1993). Isolation and characterization of a gene Involved in ethylene biosynthesis from *Arabidopsis-thaliana*. Gene **134**, 217-221.

Gomez-Gomez, L., and Carrasco, P. (1998). Differential expression of the S-adenosyl-L-methionine synthase genes during pea development. Plant Physiology **117**, 397-405.

Gomez-Jimenez, M. D., Garcia-Olivares, E., and Matilla, A. J. (2001). 1-aminocyclopropane-1-carboxylate oxidase from embryonic axes of germinating chick-pea (*Cicer arietinum* L.) seeds: cellular immunolocalization and alterations in its expression by indole-3-acetic acid, abscisic acid and spermine. Seed Science Research **11**, 243-253.

Gong, Y. P., and Mattheis, J. P. (2003). Effect of ethylene and 1-methylcyclopropene on chlorophyll catabolism of broccoli florets. Plant Growth Regulation **40**, 33-38.

Grbic, V., and Bleecker, A. B. (1995). Ethylene regulates the timing of leaf senescence in *Arabidopsis*. Plant Journal **8**, 595-602.

Guo, H. W., and Ecker, J. R. (2004). The ethylene signaling pathway: new insights. Current Opinion in Plant Biology **7**, 40-49.

Guzman, P., and Ecker, J. R. (1990). Exploiting the triple response of *Arabidopsis* to identify ethylene-related mutants. Plant Cell **2**, 513-523.

Hall, A. E., and Bleecker, A. B. (2003). Analysis of combinatorial loss-of-function mutants in the *Arabidopsis* ethylene receptors reveals that the *ers1 etr1* double mutant has severe developmental defects that are EIN2 dependent. Plant Cell **15**, 2032-2041.

Hamilton, A. J., Bouzayen, M., and Grierson, D. (1991). Identification of a tomato gene for the ethylene-forming enzyme by expression in yeast. Proceedings of the National Academy of Sciences of the United States of America **88**, 7434-7437.

Hamilton, A. J., Lycett, G. W., and Grierson, D. (1990). Antisense gene that Inhibits synthesis of the hormone ethylene in transgenic plants. Nature **346**, 284-287.

Hao, D. Y., Ohme-Takagi, M., and Sarai, A. (1998). Unique mode of GCC box recognition by the DNA-binding domain of ethylene-responsive element-binding factor (ERF domain) in plant. Journal of Biological Chemistry **273**, 26857-26861.

Harper, R. M., Stowe-Evans, E. L., Luesse, D. R., Muto, H., Tatematsu, K., Watahiki, M. K., Yamamoto, K., and Liscum, E. (2000). The NPH4 locus encodes the auxin response factor ARF7, a conditional regulator of differential growth in aerial *Arabidopsis* tissue. Plant Cell **12**, 757-770.

Harpham, N. V. J., Berry, A. W., Knee, E. M., Rovedahoyos, G., Raskin, I., Sanders, I. O., Smith, A. R., Wood, C. K., and Hall, M. A. (1991). The effect of ethylene on the growth and development of wild-type and mutant *Arabidopsis-thaliana*. Annals of Botany **68**, 55-61.

Harpster, M., Howie, W., and Dunsmuir, P. (1996). Characterization of a PCR fragment encoding 1-aminocyclopropane-1-carboxylate synthase in pepper (*Capsicum annuum*). Journal of Plant Physiology **147**, 661-664.

Hay, M. J. M., Brock, J. L., and Thomas, V. J. (1989). Density of *Trifolium-repens* plants in mixed swards under intensive grazing by sheep. Journal of Agricultural Science **113**, 81-86.

Henderson, J., Lyne, L., and Osborne, D. J. (2001). Failed expression of an endo-beta-1,4-glucanhydrolase (cellulase) in a non-abscinding mutant of *Lupinus angustifolius* cv Danja. Phytochemistry **58**, 1025-1034.

Hoffman, N. E., Fu, J. R., and Fayang, S. (1983). Identification and metabolism of 1-(malonylamino)cyclopropane-1-carboxylic acid in germinating peanut seeds. Plant Physiology **71**, 197-199.

Hoffman, N. E., and Yang, S. F. (1980). Changes of 1-aminocyclopropane-1-carboxylic acid content in ripening fruits in relation to their ethylene production-rates. Journal of the American Society For Horticultural Science **105**, 492-495.

Hua, J., Chang, C., Sun, Q., and Meyerowitz, E. M. (1995). Ethylene Insensitivity Conferred by Arabidopsis Ers Gene. Science **269**, 1712-1714.

Hua, J., and Meyerowitz, E. M. (1998). Ethylene responses are negatively regulated by a receptor gene family in *Arabidopsis thaliana*. Cell **94**, 261-271.

Hua, J., Sakai, H., Nourizadeh, S., Chen, Q. H. G., Bleecker, A. B., Ecker, J. R., and Meyerowitz, E. M. (1998). EIN4 and ERS2 are members of the putative ethylene receptor gene family in Arabidopsis. Plant Cell **10**, 1321-1332.

Huang, H., Mizukami, Y., Hu, Y., and Ma, H. (1993). Isolation and characterization of the binding sequences for the product of the *Arabidopsis* floral homeotic gene *Agamous*. Nucleic Acids Research **21**, 4769-4776.

Huang, H., Tudor, M., Weiss, C. A., Hu, Y., and Ma, H. (1995). The *Arabidopsis* MADS-box gene *Agl3* is widely expressed and encodes a sequence-specific DNA-binding Protein. Plant Molecular Biology **28**, 549-567.

Huang, P. L., Do, Y. Y., Huang, F. C., Thay, T. S., and Chang, T. W. (1997). Characterization and expression analysis of a banana gene encoding 1-aminocyclopropane-1-carboxylate oxidase. Biochemistry and Molecular Biology International **41**, 941-950.

Huang, P. L., Parks, J. E., Rottmann, W. H., and Theologis, A. (1991). 2 genes encoding 1-aminocyclopropane-1-carboxylate synthase in zucchini (*Cucurbita-Pepo*) are clustered and similar but differentially regulated. Proceedings of the National Academy of Sciences of the United States of America **88**, 7021-7025.

Hunter, D. (1998). Characterisation of ACC oxidase During Leaf maturation and Senescence in White Clover. PhD Thesis, Detartment of Plant Biology and Biotechnology, Massey University, Palmerston North, NZ.

Hunter, D. A., Yoo, S. D., Butcher, S. M., and McManus, M. T. (1999). Expression of 1-aminocyclopropane-1-carboxylate oxidase during leaf ontogeny in white clover. Plant Physiology **120**, 131-141.

Hyodo, H., Hashimoto, C., Morozumi, S., Hu, W. Z., and Tanaka, K. (1993). Characterization and Induction of the activity of 1-aminocyclopropane-1-carboxylate oxidase in the wounded mesocarp tissue of *Cucurbita-maxima*. Plant and Cell Physiology **34**, 667-671.

Imaseki, H. (1991). The biochemistry of ethylene biosynthesis. The Plant Hormone Ethylene Eds, CRC Press, Boca Raton, USA, 1-20.

Ishiguro, S., and Nakamura, K. (1994). Characterization of a cDNA encoding a novel DNA-binding protein, SPF1, that recognizes SP8 sequences in the 5' upstream regions of genes coding for sporamin and beta-amylase from sweet potato. Mol Gen Genet **244**, 563-571.

Itzhaki, H., Maxson, J. M., and Woodson, W. R. (1994). An ethylene-responsive enhancer element is involved in the senescence-related expression of the carnation glutathione-S-transferase (GST1) gene. Proc Natl Acad Sci U S A **91**, 8925-8929.

Jaya, E. S. K. D. (2003). Studies of the expression of *TR-ACO* genes in white clover. Diploma Thesis, Detartment of Plant Biology and Biotechnology, Massey University, Palmerston North, NZ.

Jeon, J. S., Lee, S., Jung, K. H., Jun, S. H., Kim, C., and An, G. (2000). Tissue-preferential expression of a rice a-tubulin gene, *OsTubA1*, mediated by the first intron1. Plant Physiology **123**, 1005-1014.

Jin, E. S., Lee, J. H., Park, J. A., and Kim, W. T. (1999). Temporal and spatial regulation of the expression of 1-aminocyclopropane-1-carboxylate oxidase by ethylene in mung bean (*Vigna radiata*). Physiologia Plantarum **105**, 132-140.

John, P. (1997). Ethylene biosynthesis: The role of 1-aminocyclopropane-1-carboxylate (ACC) oxidase, and its possible evolutionary origin. Physiologia Plantarum **100**, 583-592.

John, P., Iturriagagoitia-Bueno, T., Lay, V., Thomas, P., Hedderson, T., Prescott, A., Gibson, E., and Schofield, C. (1997). 1-aminocyclopropane-1-carboxylate-oxidase: molecular structure and catalytic function. Biology and Biotechnology of the Plant Hormone Ethylene, Kluwer Academic, Dordrecht, The Netherlands, 15-22.

Kadyrzhanova, D., McCully, T., Jaworski, S., Ververidis, P., Vlachonasios, K., Murakami, K., and Dilley, D. (1997). Structure-function analysis of ACC oxidase by site-directed mutagenesis. Biology and Biotechnology of the Plant Hormone Ethylene, Kluwer Academic, Dordrecht, The Netherlands, 5-13.

Kaneta, T., Kakimoto, T., and Shibaoka, H. (1997). Gibberellin A(3) causes a decrease in the accumulation of mRNA for ACC oxidase and in the activity of the enzyme in azuki bean (*Vigna angularis*) epicotyls. Plant and Cell Physiology **38**, 1135-1141.

Kathiresan, A., Nagarathna, K. C., Moloney, M. M., Reid, D. M., and Chinnappa, C. C. (1998). Differential regulation of 1-aminocyclopropane-1-carboxylate synthase gene family and its role in phenotypic plasticity in *Stellaria longipes*. Plant Molecular Biology **36**, 265-274.

Kawalleck, P., Plesch, G., Hahlbrock, K., and Somssich, I. E. (1992). Induction by fungal elicitor of S-adenosyl-L-methionine synthetase and S-adenosyl-L-homocysteine hydrolase messenger-RNas in cultured-cells and leaves of *Petroselinum-crispum*. Proceedings of the National Academy of Sciences of the United States of America **89**, 4713-4717.

Kende, H. (1993). Ethylene biosynthesis. Annual Review of Plant Physiology and Plant Molecular Biology **44**, 283-307.

Kepczynski, J., and Kepczynska, E. (1997). Ethylene in seed dormancy and germination. Physiologia Plantarum **101**, 720-726.

Kim, C. S., Kwak, J. M., Nam, H. G., Kim, K. C., and Cho, B. H. (1994). Isolation and characterization of 2 cDNA clones that are rapidly induced during the wound response of *Arabidopsis-thaliana*. Plant Cell Reports **13**, 340-343.

Kim, J. H., Kim, W. T., and Kang, B. G. (2001). IAA and N-6-benzyladenine inhibit ethylene-regulated expression of ACC oxidase and ACC synthase genes in mungbean hypocotyls. Plant and Cell Physiology **42**, 1056-1061.

Kim, J. H., Kim, W. T., Kang, B. G., and Yang, S. F. (1997). Induction of 1-aminocyclopropane-1-carboxylate oxidase mRNA by ethylene in mung bean hypocotyls: Involvement of both protein phosphorylation and dephosphorylation in ethylene signaling. Plant Journal **11**, 399-405.

Kim, W. T., and Yang, S. F. (1994). Structure and expression of cDNAs encoding 1-aminocyclopropane-1-carboxylate oxidase homologs isolated from excised mung bean hypocotyls. Planta **194**, 223-229.

Kim, Y. S., Choi, D., Lee, M. M., Lee, S. H., and Kim, W. T. (1998). Biotic and abiotic stress-related expression of 1-aminocyclopropane-1-carboxylate oxidase gene family in *Nicotiana glutinosa* L. Plant and Cell Physiology **39**, 565-573.

Lashbrook, C. C., Tieman, D. M., and Klee, H. J. (1998). Differential regulation of the tomato ETR gene family throughout plant development. Plant Journal **15**, 243-252.

Lasserre, E., Bouquin, T., Hernandez, J. A., Bull, J., Pech, J. C., and Balague, C. (1996). Structure and expression of three genes encoding ACC oxidase homologs from melon (*Cucumis melo* L). Molecular & General Genetics **251**, 81-90.

Lasserre, E., Godard, F., Bouquin, T., Hernandez, J. A., Pech, J. C., Roby, D., and Balague, C. (1997). Differential activation of two ACC oxidase gene promoters from melon during plant development and in response to pathogen attack. Molecular & General Genetics **256**, 211-222.

Lee, M. M., Lee, S. H., and Park, K. Y. (1997). Effects of spermine on ethylene biosynthesis in cut carnation (*Dianthus caryophyllus* L) flowers during senescence. Journal of Plant Physiology **151**, 68-73.

Lehman, A., Black, R., and Ecker, J. R. (1996). *HOOKLESS1*, an ethylene response gene, is required for differential cell elongation in the *Arabidopsis* hypocotyl. Cell **85**, 183-194.

Lelievre, J. M., Latche, A., Jones, B., Bouzayen, M., and Pech, J. C. (1997). Ethylene and fruit ripening. Physiologia Plantarum **101**, 727-739.

Li, N., and Mattoo, A. K. (1994). Deletion of the carboxyl-terminal region of 1-aminocyclopropane-1-carboxylic acid synthase, a key protein in the biosynthesis of ethylene, results in catalytically hyperactive, monomeric enzyme. Journal of Biological Chemistry **269**, 6908-6917.

Liang, X. W., Abel, S., Keller, J. A., Shen, N. F., and Theologis, A. (1992). The 1-aminocyclopropane-1-carboxylate synthase gene family of *Arabidopsis-thaliana*. Proceedings of the National Academy of Sciences of the United States of America **89**, 11046-11050.

Lincoln, J. E., Campbell, A. D., Oetiker, J., Rottmann, W. H., Oeller, P. W., Shen, N. F., and Theologis, A. (1993). *Le-ACS4*, a fruit ripening and wound-induced 1-aminocyclopropane-1-carboxylate synthase gene of tomato (*Lycopersicon-esculentum*) - expression in *Escherichia-coli*, structural characterization, expression characteristics, and phylogenetic analysis. Journal of Biological Chemistry **268**, 19422-19430.

Liu, J. H., LeeTamon, S. H., and Reid, D. M. (1997). Differential and wound-inducible expression of 1-aminocyclopropane-1-carboxylate oxidase genes in sunflower seedlings. Plant Molecular Biology **34**, 923-933.

Liu, J. H., Mukherjee, I., and Reid, D. M. (1990). Adventitious rooting in hypocotyls of sunflower (*Helianthus-annuus*) seedlings .3. the role of ethylene. Physiologia Plantarum **78**, 268-276.

Liu, Y. D., and Zhang, S. Q. (2004). Phosphorylation of 1-aminocyclopropane-1-carboxylic acid synthase by MPK6, a stress-responsive mitogen-activated protein kinase, induces ethylene biosynthesis in Arabidopsis. Plant Cell **16**, 3386-3399.

Lohman, K. N., Gan, S. S., John, M. C., and Amasino, R. M. (1994). Molecular analysis of natural leaf senescence in *Arabidopsis-thaliana*. Physiologia Plantarum **92**, 322-328.

Machackova, I., Chauvaux, N., Dewitte, W., and vanOnckelen, H. (1997). Diurnal fluctuations in ethylene formation in *Chenopodium rubrum*. Plant Physiology **113**, 981-985.

Manning, K. (1988). Detoxification of cyanide by plants and hormone action. Ciba Foundation Symposia **140**, 92-110.

Martin, M. N., Cohen, J. D., and Saftner, R. A. (1995). A new 1-aminocyclopropane-1-carboxylic acid-conjugating activity in tomato fruit. Plant Physiology **109**, 917-926.

Martin, M. N., and Saftner, R. A. (1995). Purification and characterization of 1-aminocyclopropane-1-carboxylic acid N-malonyltransferase from tomato fruit. Plant Physiology **108**, 1241-1249.

Maunders, M. J., Holdsworth, M. J., Slater, A., Knapp, J. E., Bird, C. R., Schuch, W., and Grierson, D. (1987). Ethylene stimulates the accumulation of ripening-related messenger-RNAs in tomatoes. Plant Cell and Environment **10**, 177-184.

Mayne, M. B., Coleman, J. R., and Blumwald, E. (1996). Differential expression during drought conditioning of a root-specific S-adenosylmethionine synthetase from jack pine (*Pinus banksiana* Lamb) seedlings. Plant Cell and Environment **19**, 958-966.

Mbeguie-A-Mbeguie, D., Chahine, H., Gomez, R. M., Gouble, B., Reich, M., Audergon, J. M., Souty, M., Albagnac, G., and Fils-Lycaon, B. (1999). Molecular cloning and expression of a cDNA encoding 1-aminocyclopropane-1-carboxylate (ACC) oxidase from apricot fruit (*Prunus armeniaca*). Physiologia Plantarum **105**, 294-303.

McGarvey, D. J., and Christoffersen, R. E. (1992). Characterization and kinetic-parameters of ethylene-forming enzyme from avocado fruit. Journal of Biological Chemistry **267**, 5964-5967.

Miller, J. D., Arteca, R. N., and Pell, E. J. (1999). Senescence-associated gene expression during ozone-induced leaf senescence in *Arabidopsis*. Plant Physiology **120**, 1015-1023.

Moeder, W., Barry, C. S., Tauriainen, A. A., Betz, C., Tuomainen, J., Utriainen, M., Grierson, D., Sandermann, H., Langebartels, C., and Kangasjarvi, J. (2002). Ethylene synthesis regulated by biphasic induction of 1-aminocyclopropane-1-carboxylic acid synthase and 1-aminocyclopropane-1-carboxylic acid oxidase genes is required for hydrogen peroxide accumulation and cell death in ozone-exposed tomato. Plant Physiology **130**, 1918-1926.

Monoz De Rueda, P., Gallardo, M., Matilla, A. J., and Sanchez-Calle, I. M. (1995). Preliminary characterization of 1-aminocyclopropane-1-carboxylate oxidase properties from embryonic axes of chick pea (*Cicer arietinum* L.) seeds. Journal of Experimental Botany **46**, 695-700.

Montgomery, J., Goldman, S., Deikman, J., Margossian, L., and Fischer, R. L. (1993). Identification of an ethylene-responsive region in the promoter of a fruit ripening gene. Proceedings of the National Academy of Sciences of the United States of America **90**, 5939-5943.

Moon, H., and Callahan, A. M. (2004). Developmental regulation of peach ACC oxidase promoter - GUS fusions in transgenic tomato fruits. Journal of Experimental Botany **55**, 1519-1528.

Morillon, R., Lienard, D., Chrispeels, M. J., and Lassalles, J. P. (2001). Rapid movements of plants organs require solute-water cotransporters or contractile proteins. Plant Physiology **127**, 720-723.

Moussatche, P., and Klee, H. J. (2004). Autophosphorylation activity of the *Arabidopsis* ethylene receptor multigene family. Journal of Biological Chemistry **279**, 48734-48741.

Moya-Leon, M. A., and John, P. (1995). Purification and biochemical-characterization of 1-aminocyclopropane-1-carboxylate oxidase from banana fruit. Phytochemistry **39**, 15-20.

Moysset, L., Solesugranes, L., and Simon, E. (1991). Changes in morphometry and elemental composition of *Robinia-pseudoacacia* pulvinar motor cells during leaflet movements. Journal of Experimental Botany **42**, 1315-1323.

Naik, P. K., and Mohapatra, P. K. (2000). Ethylene inhibitors enhanced sucrose synthase activity and promoted grain filling of basal rice kernels. Australian Journal of Plant Physiology **27**, 997-1008.

Nakajima, N., Matsuyama, T., Tamaoki, M., Saji, H., Aono, M., Kubo, A., and Kondo, N. (2001). Effects of ozone exposure on the gene expression of ethylene biosynthetic enzymes in tomato leaves. Plant Physiology and Biochemistry **39**, 993-998.

Nakajima, N., Mori, H., Yamazaki, K., and Imaseki, H. (1990). Molecular-cloning and sequence of a complementary-DNA encoding 1-aminocyclopropane-1-carboxylate synthase induced by tissue wounding. Plant and Cell Physiology **31**, 1021-1029.

Nakamura, M., Tsunoda, T., and Obokata, J. (2002). Photosynthesis nuclear genes generally lack TATA-boxes: a tobacco photosystem I gene responds to light through an initiator. Plant Journal **29**, 1-10.

Nakatsuka, A., Murachi, S., Okunishi, H., Shiomi, S., Nakano, R., Kubo, Y., and Inaba, A. (1998). Differential expression and internal feedback regulation of 1-aminocyclopropane-1-carboxylate synthase, 1-aminocyclopropane-1-carboxylate oxidase, and ethylene receptor genes in tomato fruit during development and ripening. Plant Physiology **118**, 1295-1305.

Nie, X. Z., Singh, R. P., and Tai, G. C. C. (2002). Molecular characterization and expression analysis of 1-aminocyclopropane-1-carboxylate oxidase homologs from potato under abiotic and biotic stresses. Genome **45**, 905-913.

Oeller, P. W., Wong, L. M., Taylor, L. P., Pike, D. A., and Theologis, A. (1991). Reversible inhibition of tomato fruit senescence by antisense RNA. Science **254**, 437-439.

Oetiker, J. H., Olson, D. C., Shiu, O. Y., and Yang, S. F. (1997). Differential induction of seven 1-aminocyclopropane-1-carboxylate synthase genes by elicitor in suspension cultures of tomato (*Lycopersicon esculentum*). Plant Molecular Biology **34**, 275-286.

Olson, D. C., Oetiker, J. H., and Yang, S. F. (1995). Analysis of *Le-ACS3*, a 1-aminocyclopropane-1-carboxylic acid synthase gene expressed during flooding in the roots of tomato plants. Journal of Biological Chemistry **270**, 14056-14061.

Olson, D. C., White, J. A., Edelman, L., Harkins, R. N., and Kende, H. (1991). Differential expression of 2 genes for 1-aminocyclopropane-1-carboxylate synthase in tomato fruits. Proceedings of the National Academy of Sciences of the United States of America **88**, 5340-5344.

Osborne, D. (1991). Ethylene in leaf ontogeny and abscission. The Plant Hormone Ethylene CRC Press, Boca Raton, Florida, USA, 193-214.

Osborne, D. J., Walters, J., Milborrow, B. V., Norville, A., and Stange, L. M. C. (1996). Evidence for a non-ACC ethylene biosynthesis pathway in lower plants. Phytochemistry **42**, 51-60.

Ouaked, F., Rozhon, W., Lecourieux, D., and Hirt, H. (2003). A MAPK pathway mediates ethylene signaling in plants. Embo Journal **22**, 1282-1288.

Ouvrard, O., Cellier, F., Ferrare, K., Tousch, D., Lamaze, T., Dupuis, J. M., and CasseDelbart, F. (1996). Identification and expression of water stress- and abscisic acid-regulated genes in a drought-tolerant sunflower genotype. Plant Molecular Biology **31**, 819-829.

Park, K. Y., Drory, A., and Woodson, W. R. (1992). Molecular-cloning of an 1-aminocyclopropane-1-carboxylate synthase from senescing carnation flower petals. Plant Molecular Biology **18**, 377-386.

Peck, S. C., and Kende, H. (1998). A gene encoding 1-aminocyclopropane-1-carboxylate (ACC) synthase produces two transcripts: elucidation of a conserved response. Plant Journal **14**, 573-581.

Peiser, G., and Yang, S. F. (1998). Evidence for 1-(malonylamino) cyclopropane-1-carboxylic acid being the major conjugate of aminocyclopropane-1-carboxylic acid in tomato fruit. Plant Physiology **116**, 1527-1532.

Peleman, J., Saito, K., Cottyn, B., Engler, G., Seurinck, J., Vanmontagu, M., and Inze, D. (1989). Structure and expression analyses of the S-adenosylmethionine synthetase gene family in *Arabidopsis-thaliana.* Gene **84**, 359-369.

Penmetsa, R. V., and Cook, D. R. (1997). A legume ethylene-insensitive mutant hyperinfected by its rhizobial symbiont. Science **275**, 527-530.

Penninckx, I., Eggermont, K., Terras, F. R. G., Thomma, B., DeSamblanx, G. W., Buchala, A., Metraux, J. P., Manners, J. M., and Broekaert, W. F. (1996). Pathogen-induced systemic activation of a plant defensin gene in *Arabidopsis* follows a salicylic acid-independent pathway. Plant Cell **8**, 2309-2323.

Petruzzelli, L., Coraggio, I., and Leubner-Metzger, G. (2000). Ethylene promotes ethylene biosynthesis during pea seed germination by positive feedback regulation of 1-aminocyclo-propane-1-carboxylic acid oxidase. Planta **211**, 144-149.

Petruzzelli, L., Harren, F., and Reuss, J. (1994). Patterns of C_2H_4 production during germination and seedling growth of pea and wheat as indicated by a laser-driven photoacoustic system. Environmental and Experimental Botany **34**, 55-61.

Pirrung, M. C., Cao, J., and Chen, J. (1995). Ethylene biosynthesis .12. analog approach to the active-site topography of the ethylene-forming enzyme - novel hydroxamate inhibitors. Journal of Organic Chemistry **60**, 5790-5794.

Pirrung, M. C., Kaiser, L. M., and Chen, J. (1993). Purification and properties of the apple fruit ethylene-forming enzyme. Biochemistry **32**, 7445-7450.

Pogson, B. J., Downs, C. G., and Davies, K. M. (1995). Differential expression of 2 1-aminocyclopropane-1-carboxylic acid oxidase genes in broccoli after harvest. Plant Physiology **108**, 651-657.

Ramassamy, S., Olmos, E., Bouzayen, M., Pech, J. C., and Latche, A. (1998). 1-aminocyclopropane-1-carboxylate oxidase of apple fruit is periplasmic. Journal of Experimental Botany **49**, 1909-1915.

Rasori, A., Bertolasi, B., Furini, A., Bonghi, C., Tonutti, P., and Ramina, A. (2003). Functional analysis of peach ACC oxidase promoters in transgenic tomato and in ripening peach fruit. Plant Science **165**, 523-530.

Raven, P., Evert, R., and Eichhorn, S. (1999). Biology of Plants, 6th ed. Worth Publishers, New York, USA.

Reid, M. (1995). Ethylene in plant growth, development and senescence. Plant Hormones, Physiology, Biochemistry and Molecular Biology 2nd ed. Kluwer Academic, Dordrecht, The Netherlands, 486-508.

Reinhardt, D., Kende, H., and Boller, T. (1994). Subcellular-localization of 1-aminocyclopropane-1-carboxylate oxidase in tomato cells. Planta **195**, 142-146.

Riechmann, J. L., and Meyerowitz, E. M. (1997). MADS domain proteins in plant development. Biological Chemistry **378**, 1079-1101.

Riechmann, J. L., Wang, M. Q., and Meyerowitz, E. M. (1996). DNA-binding properties of *Arabidopsis* MADS domain homeotic proteins APETALA1, APETALA3, PISTILLATA and AGAMOUS. Nucleic Acids Research **24**, 3134-3141.

Robatzek, S., and Somssich, I. E. (2002). Targets of *AtWRKY6* regulation during plant senescence and pathogen defense. Genes & Development **16**, 1139-1149.

Rodriguez, S. D., Lopez, B., and Chaves, A. R. (1999). Changes in polyamines and ethylene during the development and ripening of eggplant fruits (*Solanum melongena*). Journal of Agricultural and Food Chemistry **47**, 1431-1434.

Roman, G., Lubarsky, B., Kieber, J. J., Rothenberg, M., and Ecker, J. R. (1995). Genetic-analysis of ethylene signal-transduction in *Arabidopsis-thaliana* - 5 novel mutant loci Integrated Into a stress-response pathway. Genetics **139**, 1393-1409.

Rombaldi, C., Lelievre, J. M., Latche, A., Petitprez, M., Bouzayen, M., and Pech, J. C. (1994). Immunocytolocalization of 1-aminocyclopropane-1-carboxylic acid oxidase in tomato and apple fruit. Planta **192**, 453-460.

Ross, G. S., Knighton, M. L., and Layyee, M. (1992). An ethylene-related cDNA from ripening apples. Plant Molecular Biology **19**, 231-238.

Rottmann, W. H., Peter, G. F., Oeller, P. W., Keller, J. A., Shen, N. F., Nagy, B. P., Taylor, L. P., Campbell, A. D., and Theologis, A. (1991). 1-aminocyclopropane-1-carboxylate synthase in tomato is encoded by a multigene family whose transcription is induced during fruit and floral senescence. Journal of Molecular Biology **222**, 937-961.

Ruperti, B., Bonghi, C., Rasori, A., Ramina, A., and Tonutti, P. (2001). Characterization and expression of two members of the peach 1-aminocyclopropane-1-carboxylate oxidase gene family. Physiologia Plantarum **111**, 336-344.

Sakai, H., Hua, J., Chen, Q. H. G., Chang, C. R., Medrano, L. J., Bleecker, A. B., and Meyerowitz, E. M. (1998). ETR2 is an ETR1-like gene involved in ethylene signaling in *Arabidopsis*. Proceedings of the National Academy of Sciences of the United States of America **95**, 5812-5817.

Sambrook, J., Fritsch, E. F., Maniatis, T., and . (1989). Molecular Cloning: A Laboratory Manual 2nd ed. Cold Spring Harbor Laroratory Press, New York **1**.

Sato, T., and Theologis, A. (1989). Cloning the messenger-RNA encoding 1-aminocyclopropane-1-carboxylate synthase, the key enzyme for ethylene biosynthesis in plants. Proceedings of the National Academy of Sciences of the United States of America **86**, 6621-6625.

Satoh, S., and Esashi, Y. (1984). Changes in ethylene production and in 1-aminocyclopropane-1-carboxylic acid (ACC) and malonyl-ACC contents of cocklebur seeds during their development. Plant and Cell Physiology **25**, 1277-1283.

Satoh, S., and Esashi, Y. (1986). Inactivation of 1-aminocyclopropane-1-carboxylic acid synthase of etiolated mung bean hypocotyl segments by its substrate, S-adenosyl-$_L$-methionine. Plant and Cell Physiology **27**, 285-291.

Schaller, G. E., and Bleecker, A. B. (1995). Ethylene-binding sites generated in yeast expressing the *Arabidopsis Etr1* Gene. Science **270**, 1809-1811.

Schaller, G. E., Ladd, A. N., Lanahan, M. B., Spanbauer, J. M., and Bleecker, A. B. (1995). The ethylene response mediator *Etr1* from *Arabidopsis* forms a disulfide-linked dimer. Journal of Biological Chemistry **270**, 12526-12530.

Schroder, G., Eichel, J., Breinig, S., and Schroder, J. (1997). Three differentially expressed S-adenosylmethionine synthetases from *Catharanthus roseus*: Molecular and functional characterization. Plant Molecular Biology **33**, 211-222.

Sfakiotakis, E., Antunes, M., Stavroulakis, G., Niklis, N., Ververidis, P., and Gerasopoulos, D. (1997). Ethylene biosynthesis and its regulation in ripening "Hayward" kiwifruit. Biology and Biotechnology of the Plant Hormone Ethylene, Kluwer Academic, Dordrecht, The Netherlands, 47-56.

Sharp, P. A. (1994). Split gene and RNA splicing. Cell **77**, 805-815.

Shinshi, H., Usami, S., and Ohmetakagi, M. (1995). Identification of an ethylene-responsive region in the promoter of a tobacco class-I chitinase gene. Plant Molecular Biology **27**, 923-932.

Shiomi, S., Yamamoto, M., Ono, T., Kakiuchi, K., Nakamoto, J., Nakatsuka, A., Kubo, Y., Nakamura, R., Inaba, A., and Imaseki, H. (1998). cDNA cloning of ACC synthase and ACC oxidase genes in cucumber fruit and their differential expression by wounding and auxin. Journal of the Japanese Society For Horticultural Science **67**, 685-692.

Sisler, E. C., Dupille, E., and Serek, M. (1996). Effect of 1-methylcyclopropene and methylenecyclopropane on ethylene binding and ethylene action on cut carnations. Plant Growth Regulation **18**, 79-86.

Sisler, E. C., and Serek, M. (1997). Inhibitors of ethylene responses in plants at the receptor level: Recent developments. Physiologia Plantarum **100**, 577-582.

Slater, A., Maunders, M. J., Edwards, K., Schuch, W., and Grierson, D. (1985). Isolation and characterization of cDNA clones for tomato polygalacturonase and other ripening-related proteins. Plant Molecular Biology **5**, 137-147.

Smalle, J., Haegman, M., Mertens, J., Vangronsveld, J., Van Montagu, M., and Van Der Straeten, D. (1999). The expression pattern of the *Arabidopsis* ACC synthase gene 1 during rosette leaf development. Journal of Experimental Botany **50**, 1561-1566.

Smith, C. J. S., Slater, A., and Grierson, D. (1986). Rapid appearance of an messenger-RNA correlated with ethylene synthesis encoding a protein of molecular-weight 35000. Planta **168**, 94-100.

Smith, J. J., and John, P. (1993). Activation of 1-aminocyclopropane-1-carboxylate oxidase by bicarbonate carbon-dioxide. Phytochemistry **32**, 1381-1386.

Solano, R., Stepanova, A., Chao, Q. M., and Ecker, J. R. (1998). Nuclear events in ethylene signaling: a transcriptional cascade mediated by ETHYLENE-INSENSITIVE3 and ETHYLENE-RESPONSE-FACTOR1. Genes & Development **12**, 3703-3714.

Song, J. D., Lee, D. H., Rhew, T. H., and Lee, C. H. (2003). Wound-induced expression of ACC synthase genes in etiolated mung bean hypocotyls. Journal of Plant Biology **46**, 199-203.

Stalberg, K., Ellerstom, M., Ezcurra, I., Ablov, S., and Rask, L. (1996). Disruption of an overlapping E-box/ABRE motif abolished high transcription of the *napA* storage-protein promoter in transgenic *Brassica napus* seeds. Planta **199**, 515-519.

Tabor, C. W., and Tabor, H. (1984). Methionine adenosyltransferase (S-adenosylmethionine synthetase) and S-adenosylmethionine decarboxylase. Advances in Enzymology and Related Areas of Molecular Biology **56**, 251-282.

Tang, X. Y., Gomes, A., Bhatia, A., and Woodson, W. R. (1994). Pistil-specific and ethylene-regulated expression of 1-aminocyclopropane-1-carboxylate oxidase genes in petunia flowers. Plant Cell **6**, 1227-1239.

Tang, X. Y., Wang, H., Brandt, A. S., and Woodson, W. R. (1993). Organization and structure of the 1-aminocyclopropane-1-carboxylate oxidase gene family from *Petunia-hybrida*. Plant Molecular Biology **23**, 1151-1164.

Tayeh, M. A., Howe, D. L., Salleh, H. M., Sheflyan, G. Y., Son, J. K., and Woodard, R. W. (1999). Kinetic and mutagenic evidence for the role of histidine residues in the *Lycopersicon esculentum* 1-aminocyclopropane-1-carboxylic acid oxidase. Journal of Protein Chemistry **18**, 55-68.

TenHave, A., and Woltering, E. J. (1997). Ethylene biosynthetic genes are differentially expressed during carnation (*Dianthus caryophyllus* L) flower senescence. Plant Molecular Biology **34**, 89-97.

Theologis, A., Zarembinski, T. I., Oeller, P. W., Liang, X. W., and Abel, S. (1992). Modification of fruit ripening by suppressing gene-expression. Plant Physiology **100**, 549-551.

Thomas, H., and Stoddart, J. L. (1980). Leaf senescence. Annual Review of Plant Physiology and Plant Molecular Biology **31**, 83-111.

Tieman, D. V., Taylor, M. G., Ciardi, J. A., and Klee, H. J. (2000). The tomato ethylene receptors NR and LeETR4 are negative regulators of ethylene response and exhibit functional compensation within a multigene family. Proceedings of the National Academy of Sciences of the United States of America **97**, 5663-5668.

Todorov, D. T., Karanov, E. N., Smith, A. R., and Hall, M. A. (2003). Chlorophyllase activity and chlorophyll content in wild type and *eti 5* mutant of *Arabidopsis thaliana* subjected to low and high temperatures. Biologia Plantarum **46**, 633-636.

Trebitsh, T., Staub, J. E., and Oneill, S. D. (1997). Identification of a 1-aminocyclopropane-1-carboxylic acid synthase gene linked to the female (F) locus that enhances female sex expression in cucumber. Plant Physiology **113**, 987-995.

Tsai, D. S., Arteca, R. N., Bachman, J. M., and Phillips, A. T. (1988). Purification and characterization of 1-aminocyclopropane-1-carboxylate synthase from etiolated mung bean hypocotyls. Archives of Biochemistry and Biophysics **264**, 632-640.

Tuomainen, J., Betz, C., Kangasjarvi, J., Ernst, D., Yin, Z. H., Langebartels, C., and Sandermann, H. (1997). Ozone induction of ethylene emission in tomato plants: regulation by differential accumulation of transcripts for the biosynthetic enzymes. Plant Journal **12**, 1151-1162.

Ulker, B., and Somssich, I. E. (2004). WRKY transcription factors: from DNA binding towards biological function. Current Opinion in Plant Biology **7**, 491-498.

Van Der Straeten, D., Van Wiemeersch, L., Goodman, H. M., and Vanmontagu, M. (1990). Cloning and sequence of 2 different cDNAs encoding 1-aminocyclopropane-1-carboxylate synthase in tomato. Proceedings of the National Academy of Sciences of the United States of America **87**, 4859-4863.

Van Der Straeten, D., Van Wiemeersch, L., Van Damme, J., Goodman, H., and Van Montagu, M. (1989). Purification and amino acid sequence analysis of 1-amioncyclopropane-1-carboxylic acid synthase from tomato pericarp. Biochemical and Physiological Aspects of Ethylene Production in Lower and Higher Plants, Kluwer Academic, Dordrecht, The Netherlands, 93-100.

Ververidis, P., and John, P. (1991). Complete recovery Invitro of ethylene-forming enzyme-activity. Phytochemistry **30**, 725-727.

Vioque, B., and Castellano, J. M. (1994). *In-vitro* recovery of ACC oxidase from fruit of pear fruit (*Pyrus-communis* cv Blanquilla). Revista Espanola De Ciencia Y Tecnologia De Alimentos **34**, 643-652.

Voesenek, L., Benschop, J. J., Bou, J., Cox, M. C. H., Groeneveld, H. W., Millenaar, F. F., Vreeburg, R. A. M., and Peeters, A. J. M. (2003). Interactions between plant hormones regulate submergence-induced shoot elongation in the flooding-tolerant dicot Rumex palustris. Annals of Botany **91**, 205-211.

Vogel, J. P., Woeste, K. E., Theologis, A., and Kieber, J. J. (1998). Recessive and dominant mutations in the ethylene biosynthetic gene *ACS5* of *Arabidopsis* confer cytokinin insensitivity and ethylene overproduction, respectively. Proceedings of the National Academy of Sciences of the United States of America **95**, 4766-4771.

Vrebalov, J., Ruezinsky, D., Padmanabhan, V., White, R., Medrano, D., Drake, R., Schuch, W., and Giovannoni, J. (2002). A MADS-box gene necessary for fruit ripening at the tomato ripening-inhibitor (Rin) locus. Science **296**, 343-346.

Wachter, R., Langhans, M., Aloni, R., Gotz, S., Weilmunster, A., Koops, A., Temguia, L., Mistrik, I., Pavlovkin, J., Rascher, U., *et al.* (2003). Vascularization, high-volume solution flow, and localized roles for enzymes of sucrose metabolism during tumorigenesis by *Agrobacterium tumefaciens*. Plant Physiology **133**, 1024-1037.

Wang, K. L. C., Yoshida, H., Lurin, C., and Ecker, J. R. (2004). Regulation of ethylene gas biosynthesis by the *Arabidopsis* ETO1 protein. Nature **428**, 945-950.

Whittaker, D. J., Smith, G. S., and Gardner, R. C. (1997). Expression of ethylene biosynthetic genes in *Actinidia chinensis* fruit. Plant Molecular Biology **34**, 45-55.

Woltering, E. J., and Devrije, T. (1995). Ethylene - a tiny molecule with great potential. Bioessays **17**, 287-290.

Woodson, W. R., Park, K. Y., Drory, A., Larsen, P. B., and Wang, H. (1992). Expression of ethylene biosynthetic-pathway transcripts in senescing carnation flowers. Plant Physiology **99**, 526-532.

Yamagami, T., Tsuchisaka, A., Yamada, K., Haddon, W. F., Harden, L. A., and Theologis, A. (2003). Biochemical diversity among the 1-amino-cyclopropane-1-carboxylate synthase isozymes encoded by the *Arabidopsis* gene family. Journal of Biological Chemistry **278**, 49102-49112.

Yamauchi, D. (2001). A TGACGT motif in the 5'-upstream region of alpha-amylase gene from *Vigna mungo* is a *cis*-element for expression in cotyledons of germinated seeds. Plant Cell Physiol **42**, 635-641.

Yang, C. Y., Chu, F. H., Wang, Y. T., Chen, Y. T., Yang, S. F., and Shaw, J. F. (2003). Novel broccoli 1-aminocyclopropane-1-carboxylate oxidase gene (*Bo-ACO3*) associated with the late stage of postharvest floret senescence. Journal of Agricultural and Food Chemistry **51**, 2569-2575.

Yang, S. F., and Dong, J. G. (1993). Recent progress in research of ethylene biosynthesis. Botanical Bulletin of Academia Sinica **34**, 89-101.

Yang, S. F., and Hoffman, N. E. (1984). Ethylene biosynthesis and its regulation in higher-plants. Annual Review of Plant Physiology and Plant Molecular Biology **35**, 155-189.

Yip, W. K., Dong, J. G., and Yang, S. F. (1991). Purification and characterization of 1-aminocyclopropane-1-carboxylate synthase from apple fruits. Plant Physiology **95**, 251-257.

Yoo, S. (1999). Molecular characterisation of ethylene biosynthesis during leaf ontogeny in white clover. PhD Thesis, Detartment of Plant Biology and Biotechnology, Massey University, Palmerston North, NZ.

Yoshiyama, M., Maruyama, A., Atsumi, T., and Esashi, Y. (1996). Mechanism of action of C_2H_4 in promoting the germination of cocklebur seeds .3. A further enhancement of priming effect with

nitrogenous compounds and C_2H_4 responsiveness of seeds. Australian Journal of Plant Physiology **23**, 519-525.

Yu, D., Chen, C., and Chen, Z. (2001). Evidence for an important role of WRKY DNA binding proteins in the regulation of NPR1 gene expression. Plant Cell **13**, 1527-1540.

Yu, S. J., Kim, S., Lee, J. S., and Lee, D. H. (1998). Differential accumulation of transcripts for ACC synthase and ACC oxidase homologs in etiolated mung bean hypocotyls in response to various stimuli. Molecules and Cells **8**, 350-358.

Yu, Y. B., Adams, D. O., and Yang, S. F. (1979). Regulation of auxin-induced ethylene production in mung bean hypocotyls - role of 1-aminocyclopropane-1-carboxylic acid. Plant Physiology **63**, 589-590.

Zarembinski, T. I., and Theologis, A. (1994). Ethylene biosynthesis and action - a case of conservation. Plant Molecular Biology **26**, 1579-1597.

Zhang, X. S., Zheng, C. C., and O'Neil, S. D. (1999). Expression of ethylene biosynthetic genes regulated by pollination-associated factors in *Doritaenopsis hybrida* flowers. Acta Botanica Sinica **41**, 468-+.

Zhang, Z. G., Zhou, H. L., Chen, T., Gong, Y., Cao, W. H., Wang, Y. J., Zhang, J. S., and Chen, S. Y. (2004). Evidence for serine/threonine and histidine kinase activity in the tobacco ethylene receptor protein NTHK2. Plant Physiology **136**, 2971-2981.

Zhao, X. C., Qu, X., Mathews, D. E., and Schaller, G. E. (2002). Effect of ethylene pathway mutations upon expression of the ethylene receptor ETR1 from *Arabidopsis*. Plant Physiology **130**, 1983-1991.